

---

Final Report for Research Project

**INTEGRATIVE INFORMATION SYSTEM DESIGN FOR  
FLORIDA DEPARTMENT OF TRANSPORTATION**

*A framework for structural health monitoring of movable bridges*

---

**F. Necati Catbas, Ph.D.**, Principal Investigator

**Ricardo Zaurin, Melih Susoy, Mustafa Gul**, Graduate Assistants

Civil and Environmental Engineering Department, University of Central Florida  
4000 Central Florida Boulevard, PO Box 162450, Orlando, Florida 32816  
Tel: 407-823-3743 and Fax: 407-823-3315

---

A Report on a Research Project Sponsored by

Florida Department of Transportation

Contract No.: BD548 - RPWO#11

**Marcus Ansley, P.E.**, Project Manager, FDOT

---

June 2007

## **DISCLAIMER**

The opinions, findings, and conclusions expressed in this publication are those of the authors and not necessarily those of the State of Florida Department of Transportation.

## UNIT CONVERSION TABLE

To convert from	To	Multiply by
Inch	centimeter	2.54
square inch	square centimeter	6.4516
kip	kiloNewton (kN)	4.44747
kip/sq.in. (ksi)	kN/sq.m (kPa)	6,894.28
kip-foot	kN-meter	1.3556
btu	joule	1,055
btu/hr.	watt	0.2931
degrees Fahrenheit – 32	degrees celcius	0.5555
lb/cu.in.	kgs./cu.m	27,680
btu/sq.ft./min.	watts/sq.in.	0.122

**Technical Report Documentation Page**

1. Report No.		2. Government Accession No.		3. Recipient's Catalog No.	
4. Title and Subtitle  Integrative Information System Design for Florida Department of Transportation <i>A Framework for Structural Health Monitoring of Movable Bridges</i>				5. Report Date June 2007	
				6. Performing Organization Code UCF	
7. Author(s) F. Necati Catbas, Melih Susoy, Ricardo Zaurin and Mustafa Gul				8. Performing Organization Report No.	
9. Performing Organization Name and Address University of Central Florida Civil and Environmental Engineering Department Engineering Bldg Room 211 Orlando, FL 32816				10. Work Unit No. (TRAIS)	
				11. Contract or Grant No. BD548/RPWO 11	
12. Sponsoring Agency Name and Address Florida Department of Transportation Research Center, MS 30 605 Suwannee Street Tallahassee, FL 32310				13. Type of Report and Period Covered Final Report November 2004 – April 2007	
				14. Sponsoring Agency Code FDOT	
15. Supplementary Notes					
16. Abstract Bridges constitute critical nodes of transportation systems, and therefore, ensuring their continuous operation is of utmost importance for safe and efficient transportation. Currently, visual inspections and simplified analysis techniques are employed for condition assessment and for decision making about bridges. A novel approach to bridge condition assessment is Structural Health Monitoring (SHM), defined as the measurement of operating and loading environment and critical responses of a system to track and evaluate incidents, anomalies, damage and deterioration. The objective of this project is to develop an SHM framework for integrative information system design. This framework is expected to improve bridge safety and to have efficient operation, effective and low cost maintenance by taking advantage of new technological advances. Movable bridges are considered as focus bridge type, because these bridges exhibit various structural, maintenance and operational problems. In this study, inspection and maintenance records of the movable bridges are analyzed to determine the current condition of these bridges as given in these reports. Then, numerical and experimental studies are developed and conducted. Data processing and some novel analysis methods that are being employed by the writers are summarized along with examples from laboratory studies. These analysis methods include statistical pattern recognition methods, parameter estimation with sensor fusion and model updating, estimation of reliability and prediction of future performance using Bayesian updating with monitor data, and possible use of computer vision. These algorithms have to be coupled with data monitoring front panels which can be used by engineers and other users. In this study, a data monitoring front panel, which makes it available to monitor multiple sensors is also developed and presented. Concepts for data management and use of information technologies for efficient and effective use of structural health monitoring data are discussed. Also, critical components and locations of movable bridges are summarized for monitoring purposes. In addition to structural components, Hopkins frame, trunnions, live load shoes, shafts, span locks electrical motors, gear boxes and open gears are determined to be candidates for monitoring. An application such as described in this report can be expected to mitigate the problems, improve future designs and reduce the maintenance costs. Further studies and field demonstrations are necessary to evaluate the real life performance of the technologies and methods as well as to quantify the cost-benefit ratio of integrated SHM applications.					
17. Key Word Structural Health Monitoring, Movable bridges, sensors, data acquisition, data processing				18. Distribution Statement	
19. Security Classif. (of this report) Unclassified		20. Security Classif. (of this page) Unclassified		21. No. of Pages 231	22. Price NA

## **ACKNOWLEDGEMENTS**

This report is made possible through the support of the Florida Department of Transportation (FDOT), and the guidance, suggestions and feedback of the FDOT central office and district engineers. Messrs. Marcus Ansley, Angel Rodriguez, Richard Kerr and Richard Long were very instrumental in the development of this project with their continuous input. Especially, Mr. Marcus Ansley provided important feedback to develop a monitoring framework throughout the project and also gave his review for the report. Mr. Alberto Sardinias (from District 4) is to be acknowledged for sharing his experience on movable bridges, and for making arrangements for site visits. District facilities engineers Messrs. Ron Meade, Seta Koroitamoudou (from District 5) provided relevant data, as well as shared their knowledge. Messrs. Lee Smith and Duane Robertson from the FDOT Materials Laboratory at Gainesville provided valuable information about the movable bridges. They are also acknowledged for conducting tests and providing the data. Former graduate students Mr. Kevin Francoforte, Mr. Jason Burkett and Mr. Pavel Babenko have been contributors to the development work presented in this report.

## **PREFACE**

The report describes and presents the background, methodology, and results of a research project conducted by University of Central Florida researchers and funded by the Florida Department of Transportation.

# **EXECUTIVE SUMMARY**

## **Background**

Bridges constitute critical nodes of transportation systems, and therefore, ensuring their continuous operation is of utmost importance for safe and efficient transportation. Currently, visual inspections and simplified analysis techniques are employed for condition assessment and for decision making about bridges. Despite limitations, visual inspection remains today the most commonly practiced damage detection method. A novel approach to bridge condition assessment is Structural Health Monitoring (SHM), or more specifically Bridge Health Monitoring. SHM can be defined as the measurement of a bridge's operating and loading environment through use of a system to track and evaluate incidents, anomalies, damage and deterioration. With a proper design, SHM is expected to improve bridge evaluation and management techniques through instrumentation, sensing, data processing, use of analytical methods, data evaluation algorithms and data management. SHM utilizes advanced technology to capture the critical inputs and responses of a structural system in order to understand the root causes of problems as well as to track responses to predict future behavior.

## **Objective and Scope**

The objective of this project is to develop a structural health monitoring operational framework for an integrative information system design to improve bridge safety, enhance efficiency and enable effective and low cost maintenance through use of new technological advances. An integrative information system within an SHM framework can facilitate information sharing and use by FDOT groups focusing on areas such as structures, maintenance and operations that have similar data needs. While new technologies offer promise, there are several issues that need further research. These are a) managing data by means of methods and procedures developed for data collection, use and evaluation, b) identification of critical features that need to be monitored for safety,

maintenance and operation by means of statistical analysis, c) organization and use of the most critical and desirable data and information for decision making, d) demonstration of ideas and concepts.

In this project, a framework for different SHM applications has been developed by identifying current issues affecting the maintenance of movable bridges and conducting numerical and experimental studies. Movable bridges are considered “focus” bridge types, because they exhibit various structural, maintenance and operational issues. For example, movable bridges were reported to be about a hundred times more costly to repair and maintain than fixed highway bridges because service includes not just structural systems but also mechanical and electrical systems. Due to their significantly higher cost of maintenance, increasing efficiency of movable bridge management practices would have a higher benefit for monitoring demonstration purposes.

### **Project Tasks, Findings and Results**

The first task of the project is the characterization of available data and user needs. Common characteristics of Florida movable bridges and their distribution are identified from the National Bridge Inventory (NBI). In addition, existing databases, plans, inspection reports, and other relevant documents that were obtained from Districts 4 and 5 are analyzed to determine the most commonly observed movable bridge problem. Site visits, meetings with FDOT officials and district engineers, and joint field tests supplemented the data needed for understanding the condition of the bridges. A representative bridge is also identified and its inspection and maintenance records are analyzed over a 25-year period. The results of the analyses on the representative bridge helped determine plans to address or remedy critical issues. Rapid deterioration due to movements causing friction and wear of mechanical components, frequent and unexpected breakdowns of components such as drive motors, shafts, gears, racks, pinions, trunnions and limit switches require costly repair and maintenance. It is very important to detect and even predict these failures in a timely manner to prevent disruption to vehicular and marine traffic.

The second task of the project is the development of monitoring strategies. After the detailed evaluation of the inspection data of the representative bridge and communication with FDOT engineers, finite element (FE) models of the bridge are developed. The two different models which represent different levels of resolution are both calibrated using field test data. The models are used to determine levels of stresses, deflection under various load conditions. The tip deflection under single AASHTO HL-93 truck and two HL-93 trucks+lane load are determined to be 1.65 in and 4.49 in, respectively. The serviceability limit for this bridge and deck type is determined to be 5.6 in. The maximum stresses under dead load and two HL-93 trucks+lane load around trunnion, at span lock and live load shoe are determined to be ~6-12 ksi, ~10 ksi, ~15 ksi, respectively. The frequencies and mode shapes are also sensitive to damage, imbalance and structural changes. For example, it is seen that additional modes appear when span lock failure is simulated. For the undamaged condition, the first three modes are at 3.69 Hz, 4.74 Hz and 9.04 Hz. The load rating is determined to be lowest right above the live load shoes. The inventory and operating rating values under two HL-93 trucks+lane load at this location are 0.98 and 1.27, respectively. However, it is seen that under one HL-93 truck traveling at 50 mph, the lowest system reliability index is determined to be 5.79 which is far above the 3.5 (AASHTO LRFD for new design) and 2.5 (AASHTO LRFR for existing bridges). These results are valuable to determine the monitoring locations, sensing requirements and expected ranges.

The last task of the project is the design, implementation and demonstration of the integrated framework. In this task, traditional and some novel sensors and sensor networks are summarized along with criteria for the type and selection. Data acquisition systems and communications are critical components of structural health monitoring systems related with the acquisition of the data, including data collection, signal processing, synchronization, digitization and storage. A data acquisition system is proposed with different components and alternative data transmission protocols. In addition, data transmission alternatives are offered for movable bridges. Data processing and some novel analysis methods that are being developed by the writers are summarized along with examples from laboratory studies. More specifically, statistical pattern

recognition methods, parameter estimation with sensor fusion and model updating, estimation of reliability and prediction of future performance using Bayesian updating with monitored data, and the possible use of computer vision approaches are presented with examples. These algorithms have to be coupled with data monitoring front panels which can be used by engineers and other users. It should be noted that three appendices provide additional information about sensors, related laboratory studies and a brief market search for sensing and data acquisition technologies. In this study, a data monitoring front panel, which makes it available to monitor multiple sensors is also developed and presented. Concepts for data management and use of information technologies for efficient and effective use of structural health monitoring data are discussed. Finally, critical components and locations for movable bridges are summarized. In addition to structural components, Hopkins frame, trunnions, live load shoes, shafts, span locks electrical motors, gear boxes and open gears are determined to be candidates for monitoring.

## **Recommendations**

Integrated structural health monitoring offers promise for improved condition assessment and can complement current bridge management systems. An application such as described in this report can be expected to mitigate both problems and maintenance costs. Further studies and pilot applications are necessary to evaluate the real life performance of technologies and methods as well as to quantify the cost-benefit ratio of integrated SHM applications.

Finally, we note that the integrated monitoring framework proposed in this report is developed in parallel to the efforts of the Federal Highway Administration Long Term Bridge Performance Program (LTBPP), which focuses on continuous bridge monitoring applications for developing improved knowledge on performance and degradation, better design methods and performance predictive models, and advanced management decision-making tools.

# TABLE OF CONTENTS

<b>DISCLAIMER.....</b>	<b>II</b>
<b>UNIT CONVERSION TABLE .....</b>	<b>III</b>
<b>TECHNICAL REPORT DOCUMENTATION PAGE.....</b>	<b>IV</b>
<b>ACKNOWLEDGEMENTS .....</b>	<b>V</b>
<b>PREFACE .....</b>	<b>VI</b>
<b>EXECUTIVE SUMMARY .....</b>	<b>VII</b>
<b>TABLE OF CONTENTS .....</b>	<b>XI</b>
<b>LIST OF FIGURES .....</b>	<b>XVII</b>
<b>1. INTRODUCTION.....</b>	<b>1</b>
<b>1.1. Statement of the Problem.....</b>	<b>1</b>
1.1.1. Background of Bridge Inspections and Evaluations .....	2
1.1.2. New Technologies for Objective Bridge Assessment, Evaluation and Maintenance....	3
<b>1.2. Structural Health Monitoring as a Promising Approach.....</b>	<b>3</b>
1.2.1. Definition .....	3
1.2.2. Components of a Complete SHM .....	4
1.2.3. Promises of SHM.....	5
<b>1.3. Project Objectives and Goals.....</b>	<b>5</b>

<b>1.4.</b>	<b>Project Tasks .....</b>	<b>6</b>
1.4.1.	Characterization of Available Data and User Needs .....	6
1.4.2.	Development of Monitoring Strategies .....	7
1.4.3.	Design, Implement and Demonstrate the Integrated Framework .....	7
<b>2.</b>	<b>CHARACTERIZATION AND ASSESSMENT OF BRIDGES .....</b>	<b>8</b>
<b>2.1.</b>	<b>Introduction.....</b>	<b>8</b>
<b>2.2.</b>	<b>Current Bridge Inspection and Management Procedure .....</b>	<b>8</b>
2.2.1.	Bridge Inspection Program .....	8
2.2.2.	Bridge Inspections in Florida .....	9
<b>2.3.</b>	<b>Issues for Today’s Bridge Management Practice.....</b>	<b>11</b>
2.3.1.	Uncertainties in Condition Evaluation .....	11
2.3.2.	Asset Management .....	11
2.3.3.	Information Control .....	12
<b>2.4.</b>	<b>Characterization of Movable Bridges as Demonstration Example .....</b>	<b>13</b>
2.4.1.	Why Movable Bridges Selected as a Focus .....	13
2.4.2.	Movable Bridges .....	13
2.4.3.	Status of Movable Bridge Population in Florida .....	20
2.4.4.	Compilation of Data from Maintenance Offices .....	22
<b>3.</b>	<b>MONITORING DEVELOPMENT STAGES .....</b>	<b>26</b>
<b>3.1.</b>	<b>Introduction.....</b>	<b>26</b>
<b>3.2.</b>	<b>Site Visits and Meetings with FDOT Engineers – User Needs .....</b>	<b>26</b>

<b>3.3.</b>	<b>Evaluation of Inspection Data.....</b>	<b>28</b>
3.3.1.	Analysis of Inspection Data for a Subset Population .....	28
3.3.2.	Inspection Data Analysis for Christa McAuliffe Bridge over 30 Years.....	33
<b>3.4.</b>	<b>Numerical Model Development for Analytical Evaluation of Structural Performance</b>	<b>38</b>
3.4.1.	Finite Element Model Development .....	38
3.4.2.	Initial Finite Element Model with Shell Elements .....	38
3.4.3.	Modified Finite Element Model with Frame Elements.....	47
<b>3.5.</b>	<b>Comparison of the Two Models.....</b>	<b>51</b>
<b>3.6.</b>	<b>Experimental Studies Conducted at the Bridge .....</b>	<b>54</b>
3.6.1.	Field Test Data Analysis (Balance Test).....	56
<b>4.</b>	<b>MODEL CALIBRATION, SIMULATIONS AND RATING .....</b>	<b>60</b>
<b>4.1.</b>	<b>Introduction.....</b>	<b>60</b>
<b>4.2.</b>	<b>Calibration of the Model According to the Balance Condition.....</b>	<b>60</b>
<b>4.3.</b>	<b>Analysis and Load Simulation Results.....</b>	<b>61</b>
4.3.1.	Loads Used for FE Simulations .....	61
4.3.2.	Deflections .....	62
4.3.3.	Stresses.....	64
4.3.4.	Dynamic Analysis .....	67
4.3.5.	Examples of Location for Monitoring Based on FEM.....	70
<b>4.4.</b>	<b>Movable Bridge Load Rating.....</b>	<b>71</b>

4.5.	<b>Moving Load Simulation</b> .....	76
4.6.	<b>Summary of Analysis Results</b> .....	86
<b>5.</b>	<b>INTEGRATED STRUCTURAL HEALTH MONITORING DESIGN</b> .....	<b>90</b>
5.1.	<b>Introduction</b> .....	<b>90</b>
5.2.	<b>Sensors And Sensor Networks</b> .....	<b>90</b>
5.2.1.	Traditional Sensors .....	93
5.2.2.	Some Novel Sensing Technologies.....	99
5.2.3.	Wireless Sensing.....	101
5.3.	<b>Data Acquisition Systems and Communication</b> .....	<b>102</b>
5.4.	<b>Critical Components of Movable Bridges for Monitoring</b> .....	<b>105</b>
5.4.1.	Electrical Motors.....	105
5.4.2.	Gear Boxes.....	106
5.4.3.	Open Gears / Racks.....	107
5.4.4.	Hopkins Frame.....	111
5.4.5.	Trunnions .....	111
5.4.6.	Live Load Shoes.....	115
5.4.7.	Span Locks.....	116
5.4.8.	Bridge Operation (Opening/Closing).....	118
5.4.9.	Longitudinal Displacement .....	119
5.4.10.	Main Girders and Floor Beams.....	119
5.5.	<b>Data Processing and Some New Analysis Methods</b> .....	<b>122</b>

5.5.1.	Statistical Pattern Recognition .....	125
5.5.2.	Parameter Estimation with Sensor Fusion and Model Updating.....	129
5.5.3.	Estimation of Reliability using SHM Data.....	133
5.5.4.	Possible Use of Computer Vision Data for SHM.....	141
<b>5.6.</b>	<b>Data Monitoring Front Panel.....</b>	<b>145</b>
<b>5.7.</b>	<b>Data Management and Information Technologies.....</b>	<b>148</b>
<b>6.</b>	<b>CONCLUSIONS AND RECOMMENDATIONS.....</b>	<b>151</b>
<b>7.</b>	<b>REFERENCES.....</b>	<b>155</b>
<b>APPENDIX A.</b>	<b>SENSORS AND DATA ACQUISITION SYSTEMS .....</b>	<b>162</b>
<b>A.1.</b>	<b>Sensor Technology .....</b>	<b>162</b>
<b>A.2.</b>	<b>General Types of Sensors .....</b>	<b>162</b>
<b>A.3.</b>	<b>Data Acquisition Systems Currently in Use at the UCF Structures and Systems Research Laboratory.....</b>	<b>168</b>
A.3.1.	VXI System .....	168
A.3.2.	National Instruments System .....	169
A.3.3.	Campbell Scientific.....	170
A.3.4.	Other Data Acquisition Systems.....	171
<b>APPENDIX B.</b>	<b>RELATED LABORATORY STUDIES.....</b>	<b>173</b>
<b>APPENDIX C.</b>	<b>INSTRUMENTATION COMPANIES AND MARKET SEARCH.....</b>	<b>192</b>
<b>A.1.</b>	<b>Companies Related with SHM Sensor Development.....</b>	<b>192</b>
<b>A.2.</b>	<b>Sensors Market Search.....</b>	<b>199</b>

A.2.1.	Accelerometer.....	199
A.2.2.	Strain.....	201
A.2.3.	Temperature.....	203
A.2.4.	Tilt .....	203
A.2.5.	Wireless Networking .....	204
A.2.6.	Corrosion .....	205

# LIST OF FIGURES

Figure 2.1 – Movable bridge terminology (FDOT 2004).....	14
Figure 2.2 – Main types of movable bridges (Koglin 2003).....	15
Figure 2.3 – Temporary bridge adjacent to the Bridge of Lions in open position (St. Augustine, FL).....	15
Figure 2.4 – Fort Denaud Swing Bridge, Florida .....	16
Figure 2.5 – A bascule bridge on the Miami River in Florida is open to let a ship pass (Buxton-Tetteh 2004) .....	17
Figure 2.6 – Florida DOT district map .....	20
Figure 2.7 – Distribution of FDOT movable bridges .....	21
Figure 2.8 – Distribution of FDOT movable bridges according to length of maximum span (NBI 2002)...	21
Figure 2.9 – Distribution of movable bridges according to year built (NBI 2002).....	22
Figure 2.10 – Deterioration effects of corrosion on Michigan Street Bridge, Sturgeon Bay, Wisconsin (Prine and Fish 1996).....	23
Figure 2.11 – Damage to Bridge to Sullivans Island, Charleston after hurricane Hugo, 1991 Source: NOAA Photo Library ( <a href="http://www.photolib.noaa.gov/historic/nws/wea00469.htm">http://www.photolib.noaa.gov/historic/nws/wea00469.htm</a> ).....	24
Figure 3.1 – Typical element condition from an inspection report.....	29
Figure 3.2 – Analysis of inspection reports by creating spreadsheets from visual inspection data .....	30
Figure 3.3 – Average condition states of components.....	31
Figure 3.4 – Identification of common problems .....	31
Figure 3.5 – Most commonly observed movable bridge problems (District 4&5).....	32
Figure 3.6 – Case Study: Christa McAuliffe Bascule Bridge in Merritt Island, FL .....	33

Figure 3.7 – Main girder of Christa McAuliffe Movable Bridge .....	34
Figure 3.8 – Christa McAuliffe Movable Bridge elevation .....	34
Figure 3.9 – Christa McAuliffe Movable Bridge mechanical system .....	35
Figure 3.10 – Condition state: Decks .....	36
Figure 3.11 – Condition state: Movable components .....	36
Figure 3.12 – Condition state: Superstructure .....	37
Figure 3.13 – Condition state: Locks and live load shoes .....	37
Figure 3.14 – 3D CAD model of the movable bridge .....	39
Figure 3.15 – 3D CAD model; orthogonal views .....	40
Figure 3.16 – Modeling of the bascule girder .....	40
Figure 3.17 – Modeling of bascule girders with shell elements .....	41
Figure 3.18 – Detail of the pinned connection .....	41
Figure 3.19 – Model with shell elements (deck not shown) .....	42
Figure 3.20 – Rigid links between frame elements .....	42
Figure 3.21 – Detail of the steel deck (Christa McAuliffe Bridge construction plans) .....	43
Figure 3.22 – Model of the real deck .....	43
Figure 3.23 – Deformations under load .....	44
Figure 3.24 – Deck modeled using 1.45 in thick steel shell element .....	44
Figure 3.25 – Deflections under load .....	45
Figure 3.26 – Connection of two spans .....	46
Figure 3.27 – Finite element model with shell elements .....	46

Figure 3.28 – Modeling of bascule girders with frame elements.....	48
Figure 3.29 – Main girders, transverse girders, floor beams, and bracings. ....	48
Figure 3.30 – Close-up on the trunnion in the modified model.....	49
Figure 3.31 – Supports (boundary conditions) of the model (deck not shown).....	49
Figure 3.32 – Completed modified FEM (Deck not shown). ....	50
Figure 3.33 – Analysis details for the modified FEM .....	50
Figure 3.34 – Load case studied for model comparison .....	51
Figure 3.35 – Finite element models deflection comparison.....	52
Figure 3.36 – Comparison of the first three principal modes .....	53
Figure 3.37 – Desirable Balance Condition of a Bascule Bridge .....	54
Figure 3.38 – Different cases of average torque during opening and closing.....	55
Figure 3.39 – Balance test results for March 2003 .....	57
Figure 3.40 – Balance test results for February 2003 .....	57
Figure 3.41 – Balance test results for February 2006 .....	58
Figure 3.42 – Change of friction values .....	59
Figure 4.1 – Balance condition of the leaves.....	61
Figure 4.2 – HL-93 truck load.....	61
Figure 4.3 – Loading for load rating of the bridge (Two HL-93 trucks and distributed lane load).....	62
Figure 4.4 – Deflections at the center.....	63
Figure 4.5 – Von Mises stresses for Dead Load (ksi).....	64
Figure 4.6 – Von Mises stresses for Truck Load (ksi).....	65

Figure 4.7 – Von Mises stresses for Dead Load and Truck Load (ksi) .....	65
Figure 4.8 – Von Mises stresses at the THG connection for Dead Load (ksi) .....	65
Figure 4.9 – Von Mises stresses at the THG connection for Truck Load (ksi) .....	66
Figure 4.10 – Von Mises stresses at the THG connection for Dead Load and Truck Load (ksi) .....	66
Figure 4.11 – Modal analysis results: Mode 1 .....	67
Figure 4.12 – Modal analysis results: Mode 2 .....	68
Figure 4.13 – Modal analysis results: Mode 3 .....	68
Figure 4.14 – Modal analysis results: Mode 4 .....	68
Figure 4.15 – Modal analysis results: Mode 5 .....	69
Figure 4.16 – Modal analysis results: Mode 6 .....	69
Figure 4.17 – Additional mode shapes for a span-lock failure scenario .....	70
Figure 4.18 – Span lock failure simulation .....	71
Figure 4.19 – Transverse loading .....	72
Figure 4.20 – Truck position for load rating (lane load not shown) .....	72
Figure 4.21 – Section locations for load rating .....	73
Figure 4.22 – Moving Load Analysis .....	76
Figure 4.23 – Variation of Moment due to Moving Load over the Girder Locations .....	77
Figure 4.24 – Section properties of Section 1 along the girder .....	79
Figure 4.25 – Section properties of Section 2 along the girder .....	79
Figure 4.26 – Section properties of Section 3 along the girder .....	80
Figure 4.27 – Movable Bridge System Reliability Model with Parallel/Series Assembly (Lower Bound) .	84

Figure 4.28 – Instantaneous System Reliability under a Single Moving Truck (note that this is for one moving truck without lane load, wind, temperature) .....	85
Figure 4.29 – Loading position for .....	86
Figure 5.1 – Example foil type strain gages (Omega Eng.).....	94
Figure 5.2 – Example vibrating-wire type strain gages (Geokon Inc.).....	95
Figure 5.3 – Displacement gage examples (Spaceage Control).....	96
Figure 5.4 – Tiltmeter examples (Applied Geomechanics, Geokon) .....	97
Figure 5.5 – Example accelerometers (PCB) .....	97
Figure 5.6 – An example wind station for measuring wind direction, speed and temperature (Omega Inc.)	98
Figure 5.7 – Sensor array + DAQ scheme .....	103
Figure 5.8 – Data transmission with two data acquisition systems via under-water cable .....	104
Figure 5.9 - Data transmission with two data acquisition systems via wireless connection.....	104
Figure 5.10 – Data transmission with wireless sensor array.....	105
Figure 5.11. Some of the proposed metrics for Level 1 monitoring (raw data indicators) .....	124
Figure 5.12. Pattern classifier (adapted from Webb 1999).....	125
Figure 5.13 – Supervised and unsupervised learning for SHM .....	126
Figure 5.14. Some of the proposed metrics for Level 2 monitoring (identification of damage) .....	127
Figure 5.15 – Mahalanobis distance plots to detect damage case.....	129
Figure 5.16. Some of the proposed metrics for Level 3 monitoring (quantification and localization).....	130
Figure 5.17 –General methodology for parameter estimation and model updating.....	132
Figure 5.18 –Estimation of the stiffness parameters at the supports with statistical bounds.....	133

Figure 5.19 – Limit state functions (Nowak and Collins 2000).....	135
Figure 5.20 – Concept of Bayesian Updating.....	136
Figure 5.21 – Simple beam test for Bayesian updating demonstration .....	138
Figure 5.22 – Test beam .....	138
Figure 5.23 – Prior and new data for the test beam.....	139
Figure 5.24 – Updating the available data and prediction with the first data set using Bayesian.....	140
Figure 5.25 – Reliability based on SHM data.....	141
Figure 5.26 – Computer vision integration into SHM.....	142
Figure 5.27 – Data monitoring for the laboratory health monitoring setup.....	146
Figure 5.28 – Movable bridge remote monitoring system.....	147
Figure 5.29 - Database implementation.....	148
Figure 5.30 - Database functional layers .....	149
Figure 5.31 – Example framework for internet-based database .....	150
Figure 5.32 – Electrical motor.....	106
Figure 5.33 – A gear box.....	107
Figure 5.34 – Open gear / rack .....	108
Figure 5.35 – Rack details (Patton 2006) .....	108
Figure 5.36 – Area for searching is defined .....	110
Figure 5.37 – Histogram of the pixel intensities and determination of interest regions .....	110
Figure 5.38 – Detection of corrosion/indentation.....	110
Figure 5.39 – Hopkins frame girder .....	111

Figure 5.40 – Trunnion.....	112
Figure 5.41 – Instrumentation for the mechanical components (Adapted from Christa McAuliffe Bridge Construction Plans).....	113
Figure 5.42 – Instrumentation of mechanical components.....	114
Figure 5.43 – Mechanical system of the representative movable bridge (Adapted from Christa McAuliffe Bridge Construction Plans).....	115
Figure 5.44 – Live load shoe (LLS) (sketch adapted from Christa McAuliffe Bridge construction plans).....	116
Figure 5.45 – Span lock.....	117
Figure 5.46 – Instrumentation for the span lock (Adapted from Christa McAuliffe Bridge construction plans).....	117
Figure 5.47 – Opening/closing of the leaf.....	118
Figure 5.48 – Main girders in open position.....	120
Figure 5.49 – Possible instrumentation for movable bridge structural components.....	121
Figure A.1 – A strain rosette .....	163
Figure A.2 – Signal conditioning .....	169
Figure A.3 – National Instruments system in the laboratory; (a) SCXI 1001 chassis, (b) PXI 1033 chassis .....	170
Figure A.5 – Microstrain data acquisition and transmitter .....	172
Figure B.1 – Test beam .....	173
Figure B.2 – Some tests performed on the test structure.....	174
Figure B.3 – Analysis results from the instrumented beam.....	174
Figure B.4 – Grid structure in the laboratory .....	175
Figure B.5 – Results of dynamic analysis and damage scenarios.....	175

Figure B.6 – General Methodology .....	177
Figure B.7 – Test setup.....	181
Figure B.8 – Example pictures showing different BC (a) The pin support for BC1 (b) Four Duro50 pads for BC2 (c) Five Duro70 pads for BC4.....	183
Figure B.9 – Time history data (a) Ambient data (b) Data after averaging with RD plotted with the data estimated with AR (c) A closer look at the figure in (b).....	184
Figure B.10 – Analysis results for BC1, BC2 and BC3 (a) Mahalanobis distance of the AR coefficients for BC1 and BC2 (b) Clustering of the AR coefficients for BC1 and BC2 (c) Mahalanobis distance of the AR coefficients for BC1 and BC3 (d) Clustering of the AR coefficients for BC1 and BC3 (each point in the figures is coming from one data block).....	186
Figure B.11 – Mahalanobis distance of the AR coefficients $f$ for BC1, BC3 and BC4 (each point in the figures is coming from one data block).....	187
Figure B.12 – The physical grid model and test setup.....	188
Figure B.13 – Damage scenarios applied to the steel grid.....	188
Figure B.14 – Determining the threshold value for the grid.....	189
Figure B.15 – Mahalanobis distance plots for scour case.....	190
Figure B.16 – Mahalanobis distance plots for restraint supports.....	190
Figure B.17 – Mahalanobis distance plots for reduced stiffness .....	191

# **1. INTRODUCTION**

## **1.1. STATEMENT OF THE PROBLEM**

Bridges constitute critical nodes of transportation systems, and therefore, ensuring their continuous operation is of utmost importance for safe and efficient transportation. Deterioration due to environmental effects and operational loading causes bridge performance to decline, and may even result in collapse. The U.S. requires periodic bridge inspections, which should then be reported to the Federal Highway Administration (FHWA) through the National Bridge Inventory Standards (NBIS). These inspections, however, are mainly based on subjective visual inspections, while a thorough understanding of the performance and behavior of a bridge requires extensive analysis, modeling and test results.

Load rating is another method used for decision making, traffic operations, load posting and issuing permits. Load rating of bridges as described by AASHTO Manual for Condition Evaluation and Load and Resistance Factor Rating (LRFR) of Highway Bridges (2003b) is employed for more in-depth bridge evaluation practices based on numerical models and available data on the specific bridge. Bridges may be rated according to this procedure for inventory rating if the safety is of concern, or for operating rating if a special load permit is requested. Load rating analysis is generally conducted using simplified software such as BAR7 (PennDOT 2001). Using more accurate analytical model and assumptions in the load rating calculation will result in more dependable evaluation results (Catbas et al. 2005).

Highly developed analysis techniques, such as linear and nonlinear finite element modeling, can be used to simulate the structural response. Complex boundary conditions, material behavior, interactions between substructural components, and time-dependent effects have to be estimated through certain assumptions, which hinder the reliability of the model. In case of a complex, irregular, or extraordinary structure, destructive or nondestructive tests may be necessary to calculate the actual capacity, or required parameters, or to calibrate/validate the model. Destructive load tests, while precise,

cannot be carried out for in-service evaluation of structures. Therefore, condition assessment must be based on data obtained through non-destructive testing methods.

A Structural Health Monitoring (SHM) application is an integrated system formed by the collection of efforts aiming to advance decision-making. SHM can use continuous or intermittent structural monitoring via sensors. Key parameters are determined by employing analysis techniques to indicate the condition and performance of the bridge. The sophistication of SHM differs widely according to the needs and characteristics of each application. Currently, SHM is used primarily for major bridges, demonstration studies or bridges showing signs of critical distress. However, FHWA has been developing and coordinating the new Long Term Bridge Performance (LTBP) program for the implementation of SHM in a more effective manner and eventually for the development of guidelines.

While new technologies within the context of SHM exist, there is a strong need for defining an integrated approach to link data collection, evaluation techniques and efficient data management. There also needs to be a unified approach with guidelines and standards to provide consistency in bridge data collection and evaluation, so that objective comparisons for decision-making can be conducted. This is possible through an integrated SHM approach.

### **1.1.1. Background of Bridge Inspections and Evaluations**

Visual inspection is the traditional method for damage detections. However, this method has some inherent drawbacks, the first of which is the damage must have progressed far enough to be visually observable. Second, visual inspection is inherently subjective not just for identifying the implication of damage but also in the detection of damage. A study conducted by the Federal Highway Administration's NDE Center on the accuracy of visual inspection of short-to-medium span bridges concluded that at least 56% of the bridges given an average condition rating were done incorrectly (Turner-Fairbank Research Center 2005). Even if the damage is successfully identified, the final problem facing the engineer is accurately assessing its effect on the overall "health" of

the structure (Aktan et al. 2001b). Visual inspection also requires much time and effort, and may overlook locations of limited and/or no accessibility.

For extended structures, such as long-span suspension bridges, the difficulty is further compounded. Successful visual inspection of these structures is dependent on inspecting all possible damage scenarios at all critical locations, not an easily accomplished task even for an experienced inspector (Aktan et al. 2001a). Despite all these limitations, visual inspection remains today the most commonly practiced damage detection method.

### **1.1.2. New Technologies for Objective Bridge Assessment, Evaluation and Maintenance**

The state-of-the-art in SHM allows for advanced techniques with sensing devices and analysis methods to be used to capture and quantify parameters of concern. These technologies show great promise for complementing and improving current inspection techniques. However, these novel methods also introduce various challenges to the bridge engineer, such as evaluation of large amounts of data in a timely manner. Without proper guidance and established standards, jobs such as sensory systems application, data collection and analysis could prove to be a burden for the bridge engineer.

The growing availability of sensors and sensing technologies is making it even easier to implement instrumentation applications on as large a scale as needed. Therefore, the main challenge is not collecting data, but making sense of it. A successful SHM needs evaluation of data into useful information in a timely manner.

## **1.2. STRUCTURAL HEALTH MONITORING AS A PROMISING APPROACH**

### **1.2.1. Definition**

Structural Health Monitoring, or SHM, is defined as the measurement of operating and loading environments and critical responses of a system to track and evaluate incidents, anomalies, damage and deterioration. With a proper design, SHM is expected to advance bridge evaluation and management approach through

instrumentation, sensing, data processing, use of analytical methods, data evaluation algorithms and data management techniques, at the project level as well as the network level. SHM utilizes advanced technology to capture the critical inputs and responses of a structural system with various types of sensors and analysis methods as part of the health monitoring framework to understand the root causes of the problem as well as to track responses to predict future behavior.

### **1.2.2. Components of a Complete SHM**

A complete SHM application is created by many interacting components, which may be added or subtracted according to the specific needs of each application, but the main categories may be broadly summarized as follows (Catbas et al. 2004);

Experimental Components: Include the selection of sensory devices, instrumentation locations, measurement types, and tests, such as static, dynamic or localized non-destructive testing. General categories can be listed as geometry monitoring, controlled testing (which may be static or dynamic, nondestructive or destructive) and continuous monitoring. Acquiring data from the sensor devices, signal conditioning, and transferring the data to main terminals is part of the data acquisition component. Data acquisition systems provide the excitation, initial filtering, collection and analog-to-digital conversion of the signals as well as storage in the appropriate format.

Analytical Components: Composed of all analysis tools necessary for extracting the required information from the data. Analytical components may be drafting, modeling and structural analysis techniques along with the instrumentation, as well as data processing and algorithms such as statistical pattern recognition or parameter identification. Without proper analysis techniques, we cannot expect to generate useful information from acquired sensor data.

Information Technology: Represents all the methods and framework through which the information is stored, managed and shared. A successful IT application also provides access to the information through visualization and user interfaces. This is a key

component of SHM applications by providing the backbone and their design vary widely according to the requirements of the application.

### **1.2.3. Promises of SHM**

With recent rapid developments in electronics and communications, sensor technologies have developed such that costs are reduced, accuracies are improved and novel approaches such as wireless sensing, fiber-optic sensors, MEMS (microelectromechanics) sensors, distributed networking and internet-based data acquisition are introduced. Now it is more feasible to acquire data about the status of structural responses, such as strain, displacement, vibration, and environmental effects, such as wind speed, temperature and earthquake excitation. For an effective implementation, it is important to integrate novel experimental technologies, analytical methods and information technologies for determining the structural condition. SHM offers accurate information and detection of distress that visual inspections cannot reveal. SHM can be employed for obtaining global and local structural parameters, data for structural identification (geometric/ FE model calibration), effective maintenance and operation. It can also be used for improving future designs. Diagnosing pre- & post-hazard conditions for emergency management can also be facilitated by SHM.

### **1.3. PROJECT OBJECTIVES AND GOALS**

The ultimate objective of the project is to develop an SHM framework for integrative information system design to enable FDOT to improve practices and provide the best possible transportation infrastructure by taking advantage of new technological advances. In order to develop an integration information system, three groups within FDOT (structures, maintenance, operations) were identified that would have similar data needs and could provide feedback and guidance. A kick-off meeting with structures, maintenance and operations engineers was held in Tallahassee. Based on the valuable feedback that was received during the kick-off meeting and other subsequent meetings and communications, the initial scope of the project was revised approximately six months after the start. New objectives include:

- Managing data effectively and efficiently. Development of policies and approaches for consistent structural health monitoring applications within the organizations for mitigation of possible problems inconsistencies for data collection, sharing and data comparing within each FDOT district.
- Identifying critical features that need to be monitored for safety, maintenance and operation. Development of monitoring strategies based on statistical information extracted from the data and engineering heuristics.
- Organizing the most critical and desirable data and information. It is known that statistical tools could be made available to approximate the current condition, provided that the data is well organized. Efficient storage, organization and availability of the data would make it possible to plan ahead.
- Demonstrating the ideas and concepts of this study by integrating data and information for the movable bridges.

As a result, the main goal of the current project is to develop an SHM framework that will serve the different users of FDOT for bridge management and operations within an Integrative Information System context. The first goal of the project is: To identify the challenges and inefficiencies in bridge monitoring, data management and information control procedures to improve and supplement current bridge management methods by establishing a general SHM framework that can be employed by different districts and offices. Another major goal will be to provide guidelines, standards and a demonstration study for future applications that can be carried in a more uniform manner with all critical components of SHM taken into consideration. The project focuses on exploring the use of advanced information technology demonstrations for movable bridges as a case study.

#### **1.4. PROJECT TASKS**

##### **1.4.1. Characterization of Available Data and User Needs**

- Characterize interacting systems with all the critical parameters affecting component and individual system performances.
- Characterize data needs, existing data, information and knowledge available in the existing FDOT databases. Communicate with FDOT engineers on the preliminary

design of the integrated system for legacy as well as new and objective field data to be collected. Collect and analyze FDOT's existing data and information assets, which exist in a variety of databases and in hard-copy formats, with the specific focus on the movable bridges.

- Identify and collect data/information such as the inspection and maintenance reports, analytical and experimental data for existing condition evaluation and load rating reports by closely working with structures, maintenance and operations engineers.

#### **1.4.2. Development of Monitoring Strategies**

- Investigate and identify the critical features that need to be monitored for safety, maintenance and operation to enable successful development of monitoring strategies based on statistical information extracted from the data and engineering heuristics.
- Investigate and define the sensing and data acquisition and other related hardware for possible standardized structural health monitoring practices.
- Conduct benchmark tests and evaluation studies in the laboratory in order to exemplify the application of the structural health monitoring hardware components.

#### **1.4.3. Design, Implement and Demonstrate the Integrated Framework**

- Design, implement and demonstrate a framework that will use the state-of-the-art approaches for collecting and analyzing data to generate valuable and useable information and knowledge for decision making. The system will include data and information for the selected movable bridges. Possible monitoring designs will be developed in such a way that the most critical and desirable data and information about movable bridges can be generated, analyzed timely and utilized to help decision making for maintenance, structural repairs and operations. In addition, the PI and his students will investigate the use of statistical tools that can be embedded in the integrated SHM framework to approximate the current condition. Efficient storage, organization and easy and timely availability of the data are important issues for a complete SHM framework.

## **2. CHARACTERIZATION AND ASSESSMENT OF BRIDGES**

### **2.1. INTRODUCTION**

In order to address the issues related to decision making for bridge management and accomplish the project tasks, it is important to review the current condition of bridges and bridge management practice in the nation and in Florida. First, the current approach for bridge inspection and decision-making process was investigated. Then the movable bridge population was evaluated with this understanding. General characteristics of the movable bridges in terms of the main parameters such as geometry, type and condition were analyzed and summarized.

### **2.2. CURRENT BRIDGE INSPECTION AND MANAGEMENT PROCEDURE**

#### **2.2.1. Bridge Inspection Program**

The National Bridge Inspection Standards (NBIS) applies to all structures defined as bridges located on all public roads. In accordance with the AASHTO (American Association of State Highway and Transportation Officials) Transportation Glossary, a “bridge” is defined as a structure including supports erected over a depression or an obstruction, such as water, highway, or railway, and having a track or passageway for carrying traffic or other moving loads, and having an opening measured along the center of the roadway of more than 6.1 m (20 feet). These openings are between undercopings of abutments or spring lines of arches, or extreme ends of openings for multiple boxes. A bridge may also include multiple pipes, where the clear distance between openings is less than half of the smaller contiguous opening.

NBIS regulates that each highway department shall include a bridge inspection organization capable of performing inspections, preparing reports, and determining ratings in accordance with the Manual for Condition Evaluation of Bridges (AASHTO 2003a). Inspection records and bridge inventories are to be prepared and maintained.

According to NBIS, location, description, inspection frequency and procedures for fracture critical members (members of a bridge whose failure will probably cause a

portion of or the entire bridge to collapse), underwater members and special features are to be listed for each bridge, with their previous inspection dates. Each bridge is to be inspected at regular intervals not to exceed two years, or less depending on such factors as age, traffic characteristics, state of maintenance, and known deficiencies. The inspections are conducted by a team of qualified personnel. In order to qualify as an inspector, professional engineer registration or a minimum 10 years of experience in bridge inspection assignments is needed together with the completion of the comprehensive training course (AASHTO 1983).

### **2.2.2. Bridge Inspections in Florida**

The findings and results of bridge inspection are recorded on standard forms. These inspection reports have to be kept by the state DOTs and reported to the FHWA in required formats. For many states, including Florida, inspection data are stored and used by means of software such as PONTIS or BRIDGIT. Each state prepares and maintains an inventory of all bridge structures. Inventory and appraisal data must be collected and retained within the various departments of the state organization for collection by the Federal Highway Administration as needed. A tabulation of this data is contained in the structure inventory and appraisal sheet distributed by the Federal Highway Administration (FHWA 1995).

Florida Department of Transportation (FDOT) inspectors must be either state-licensed professional engineers or they must complete the National Highway Institute course in bridge inspection and meet FDOT's experience requirements (FHWA 2003). FDOT's development program classifies the inspectors' recommendations into three categories:

- Routine maintenance
- Periodic maintenance and repair
- Replacements

Once the inspectors' recommendations are sorted into the three categories above, the next step is to create work orders. Work orders are given priority ratings from 1 to 4,

priority 1 being an emergency situation requiring work to be completed within 60 days; priority 2, an urgent situation with a 180-day limitation; priority 3, routine work to be done within 1 year; and priority 4, no immediate deadline but information is provided. All work orders are scheduled and performed by the districts or by an independent asset management contractor (FHWA 2005).

FDOT has implemented PONTIS, a Bridge Management System, to provide decision support to engineers in the headquarters and district offices as they make routine policy, programming, and budgeting decisions regarding the preservation and improvement of the state's bridges. A Feasible Action Review Committee (FARC) in each district office is responsible for reviewing and prioritizing the needs identified by the inspectors. FARC uses the Project-Level Analysis Tool (PLAT), an integrated software customized for FDOT. PLAT is a project-level decision support framework that complements and builds on PONTIS' existing network-level analysis. Specific models include:

- Accident risk and user cost due to roadway width and alignment deficiencies
- User cost of load capacity, vertical clearance restrictions, and movable bridge openings
- Project-level prediction models for bridge element conditions and costs
- Prediction of economics of scale and scoping possibilities.

These new PLAT models are displayed graphically in a spreadsheet format as an aid in decision making. Engineers use PLAT to determine the economic health of a structure, and they use it as a design tool for candidate projects to program into the management process. When the engineer modifies a candidate by changing the element action selections, quantities, or various cost factors, PLAT responds, immediately updating its predictive results. This new project-level decision support framework complements and builds on the existing network-level analysis in PONTIS. Florida is one of the few States integrating PONTIS to do network-level analysis applications (Thompson et al. 2003; FHWA 2005).

## **2.3. ISSUES FOR TODAY'S BRIDGE MANAGEMENT PRACTICE**

### **2.3.1. Uncertainties in Condition Evaluation**

The ability to monitor the condition of a bridge structure to capture the structural parameters or changes in condition is of significant interest to many bridge owners. Traditionally, visual inspections have been used. Inspectors follow a scheduled plan, every two years in most cases, to identify which bridges need preventative maintenance, minor or major repair work, or replacement. A bridge that meets the standards is defined as not showing evidence of structural deterioration, not being limited by weight restrictions or not needing preventative maintenance. One big problem with this subjective approach is that if damage occurs gradually, it may not be observed by inspectors. If access to some parts is difficult, observations are done from a distance and are not always accurate. Shortcomings of visual inspections are well-documented in a study by FHWA Turner-Fairbank Research Center (Turner-Fairbank 2005). Unless great damage is present, no inspection will be done outside of the scheduled plan. Even if the damage is successfully identified, the final problem facing the engineer is accurately assessing its effect on the overall health of the structure (Aktan et al. 2001b).

Obviously, the major issue is not obtaining measurements, but rather how to process, analyze and convert the data into useful information about the condition and performance of the bridges. In addition, it is important to provide the bridge owners with the future performance predictions for decision making such as condition-based maintenance scheduling.

### **2.3.2. Asset Management**

The task of maintaining a large bridge population in good condition requires considerable effort and budget. In addition to that, the fact that the bridge population is aging means ever-increasing costs for maintenance. State departments of transportation and districts allocate a certain proportion of their total budget to preservation. The available maintenance budget should be allocated to routine maintenance and retrofitting a portion of bridges showing deficiency. To determine funding priorities, network-level

analysis needs to be carried out. The analysis should consider the total cost-benefit trade-off, which requires both detailed structural condition analysis and condition predictions for alternative actions. Decisions based merely on condition ratings and simplified structural analyses with high uncertainty would not be efficient. Objective assessment of the condition using new, cost-effective technologies and condition-based maintenance is becoming crucial.

### **2.3.3. Information Control**

The information generated by districts are used by FDOT Headquarters for maintenance, repair prioritization and resource allocation. Information obtained by different offices in the DOT and districts over different counties can be incompatible, due to insufficient standardization of data collection and management. Bridge inspection and maintenance data are kept with PONTIS software, commonly adopted in Florida. However, this information is localized and each district manages its own inspection results. Since ownership and responsibility of data collection and collected data are the responsibility of independent districts, that may result in inconsistencies and inefficiencies in managing the data by FDOT headquarters.

Information management is the key for efficient transportation asset management. Information related to condition and operation of highway bridges are required by numerous branches of state departments of transportation. For example, bridge performance information is to be used by the maintenance office for monitoring the performance and planning repair and rehabilitation operations. The structural design office needs the same information to derive and validate data for modeling and analysis. The division associated with traffic operations needs certain data related with bridge usage, which is also of concern for structures and maintenance groups. Lack of communication and information exchange between these offices may be a major problem causing collection of duplicate data or delays. Similarly, an SHM design should also recognize these challenges and provide a standardized platform for applications by various users.

## **2.4. CHARACTERIZATION OF MOVABLE BRIDGES AS DEMONSTRATION EXAMPLE**

### **2.4.1. Why Movable Bridges Selected as a Focus**

The Florida Department of Transportation (FDOT) bridge inventory includes a large number of movable bridges. For the current research project, the movable bridges were chosen due largely based upon the following distinctions:

- High maintenance cost of movable bridges (the average maintenance cost is about 100 times that of fixed bridges per square ft)
- Frequency of breakdowns due to the high number of movable parts
- Malfunctions cause not only problems in land traffic, but also marine traffic
- Difficulties in determining the root cause(s) of breakdown and predicting future breakdowns

As a result, FDOT engineers indicated that the movable bridges would provide a better demonstration case, while improvements through the conducted study will have more significant benefits.

### **2.4.2. Movable Bridges**

#### ***2.4.2.1 Definition of a Movable Bridge***

A movable bridge is a structure which has movable components operated by various types of machinery to open the passageway for maritime traffic. Movable bridges are employed when the vertical clearance of the bridge carrying the roadway/pedestrian way over a river, canal or any water body is not sufficient for the vessels traveling over the waterway. A movable bridge is a viable alternative to a high fixed bridge over the waterway, however, they also contain significant drawbacks and problems, which are to be mentioned specifically in the following sections. In certain cases, where aesthetics and dimensional constraints dominate the design, movable bridges constitute the only choice.

### 2.4.2.2 Movable Bridge Terminology

Although highly variable in type, configuration and geometry, common terminology and features for movable bridges are shown given in Figure 2.1. Movable bridges have approach spans, movable spans, operator room, machinery room, traffic gates and span locks. Typically, they are over a channel or a similar waterway. Fenders are often installed to protect the piers.

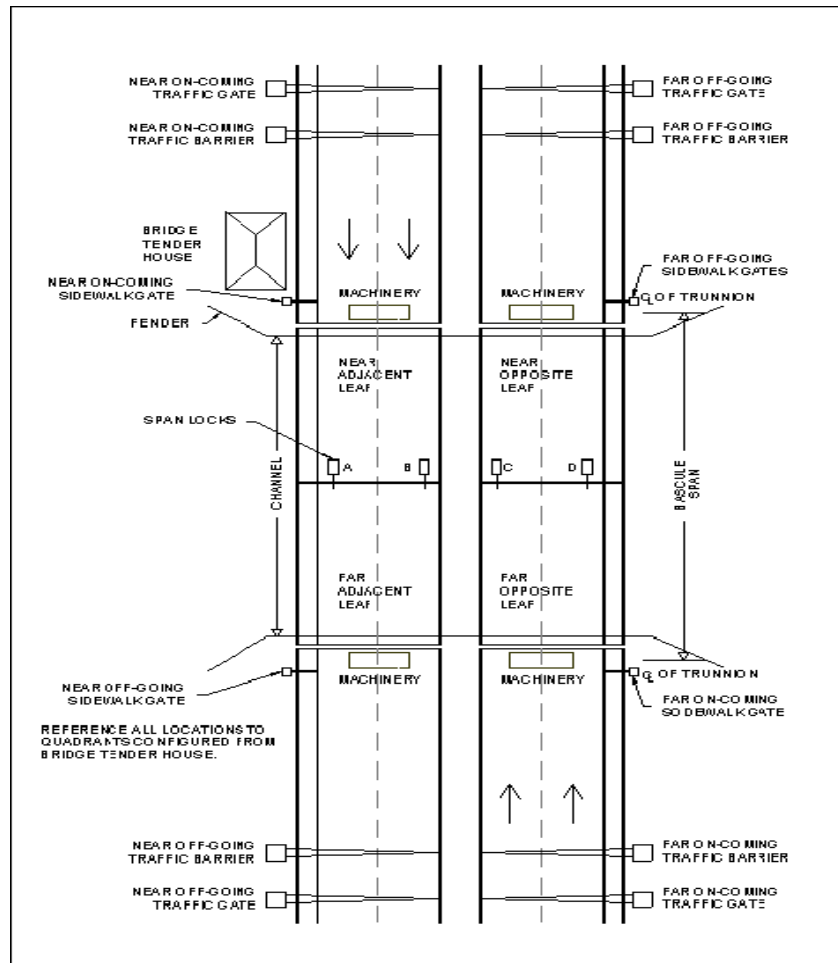


Figure 2.1 – Movable bridge terminology (FDOT 2004)

Although this schematic is for the most common type, there are several kinds of movable bridges. Three main types are shown in Figure 2.2, which are to be explained in detail in the following section.

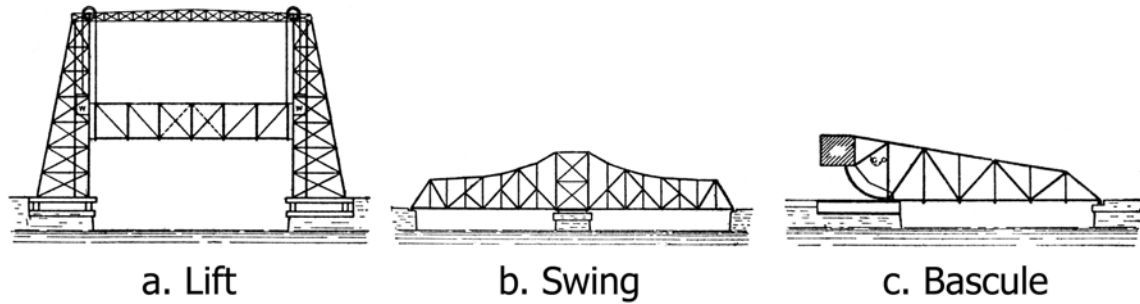


Figure 2.2 – Main types of movable bridges (Koglin 2003)

### 2.4.2.3 Types of Movable Bridges

#### Lift Type Bridge

Vertical lift bridges use cables, pulleys, motors and counterweights to raise a section of the bridge vertically. The classical lifting bridge is used in urban areas with scarce space for bridging inland waterways. Overhead clearance for navigation is limited, however, these bridges have the advantage over bascule bridges in that they can be made of any length feasible for a simple span. Disadvantages are a high initial cost and expensive operation (Buxton-Tetteh 2004). The temporary lift bridge shown in Figure 2.3 is a typical example for lift type movable bridges.



Figure 2.3 – Temporary bridge adjacent to the Bridge of Lions in open position (St. Augustine, FL)

## Swing Type Bridges

Swing bridges rotate their spans on a pedestal, allowing vessels to move past on either side. The swing bridge over the Caloosahatchee River, Florida (Figure 2.4) is an example of a pedestal type swing bridge. Swing bridges do not move vertically, therefore, operation is easier. However, the pedestal is usually located in the middle of the channel, creating a navigation hazard.



Figure 2.4 – Fort Denaud Swing Bridge, Florida

## Bascule Type Bridges

A bascule bridge is a drawbridge with a counterweight that continuously balances the span, or "leaf", throughout the entire upward swing in providing clearance for boat traffic.

Bascule bridges have interior spans called "leaves" that rotate upward and away from the centerline of the river, providing clear passage for river traffic. Unlike the vertical lift bridges, when opened, there is no vertical obstacle to river traffic. They rotate about trunnions or roll back on circular segments, or have a combined motion of turning

and rolling, and are counterweighted to reduce the power required for operation. There are motors that turn the reduction gears connected to shafts and gears. These gears are connected to rack assemblies, which are mounted on the counterweights. Bascule bridges are made in one leaf, or in two leaves that meet in the center. The two-leaf bridges have a locking device at the ends, and are arranged to act as cantilevers when closed, and sometimes as three-hinged arches. The span locks keep the ends of the leaves from bouncing as traffic passes over them.

Bascule bridges with one leaf or symmetrical bascule bridges with two leaves have an opening angle of up to  $85^\circ$  to create optimum clearance for navigation without upper limitation. In case of navigation channels near the coast which are also used by large deep-sea vessels bascule bridges are particularly appropriate because they offer unlimited overhead clearance and their large spans are able to cope with wide shipping channels. In urban areas with scarcity of space and no possibility of high access for cross traffic, bascule bridges offer a solution for the "crossing" of road and waterborne traffic (Koglin 2003).

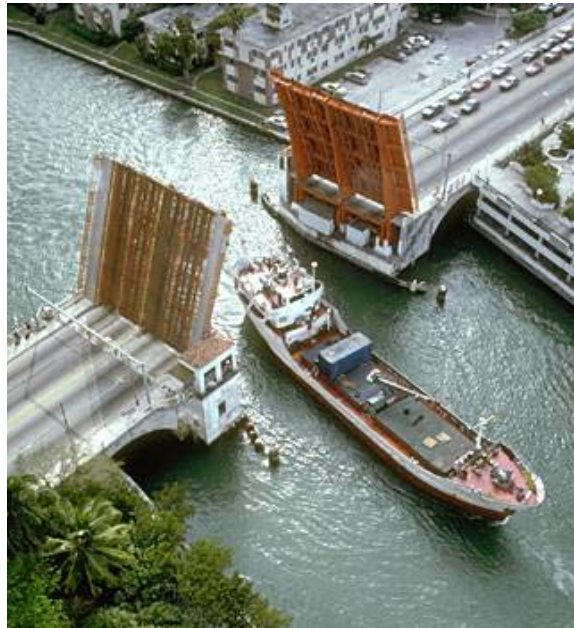


Figure 2.5 – A bascule bridge on the Miami River in Florida is open to let a ship pass (Buxton-Tetteh 2004)

#### ***2.4.2.4 Movable Bridge Inspections***

Movable bridges are subject to regular NBI inspections, as well as underwater inspections. Regular inspections have been expanded to cover mechanical, electrical and other special components, which are also rated according to similar guides. Inspection procedures for some movable bridge elements are summarized as example.

Open gearings: Alignment and wear of open gearings are inspected. Grease patterns are checked for signs of misalignment and tooth surface is inspected for deterioration and cracks. If present, proper alignment of pitch-lines is checked.

Enclosed gearings: Alignment and wear is also a major concern for enclosed gearings. The gearing is visually inspected through inspection ports, reducer supports are examined for cracks or deterioration, bolting is checked for tightness. Also checked are the oil level, leaks on the box and seals. Operating sounds are checked for abnormal noises. Oil sample is taken from bottom of box for chemical analysis.

Bearings: There are different inspection procedures for different types of bearings. For sleeve bearings, cracks, damage or deterioration are inspected. Anti-Friction bearing is a ball or roller-type bearing; a bearing that does not resist horizontal or frictional loads. This kind of bearing is inspected for cracks, damage or deterioration. Bolts should be checked for tightness. Rollers and racers are inspected visually by opening the housing and checking for internal contamination. For trunnion bearings, cracks, damage or deterioration is inspected. In addition, grease is examined for contamination. For all types of bearings, bolts are checked for tightness, and any unusual noise, movement or excessive heat is noted during operation. While pumping lubricant into bearings, it is checked whether the lubricant is exiting the bearing properly and expelled lubricant is inspected for signs of contamination.

Shafts and couplings: The force transfer mechanism that carry the torque produced by the motor or the hydraulic drive to the gears is provided by shafts and couplings. Keyways and shoulders are possible locations to observe cracks. Corrosion is checked over the shafts and couplings. On the couplings, tightness of flange bolts are

tried and proper lubrication and leakage is checked. Then, machinery is operated to observe shafts and couplings for excessive movements, vibration or noise while operating. The coupling should be a tight fit on the shaft.

Cylinders: Exterior housing of buffer cylinders is checked for deterioration. Mounting bolts are examined and the piston is observed for full movement during operation. Presence of air leakage is inspected by listening.

Live load shoes: Mounting bolts of live load bearings are checked for tightness. Bolts and shims are examined for deterioration, contact surfaces are inspected for wear. Also, under live load, there should be full continuous contact between the sole and bearing plates.

Span locks: Span locks are also inspected in detail. Common types of span locks include fixed center locks, mechanical center locks, rear locks and end locks. First, the span locks are checked for proper lubrication, cracks or damage and then for movement under traffic. Mounting bolts are examined for tightness. Fixed center locks are checked for uneven or excessive wear. Proper alignment and operation should be ensured for mechanical center locks. Also, lock bars and receivers are checked for excessive wear.

Castings: Alignment and wear for segmental and track castings are inspected by checking tread surfaces which should be clean and free of lubricant and debris, and free of excessive wear. Surfaces of alignment lugs are examined for excessive wear or cracks. Mounting bolts are checked for tightness, keyways are checked for cracks and, during operation, unusual noise or movement is recorded.

Mechanical and electrical systems of movable bridges are inspected and maintained continuously, since it is essential to keep all the components in optimum condition to prevent breakdowns. Maintenance of movable bridges in Florida is usually contracted to private companies, which conduct and supervise day-to-day checks and maintenance.

### 2.4.3. Status of Movable Bridge Population in Florida

Florida is divided into seven geographic districts and one Turnpike district, as shown in Figure 2.6. Each district is responsible for element-level inspections of Florida's 11,100 bridges (6,300 State highway bridges and 4,800 local bridges). FDOT's inventory of 98 movable bridges includes 3 lift type, 94 bascule type, and 1 swing-type bridge. To maintain, manage, and evaluate the needs of the State's bridge inventory, five personnel in the state maintenance office and two programming personnel coordinate with the districts, the work program office, and the offices of planning and engineering support services.

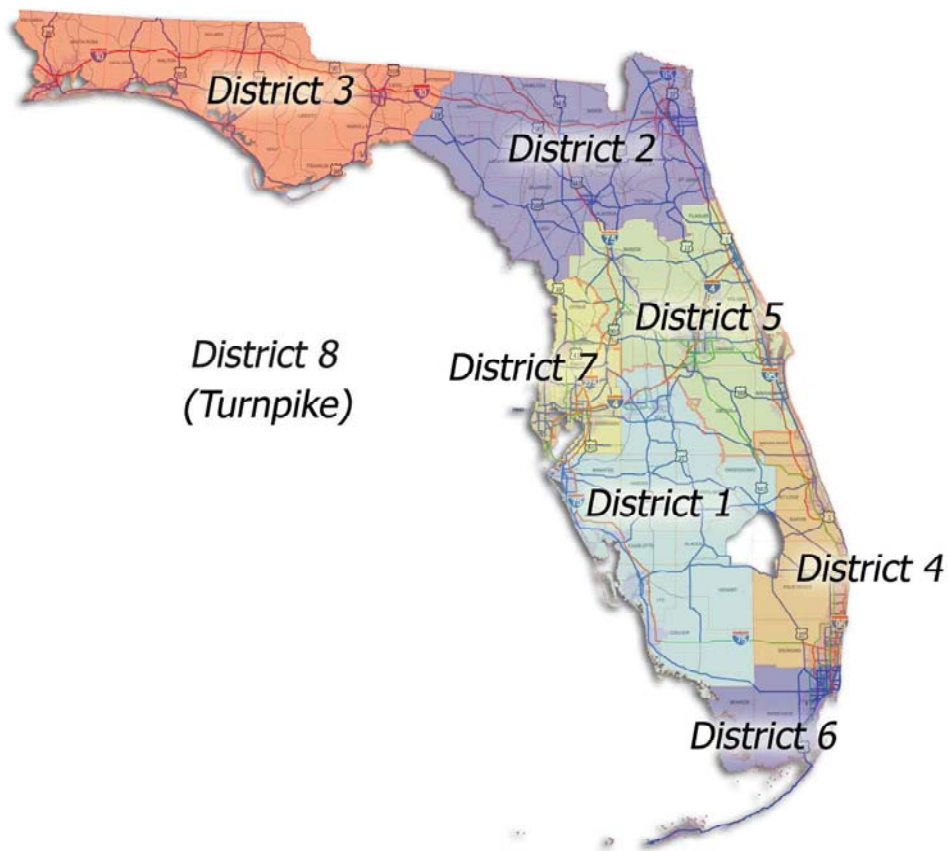


Figure 2.6 – Florida DOT district map

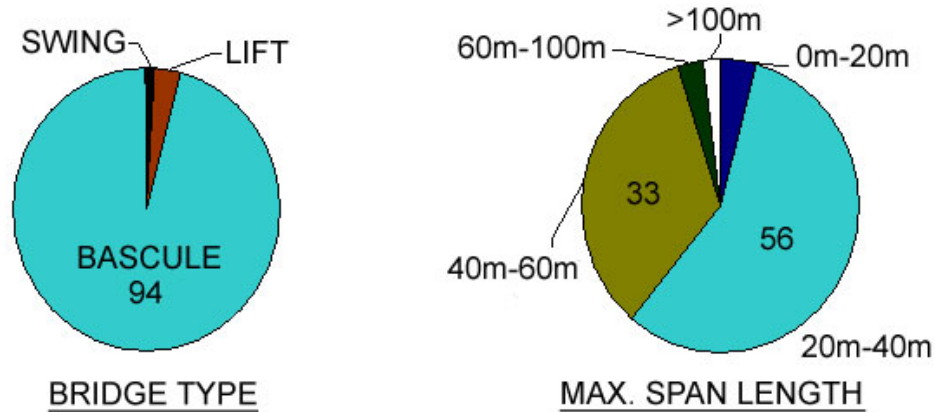


Figure 2.7 – Distribution of FDOT movable bridges

The majority of the movable bridges in Florida state system have main spans between 20m and 40m (~65 to 135ft), and those with less than 20m (~65ft) or more than 60m(~200ft) are very rare. The average span length is about 37m (121ft). Almost half of this bridge population is 40 to 50 years old, with the average of 42.5 years. Distribution of the movable bridges with respect to span length and year built are shown in Figures 2.8 and 2.9 respectively.

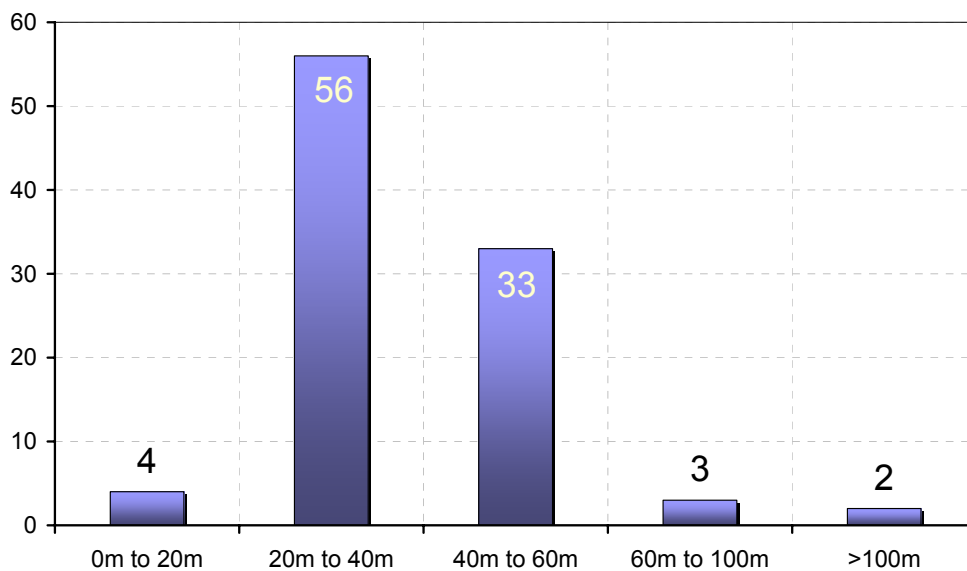


Figure 2.8 – Distribution of FDOT movable bridges according to length of maximum span (NBI 2002)

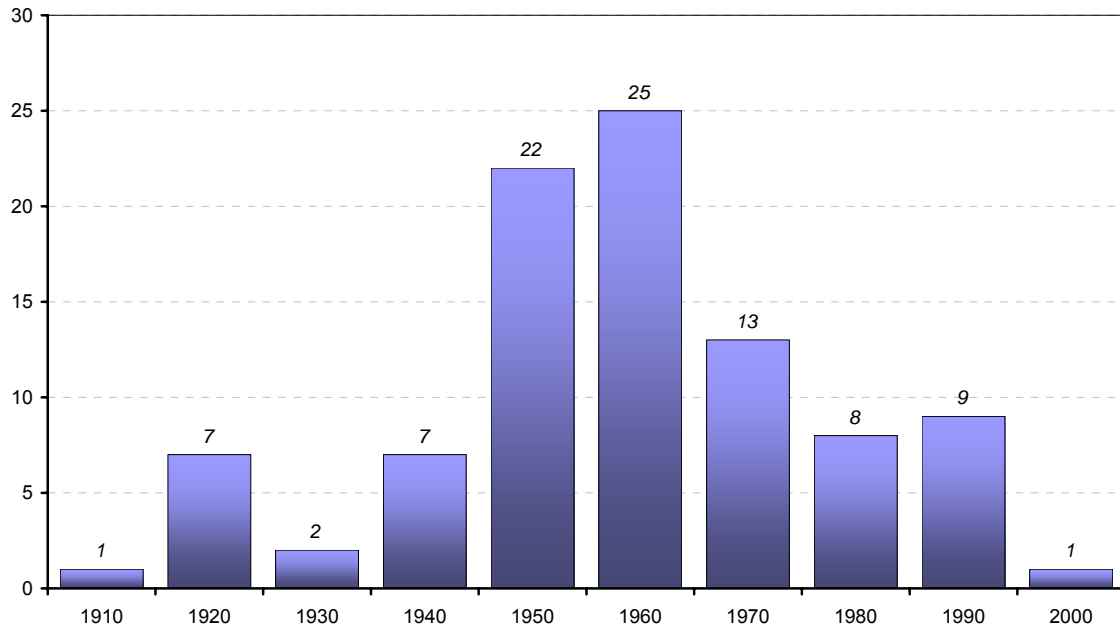


Figure 2.9 – Distribution of movable bridges according to year built (NBI 2002)

## 2.4.4. Compilation of Data from Maintenance Offices

### 2.4.4.1 Most Common Issues According to Maintenance Data and Expert Opinions

The researchers conducted visits to Districts 4 and 5 to interview the engineers about movable bridges. Some of the key points are as follows:

#### **Rapid Deterioration**

Movable bridges are subject to harsh conditions since they are located over waterways, and often close to the coast, which constitute conditions suitable for corrosion, causing section losses as shown in Figure 2.10 and that hurricane wind forces are more significant closer to the coastal regions. Another important reason for the rapid deterioration observed in movable bridges is that movements cause friction and wear of the structural and mechanical components. Fatigue can be a problem due to the reversal or the fluctuation of stresses as the spans open and close. Any member or connection subject to such stress variations should be carefully inspected for fatigue failure (FHWA Report 2002). Even with regular maintenance is provided, continuous downgrading of all parts of such complex bridges is inevitable.



Figure 2.10 – Deterioration effects of corrosion on Michigan Street Bridge, Sturgeon Bay, Wisconsin  
(Prine and Fish 1996)

### **Frequent and Unexpected Breakdowns**

Unexpected breakdowns are reported to occur on average 2 to 3 times a month. Malfunctions are usually results of electrical problems. Limit switches that regulate the operation sequence of the bridge are among the most vulnerable components. There may be more than thirty limit switches on a movable bridge, and failure of any one of these causes the operation to halt. The case is similar for other electrical components, too, such as cables, fuses, or junction boxes, since they are exposed to harsh environmental conditions, and frequent use.

Another major reason for breakdown is the mechanical system of the bridge, including the drive motor, shafts, gears, racks, pinions and the trunnions. The drive motor components and the gears need continuous maintenance, lubrication and checking. Still, the movable parts deteriorate very quickly due to fatigue and wear, and fail unexpectedly.

One of the most problematic and equally critical components is the span lock and its drive system. This linking bar locks the opposite leaves of double-bascule spans, providing a safer load distribution and preventing excessive deflections and vibrations. For opening the leaves, the locking bar needs to be withdrawn, triggering the associated

limit switch for clearance. Due to frequent operation and fatiguing live load, these critical parts tend to malfunction often, usually losing proper alignment, or even breaking or severing. All mechanical components are subject to corrosion, due to high humidity and extreme conditions at the site.

Also, movable bridges constantly suffer the wearing effect of opening/closing operations. All movable parts, as well as the relatively slender structural members, are subject to fatigue stresses produced by these effects, in addition to live load and wind forces. Hurricane events also create a significant hazard to these structures, causing failure due to heavy wind loading, or indirectly, such as a vessel hit (Figure 2.11).



Figure 2.11 – Damage to bridge to Sullivans Island, Charleston after hurricane Hugo, 1991  
Source: NOAA Photo Library (<http://www.photolib.noaa.gov/historic/nws/wea00469.htm>)

### **High Maintenance Cost**

Unit maintenance cost for a movable bridge is approximately 100 times higher than that of a fixed bridge. The high cost is associated with the complex operation system and mechanical parts requiring special expertise, and with rapid deterioration causing more extensive repair works. Almost all parts need to be frequently checked and maintained. On-site maintenance is usually performed by private contractors, who

employ up to two personnel overseeing the proper performance of the bridge. Unlike fixed bridges, deterioration of movable bridges is quite rapid; therefore, major maintenance is required with much higher frequency. As mentioned earlier, although the number of movable bridges makes up a very small fraction of the total number of bridges, the cost of these major maintenance tasks usually constitute a large portion of the total maintenance budget. Repair time is a major constraint, in case of unexpected failures, which increases the cost.

### **Difficulty of Repair Works**

A minor or major malfunction of any component can cause an unexpected failure of bridge operation. In such a case, the bridge operator reports to the maintenance and repair personnel, who drive to the site, investigate and determine the cause of breakdown, and head back to collect the necessary equipment for the repair work. Locating the sources of electrical problems take longer, while mechanical issues are generally more difficult to fix. The repair tasks proceed around the clock, because the malfunction of the bridge would disrupt the traffic, blocking either or both transportation routes. Considerable time is spent initially due to not knowing the cause of the failure. Also, due to the complex mechanisms of the movable system, repairs works are difficult and costly.

### **3. MONITORING DEVELOPMENT STAGES**

#### **3.1. INTRODUCTION**

This chapter summarizes the methodology followed for obtaining and processing the necessary information for identifying, quantifying and documenting the existing condition of bridges. Our research team used a variety of sources such as inspection reports, construction plans, opinions and suggestions of FDOT engineers, site visits to various bridges and data from field tests. In addition, numerical models such as FE models, have to be employed to develop an effective monitoring system. Our research team developed a numerical model for characterization of the structural behavior. The data collected and processed as described in this chapter formed the foundation of the studies conducted to characterize the bridges and develop an instrumentation scheme.

#### **3.2. SITE VISITS AND MEETINGS WITH FDOT ENGINEERS – USER NEEDS**

One of the major sources of information for the project was interaction and meetings with FDOT staff in the district offices and headquarters. In addition to recommendations from FDOT engineers, several site visits to selected movable bridges were conducted. During the site visits, information about the bridges were collected, pictures of critical areas were taken, routine maintenance and tests conducted by FDOT personnel were observed and recorded.

The kick-off meeting for the project in Tallahassee helped shape the initial directions for the research by defining the scope as the information generation and use for movable bridge problems and maintenance issues. Other general problems such as information management and sharing, compatibility of data, communication between offices, different districts, and lack of standards in advanced assessment techniques were also discussed. This meeting provided input from a broad perspective of FDOT, from Marc Ansley, Richard Kerr, John Harris, Elizabeth Birriel and Richard Long. Many attendees also addressed the issue of making use of collected data efficiently and effectively.

Another meeting was conducted in the FDOT Laboratories in Tallahassee, for briefing on the progress in the project and discussion on the direction of the studies and expected outcomes. Project tasks were revisited and discussed to further clarify the details and the desired deliverables.

FDOT District 5 facilities engineers provided valuable guidance in two meetings at their district headquarters in DeLand. District 5 (responsible for the Central Florida region including Orlando, Daytona Beach and vicinity) supplied inspection reports for all their movable bridges and opinions from maintenance engineers, as well as maintenance contractors, regarding the most common and critical issues with movable bridges. District 5 engineers confirmed that the movable bridges are the most problematic type of structures in the bridge population. It was also expressed that an automated condition evaluation system would be invaluable during extreme natural occurrences, reflecting their experience from recent hurricanes affecting a large population of bridges over a wide area.

FDOT Materials Laboratory in Gainesville was visited to note the tests and methods dealing with corrosion on bridge structural elements. Corrosion was already pointed out as one of the most critical factors that cause rapid deterioration of movable bridges. Related information was exchanged with FDOT Materials Laboratory engineers, who hosted the research group and introduced the laboratory.

Site visits were conducted to movable bridges in District 5 in order to aid the tasks of model development and analysis of available inspection/maintenance data. The researchers were more familiarized with movable bridge structure and operation with different types of mechanical systems. We visited the Christa McAuliffe Bridge in Merritt Island with the Balance Testing team from FDOT Gainesville Laboratory to observe and collect data from a routine balance test. Movable bridge specialists briefed the researchers on the balance test background and procedure. The balance testing team provided additional information with their expertise on movable bridges, and copied the collected data to the researchers after the test. Documentation on the test procedures was also received.

In another meeting at the FDOT Headquarters in Tallahassee, we briefed attendees on current progress in the project and heard comments and suggestions for the next steps. One of the main outcomes of the meetings was the move to select a specific movable bridge and demonstrate the implementation of the monitoring system and its integration into bridge management.

A site visit to a number of movable bridges in District 4, as well as to the district headquarters was conducted. District maintenance engineers, indicated a need for monitoring some maintenance tasks to be able to assess if routine maintenance was being performed satisfactorily. Preventive maintenance was presented as a critical measure in preventing failures and more costly repairs and prepared a summary of desired aspects of a maintenance monitoring system which was given to the researchers. We visited a number of bridges and district engineers shared their experience on critical components with most common modes of failure, and issues for monitoring the condition of these elements.

### **3.3. EVALUATION OF INSPECTION DATA**

#### **3.3.1. Analysis of Inspection Data for a Subset Population**

Inspection reports are the main source of data on the condition of bridges. These reports are generated for each regular NBI inspection and other special inspections (underwater, electrical, etc.). After 1999, inspection reports started following NBI standards and condition ratings defined by PONTIS on a scale of 5. A typical inspection report includes the general characteristics of the bridge such as, location, age, dimensions, type and date of inspection, and the inspection team on the first page. Then, each element subject to inspection is listed according to its category, and the total quantity (area, length, etc.) is distributed to appropriate condition states according to their definitions.

FLORIDA DEPARTMENT OF TRANSPORTATION  
BRIDGE MANAGEMENT SYSTEM  
BRIDGE INSPECTION REPORT

PAGE: 3 OF 37  
INSPECTION DATE: 6/28/99 VTCH

**ELEMENT**

BRIDGE NUMBER: 2  
DISTRICT: 05  
UNIT: 0 DECKS  
ELEMENT CATEGORY: Decks/Slabs

ELEMENT/ENV: 28/4 Steel Deck/Open Grid 330 sq.m.

CONDITION STATE	DESCRIPTION	QUANTITY	RECOMMENDED FEASIBLE ACTION
1	There is no corrosion. The paint system, if any, is sound. The connectors (welds, rivets, bolts, nuts, etc.) are in good condition. The steel deck, if any, may be showing early signs of corrosion.	330	0 Do Nothing
2	There is light corrosion. The paint system, if any, may be showing early signs of corrosion. The connectors (welds, rivets, bolts, nuts, etc.) are in good condition. The steel deck, if any, may be showing early signs of corrosion.	0	
3	Surface corrosion has formed. The paint system is no longer fully effective. There is no loss of section. The connectors may be starting to show signs of distress - cracked welds or broken rivets.	0	
4	Corrosion is moderate. Surface pitting may be present but any section loss is incidental. Numerous connectors are failing at scattered locations. The strength or serviceability of the section is not yet affected.	0	
5	Corrosion is advanced. Numerous connectors have failed. Section loss and/or connectivity is sufficient to warrant analysis to ascertain the impact on the ultimate strength and/or serviceability of either the element or the bridge.	0	

**NOTES**

**ELEMENT INSPECTION NOTES:**  
The steel sidewalk on the west side of the north bascule leaf has an area approximately 1'-9" x 8" which has peeled with moderate corrosion and minor pitting. See photo #1. There are several random areas throughout with slight corrosion present. Also, the quantity of the sidewalk (steel plate) was figured in with the steel open grid. The sidewalk length was 105' and width was 4'-5". Previous Corrective Action -The open grid decking was replaced. The sidewalk had fasteners installed of sufficient length to connect to the sidewalk and support angle. Some areas at the end of the sidewalk had missing fasteners due to no angle to connect to.

REPORT ID: INSP002 (detailed) PRINTED: 8/16/99 17:09:47

Figure 3.1 – Typical element condition from an inspection report

Inspection notes for each element follow the condition ratings. These notes are documented along with related photographs. Recommended actions are specified for each deficient element. Finally, NBI data pertaining to the bridge can be found, sometimes with sufficiency rating calculations and notes.

Although it is acknowledged that condition ratings are subjective and limited, analysis of current and past inspection reports can provide valuable representative information for the general condition and critical components of movable bridges. Data from recent inspection reports for movable bridges in FDOT Districts 4 and 5 were analyzed to investigate the most common problems and identify which components experience the highest number of them. Figure 3.1 is a screenshot from the spreadsheet developed to analyze the data from the inspection reports. For all bridges, the average condition state was recorded, as well as the observed problem from any notes of the

inspector. With this analysis, average condition states for each component in the bridge population were obtained. Also, observed problems were tallied to identify the problems related with each component and analyze those most commonly observed.

3	A	B	C	D	E	F	G	H	I	J	K	L	M	N	O	P	Q	R	S	T	U	V	W	X	Y	Z	AA	AB	AC	AD	AE	AF	AG	AH	AI	AJ	AK	AL	AM	AN	AO	AP	AQ	AR	AS	AT	AU							
4	UNIT	ELEM CATEGORY	ELEMENT	District	BR0001	BR0002	BR0003	BR0004	BR0005	BR0006	BR0007	BR0008	BR0009	BR0010	BR0011	BR0012	BR0013	BR0014	BR0015	BR0016	BR0017	BR0018	BR0019	BR0020	BR0021	BR0022	BR0023	BR0024	BR0025	BR0026	BR0027	BR0028	BR0029	BR0030	BR0031	BR0032	BR0033	BR0034	BR0035	BR0036	BR0037	BR0038	BR0039	BR0040	BR0041	BR0042	BR0043	BR0044	BR0045					
5	I. Decks	Decks/Slabs	a. Bare Concrete Deck	Average Condition State	1	2	1	2	3	2	2	2	2	1	1	1	1	1	1	2	1	2	2	3	2	2	2	2	1	2	1	2	1	1	1	1	1	1	1	1	1	1	1	1	1	1	3	3	2	2				
6				• Section loss																																																		
7				• Corrosion																																																		
8				• Missing fasteners																																																		
9				• Cracking																																																		
10				• Exposed rebar																																																		
11				• Delamination/spalls																																																		
12				Average Condition State	1	3	1	1	1	2	1	3	3	3	1	1	1	1	1	1	1	1	1	1	1	1	1	1	1	1	1	1	1	1	1	1	1	1	1	1	1	1	1	1	1	1	1	1	1	1	1	1		
13				• Section loss																																																		
14				• Surface corrosion																																																		
15				• Surface cracks																																																		
16				• Missing fasteners																																																		
17				• Cracked welds/broken rivets																																																		
18				Average Condition State	1	2	3	3	1	2	1	3	3	3	1	1	1	1	1	1	2	1	1	1	1	1	1	1	1	1	1	1	1	1	1	1	1	1	1	1	1	1	1	1	1	1	1	1	1	1	1	1	1	
19				• Delamination/spalls																																																		
20				• Corrosion																																																		
21				• Section loss																																																		
22				• Cracked welds/broken rivets																																																		
23				Average Condition State																																																		
24				• Cracking																																																		
25				• Delamination/spalls																																																		
26				Average Condition State																																																		
27				• Cracking																																																		
28				Average Condition State	3	3		1	1	1	1	1	1	1	1	1	1	1	1	1	1	1	1	1	1	1	1	1	1	1	1	1	1	1	1	1	1	1	1	1	1	1	1	1	1	1	1	1	1	1	1	1		
29				• Seepage																																																		
30				• Delamination/spalls																																																		
31				• Adhesion failures																																																		
32				Average Condition State	11	12	1	11	3	1	3	1	1	1	1	1	1	1	1	1	1	1	1	1	1	1	1	1	1	1	1	1	1	1	1	1	1	1	1	1	1	1	1	1	1	1	1	1	1	1	1	1		
33				• Adhesion failures																																																		
34				• Delamination/spalls																																																		
35				• Seepage																																																		
36				Average Condition State																																																		
37				• Delamination and bond loss																																																		

Figure 3.2 – Analysis of inspection reports by creating spreadsheets from visual inspection data

Based on this analysis, nine common types of damage were identified for all components. For every component, the total number of occurrences of a particular type of problem was indicated.

The inspection data were then plotted and analyzed to review the condition of movable bridges in Districts 4 & 5. In Figure 3.3, the element types and their averaged conditions are shown. In this figure, best condition and worst condition are given as “1” and “5”, respectively. Steel decks and movable components, on the average, have the lowest condition state.

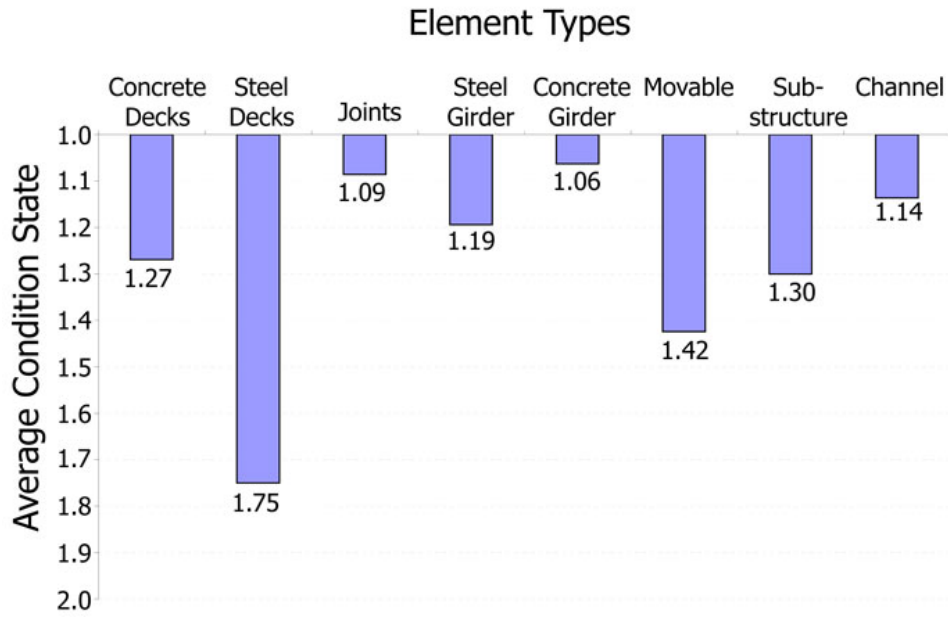


Figure 3.3 – Average condition states of components

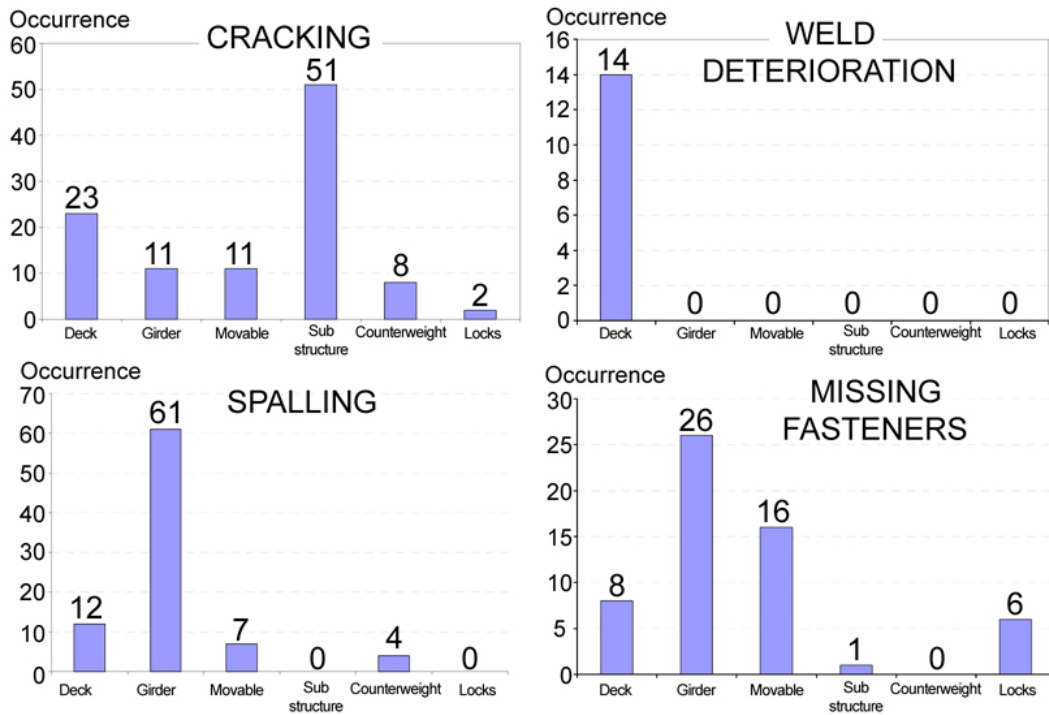


Figure 3.4 – Identification of common problems

For the superstructure, the most common problems were observed were for the deck, main girder and transverse girder elements. For steel girders, section loss resulting from corrosion was the main source of problems. Cracking and missing fasteners were the next most common. The most common problems are given in Figure 3.4.

Movable components include all mechanical parts and machinery that operate for opening and closing of the bridge. Analysis of the data from inspection reports shows that misalignment, leaking and inadequate lubrication are the most significant causes of breakdowns. Span locks are found to be the most problematic component among the movable elements.

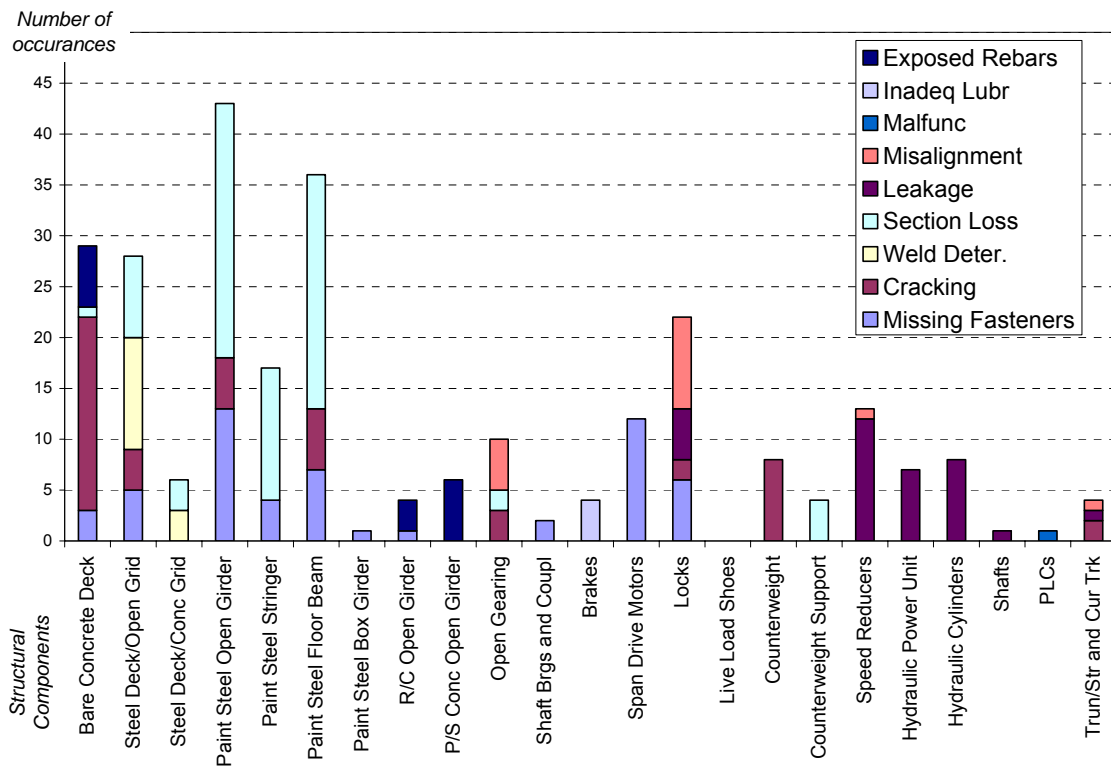


Figure 3.5 – Most commonly observed movable bridge problems (District 4&5)

Analysis of inspection reports shows components with the most frequent problems. This analysis is based on subjective visual inspections, and do not consider the impact of each type of failure, it provides a guide indicating the problematic elements.

### 3.3.2. Inspection Data Analysis for Christa McAuliffe Bridge over 30 Years

Bascule bridges constitute by far the majority of movable bridge types. Based on this analysis and interaction with FDOT structures and maintenance engineers, the bascule type was selected for detailed investigation, and the movable bridge over Florida SR-3, known as Christa McAuliffe Bridge, was selected as the representative bridge considering its type, span length, age, opening frequency, type of traffic and accessibility (Figure 3.6).

The selected representative movable span has the structure number 700072, and is the south-bound span of two parallel spans on SR-3, crossing the Barge Canal in Merritt Island, FL. This span was constructed in 1961, and underwent extensive rehabilitation twice, in 1994-1995 and again in 1999-2003. It has double bascule leaves, each 70-ft long, and 40-ft wide, carrying two traffic lanes. The representative bridge opens about 6 to 7 times a day.

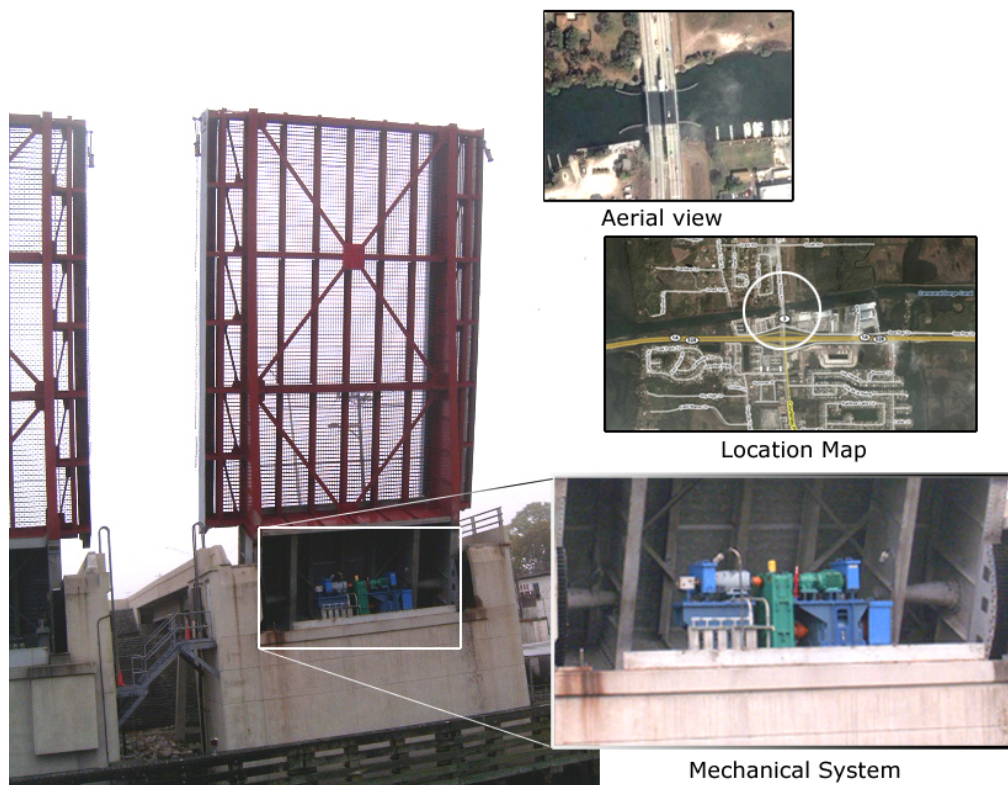


Figure 3.6 – Case Study: Christa McAuliffe Bascule Bridge in Merritt Island, FL

Christa McAuliffe is of the most common bascule type, with a rack-and-pinion mechanism. The bascule leaves are lifted horizontally at the point of the trunnions, which are the pivot points on the main girders (Figure 3.7). The weight of the span is balanced with a counterweight that minimizes the required torque to lift the leaf. The counterweight is made of cast-in-place concrete. In the closed position, the girder rests on a support called ‘live load shoe’ on the pier and traffic loads are not transferred to the mechanical system.

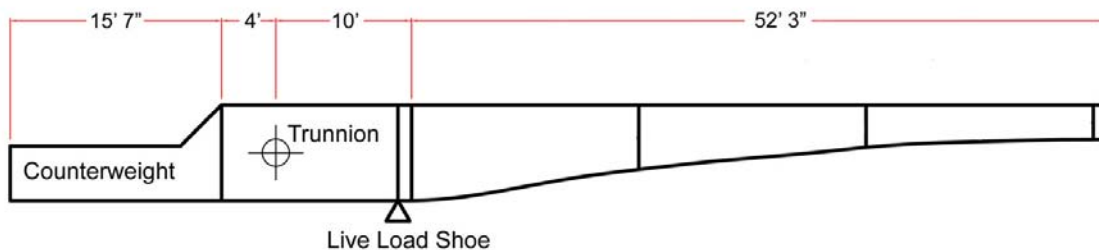


Figure 3.7 – Main girder of Christa McAuliffe Movable Bridge

The movable bridge also involves fixed components, such as reinforced concrete piers and approach spans. The counterweight of the main girder stays below the approach span deck in the closed position. When the bridge is opening, the leaves rotate upwards, and the counterweight goes down. The elevation view of the Christa McAuliffe Bridge is shown in Figure 3.8.

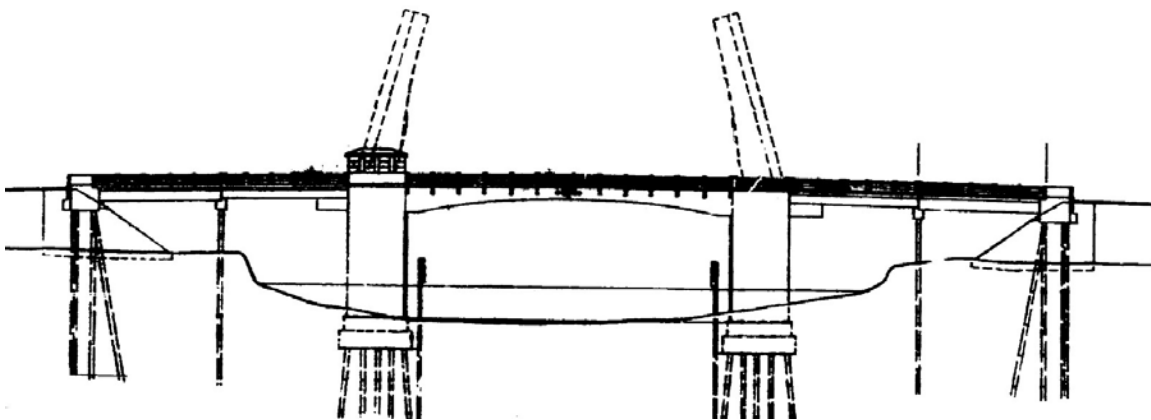


Figure 3.8 – Christa McAuliffe Movable Bridge elevation (adapted from Christa McAuliffe Bridge construction plans)

The schematic of the mechanical system that operates the movable bridge is shown in Figure 3.9. The driving torque is generated by an electrical motor, which is then distributed to the drive shafts via the gear box. The gear box involves an assembly of gears operating similar to automobile differentials, and provides equal lifting of both sides. The drive shafts transmit the torque to the final gear called the pinion, which engages the rack assembly, which is directly attached to the main girder.

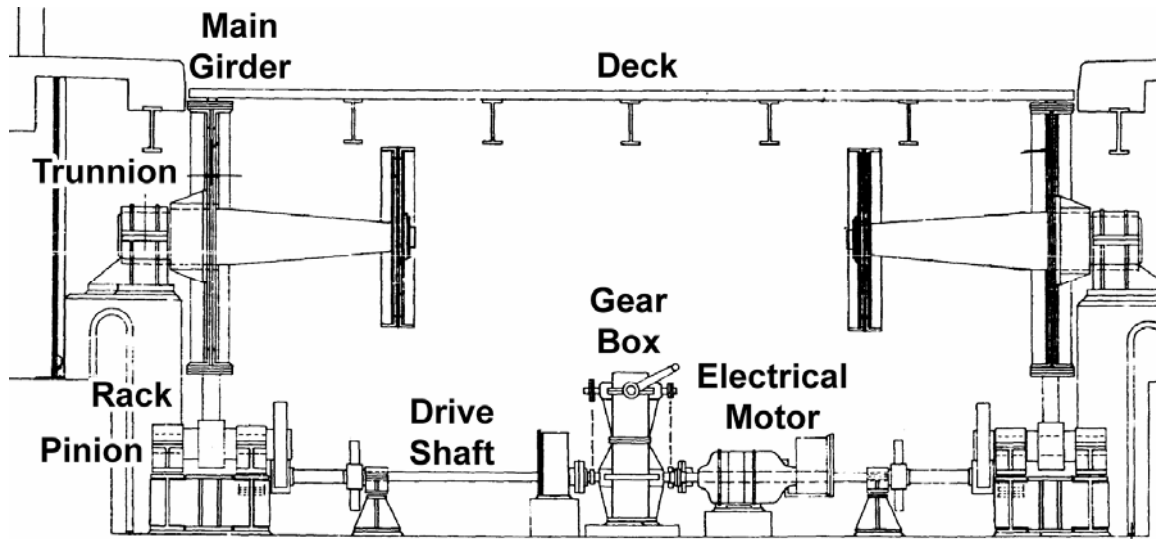


Figure 3.9 – Christa McAuliffe Movable Bridge mechanical system (adapted from Christa McAuliffe Bridge construction plans)

Inspection reports of the representative bridge were analyzed in order to track the change of condition states over a 25-year period. Examples of the analysis are given in Figures 3.10 to 3.13, showing the condition state of steel girders and some movable parts through years. It should be noted that prior to 1980's movable parts were not assigned any condition state number, therefore those were not included.

These figures clearly indicate the deterioration pattern and effect of rehabilitation. The condition of steel girder elements starts deteriorating after 7 or 8 years with the effect of surface corrosion, section loss and operating impacts causing bents and misalignment. Each rehabilitation effort, shown as striped regions, produces a positive effect on the condition state. The downward drift is much more rapid for the case of movable parts,

since they are subjected to heavy fatigue effects, and are very sensitive to alignment, lubrication and proper maintenance.

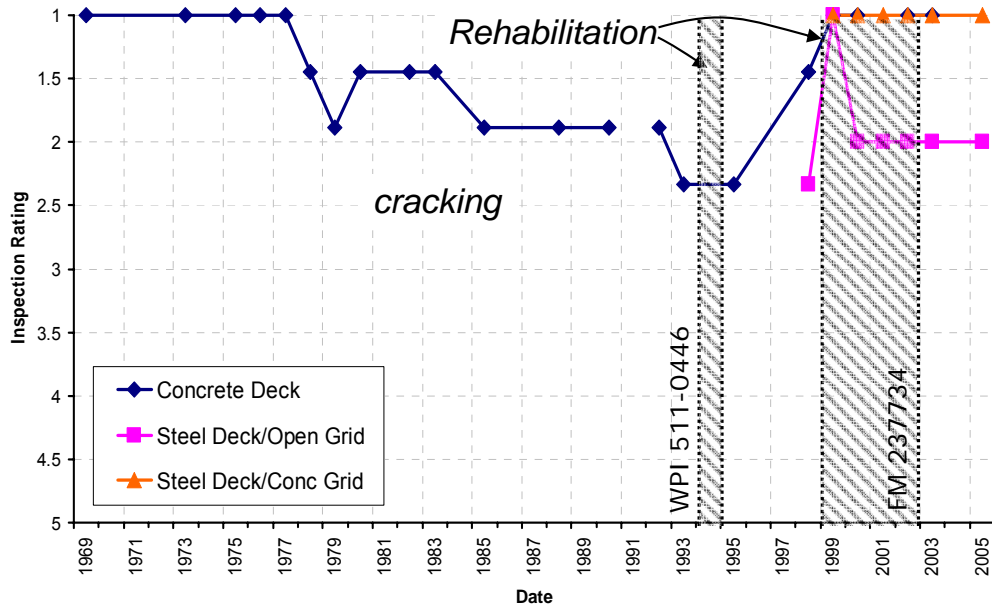


Figure 3.10 – Condition state: Decks

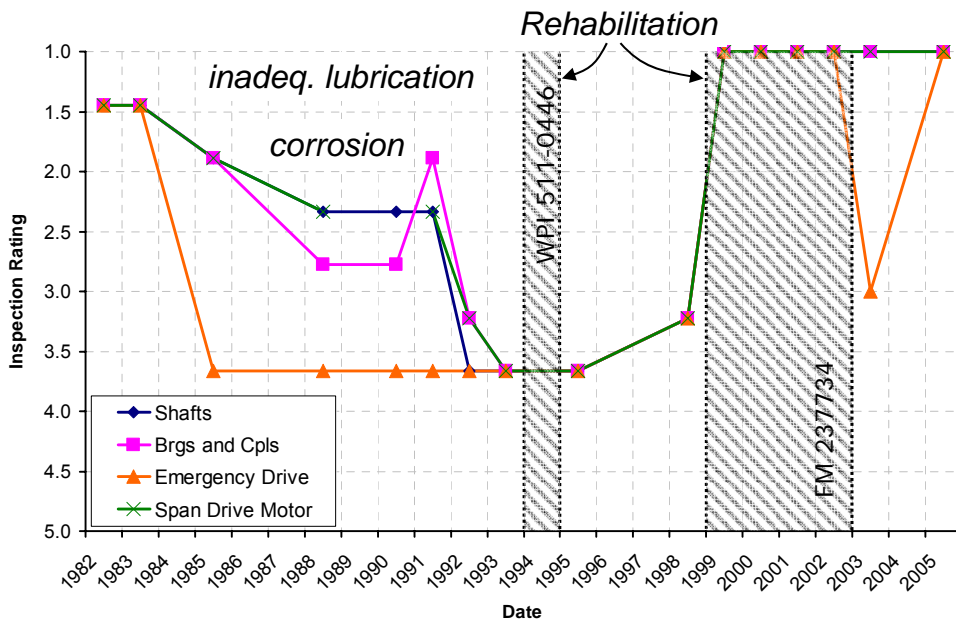


Figure 3.11 – Condition state: Movable components

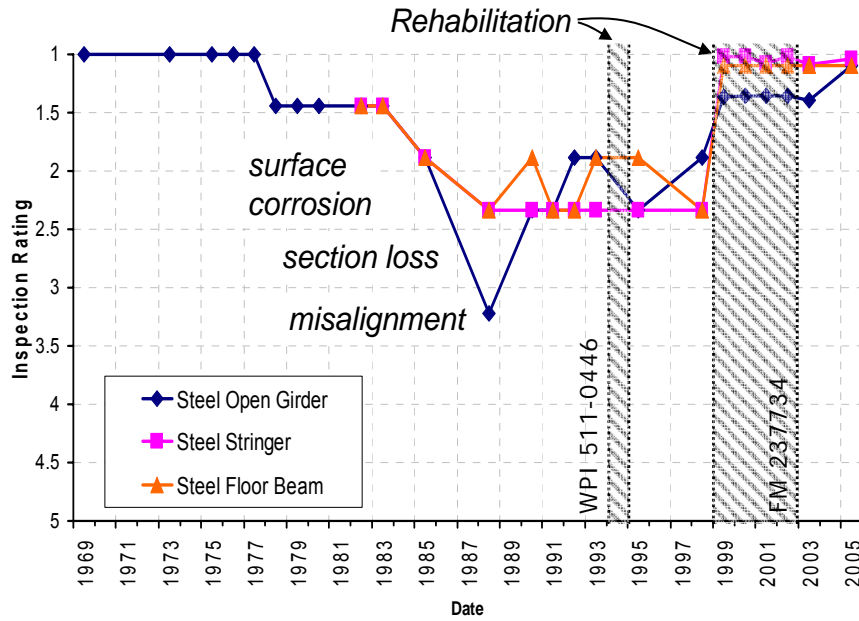


Figure 3.12 – Condition state: Superstructure

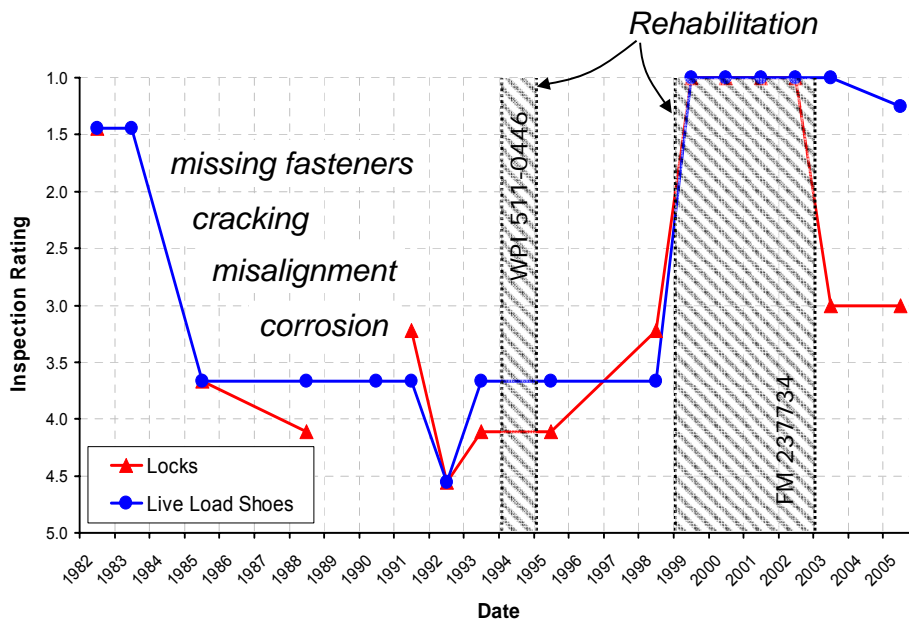


Figure 3.13 – Condition state: Locks and live load shoes

Although the condition states are obtained by visual inspections, whose subjectivity and limitations are well-documented, they show a trend of bridge condition during its lifetime. The deterioration patterns can be identified and modeled, making it

possible to predict the future condition and effects of rehabilitation. Here, structural health monitoring can provide a benefit for reducing the uncertainty in the component condition appraisal process and supplying dependable data for deterioration analysis. Accurate structural capacity or a reliability index of each component can be derived with SHM data, and deterioration models can be constructed by applying the Bayesian updating method to collected data.

### **3.4. NUMERICAL MODEL DEVELOPMENT FOR ANALYTICAL EVALUATION OF STRUCTURAL PERFORMANCE**

#### **3.4.1. Finite Element Model Development**

Finite Element Modeling is the analysis method based on discretization of structures to solve the governing equations of mechanics. Computer programs are used to model the structure. Data from the model are translated into assembled stiffness matrices to be solved for the input load cases. Finite Element Modeling allows for predicting the structural response to various loading simulations with much higher accuracy than the usual simplified analysis techniques.

Development of a Finite Element Model requires attention to the underlying equations for the elements defined to represent structural components. Appropriate finite elements should be used to conduct a behavior as similar as possible to the actual structure. Also, discretizations, connections and constraints of the elements are as important as matching the geometric requirements. A thorough inspection and verification stage is crucial to ensure the model has the intended behavior. Two levels of verification are element-by-element checking and checking the model behavior for different analysis cases.

#### **3.4.2. Initial Finite Element Model with Shell Elements**

An initial model was developed by modeling the main girders with shell elements. The main girder is a built-up plate girder made out of multiple layers of steel plates. Both the thickness and the section depth are variable, to provide sufficient capacity at all

sections with minimum weight. Flange thickness is also variable, with changing thickness and number of steel plates through the length of the girder.

Original construction plans were used to build the CAD and Finite Element models of the bridge. Model creation was also assisted by the notes and pictures obtained from site visits to the movable bridge (Figure 3.14 and Figure 3.15).

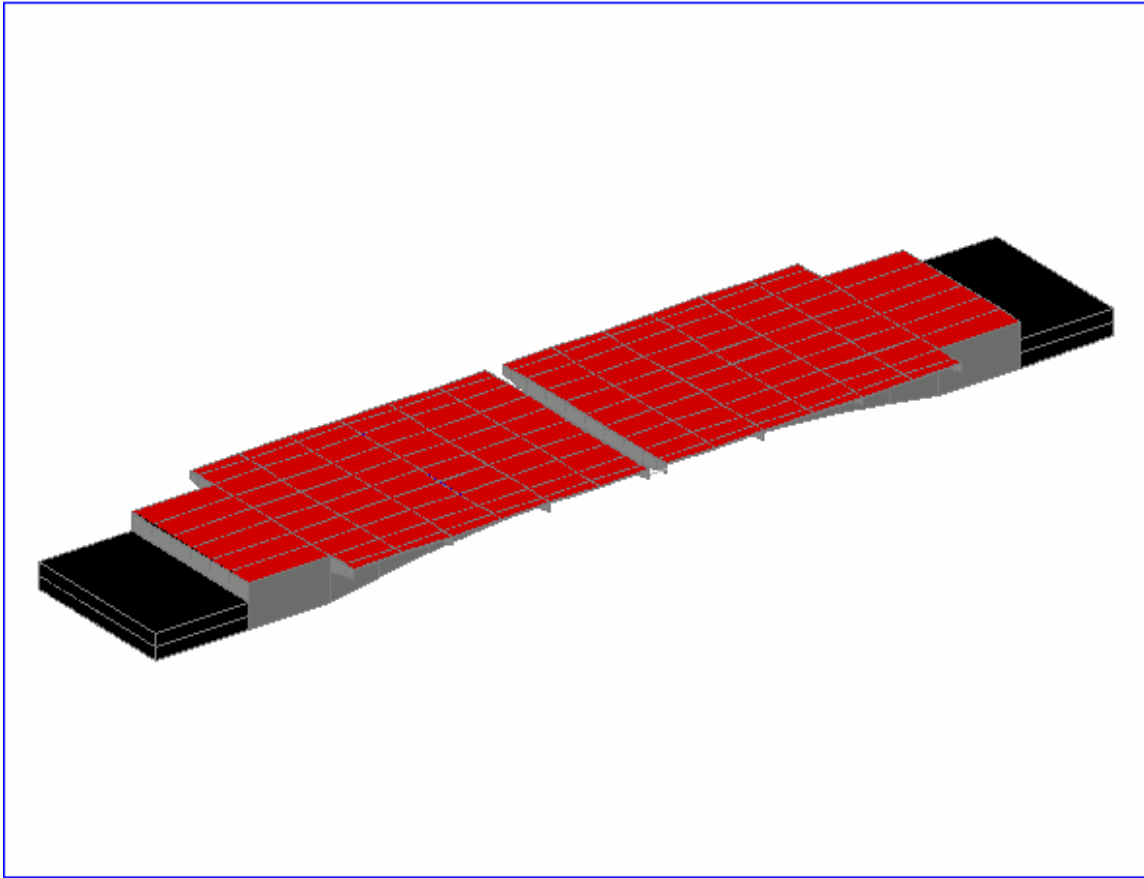


Figure 3.14 – 3D CAD model of the movable bridge

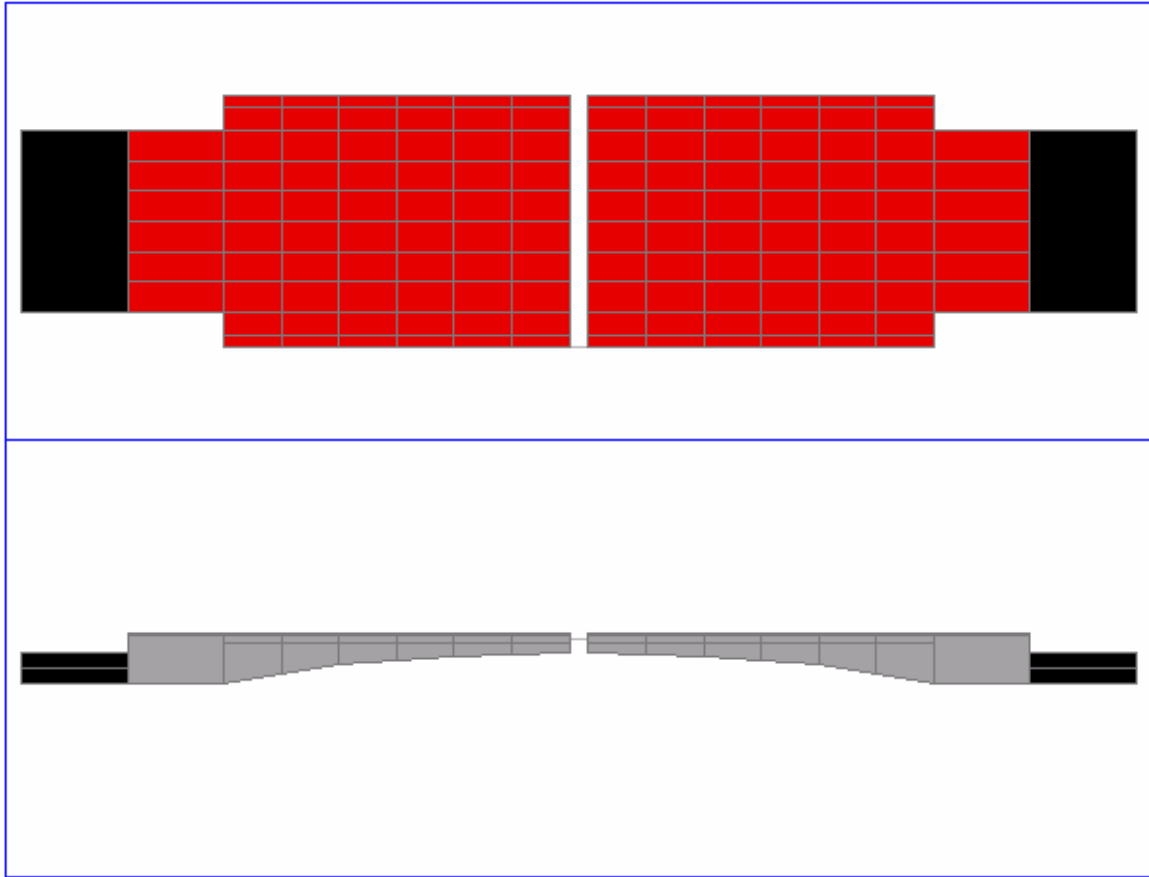


Figure 3.15 – 3D CAD model; orthogonal views

The main girder was modeled by using two shell elements for the flanges and one shell element for the web. Due to the thickness of the elements, their nodes do not match; therefore, connectivity was satisfied by assigning rigid links as shown in Figure 3.16. The depth of the girder web varies following a parabolic function, which can be replicated with shells of varying depth (Figure 3.17).

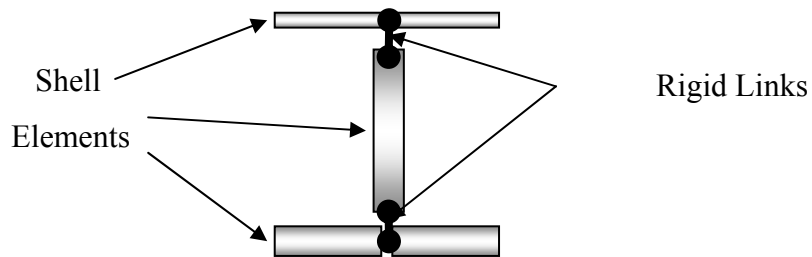


Figure 3.16 – Modeling of the bascule girder

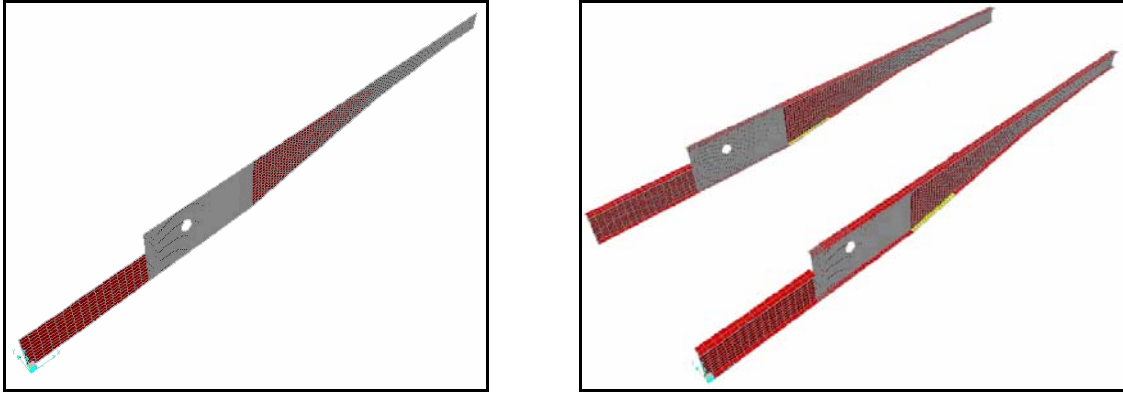


Figure 3.17 – Modeling of bascule girders with shell elements

The trunnion was modeled as a circular region connected to the girder shells with rigid links. This rigid region representing the trunnion-hub-girder (THG) assembly was assumed to be including the effects of the stiffeners at the trunnion.

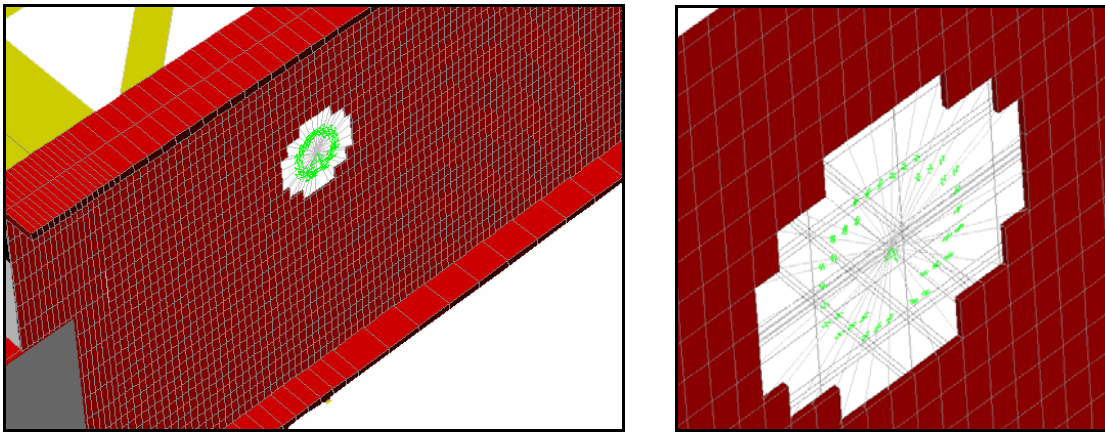


Figure 3.18 – Detail of the pinned connection

For all remaining beam members, meaning floor beams, transverse beams and bracings members, frame elements were employed. In the case of variable linear section members, also variable frame section elements were used (Figure 3.19).

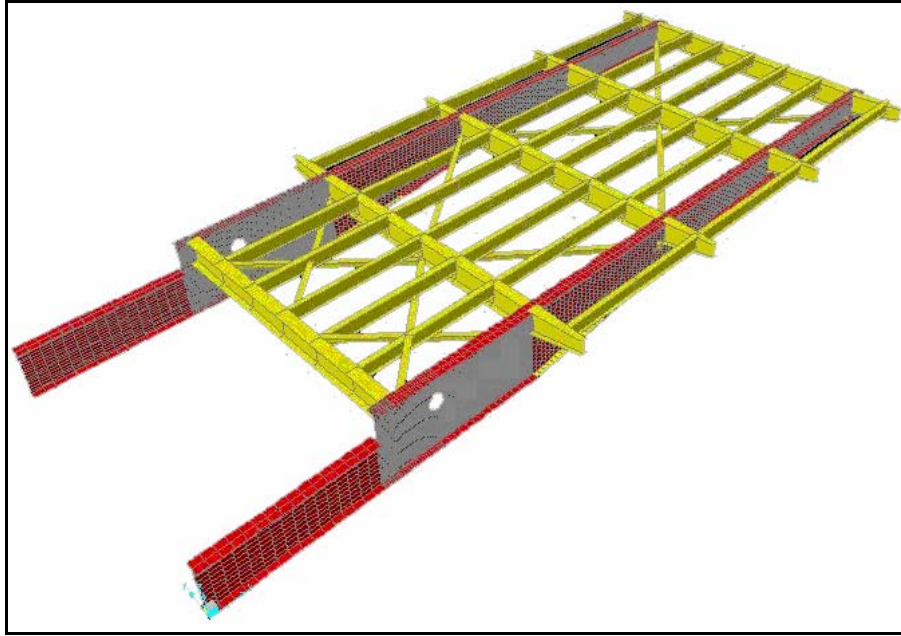


Figure 3.19 – Model with shell elements (deck not shown)

It is important to note that because different frame elements, like W27×102 and W16×36 have different centers of gravity, a rigid link between them is necessary to ensure a good model (Figure 3.20).

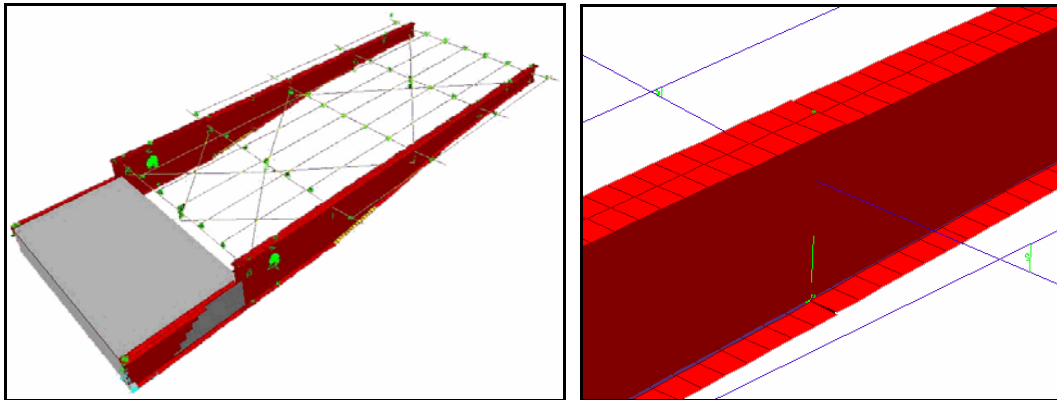


Figure 3.20 – Rigid links between frame elements

The deck of the movable bridge is steel grid type, built by closely arranged and welded thin plate members providing maximum bending resistance with minimum self-weight. Details are given in Figure 3.21, which is from the original construction plans.

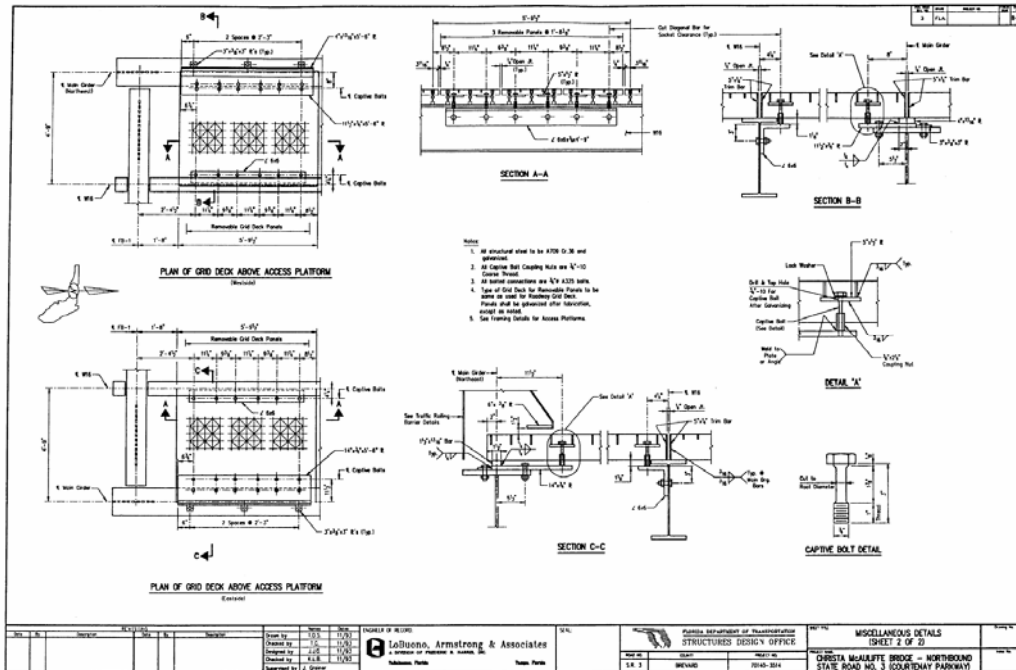


Figure 3.21 – Detail of the steel deck (Christa McAuliffe Bridge construction plans)

This same type of structure could be modeled in the Finite Element Model using frame elements (Figure 3.22), but the processing time would be very long and generation of element would take a long time as well. That is why, a simpler deck was employed, formed by shell elements equivalent to the real deck of the bridge.

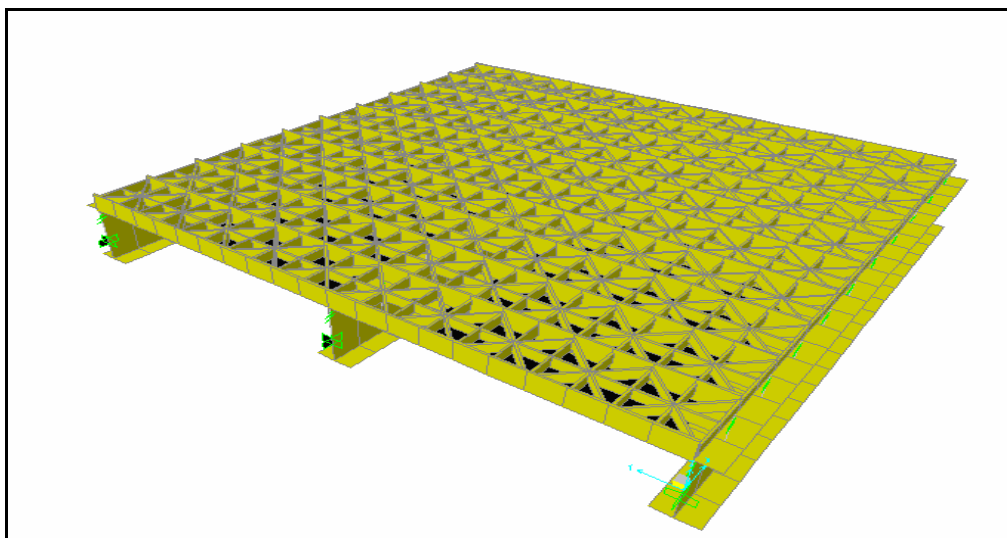


Figure 3.22 – Model of the real deck

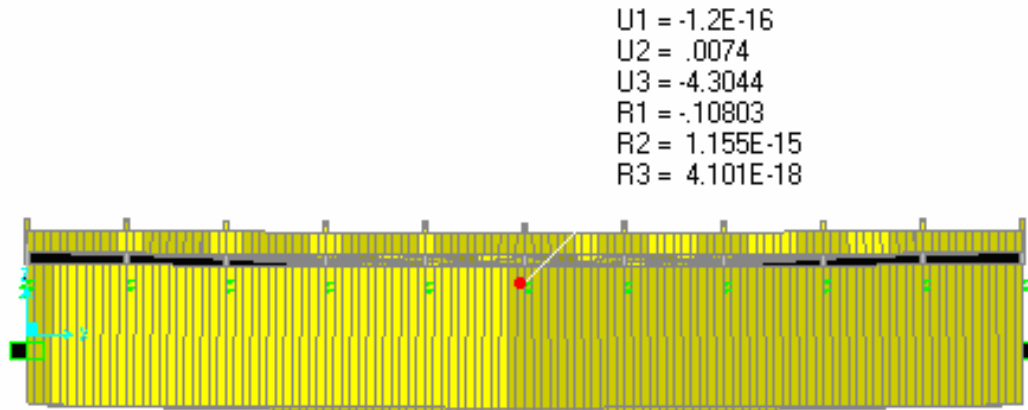


Figure 3.23 – Deformations under load (frame representation)

The same deck was modeled using steel shell elements of different thickness and the best match was for 1.45 in thickness element.

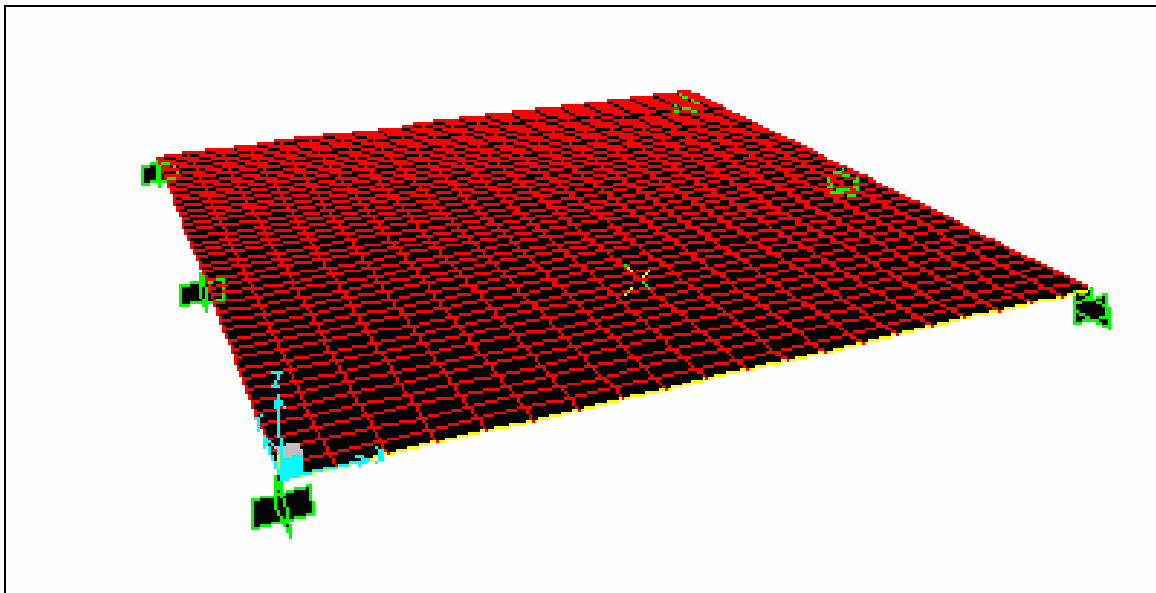


Figure 3.24 – Deck modeled using 1.45 in thick steel shell element

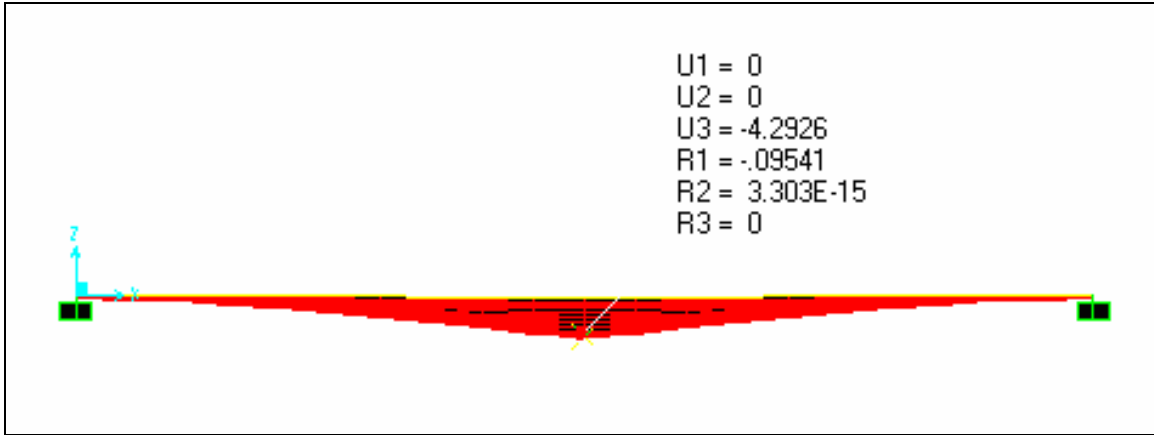


Figure 3.25 – Deflections under load (shell representation)

Comparing the results for deflection and rotations it is evident that the modeled finite element deck behaves similarly to the real one with only a minimum error (Figures 3.23 to 3.25).

The connection between the two spans was modeled using rigid links and the moments at the contact points were released. Therefore, it was assumed that the shear force was completely transferred between the two leaves, which is the desired function of the span lock (Figure 3.26). Since recent changes in design standards require that the span locks should not be considered as load transferring members, the model was analyzed with and without the effect of span locks.

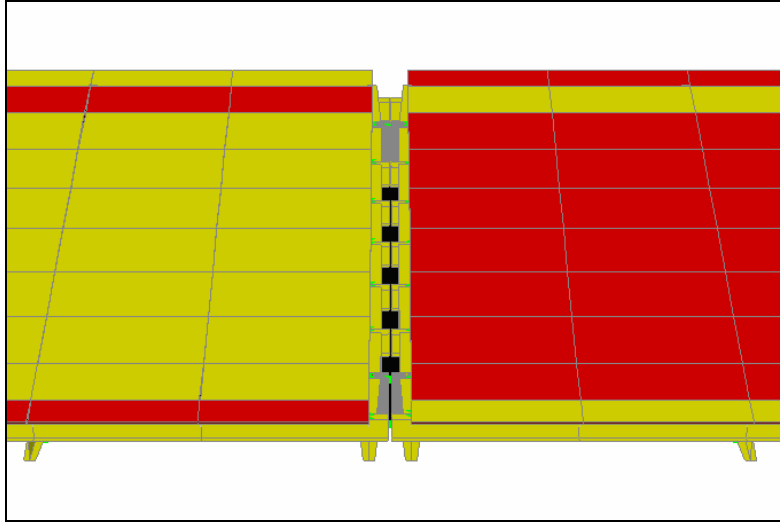


Figure 3.26 – Connection of two spans

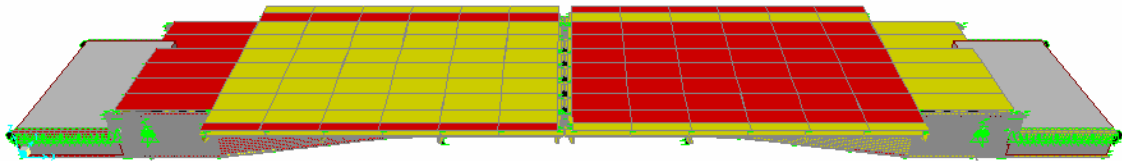


Figure 3.27 – Finite element model with shell elements

This initial model is formed by 230 elements, 29498 shell elements, 2 solid elements, 4,473 links and 26,808 constrains formed. This model consists of 11,133 master degrees of freedoms and was solved with a system of 178,507 equilibrium equations and 4,745,459 non-zero stiffness terms. The system was solved using a desktop computer with Pentium-4, 2.4GHz CPU clock, 1.0 GB memory ram, and the computational time was 16:14 min as shown in Figure 3.28.

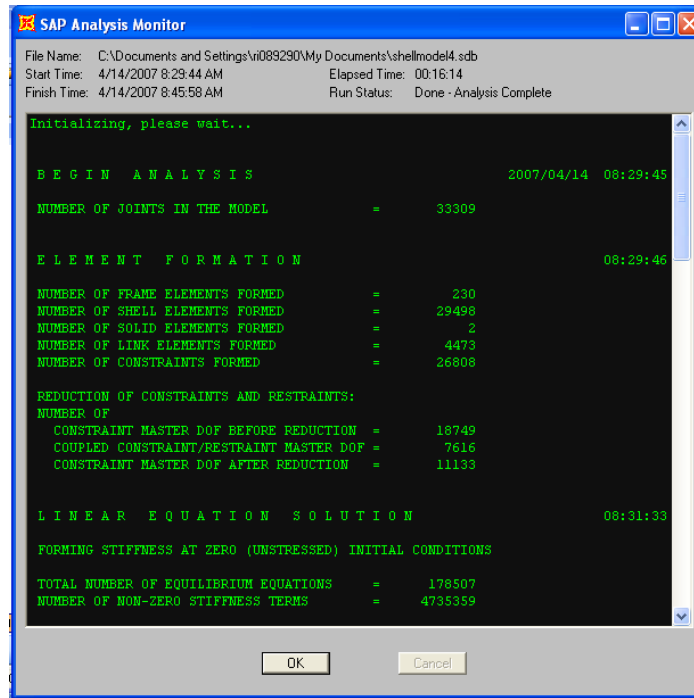


Figure 3.28 – Summary of initial finite element model

### 3.4.3. Modified Finite Element Model with Frame Elements

Since the computational time and complexity of the initial finite element with shell elements is large, a modified model was developed, replacing the main girders with variable cross-section frame elements (Figure 3.29).

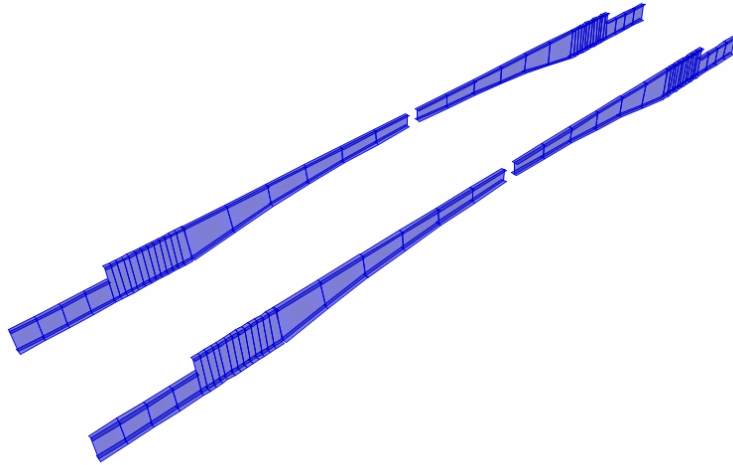


Figure 3.29 – Modeling of bascule girders with frame elements

Transverse girders, floor girders and bracings were also simulated using frame elements (Figure 3.30). All the members were interconnected using rigid links at their center of gravity, transmitting moment and other internal forces accordingly.

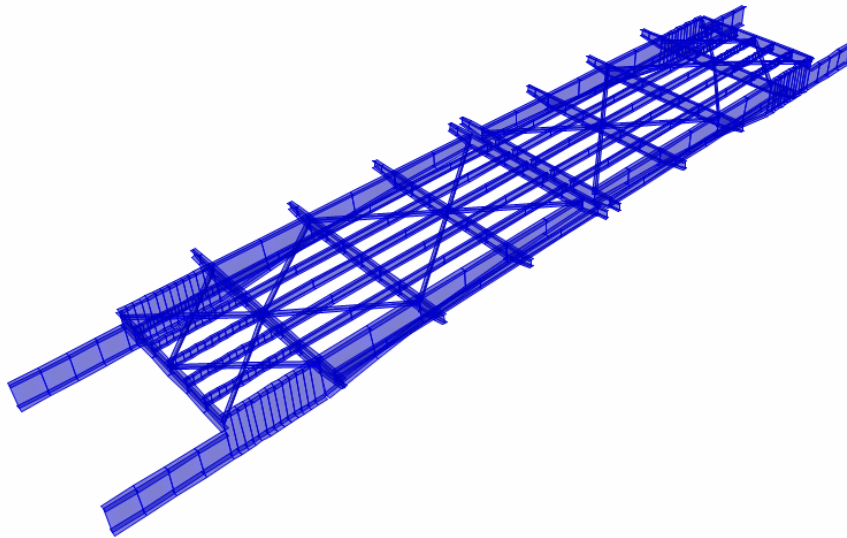


Figure 3.30 – Main girders, transverse girders, floor beams, and bracings.

Counterweight was simulated using solid concrete elements. The deck was modeled using 1.45 in. steel shell elements as explained in section 3.4.1. For this model, the trunnion was defined as a pin connection, instead of a rigid area. The live load shoe

(LLS) was again defined as a roller support, since the leaves only rest on the LLS at closed position (Figure 3.31 and Figure 3.32). Figure 3.33 represents the complete modified FEM.

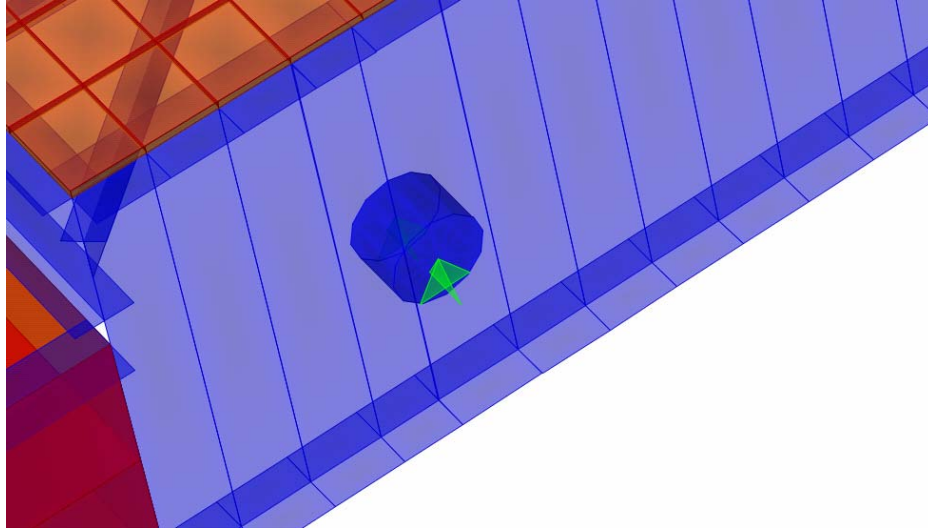


Figure 3.31 – Close-up on the trunnion in the modified model

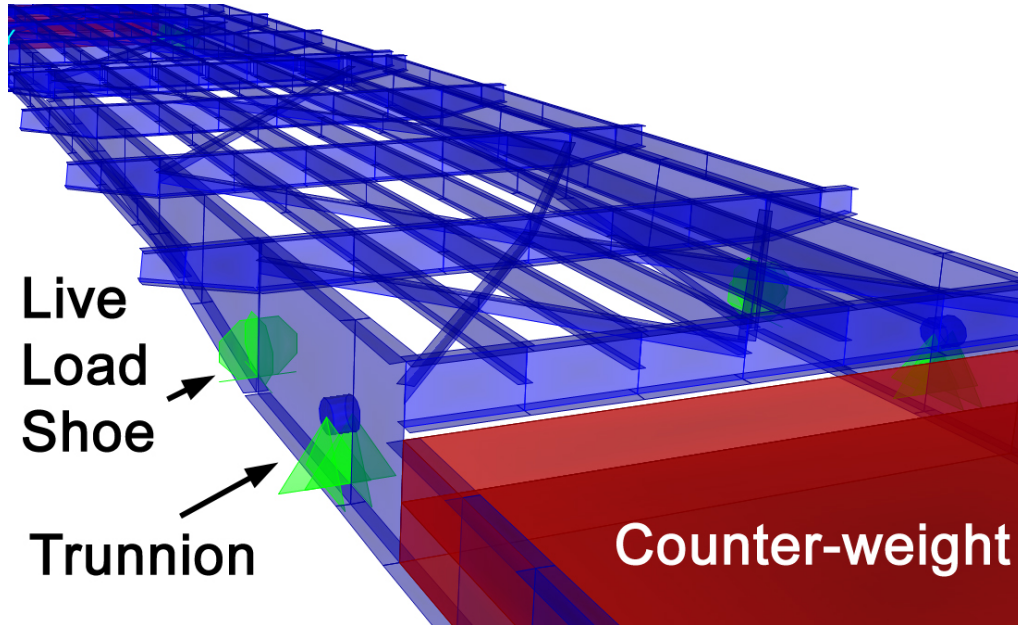


Figure 3.32 – Supports (boundary conditions) of the model (deck not shown)

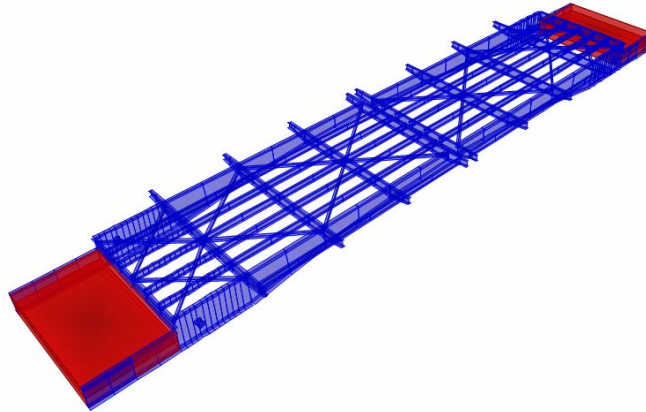


Figure 3.33 – Completed modified FEM (Deck not shown).

This model is formed by 454 frame elements, 3098 shell elements, 4 solid elements, 450 links and 2706 constrains formed. This model consists of 1480 master degrees of freedoms and was solved with a system of 18,256 equilibrium equations and 470,034 non-zero stiffness terms. The system was analyzed for static loads using a desktop computer Pentium 4 CPU 2.4 GHz, 1.00 GB of RAM and the computational time was 57 sec. as shown in Figure 3.34.

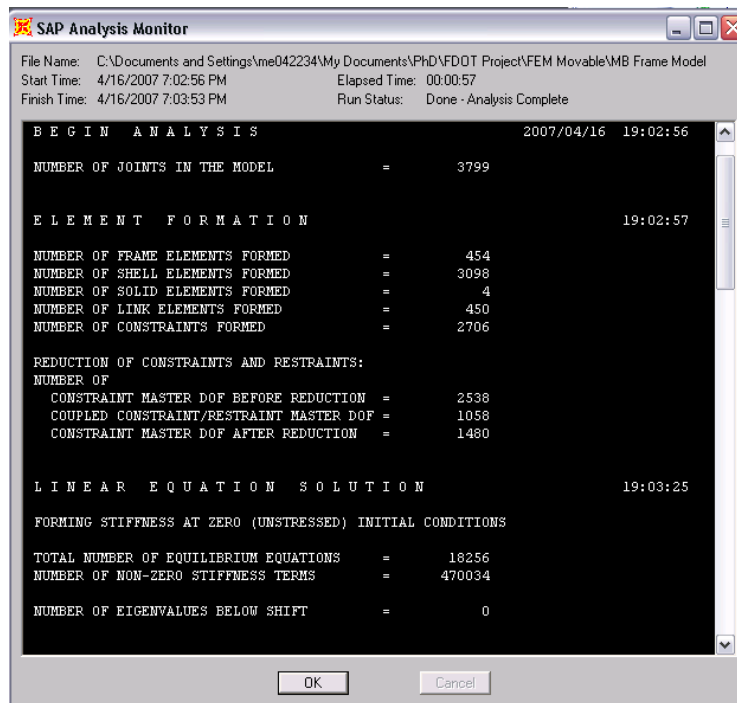


Figure 3.34 – Analysis details for the modified FEM

### 3.5. COMPARISON OF THE TWO MODELS

Both models were compared to be sure they simulate the bridge in the same way. The validity of the modified model was ensured by obtaining responses for the same loading and analysis cases. The first structural response to compare the two models was the tip deflection under static loading. For this purpose, a load corresponding to an HL-93 Truck was placed on both models as show in Figure 3.35.

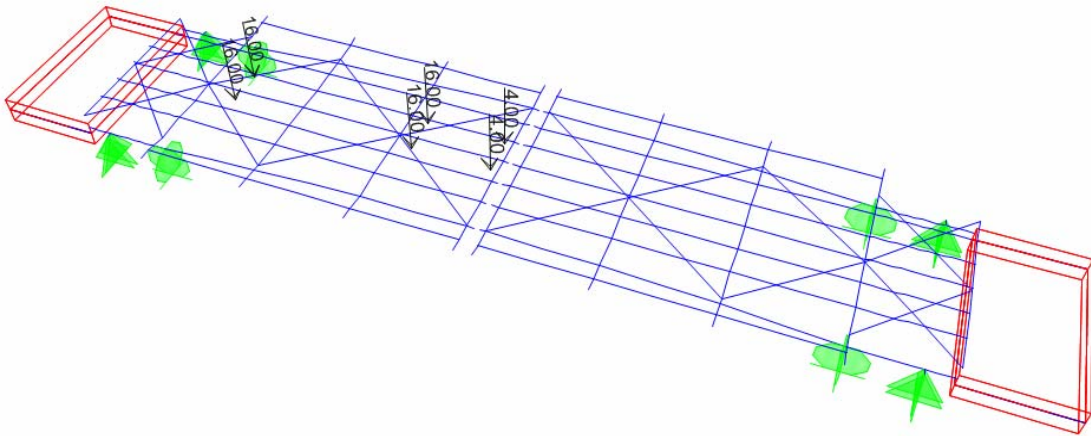


Figure 3.35 – Load case studied for model comparison

In Figure 3.36 results for deflection on the tip of the leaves are shown for both, the initial and the modified model.

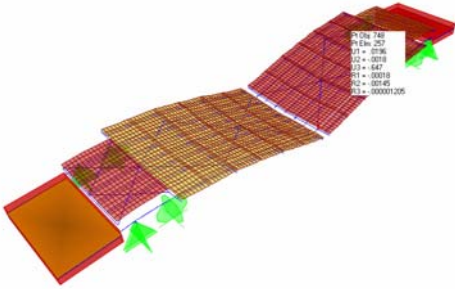
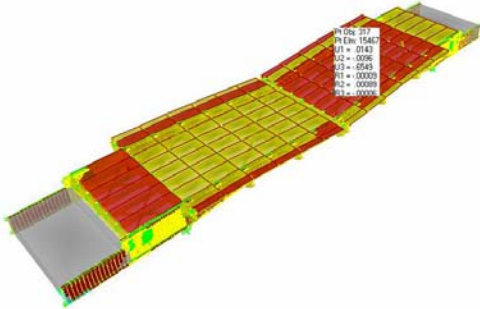
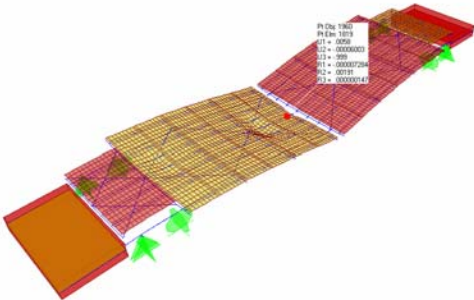
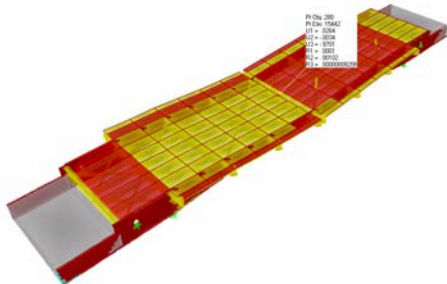
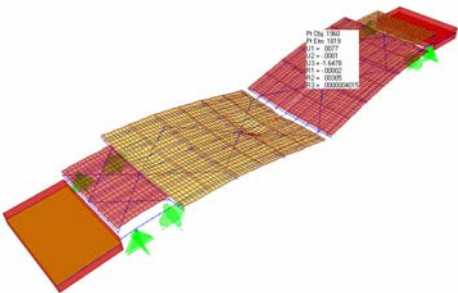
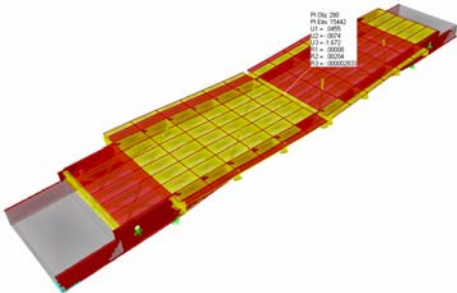
Modified Model with Frames	Initial Model with Shells
 <p data-bbox="240 653 672 688">Dead Load Deflection = 0.647 in.</p>	 <p data-bbox="821 646 1248 682">Dead Load Deflection = 0.655 in</p>
 <p data-bbox="240 1113 630 1148">(Truck) Deflection = 0.999 in.</p>	 <p data-bbox="821 1113 1211 1148">(Truck) Deflection = 0.970 in.</p>
 <p data-bbox="240 1570 716 1606">(Dead+Truck) Deflection = 1.648 in.</p>	 <p data-bbox="821 1570 1281 1606">(Dead+Live) Deflection = 1.672 in.</p>

Figure 3.36 – Finite element models deflection comparison

Dynamic properties for both models were also compared and indicate behavioral similarity. Comparison of the first three mode shapes shows an almost perfect match (Figure 3.37).

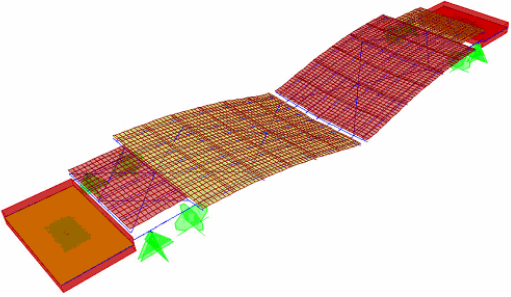
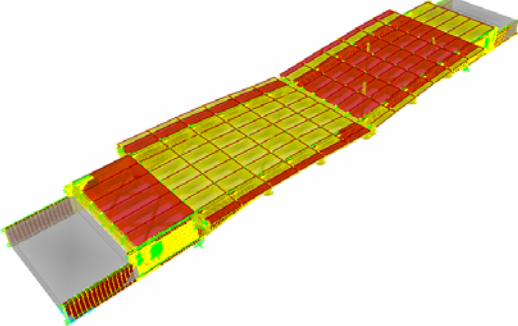
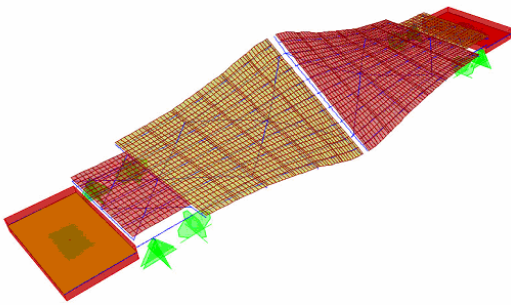
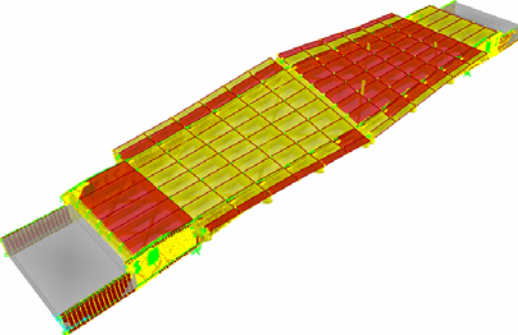
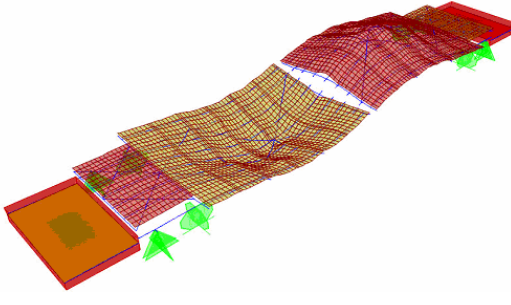
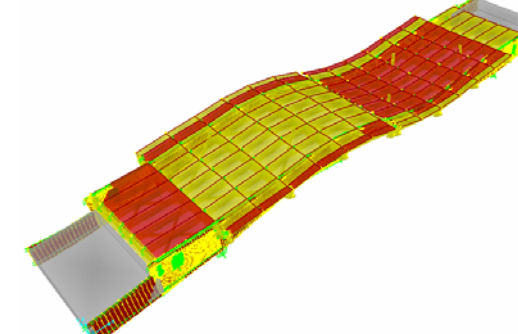
Modified Model with Frames	Initial Model with Shells
 <p data-bbox="337 653 704 684">T = 0.271 s    f = 3.69 Hz</p>	 <p data-bbox="915 653 1282 684">T = 0.272 s    f = 3.68 Hz</p>
 <p data-bbox="337 1108 704 1140">T = 0.211 s    f = 4.74 Hz</p>	 <p data-bbox="915 1098 1282 1129">T = 0.196 s    f = 5.10 Hz</p>
 <p data-bbox="337 1545 704 1577">T = 0.111 s    f = 9.04 Hz</p>	 <p data-bbox="915 1551 1282 1583">T = 0.112 s    f = 8.93 Hz</p>

Figure 3.37 – Comparison of the first three principal modes

Based on these comparative results, all further calculations were done using the modified model, mainly because computational time was reduced by 94% without losing

accuracy. The initial model was only used to obtain stress distribution over the girder when necessary.

### 3.6. EXPERIMENTAL STUDIES CONDUCTED AT THE BRIDGE

Movable bridge operation is based on the balance of the span weight and the counterweight. When the weights of the leaf and counterweight are in equilibrium about the pivot point (trunnion), they are in what is called balanced condition. However, this is not the desired configuration. Weights of the leaf and counterweight should be distributed in such a way that the leaf can be closed manually without too much effort in the event of a power failure. There are no accepted standards for this weight distribution, however, maintenance engineers agree that this condition should make the leaf drift slowly downward without power during most of the closing operation. At the same time, the motor should make the minimum torque to overcome the static friction.

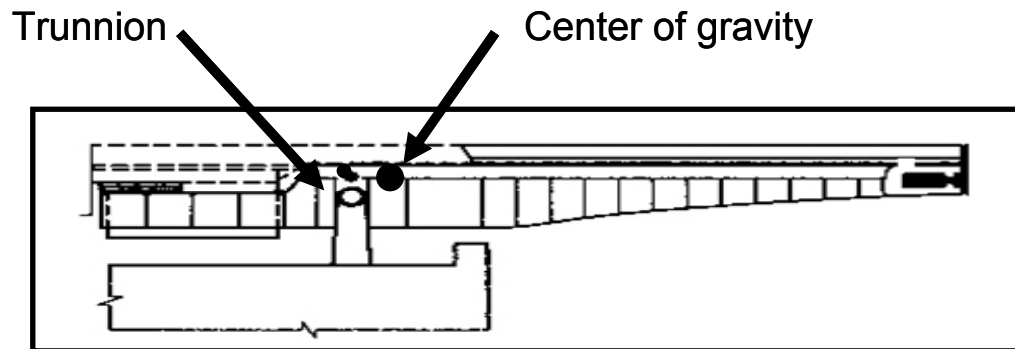


Figure 3.38 – Desirable Balance Condition of a Bascule Bridge

The Florida Department of Transportation is using Bascule Bridge Balance Tests (Malvern et al. 1982) for evaluating the balance state and verify the functioning of the shaft-gear-trunnion system. A test team of engineers from the FDOT State and Materials Office in Gainesville conducts these tests by visiting the bridges annually, or whenever there is a rehabilitation or alteration, which could change its balance condition. The test is performed by mounting strain sensors on the main drive shafts to obtain the torsional shear strain. These data are used to calculate the torque during opening and closing of the leaves, recorded in conjunction with the opening angle, which is obtained by a tiltmeter

near the trunnion. Typical plots of average torque (AVT), which is the average of opening and closing torques, with respect to the opening angle  $\theta$ , are given in Figure 3.39. The average torque changes with the horizontal distance between the trunnion and center of gravity, thus, it is a cosine curve. The positive region of this plot is unbalance towards the leaf side, and the negative region corresponds to unbalance towards the counter-weight (heel) side.

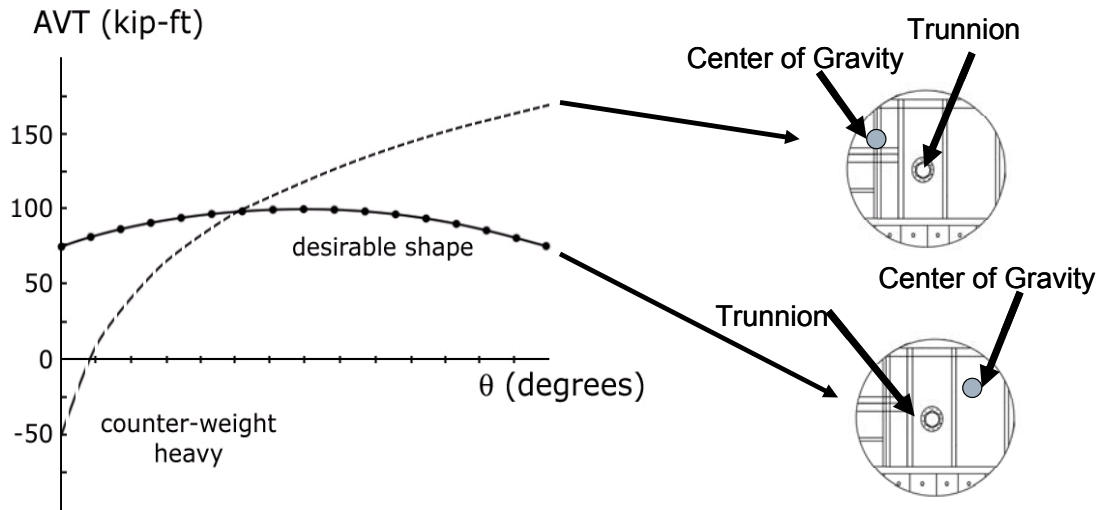


Figure 3.39 – Different cases of average torque during opening and closing

AVT is affected by environmental conditions, such as wind, and the friction in the system, which acts in the opposite direction of the movement. The friction is obtained from the difference between the opening and closing torques, as per the equation below;

$$T_f = \frac{T_o - T_c}{2} \quad (3.1)$$

where  $T_f$  is the friction torque,  $T_o$  is the opening torque and  $T_c$  is the closing torque. The friction number is indicative of lubrication on the trunnion, rack and gears, as well as related mechanical problems. Although there are no quantitative limits, maintenance is required when the friction number is calculated to be relatively high, in comparison with the previous values.

### **3.6.1. Field Test Data Analysis (Balance Test)**

The writers and FDOT personnel conducted bridge balance tests on two different movable bridges. The bridges were instrumented as described before. The raw data were provided by FDOT to the writers for analysis. In addition, the writers obtained data from past studies to track the bridge balance characteristics. Also, it is essential to determine the correlation between environmental conditions such as wind and the bridge balance, which may vary depending on when the test is conducted. The writers plan to collect environmental data in their future tests.

Average torque and friction torque were calculated and plotted against the rotation angle for Christa McAuliffe Bridge (Figure 3.40). The comparison of the three tests performed on different dates shows that the balance test results change significantly, affected by all rehabilitation, alteration and maintenance works, as well as due to possible deterioration effects. Although reduction of the total imbalance and friction can be associated with the overall rehabilitation work, the root reasons of the change in imbalance and friction numbers should be further explored. In the current practice, the change in friction with respect to baseline is considered and some rules of thumb in terms of bridge balance are employed based on the engineers' experience. To track the bridge balance and imbalance and their interaction with other phenomena such as environmental effects, it is clear that the balance tests should be part of the movable bridge SHM application, to be performed real-time for each bridge operation in order to track the balance condition dependably and identify the interaction of deterioration and maintenance actions.

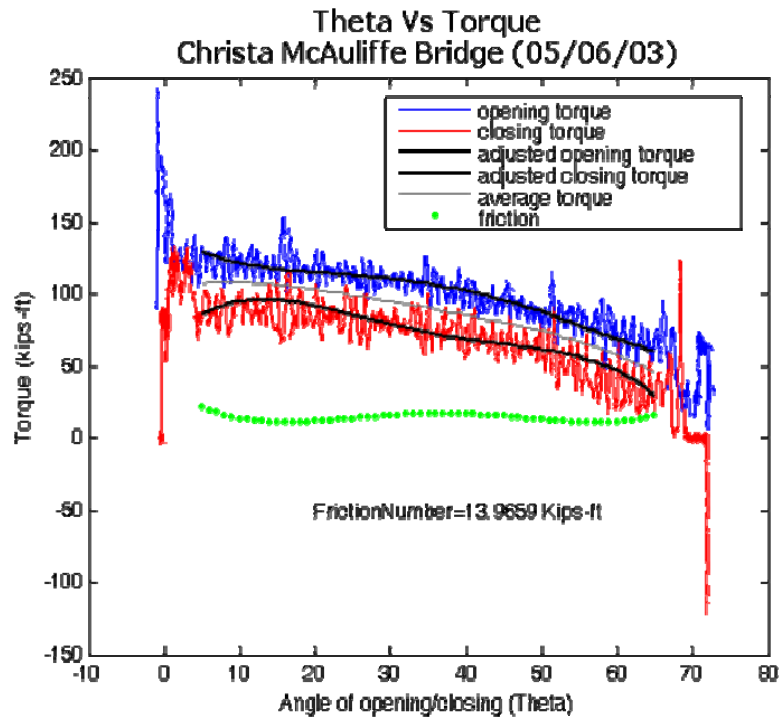


Figure 3.40 – Balance test results for March 2003

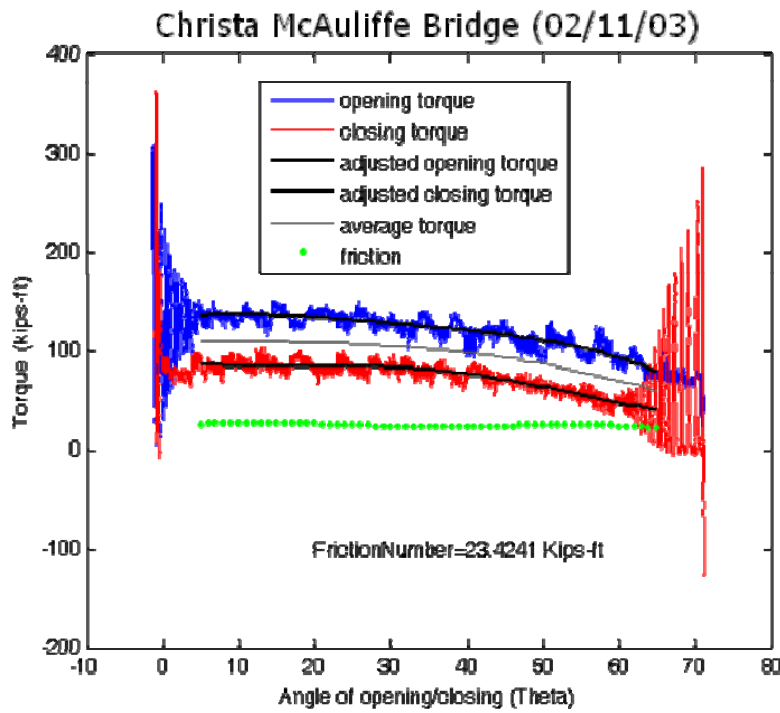


Figure 3.41 – Balance test results for February 2003

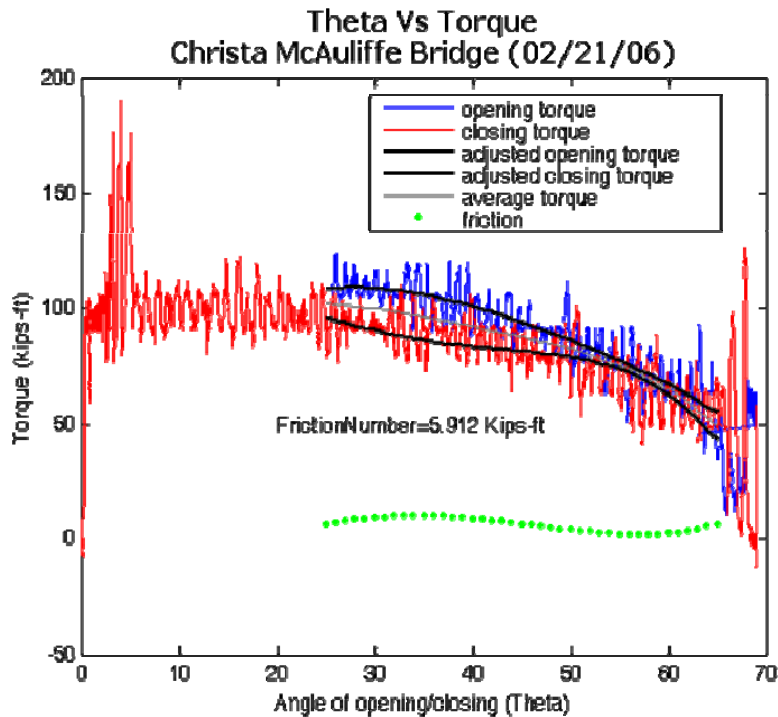


Figure 3.42 – Balance test results for February 2006

The average torque curves from the three tests at Christa McAuliffe Bridge are similar, indicating similar balance conditions. However, there does not exist a rationale to judge if the average torque values are within acceptable values. Standards need to be set, justifying the limits of average torque values and the friction numbers. As seen in Figure 3.43, friction coefficient changes radically at each test, and it can only intuitively be related to the change of condition in the system. The majority of the friction is assumed to be coming from the trunnion friction; therefore, the lubrication in the trunnion is closely related to the friction numbers. The relation between the friction number and the trunnion maintenance should be studied, and thresholds should be established for trunnion lubrication.

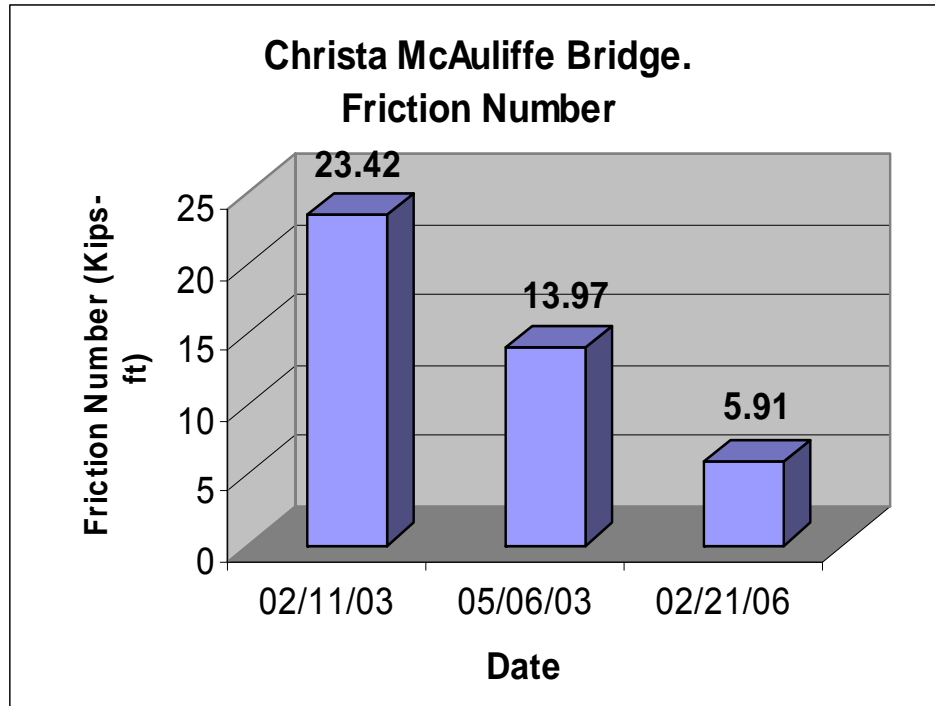


Figure 3.43 – Change of friction values

## **4. MODEL CALIBRATION, SIMULATIONS AND RATING**

### **4.1. INTRODUCTION**

In this section, the finite element model is calibrated using balance test data, and several simulations have been conducted to evaluate the response of the structure and also to determine possible instrumentation locations. As a result, analytical studies enabled the researchers to understand the structural behavior of the bridge, as well as determining the roles of the critical components, such as the trunnions, live load shoes, and the span locks. Analysis results and load rating helps with assessing the current condition of the bridge and predicting possible structural problems, therefore, enabling an instrumentation layout plan that can capture the major features identified from the analyses. All the analyses were conducted after calibrating the finite element model to match the balance data that was collected by a field test, since the balance condition is very critical for bascule cases, and the model needs to be calibrated to reflect the actual behavior.

### **4.2. CALIBRATION OF THE MODEL ACCORDING TO THE BALANCE CONDITION**

The balance condition of the leaves was made to represent the same results with the latest balance test conducted on the Christa McAuliffe movable bridge. The test was performed by FDOT Materials Lab personnel and accompanied by UCF researchers. The FDOT staff supplied the raw data and the test results, which were then analyzed by the UCF researchers. The analysis procedure and results are given in Section 3.3.1, and they were also used to calibrate the finite element model of the bridge. In order to provide the same balance condition, only a single leaf of the bridge model was analyzed, fixing at the trunnion and removing the live load shoe support. The weight of the counterweight was adjusted by iteration to match with the calculated imbalance moment.

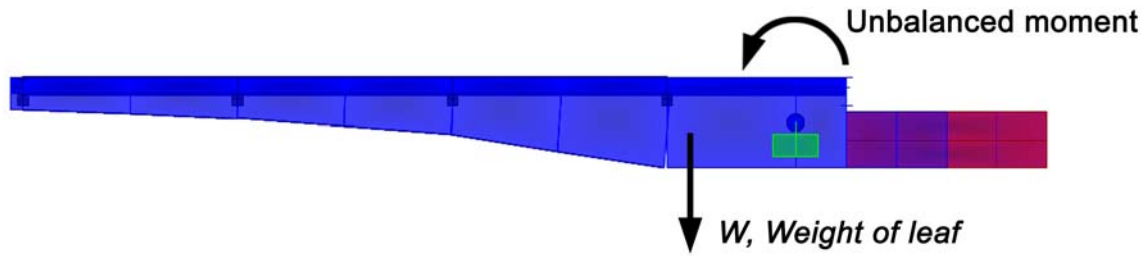


Figure 4.1 – Balance condition of the leaves

### 4.3. ANALYSIS AND LOAD SIMULATION RESULTS

#### 4.3.1. Loads Used for FE Simulations

The bridge model was analyzed under a vehicular load corresponding to the AASHTO HL-93 design truck.

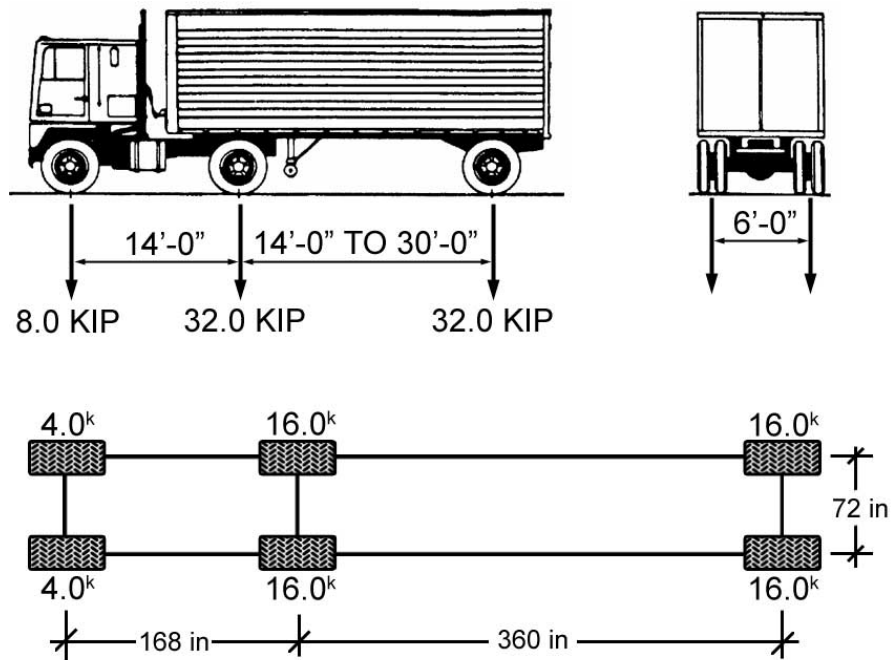


Figure 4.2 – AASHTO HL-93 Design Truck

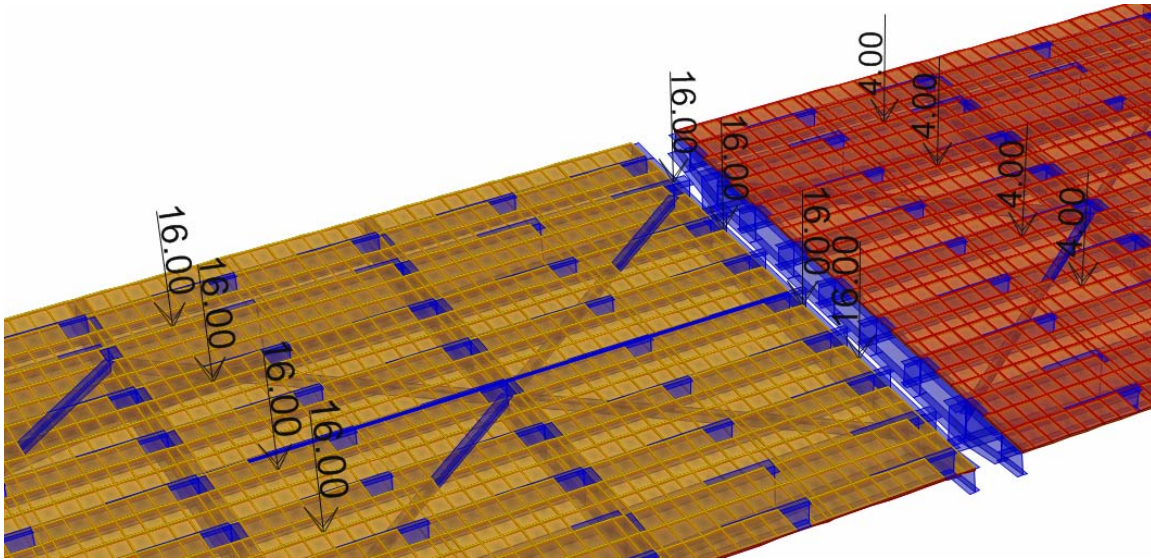


Figure 4.3 – Loading for load rating and serviceability of the bridge  
(Two HL-93 trucks and distributed lane load)

Once finished and loaded, the model realized the analysis of the bridge showing the following results.

#### 4.3.2. Deflections

Deflection was calculated from the finite element model analysis with two HL-93 standard truck loading and lane loading as specified by the AASHTO Manual. Load factors are 1.0 since deflection is a serviceability check. The allowable deflection specified is  $\delta_{\max} = L/300$  for orthotropic plate decks with vehicular load on deck (AASHTO 2.2.2.6.2), where L is the span length, 140 ft in the current case. The deflection was checked to be below this specified value. Figure 4.4 shows the deflected shape and the displacement values at the tips.

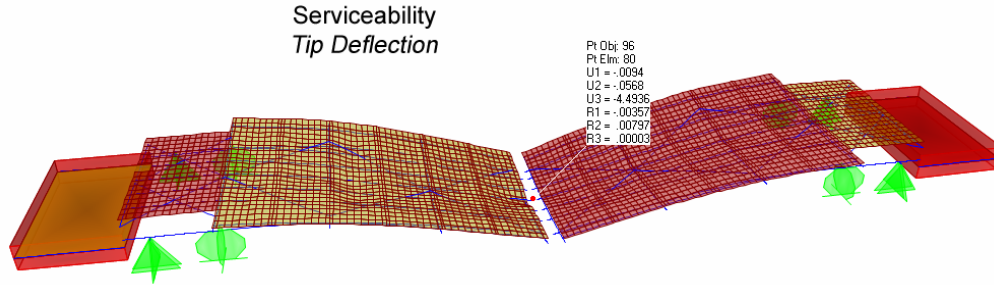


Figure 4.4 – Deflections at the center.

Values for vertical deflection at the center are -4.49 in. under serviceability load conditions and the maximum permitted, which is equal to approximately 5.6 in. Deflection was also calculated for the load cases considering only dead load, only single HL-93 truck load, and both combined. The deflection results are shown in Figures 4.5 to 4.7, for the respective load cases.

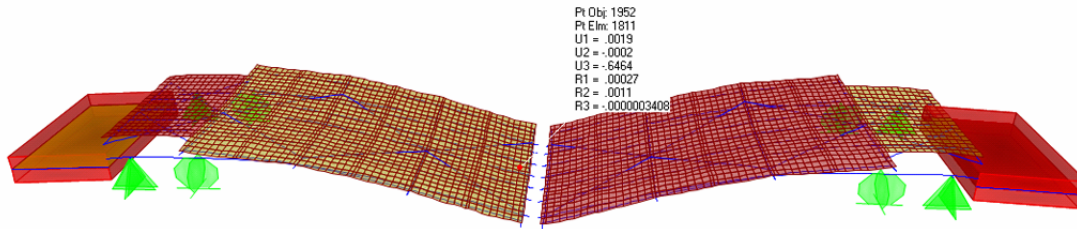


Figure 4.5 – Tip deflection for Dead Load (in)

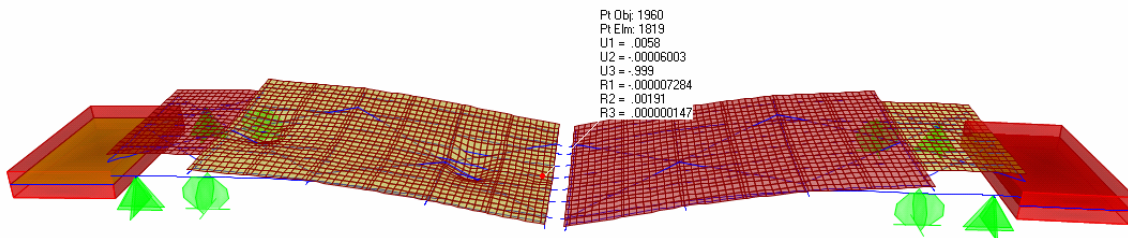


Figure 4.6 – Tip deflection for Truck Load (in)

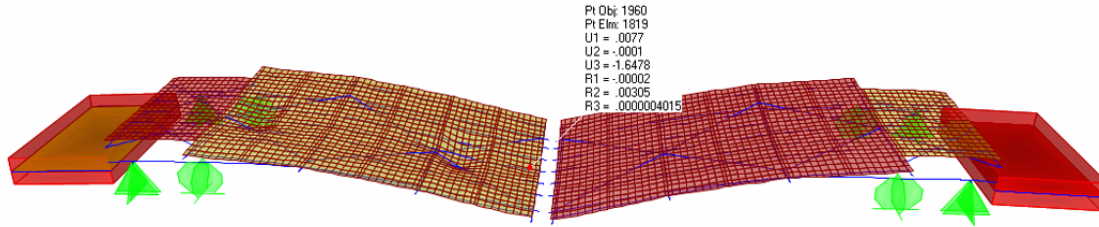


Figure 4.7 – Tip deflection for Dead Load and Truck Load (in)

### 4.3.3. Stresses

Von Mises stress, based on the yield criterion of the same name, is defined as;

$$\sigma_{vm} = \sqrt{\frac{1}{2}[(\sigma_1 - \sigma_2)^2 + (\sigma_1 - \sigma_3)^2 + (\sigma_2 - \sigma_3)^2]} \quad (4.1)$$

where  $\sigma_1$ ,  $\sigma_2$  and  $\sigma_3$  are the principal stress values at the point of concern. For steel plate structures, Von Mises stress is a better indication of the yielding condition, since the stresses are usually biaxial. The initial model with shell elements was evaluated to obtain the Von Mises stress distribution over the main girders. The initial model with shell elements was evaluated to obtain the Von Mises stress distribution over the main girders, and the results for only dead load, only truck load and combination are shown in Figures 4.5, 4.6 and 4.7, respectively. In this analysis, load factors have not been used. Von Mises stresses due to combined dead and live load are seen to be around 6-12 ksi (Figure 4.7) compared to 36 ksi yield stress of the steel girders.

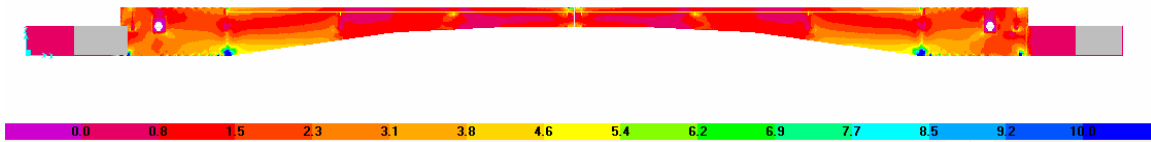


Figure 4.8 – Von Mises stresses for Dead Load (ksi)

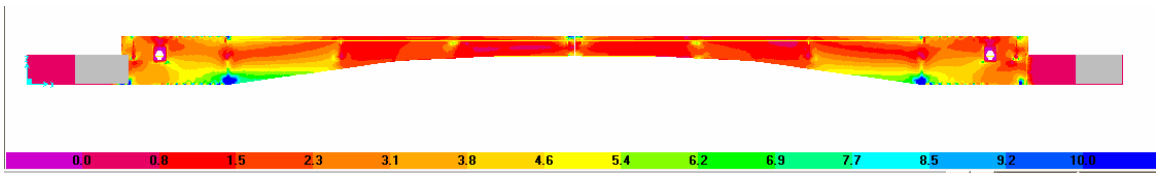


Figure 4.9 – Von Mises stresses for Truck Load (ksi)

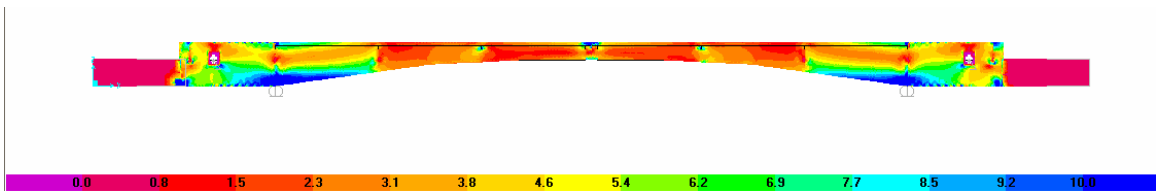


Figure 4.10 – Von Mises stresses for Dead Load and Truck Load (ksi)

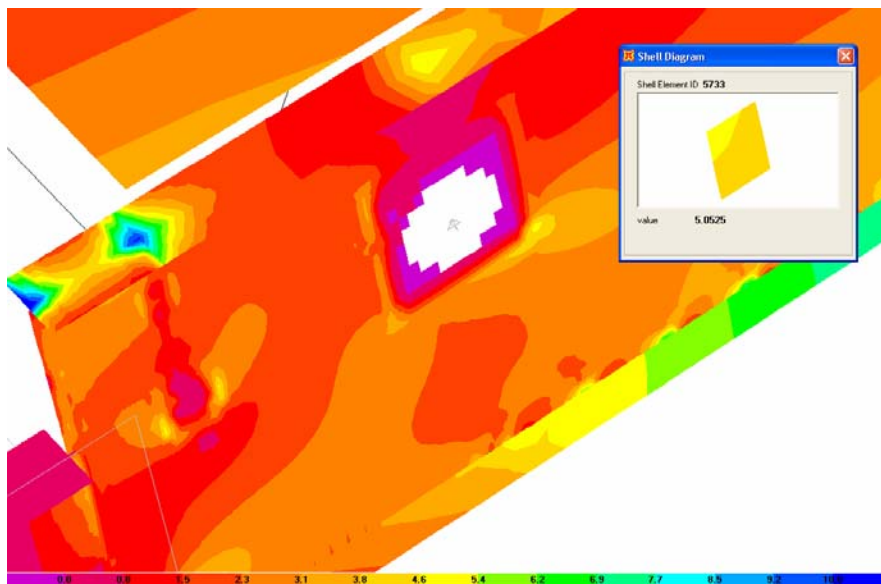


Figure 4.11 – Von Mises stresses at the THG connection for Dead Load (ksi)

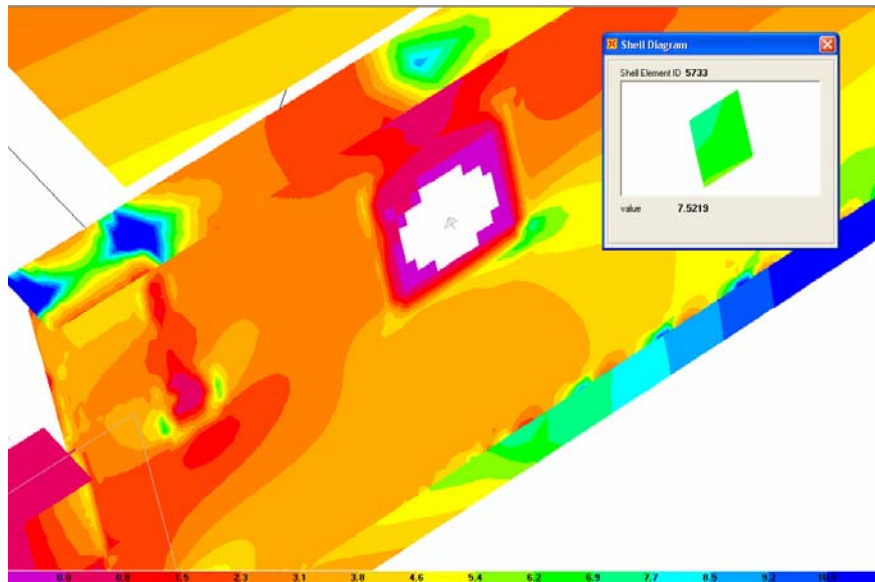


Figure 4.12 – Von Mises stresses at the THG connection for Truck Load (ksi)

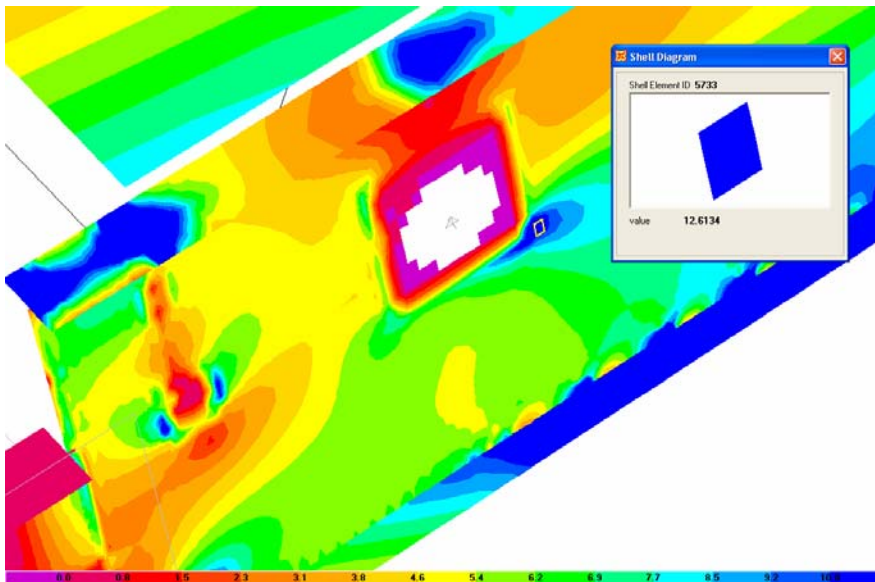


Figure 4.13 – Von Mises stresses at the THG connection for Dead Load and Truck Load (ksi)

Figures 4.8, 4.9 and 4.10 show the Von Mises stress distributions around the trunnion region for only dead load, only truck load and combined, respectively. One of the highest stress levels (around 12 Ksi) is observed at the trunnion region, since it is where the total moment is resisted (Figure 4.10). As an extreme condition, the live load

shoe was removed for this analysis in order to simulate the opening action, when all the balance is provided by the driving torque at the trunnion.

Another high stress concentration occurs at the span lock (Figure 4.7). Here, stress values of around 10 ksi were observed. It is important to notice that this is an area subjected to constant impact from the traffic and is highly susceptible to fatigue.

The live load shoes and the girder area in contact with them is another high-stress location also prone to fatigue. Stress values are around 15 ksi for these particular positions when bridge is in closed position and loaded as shown in Figure 4.3. We also note that high stress values are localized and numerical model results for stresses are to be verified with field measurements.

#### 4.3.4. Dynamic Analysis

Dynamic analysis of the finite element model provided the natural modes and frequencies of the structure. Mode shapes also provide another means of checking the model for accuracy and errors as well as global response of the bridge (Figures 4.11 to 4.16).

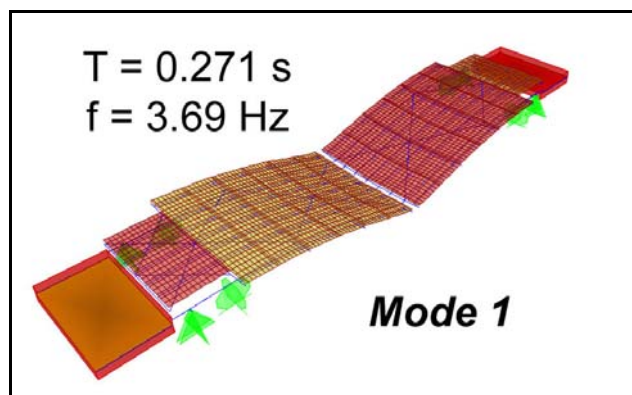


Figure 4.14 – Modal analysis results: Mode 1

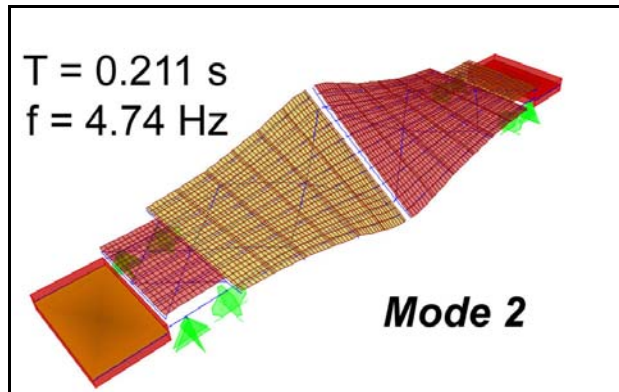


Figure 4.15 – Modal analysis results: Mode 2

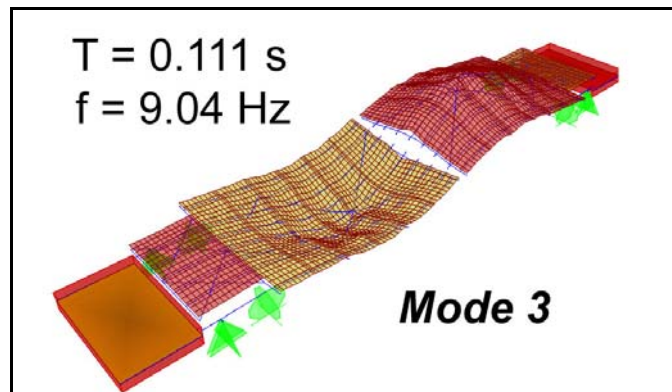


Figure 4.16 – Modal analysis results: Mode 3

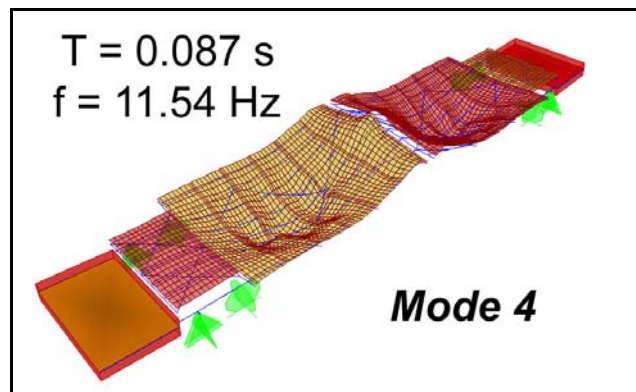


Figure 4.17 – Modal analysis results: Mode 4

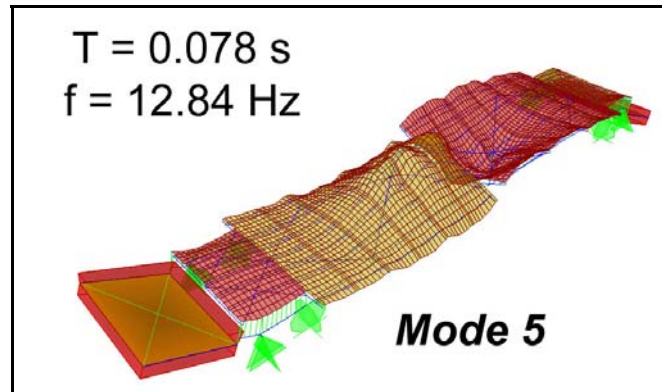


Figure 4.18 – Modal analysis results: Mode 5

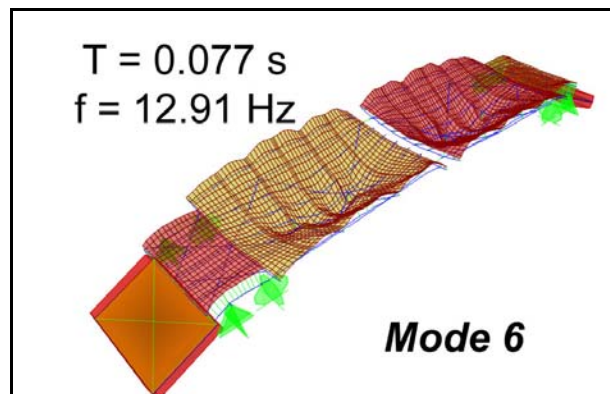


Figure 4.19 – Modal analysis results: Mode 6

Dynamic properties of bridges are mainly used for calibrating the finite element models with dynamic tests. Mode shapes indicate the behavior of the structure, helping identify most influential dynamic load types. Natural frequencies are also useful for assessing the dynamic load effect, which may excite the system with resonance. Changes in frequencies and modes are monitored for assessing damage and/or deterioration, since these effects tend to shift these parameters significantly. We also note that any major imbalance can be determined from tracking the frequencies since imbalance may be due to mass redistribution, which directly affects the dynamic properties.

Span lock failure can also be detected from dynamic properties. In a scenario where one of the span locks breaks, it is shown that the mode shapes and natural frequencies of the bridge do not differ, but new mode shapes appear in between the first

three modes. These new modes can easily be identified from vibration tests, determining instantly any failure of the span locks.

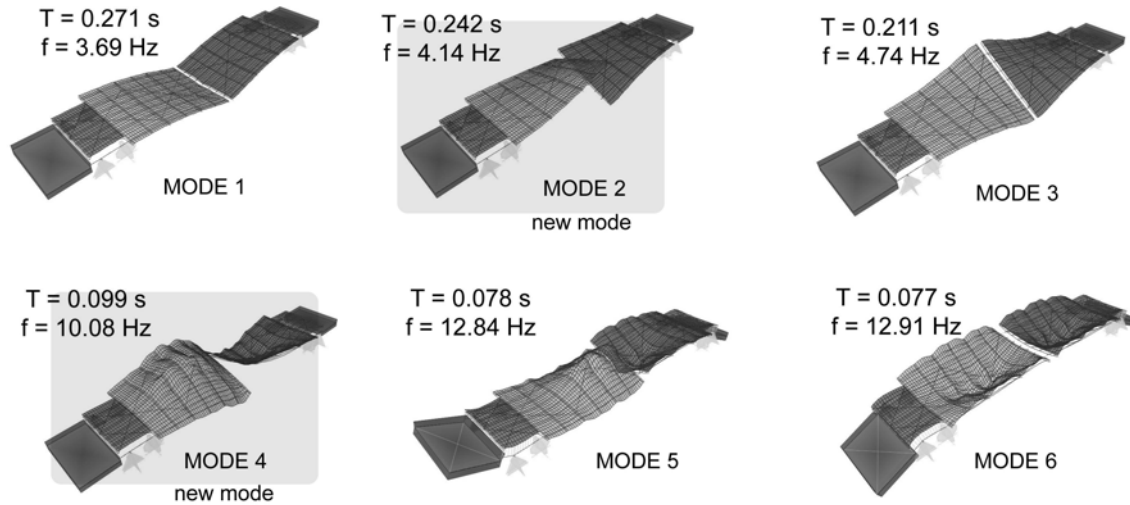


Figure 4.20 – Additional mode shapes for a span-lock failure scenario

#### 4.3.5. Examples of Location for Monitoring Based on FEM

Trunnion is the pivot point of rotation for the bascule leaf. According to FHWA, fracture critical member is “a member in tension, or with a tension element, whose failure would probably cause a portion of or the entire bridge to collapse.” (FHWA Report 2002). Therefore, trunnions can be accepted as fracture critical components for the operation of the movable bridges. The FE model also indicates high stress concentration in the vicinity of the trunnion.

Connection between the girder and the trunnion is a highly critical location, where problems such as cracking, misalignment and corrosion are commonly observed. It is a very important part of the mechanical system, and it should be monitored.

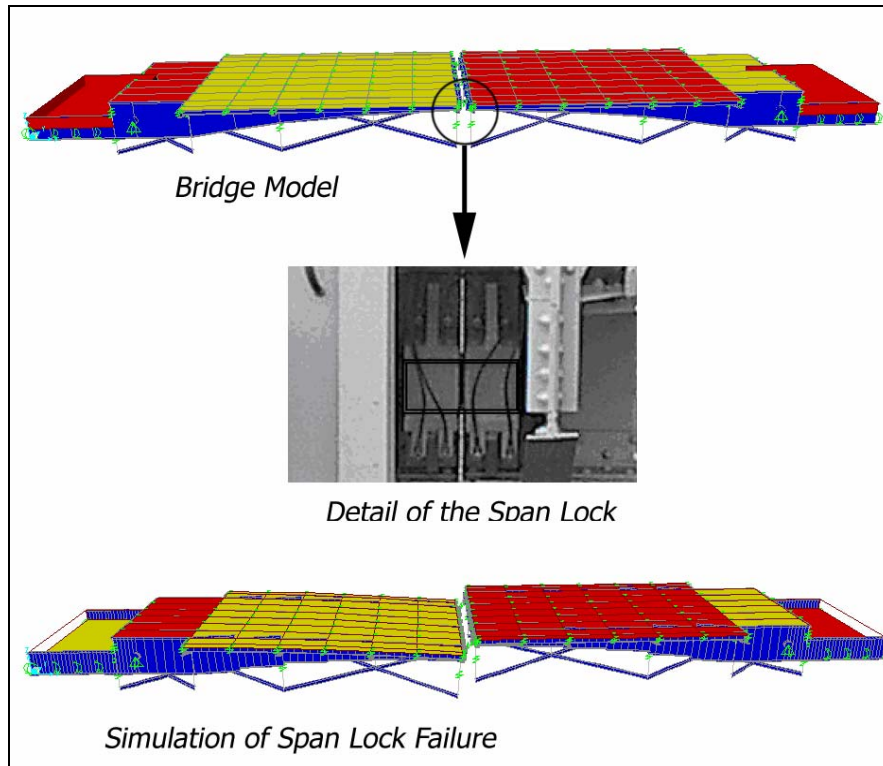


Figure 4.21 – Span lock failure simulation

Span lock, which holds the two spans together and assures the same vertical displacement of the tips is also critical. The effect of failure of the span lock was investigated by removing the links connecting both leaves at the tips in the finite element model. When the span lock is removed, the model shows that the leaves deform independently of each other causing up to approximately 1.5 in. difference in vertical displacement. Monitoring and maintenance of the span locks is essential to ensure proper function.

#### **4.4. MOVABLE BRIDGE LOAD RATING**

Load rating analysis is another approach to evaluating live load carrying capacity of the bridges. Load rating also indicates the critical locations and often load rating results of FEM can further be verified by experimental measurements.

Load rating of the movable bridge was calculated following the AASHTO Guide (AASHTO 2002). Bending capacity, including lateral torsional buckling effect, and shear

capacity were calculated as deterministic values. Critical positions of the standard (HL-93) truck load were used to obtain the maximum live load moment and shear. The sections selected for load rating are the joints at the floor beams.

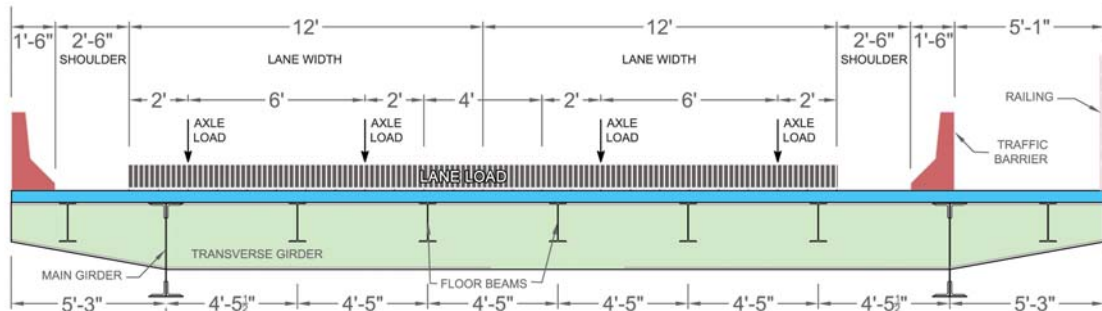


Figure 4.22 – Transverse loading

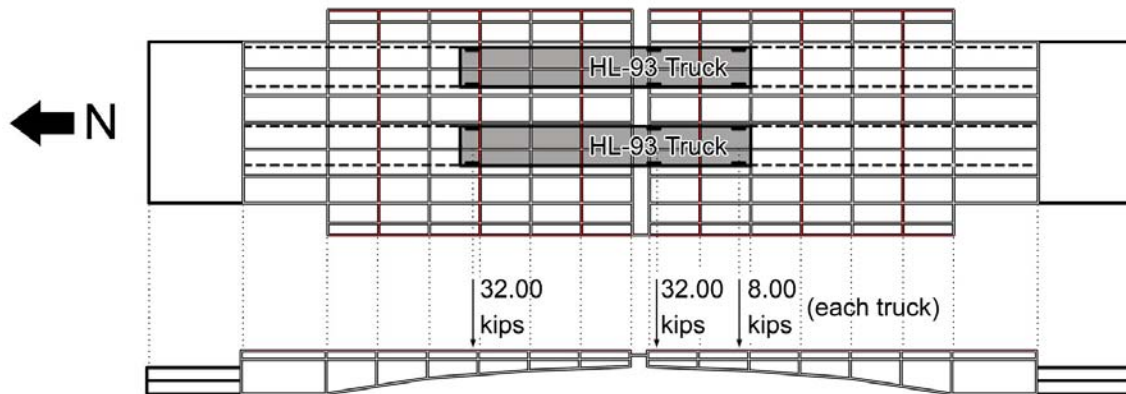


Figure 4.23 – Truck position for load rating (lane load not shown)

The transverse cross-section of the deck (Figure 4.22) shows the location of the lanes and axle positions for the HL-93 standard truck loading. Since a three-dimensional model was used, axle loads were defined as individual point loads, and lane loading was ignored. The truck was placed at the midspan of the movable bridge, for the most critical loading condition, as shown in Figure 4.23.

The load rating can be expressed as the factor of the critical live load effect to the available capacity for a certain limit state. The general formula for the rating factor is;

$$RF = \frac{C - \gamma_{DC}DC - \gamma_{DW}DW \pm \gamma_P P}{\gamma_L LL(1 + IM)} \quad (4.2)$$

where C is the factored load carrying capacity, DC is the dead load of structural components, DW is the dead load of the wearing surface, P is a dead load concentrated at a single point, LL is the live load effect, IM is the impact factor, and  $\gamma$ 's are the safety factors.

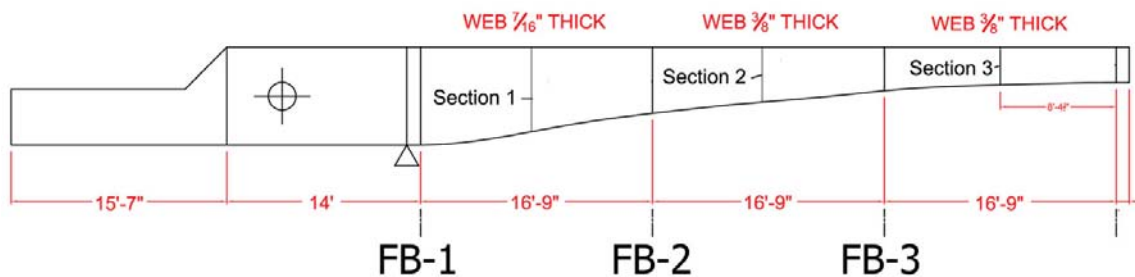


Figure 4.24 – Section locations for load rating

The load factors change according to the type of load rating, i.e., inventory load rating or operating load rating. The load ratings for the girder were calculated at the connections of the floor beams, as indicated in Figure 4.24. The capacity of the sections were calculated based on the ultimate moment capacity

$$M_u = F_y Z \quad (4.3)$$

where  $M_u$  = ultimate moment capacity;  $F_y$  = specified yield strength;  $Z$  = plastic section modulus.

The yield strength of the steel was given as 36.0 ksi. The plastic moduli was calculated from section sizes in the CAD drawing. Area of the bolts was deducted from the section size while calculating the plastic modulus. Then, following formula (1), the section moment capacities were found for the three sections as:

Table 4.1 – Section flexural capacity

<b>Location</b>	<b>Z (in<sup>3</sup>)</b>	<b>M<sub>u</sub> (kip·ft)</b>	<b>M<sub>u</sub> (kip·in)</b>
FB-1	137.5	4951.9	59422.8
FB-2	73.2	2634.8	31617.6
FB-3	29.4	1057.5	12690.0

The load effects (moments) on the sections were obtained from finite element analysis with the loading pattern shown in Figure 4.22.

Table 4.2 – Section moments from the load combination

<b>Location</b>	<b>M<sub>DL</sub> (kip·in)</b>	<b>M<sub>LL-TRUCK</sub> (kip·in)</b>	<b>M<sub>LL-LANE</sub> (kip·in)</b>
FB-1	8805.0	16579.5	4676.8
FB-2	3644.0	4321.3	1289.2
FB-3	940.4	1659.5	300.4

The dynamic impact factor is used as 33% for both inventory and operating ratings. The load factors change according to the rating type as follows;

Table 4.3 - Load factors

<b>Load Factor (<math>\gamma</math>)</b>	<b>Load Rating Case</b>	
	<b>Inventory</b>	<b>Operating</b>
DC	1.25	1.25
DW	1.25	1.25
LL+IM	1.75	1.35

According to the condition of the structural members of the bridge based on condition state or sufficiency rating, the condition factor allows for a reduction in the load rating up to 15%. Since Christa McAuliffe Bridge was recently rehabilitated, the condition factor,  $\gamma_c$ , is 1.0. The system factor was also taken as 1.0.

$$\begin{aligned}\gamma_c &= 1.0 \\ \gamma_s &= 1.0\end{aligned}\tag{4.4}$$

### Inventory Load Rating

$$\begin{aligned}\gamma_{DC} &= 1.25 \\ \gamma_{DW} &= 1.25 \\ \gamma_{LL+IM} &= 1.75\end{aligned}\begin{aligned} \text{FB-1} \quad \text{RF} &= \frac{C - \gamma_{DC}M_{DC}}{\gamma_{LL+IM}(1+IM)} = \frac{59422.8 - 1.25 \times 8805}{1.75 \times 21256.3} = 0.979 \\ \text{FB-2} \quad \text{RF} &= \frac{C - \gamma_{DC}M_{DC}}{\gamma_{LL+IM}(1+IM)} = \frac{31617.6 - 1.25 \times 3644}{1.75 \times 5610.5} = 2.072 \\ \text{FB-3} \quad \text{RF} &= \frac{C - \gamma_{DC}M_{DC}}{\gamma_{LL+IM}(1+IM)} = \frac{12690.0 - 1.25 \times 940.4}{1.75 \times 1959.9} = 2.524 \end{aligned}\tag{4.5}$$

### Operating Load Rating

$$\begin{aligned}\gamma_{DC} &= 1.25 \\ \gamma_{DW} &= 1.25 \\ \gamma_{LL+IM} &= 1.35\end{aligned}\begin{aligned} \text{FB-1} \quad \text{RF} &= \frac{C - \gamma_{DC}M_{DC}}{\gamma_{LL+IM}(1+IM)} = \frac{59422.8 - 1.25 \times 8805}{1.35 \times 21256.3} = 1.269 \\ \text{FB-2} \quad \text{RF} &= \frac{C - \gamma_{DC}M_{DC}}{\gamma_{LL+IM}(1+IM)} = \frac{31617.6 - 1.25 \times 3644}{1.35 \times 5610.5} = 2.686 \\ \text{FB-3} \quad \text{RF} &= \frac{C - \gamma_{DC}M_{DC}}{\gamma_{LL+IM}(1+IM)} = \frac{12690.0 - 1.25 \times 940.4}{1.35 \times 1959.9} = 3.272 \end{aligned}\tag{4.6}$$

Results of the load rating are tabulated in Table 4.4.

Table 4.4 – Load Ratings

Location	Load Rating	
	Inventory	Operating
FB-1	0.979	1.269
FB-2	2.072	2.686
FB-3	2.524	3.272

#### 4.5. MOVING LOAD SIMULATION

In order to determine the structural load carrying capacity, moving load simulations were carried out to obtain the reliability of the bridge in addition to the load rating. The reliability analysis incorporates a probabilistic approach with respect to the load effects and structural capacity.

The finite element model was used to simulate a standard AASHTO HL-93 truck traveling over the bridge. The truck load was applied as joint loads, with 12.5-in increments, which corresponds to about 0.015s steps for a truck traveling at 50 mph (Figure 4.25). This simulation was expected to provide the structural reliability of the bridge, and also simulate the sensor readings during a moving load for using in data-based reliability assessment.

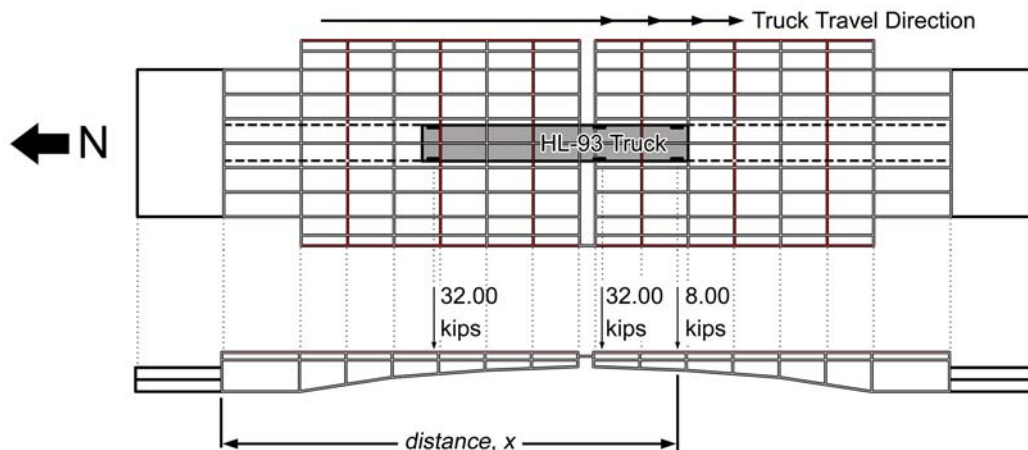


Figure 4.25 – Moving Load Analysis

The variation of moment values at each node on the main girder on the north span is shown in Figure 4.26. The horizontal axes in these graphs are the truck position, which is moving at a constant velocity.

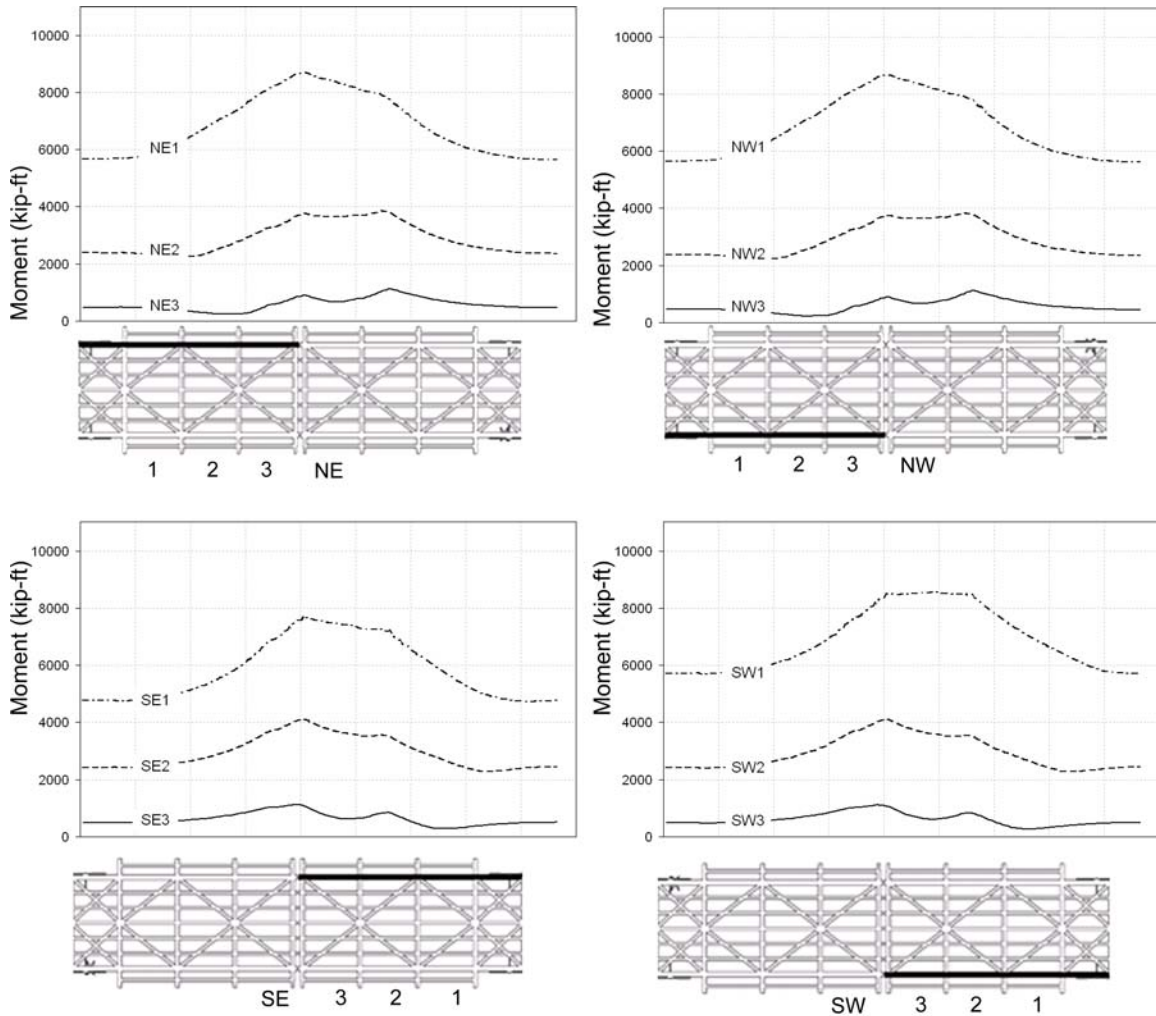


Figure 4.26 – Variation of Moment due to Moving Load over the Girder Locations

### Statistical Models of Random Variables

Probabilistic modeling of the structural capacity and load effects requires determination of the statistical parameters with the uncertainties of each parameter. Sources of variability are generally categorized as material factor (material properties), fabrication factor (imperfections) and analysis factor (assumptions, approximations) (Nowak and Collins 2000), and have been quantified by statistical studies in the literature. At least the mean value and the variance (or standard deviation, or coefficient of variation) should be known for reliability analysis. In this study, statistical distributions were used for the random variables.

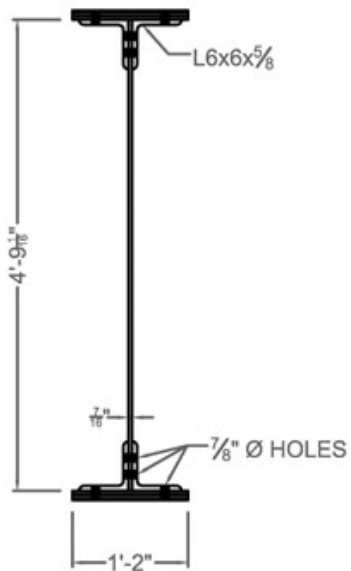
Nodal results obtained from the analytical simulation were taken as the nominal values of load effects, and assumed as normally distributed. The bias factor ( $\lambda$ ) for the load effect was taken as 1.15, and the coefficient of variation (cov) as 0.18 (Nowak 1995). Bias factor and coefficient of variation of other random variables are used as in Table 4.5. Yield strength of the structural steel was specified as 36 ksi.

Table 4.5 – Statistical Parameters of the Random Variables

<b>Variable</b>	<b>Moment of Inertia <math>I_x</math></b>	<b>Plastic Section Modulus <math>Z_x</math></b>	<b>Yield Strength <math>F_y</math></b>	<b>Truck Load <math>M_u, V_u</math></b>
$\mu$ (mean)	1.0	1.0	1.12	1.15
$\delta$ (c.o.v.)	0.05	0.05	0.0866	0.18
Type	Lognormal	Lognormal	Lognormal	Normal

Section properties were obtained for all the locations of concern over the main girders, and the cross beams. The modulus of inertia and the plastic modulus were taken as random variables, and used to calculate the yield and plastic moment capacity. The sections and corresponding properties are shown in Figure 4.27 to 4.26.

## Section 1

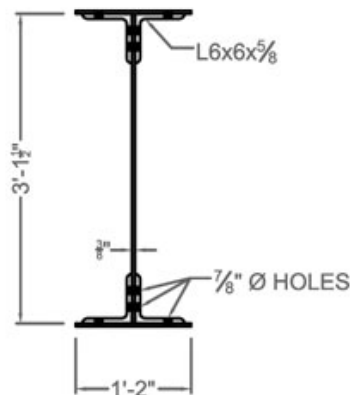


### SECTION PROPERTIES

Area:	23.0223 sq in
Perimeter:	106.1200 in
Bounding box:	X: -0.2188 -- 0.2188 in Y: -26.3112 -- 26.3113 in
Centroid:	X: 0.0000 in Y: 0.0000 in
Moments of inertia:	X: 5312.6504 sq in sq in Y: 0.3672 sq in sq in
Product of inertia:	XY: 0.0000 sq in sq in
Radii of gyration:	X: 15.1908 in Y: 0.1263 in
Principal moments (sq in sq in) and X-Y directions about centroid:	I: 0.3672 along [0.0000 -1.0000] J: 5312.6504 along [1.0000 0.0000]

Figure 4.27 – Section properties of Section 1 along the girder

## Section 2

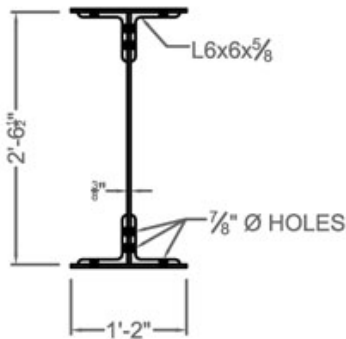


### SECTION PROPERTIES

Area:	44.1334 sq in
Perimeter:	137.5310 in
Bounding box:	X: -7.0000 -- 7.0000 in Y: -19.1250 -- 19.1250 in
Centroid:	X: 0.0000 in Y: 0.2342 in
Moments of inertia:	X: 11221.0794 sq in sq in Y: 297.9064 sq in sq in
Product of inertia:	XY: 0.0000 sq in sq in
Radii of gyration:	X: 15.9453 in Y: 2.5981 in
Principal moments (sq in sq in) and X-Y directions about centroid:	I: 297.9064 along [0.0000 -1.0000] J: 11218.6587 along [1.0000 0.0000]

Figure 4.28 – Section properties of Section 2 along the girder

### Section 3



#### SECTION PROPERTIES

Area:	40.8597 sq in
Perimeter:	121.5710 in
Bounding box:	X: -7.0000 -- 7.0000 in Y: -15.6350 -- 15.6350 in
Centroid:	X: 0.0000 in Y: 0.0000 in
Moments of inertia:	X: 7001.1138 sq in sq in Y: 297.8680 sq in sq in
Product of inertia:	XY: 0.0000 sq in sq in
Radii of gyration:	X: 13.0899 in Y: 2.7000 in
Principal moments (sq in sq in) and X-Y directions about centroid:	I: 297.8680 along [0.0000 -1.0000] J: 7001.1138 along [1.0000 0.0000]

Figure 4.29 – Section properties of Section 3 along the girder

### Component Reliability

Component reliability indices were calculated based on moment and shear failure modes. The main girders constitute the main load carrying components; therefore, they are the most critical members. Moment and shear failure modes at the sections selected for instrumentation were evaluated. Cross-beams were also considered for moment capacity.

For the moment limit state, two cases were considered; yield moment, and the plastic moment. The limit state function according to the yield moment capacity is;

$$g_M^{\text{yield}}(F_y, S_x, M_u) = F_y S_x - M_u \quad (4.7)$$

where the random variables are  $F_y$  (yield strength),  $S_x$  (section modulus) and  $M_u$  (applied moment on the section). For the plastic limit case, instead of  $S_x$ , plastic section modulus ( $Z_x$ ) was used, and the limit state function for this case;

$$g_M^{\text{plastic}}(F_y, Z_x, M_u) = F_y Z_x - M_u \quad (4.8)$$

For the shear failure limit state, two random variables were defined.  $V_r$  is the shear capacity, and it was taken as;

$$V_r = \frac{1}{3} A_w F_y \quad (4.9)$$

where  $A_w$  is the web area and  $F_y$  is the yield strength of the steel. The shear capacity was modeled as lognormally distributed. The bias factor  $\lambda_v$  was taken as 1.14 and the coefficient of variation, 0.106 (Nowak and Collins 2000). The shear load effect was again taken from finite element model results. The limit state for shear mode is;

$$g_V(V_r, V_u) = V_r - V_u \quad (4.10)$$

The defined limit state functions were evaluated at each joint to obtain the probability of failure. For nonlinear limit state functions, as in the current case, convenient first order approximations can be applied using Taylor series expansion to linearize the function with respect to the random variables. The limit state function is expanded with respect to each random variable about a certain point on the limit state surface. The linear approximation will be more accurate in the proximity of this pivot point, which is also called the design point. The coordinates of the design point are to be determined, which can be represented as values of the random variables  $(x_1^*, x_2^*, x_3^*, \dots)$ , or within the reduced variate space, as  $(z_1^*, z_2^*, z_3^*, \dots)$ . The distance from the origin to the design point in reduced variate coordinates gives the reliability index. The limit state function for plastic moment capacity was expanded around the design point as follows.

$$g(X_1, X_2, \dots, X_n) \approx g(x_1^*, x_2^*, \dots, x_n^*) + \sum_{i=1}^n (X_i - x_i^*) \left. \frac{\partial g}{\partial X_i} \right|_{(x_1^*, x_2^*, \dots, x_n^*)} \quad (4.11)$$

where  $X_1$  :  $F_y$ , the yield strength of the steel

$X_2$  :  $Z_x$ , plastic modulus of the section

$X_3$  :  $M_u$ , moment effect on the section due to dead load and moving load

The design point is calculated to be the minimum distance from the origin to the limit state surface in reduced variate space. Therefore, iteration is required for finding the design point. According to the procedure of the Rackwitz-Fiessler method (Rackwitz and Fiessler 1978), equivalent normal statistical parameters of the non-normal random variables were calculated. Since the yield strength ( $F_y$ ), plastic section modulus ( $Z_x$ ) and elastic section modulus ( $S_x$ ) were assumed as lognormally distributed, equivalent normal mean value and standard deviation of each of these random variables using the following formulae;

$$\begin{aligned}\sigma_x^e &= x^* \sigma_{\ln x} \\ \mu_x^e &= x^* \left[ 1 - \ln(x^*) + \mu_{\ln x} \right]\end{aligned}\quad (4.12)$$

Then, partial derivatives of the limit state function with respect to each random variable were obtained, and the sensitivity matrix was formed with these values. The derivatives for the plastic moment limit state were given below as an example. Partial derivatives for the other limit state functions were obtained similarly.

$$G_i = \left. \frac{\partial g}{\partial Z_i} \right|_{\text{design point}} = \left. \frac{\partial g}{\partial X_i} \right|_{\text{design point}} \frac{\partial X_i}{\partial Z_i} = \left. \frac{\partial g}{\partial X_i} \right|_{\text{design point}} \sigma_{X_i} \quad (4.13)$$

$$\begin{aligned}G_1 &= -X_2 \sigma_{X_1} \\ G_2 &= -X_1 \sigma_{X_2} \\ G_3 &= \sigma_{X_3}\end{aligned} \quad \{G\} = \begin{Bmatrix} G_1 \\ G_2 \\ G_3 \end{Bmatrix} \quad (4.14)$$

An initial design point was assumed for the first cycle of iterations, in order to obtain the first estimate of the reliability index. The iterative process was set up in MATLAB software, which used finite element output at the required nodes and computed the reliability index for all limit state functions and the system reliability for each given truck position.

## System Reliability

System reliability is a major concept in reliability analysis, because individual limit state functions are assembled together in a system model. The failure conditions are determined by the system model, since failure of one or two members may not be important due to redundancy. On the other hand, there may be critical components (fracture-critical) which have to stay intact for the structural integrity of the whole system.

System reliability can be modeled with certain assumptions, including assembling the failure limit states as parallel or series links after determining the failure modes. Evaluation of a system model is performed by reducing first the parallel components. System failure probability of parallel systems are solved by;

$$(P_f)_i = \prod_{k=1}^n (P_f)_k, \text{ n: \# of parallel members} \quad (4.15)$$

Therefore, the model is reduced to only serially connected members. Failure of each component means failure, so all the components should survive for structural integrity. So, the resulting series system can be solved by the following;

$$(P_f)_{\text{system}} = 1 - \prod_{i=1}^m [1 - (P_f)_i], \text{ m: \# of series components} \quad (4.16)$$

Parallel and series models of the movable bridge structural components were constructed according to the most general structural failure mechanisms. The main components of the system were the main girder bending failure state, main girder shear failure state, and the moment failure of the transverse beams. The main girder failure states were assumed as the failure condition at any of the monitored sections. These sections, however, are not fully independent, therefore cannot be modeled as acting in series. Accounting for the correlation of the failure probabilities at these sections, two limit cases were considered. The first case is assuming no correlation between the failure of monitored sections, which can be modeled as a series system in this case, and the

second case is modeling them as fully correlated limit states, so the failure of the main girder system depends on the section with the highest probability of failure. The system model is shown in Figure 4.30, which illustrates the lower bounding case.

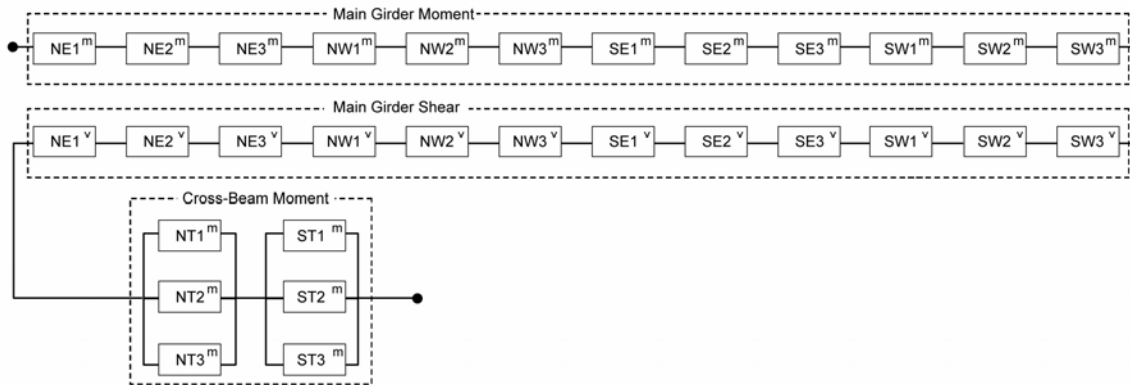


Figure 4.30 – Movable Bridge System Reliability Model with Parallel/Series Assembly (Lower Bound)

The system reliability was first calculated according to the same load case as employed for the load rating calculations. Results of the finite element analysis were used to generate the input variables, and the reliability was obtained as 3.24 for the lower bound, and 3.37 for the upper bound case and these values can be considered acceptable since AASHTO LRFD designs are based on a reliability index of 3.5 for new bridges and AASHTO Load and Resistance Factor Rating (LRFR) considers 2.5 for existing bridges.

Reliability analysis was also performed for the moving load case, where a single standard truck is simulated crossing the bridge. The results for each position of the truck were obtained from the finite element simulation and processed by the component and system reliability algorithms developed in MATLAB. The result of the system reliability analysis is plotted in Figure 4.31, for plastic moment capacity. The horizontal axis is the truck position, which can also be regarded as time. The vertical axis shows the reliability index, which changes according to the position of the truck.

It should be noted that high reliability values obtained from this analysis are due to the presence of a single truck without lane loading, and also excluding any wind load. This analysis was conducted to demonstrate the monitoring of reliability at a single

instant based on the collected measurements. The minimum reliability index was calculated as 5.79 when the middle axle of the truck arrives at the midspan. The calculated reliability is relatively high, since the simulation uses a single truck crossing the bridge without lane loads or additional load cases.

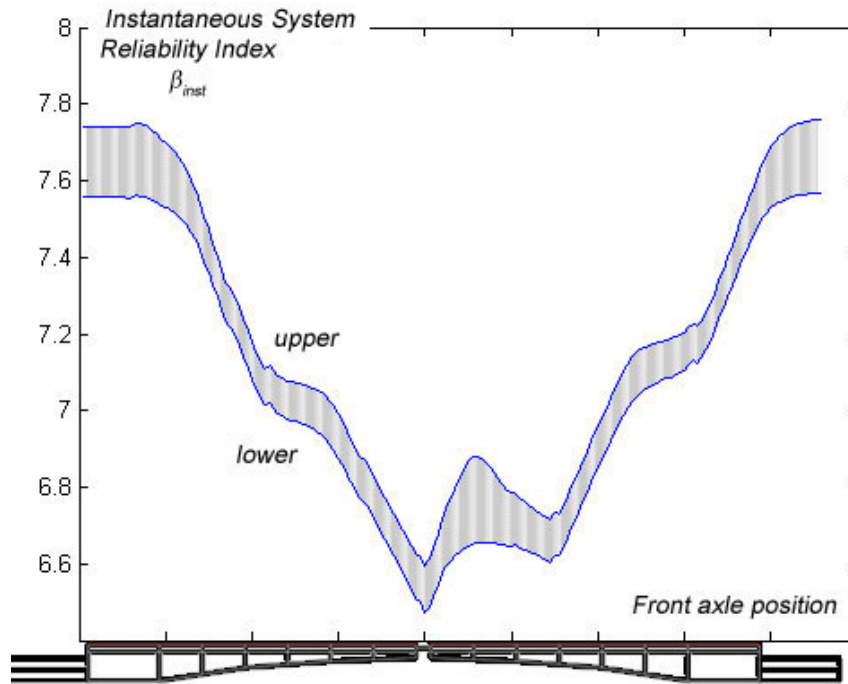


Figure 4.31 – Instantaneous System Reliability under a Single Moving Truck (note that this is for one moving truck without lane load, wind, temperature)

The reliability obtained here is not a formal reliability analysis result, since an instant in time is selected instead of the life span of the structure. This is to demonstrate the changes in reliability in real time and to layout a framework to incorporate instantaneous reliability into life-cycle reliability analysis of the structure.

Safety indices based on component or system reliability can be evaluated with much higher accuracy and confidence over the long term throughout the monitoring process. Component-based monitoring data should be assessed to produce reliability of each monitored structural component, and deterioration with time. Components to be instrumented and the parameters to be monitored should be carefully selected.

SHM techniques make it possible to retrieve information about the status of individual elements of a bridge. Since every component requires unique maintenance work, these operations can be scheduled more specifically and efficiently. Also, once individual deterioration and maintenance models are available for each critical node, a network reliability analysis can be conducted within the bridge components, in order to determine the most critical components (parallel/series reliability). Structural condition state and reliability are to be determined from component data. Reliability of the structural system depends on reliability of its components, so if there is no redundancy, the weakest link will determine the overall reliability. Presence of redundant members makes it necessary to perform a system reliability analysis, modeling the structure as parallel and/or series combinations of the components (Susoy et al. 2006a; Susoy et al. 2006b).

#### 4.6. SUMMARY OF ANALYSIS RESULTS

The results of the finite element model analysis for specific locations are shown in the table below. The results are listed according to three cases;

- Only dead load,
- Only a single standard (HL-93) truck at the tip without dead load
- Dead load and a standard truck (HL-93) at the tip

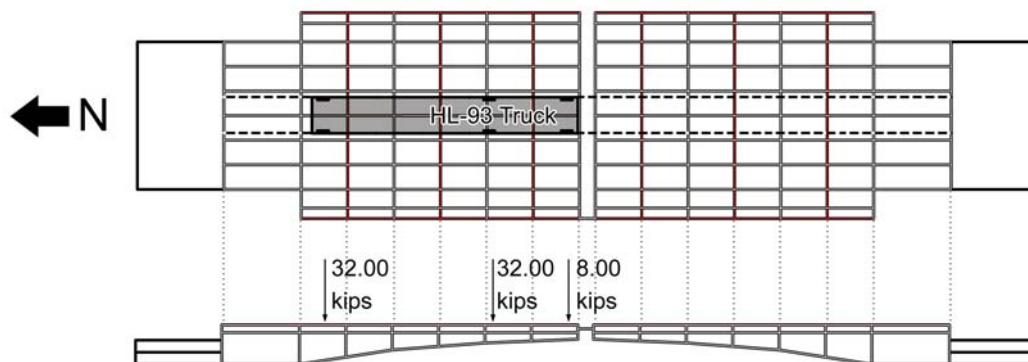


Figure 4.32 – Loading position for FEM analysis results

Vertical reactions at support locations, which are the trunnion (pin support) and live load shoe (roller support) are provided. The span-lock shear is also given as it indicates the load transfer provided by the span-lock assembly. The maximum moment on the main girders and the transverse beams are shown. Finally, the tip deflections for the mentioned load cases are included.

Table 4.6 – Summary of analysis results (reactions and deflections)

<b>Feature</b>		<b>Units</b>	<b>Dead Load</b>	<b>Truck Load*</b>	<b>Dead Load + Truck Load*</b>
<i>Reactions</i>					
1	Trunnion	(kips)	161.74	126.28	288.02
2	LL Shoe	(kips)	73.63	138.48	212.11
<i>Shear</i>					
1	V <sub>Span-Lock</sub>	(kips)	7.337	12.92	20.269
<i>Moment</i>					
1	max M <sub>girder</sub>	(kip·in)	8026.3	11223.8	19250.1
2	max M <sub>transverse</sub>	(kip·in)	383.5	1112.5	1495.6
<i>Deflection</i>					
1	δ <sub>tip</sub>	(in)	0.647	0.999	1.648

\* Single HL-93 Truck without lane load applied

\*\* Results are from FEM 2

Stress distributions over the girder and around critical regions are given in the previous sections. Results of stress distributions indicate the critical regions and aid understanding of the load transfer mechanism. Stress values around critical features such as trunnion, live load shoe and span locks are given in Table 4.7. Maximum observed stresses around the points of interest are reported, although stress values are susceptible to stress concentrations, meaning shown results can be accepted as conservative.

Table 4.7 – Summary of analysis results (stresses)

<b>Location</b>	<b>Units</b>	<b>Dead Load</b>	<b>Truck Load*</b>	<b>Dead Load + Truck Load*</b>
Trunnion	(ksi)	~5.1	~7.5	~12.6
Live load shoe	(ksi)	~6.4	~8.7	~15.1
Span lock	(ksi)	~5.2	~6.9	~12.1

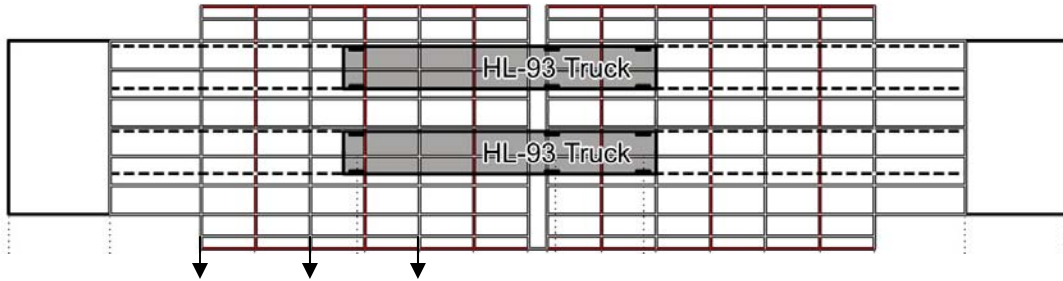
First modal frequencies and periods according to the dynamic analysis of the bridge are given in Table 4.8.

Table 4.8 – Modal frequencies and periods for the movable bridge

<b>Mode #</b>	<b>Mode Type</b>	<b>Frequency (Hz)</b>	<b>Period (s)</b>
1	Vertical	3.69	0.271
2	Torsional	4.74	0.211
3	Vertical	9.04	0.111
4	Vertical	11.54	0.087

Load rating of the main girder based on HL-93 load case (two trucks each 72 kips and a lane load of 0.64 kip/ft as shown in Figure 4.22) was calculated, and shown in Table 4.7 for the position over the live load shoe location. A load rating value below 1.0 means inadequate in terms of strength, therefore, the calculated inventory load rating is found to be slightly under 1.00. The load rating can be further investigated using actual SHM data, and rating formulation can be modified using results such as measured dynamic impact factors.

Table 4.9 – Load rating results for the main girder at the LLS



	<b>FB-1</b>	<b>FB-2</b>	<b>FB-3</b>
<b>Inventory</b>	0.979	2.072	2.254
<b>Operating</b>	1.269	2.686	3.272

The system reliability of the movable bridge was obtained as 3.24 for the lower bound, and 3.37 for the upper bound case, for the same load case with the load rating calculations.

## **5. INTEGRATED STRUCTURAL HEALTH MONITORING DESIGN**

### **5.1. INTRODUCTION**

Data from an SHM system can provide information related to structural performance as well as condition based maintenance during the monitoring period. For movable bridges, maintenance of mechanical and electrical components are as important as maintenance of structural components. The most common types of machinery and related problems need to be investigated in order to propose monitoring solutions to detect those problems, track their development, and plan for corrective action before failure. In this chapter, sensors and data acquisition systems along with data analysis and management techniques are discussed. At the end of the chapter, critical electrical, mechanical and structural components for movable bridges are summarized and possible SHM designs are presented.

### **5.2. SENSORS AND SENSOR NETWORKS**

All kinds of sensors work by transforming physical changes in the environment or the structure into a measurable signal. Sensors are desired to be insensitive to the changes in parameters other than the measured quantities. Those physical and/or environmental changes alter the response of the sensing unit to a given excitation. The relation between the ratio of response to the input excitation and the measurand is established through calibration, which is usually provided by the manufacturer and may be repeated at certain intervals.

The most basic and commonly applied types of measurement parameters are related with basic physical responses of structures, such as strain, displacement, acceleration, tilt and environmental conditions such as temperature, wind speed and direction, and humidity. There are various types of sensors with different technologies, but here, only the most widely used types and their operation principles will be described first.

In this respect, all sensors have characteristics that specify their measurement behavior, making them suitable for certain types of applications and unsuitable for others. The main characteristics of sensors we are concerned with are listed below. The basic sensor and measurement properties should be specified for all sensors by the manufacturer, and the other characteristics can be quantified with further calibration tests (Aktan et al. 2003; Dunn 2005).

Sensitivity: This is the amount of change in the output of a sensor in response to a change in a sensor's input. Sensitivity is defined as the ratio of output to input, and is an important characteristic related with the precision and accuracy of the measurement. It may be considered as the slope of the calibration line for the sensor measurement.

Resolution: The smallest measurable change in input that will produce a small but noticeable change in the sensor output. This defines how small a change in the measurand can be detected by the sensor.

Discrimination: Also referred to as the limit of detection, this is the smallest increment of a measurement that can be discerned.

Range: The maximum and minimum values of the measured occurrence that can be measured with the sensor define the range property. Sensors will not be able to capture the changes beyond those limits.

Hysteresis: The maximum deviation between the measurement obtained by increasing and decreasing values of the measurement. Hysteresis error can be caused by the sensor's physical changes to the reversal of the conditions, or the structure's inherent hysteresis behavior. It is specified as the maximum difference between the measurements taken at both situations.

Accuracy: This is the closeness of a measurement to the value defined to be the true value of the measurand. The true value refers to an accepted and traceable standard and is usually compared to the sensor measurement during calibration. Accuracy is a qualitative concept and is the combined error of nonlinearity, repeatability, and hysteresis. Accuracy

is usually expressed as a maximum positive or negative percent of the full scale (FS) of the output.

Linearity: The measurements usually do not follow the calibration curve over the entire range linearly. Linearity defines the deviation of measurements from the linear calibration line.

Repeatability: Obtaining the same output value for repeated measurements of the same quantity specifies the repeatability of the instrument.

Stability: This refers to the ability of a sensor to maintain its calibration value over an extended time period. Sensors with good stability are preferred for long-term measurements in order to avoid the errors due to the drift in the measurements. Drift is the continuous upward or downward change of measurements mostly due to environmental effects.

The measurements are subject to errors due to instrumental properties and uncertainties listed above, as well as other sources. Installation is a major source of uncertainty, since the measurement location is the point the gage is installed. Installation quality will vary widely according to the care, skill and expertise of the operator. Imprecise location, direction and alignment may cause significant errors in measurements, where improper mounting may even prevent any useful measurements at all.

Noise, considered as a random oscillation in the signal, is also inherent in all sensor measurements. The sources could be internal, such as the resistive properties and effects during signal transfer to the data acquisition device, or external from mechanical and electromagnetic fluctuations. Measurement noise can be high enough to reduce the accuracy of measurements significantly, but usually noise components can be eliminated by filtering. Filtering is the process of screening the input signal according to the desired ranges of frequency or other parameters. Filtering is explained in the following sections, as part of the data acquisition system.

The sensory system refers to the sensors and their corresponding interfacing units for input signals gathered from various monitoring equipments. In the design/selection of the types and locations of sensory systems, the following criteria should be fulfilled (Wong 2005).

- The sensory system should have the ability to capture the local and system-level responses, which could be correlated or compared with those design values;
- The sensory system is required to integrate the predictive-modeling and data interrogation processes with the sensing system design process;
- The sensory system should have the function to acquire data in a consistent and retrievable manner for long-term statistical data processing and analysis;
- All sensors should be chosen from the contemporary commercially available sensors that best match the defined sensing performance requirements;
- The sensory system should include additional measurements by removable/portable sensors to quantify changing operational and environmental conditions;
- At key locations, different types of sensors should be deployed so that cross-calibration of sensors could be carried out.

### **5.2.1. Traditional Sensors**

The most common types of sensors used in SHM applications include displacement sensors, strain sensors, vibrating wire sensors (both temperature and strain/rotation/displacement, etc.), force sensors, and temperature sensors. Displacement transducers and settlement devices can be used to measure and monitor deflection, settlement, joint openings, and other movements of bridge members. Strain sensors are normally used to measure the change in the length of an object per unit length. These conventional gages are commercially available from various suppliers with different specifications. Some of the basic characteristics and principles for these gages are given in the following;

Strain Gages: Probably the most commonly sought monitoring parameter is the strain, which is the ratio of the change of length of an element to its original length.

Strain is directly related with the stress experienced at that location, and provides direct indication of the utilized and reserve capacity of the location, section or component. For strain measurements, a reference point is not required, which is a major advantage. There are many techniques available that can be used to measure strains. The most common types used for bridge testing and monitoring applications are electrical resistance strain gages and vibrating wire strain gages.

Electrical resistance gages are usually bonded foil type, consisting of a thin foil of resistor embedded within a nonconductive plastic film. The difference in strain measurement is obtained through the change of resistance of the foil as it is stretched or compressed, together with the structural location. The resistive change is measured through circuits called ‘bridges’ to increase the accuracy of measurements by measuring the voltage difference between the legs of the bridge in accordance with the applied voltage on the bridge.

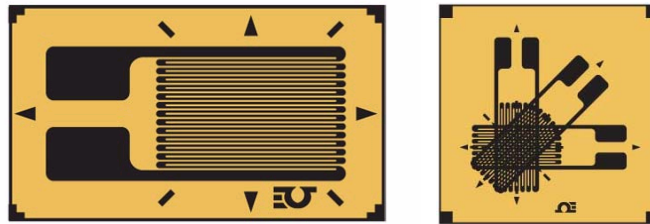


Figure 5.1 – Example foil type strain gages (Omega Eng.)

Foil strain gages measure strain in a single direction, but for measuring components of strain in multiple directions, strain gage rosettes made of two or more strain gages are also available (Figure 5.1). There are many types of resistive strain gages, which can be installed by mounting on the surface with adhesives, epoxy or welding, or by embedding inside concrete or similar material.

Vibrating wire strain gages are very reliable and robust gages that operate on the principle of natural frequency, as shown in Figure 5.2. The vibrating wire is the metal rod that is fixed on or embedded into the structure, which undergoes deformation. Tension on the wire due to extension or contraction will change its natural frequency, which is

measured by an electromagnetic coil. The output of the gage is in terms of frequency, which is converted to strain using the mathematical relations between the frequency and tensile strain.

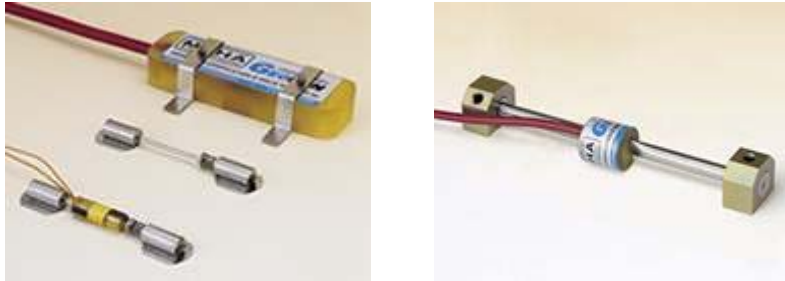


Figure 5.2 – Example vibrating-wire type strain gages (Geokon Inc.)

Vibrating wire strain gages are temperature compensated when installed on a steel member because the thermal expansion coefficient for the strain gage wire and the steel member will be nearly the same. Also, some vibrating wire gages have internal temperature sensors that allow for differentiating the temperature induced stresses on the member from mechanical stresses. Vibrating wire strain gages are significantly less stiff than the steel or concrete members on which they are typically installed, so that they do not contribute to the stiffness at that location. Most vibrating wire type sensors, including strain gages, have been shown to be very stable exhibiting very little drift over during long periods of use. Vibrating wire technology has been extended to rotation and displacement measurements also coupled with temperature sensors.

Displacement measurement: Displacement is another very useful measurement type, providing directly the deformation of the structure under consideration. Displacement is a directly useful quantity, since some standards are specified as deflection values. Among many types, cable extension transducers, linear variable differential transformers (LVDT), direct current differential transformers (DCDT) and vibrating wire crack-meters are commonly found in instrumentation applications.

Cable extension displacement sensors typically have a spool wound with a length of stainless steel cable. Extension or contraction of the cable moves the potentiometer and generates an electrical signal that is linearly proportional to the displacement. An input

excitation is necessary to receive the output readings. LVDT's include an electromechanical device that measures displacements based on the principle of mutual inductance. A high frequency AC voltage is applied to the primary coil that induces a corresponding AC voltage in the two secondary coils. The voltage induced in the secondary coils is proportional to the position of the movable core, therefore, the amplitude of output signal will be proportional to the distance the core is moved from the center position. A similar type of gage is DCRT, which works the same way as LVDT, except that it uses direct current, making it easier to supply the excitation.

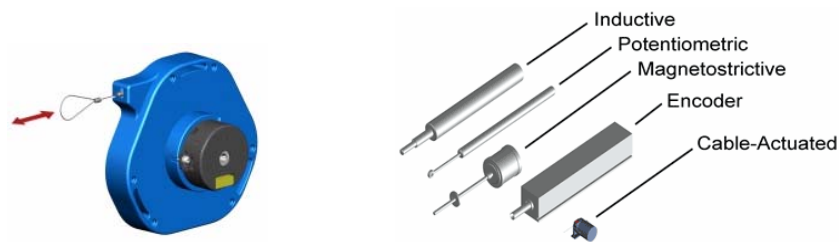


Figure 5.3 – Displacement gage examples (Spaceage Control)

Displacement gages, although widely used in localized evaluation, are not practical for large scale buildings and especially bridge structures, since they measure the dimensional difference between two points, hence requiring a reference point.

Tiltmeters: The change of inclination of a surface or a component is measured with tiltmeters. They usually encompass a pendulum mass, therefore, rotation of the device induces spring forces due to earth's gravitation. Tiltmeters might be based on electrolytic or vibrating wire principles, similar to strain gages.

Electrolytic tiltmeters sense angular movement (rotation) with respect to the vertical gravity vector through its sensing element, which is an electrolytic tilt transducer, similar to a spirit level. As the transducer tilts, internal electrodes are covered or uncovered by a conductive fluid. This process produces changes in electrical resistance when an AC excitation is passed through the transducer. These changes are measured using a voltage divider network. The resulting signal is then amplified, actively rectified

and filtered to form a high-level DC signal that is proportional to the measured angular rotation, or tilt.



Figure 5.4 – Tiltmeter examples (Applied Geomechanics, Geokon)

Vibrating wire tiltmeters operate similar to vibrating wire strain gages. Some advantages of using vibrating wire tiltmeters is that they combine high range with high sensitivity, and have excellent long-term stability. Since the sensor outputs readings in units of frequency, there is little attenuation over long cable lengths.

Accelerometers: Accelerometers capture the vibration characteristics of a structure, and are used for dynamic tests such as forced excitation, impact and ambient vibration testing. The four main types of accelerometers are piezoelectric accelerometers, piezoelectric accelerometers with internal electronics, capacitive accelerometers and servo force balance accelerometers.



Figure 5.5 – Example accelerometers (PCB)

Dynamic tests provide frequency, damping and mode shapes of the structure. Since these properties are directly related to the mass, stiffness and damping characteristics, dynamic test results provide invaluable insight to the structure. The

accelerometer should be selected according to the vibration characteristics of the structure, which should be estimated. For short to medium span bridges, a 3-50 Hz frequency band is common. For long span bridges, a 0-10 Hz band is a reasonable estimate. In terms of amplitude range, +/- 3g is a reasonable range, since the maximum amplitudes for long span bridges are in the range of 0.05g.

Environmental sensors: Environmental conditions at a test site are measured with different types of environmental sensors. These measurements most often include ambient temperature, relative humidity, and wind speed and direction. There are two common options for monitoring wind speed and direction. The first option is to use a cup anemometer equipped with a wind vane. Most cup anemometers utilize magnetic reed switches, which are frequency type devices (shown in Figure 5.6). The wind direction is sensed by a potentiometer linked to a rotating wind direction indicator. A second option for wind speed and direction measurements is to use an ultrasonic anemometer. The anemometers usually have three sensors that are offset by 120° and share the same horizontal plane.



Figure 5.6 – An example wind station for measuring wind direction, speed and temperature (Omega Inc.)

Appendix A contains more detailed information and operating principles on various sensor types, characteristics, and operation theory.

### 5.2.2. Some Novel Sensing Technologies

The sensor technology is advancing rapidly with the introduction of new technologies on sensing the ordinary parameters, such as displacement and strain. There are novel techniques allowing better range, resolution and accuracy, that also make it possible to measure phenomena that could not be measured directly.

Fiberoptic technology is utilizing the novel materials and their light-transmitting properties to accurately register changes in length. Fiberoptic sensors are generally used for measurement of strain, displacement and acceleration with no sensitivity for temperature changes. They are also very stable and reliable over long-term measurement, and especially practical for embedding sensor arrays within concrete blocks, such as in dams and piles. The sensor sizes have huge variation, and many different types are available according to type of application.

Another new technology makes use of ultrasonic signals. Ultrasonic signals are like audible sound waves, except the frequencies are much higher. Ultrasonic transducers have piezoelectric crystals, which resonate to a desired frequency and convert electric energy into acoustic energy and vice versa. An output signal is produced to perform some kind of indicating or control function. A minimum distance from the sensor is required to provide a time delay so that the "echoes" can be interpreted. Variables which can effect the operation of ultrasonic sensing include: target surface angle, reflective surface roughness or changes in temperature or humidity. The targets can have any kind of reflective form-even round objects. Accordingly, ultrasonic sensors are used for detecting and measuring discrete distances to moving objects with high resistance to external disturbances such as vibration, infrared radiation, ambient noise, and EMI radiation. They are most typically used for motion control, proximity, detection and liquid levels.

Corrosion is one of the main concerns for bridges near or over water bodies or in other corrosive environments, and both engineers and researchers are working on different methods for quantifying and remedying corrosion. Although corrosion sensors are not widely used, there are currently a number of corrosion sensors available in the

market. Corrosion sensors detect and measure corrosion usually either by detecting the chemical agents causing corrosion, or have a corroding component itself to passively track the corrosion. Electrochemical methods such as corrosion potential, linear polarization resistance and chloride level involve the use of an embedded reference electrode. The non-electrochemical method involves using the macrocell system to determine whether the corrosion occurs or not, instead of the rate of corrosion. The sensor elements are stable and durable because no reference electrode is used. Various macrocell sensor systems have been developed and used to monitor the corrosion risk of new concrete structures. Macrocell sensor systems utilize a galvanic current that flows between two metal materials. These materials have different potentials when they are interconnected. Macrocell sensor systems consist of sacrificial carbon-steel anodes mounted at different depths from the surfaces. Although the measured galvanic currents between the so-called sacrificial anode and cathode can detect the time to depassivation and the severity of depassivation, no information regarding the corrosion rate of the steel can be obtained since they can not provide instantaneous information of corrosion.

Another novel technology, Microelectromechanical Systems (MEMS), focuses on very small scaled systems. Although application of MEMS sensors are very wide as part of sensing systems in electronic devices or cars, their use is limited in SHM applications. However, their promise is high as many types of MEMS sensors are becoming available commercially, and their extremely small size is a major benefit. Various vendors market MEMS-based sensors such as accelerometers.

Acoustic Emission (AE) monitoring systems are being considered due to their capacity to detect very small defects in metals. For example, an array of high frequency sensors that operate continuously is used to detect the energy that is released when a steel wire or member fails. Therefore, AE sensors can be used to detect cracks or failures, also indicating the location of the occurrence. Some specific acoustic emission devices are designed for measurement of very high frequency phenomena particularly on machine structures for crack formation investigations, fatigue studies and machine tool diagnostics. The covered frequency ranges are from 50 kHz to 900 kHz depending on the sensor. AE above 50 kHz in the surface of metallic components or structures results from

plastic deformation of materials, crack formation and growth, fracturing or friction. Application examples are monitoring of processes, tools and machines in metal cutting as well as forming operations. Some sensors have rugged construction and tightly welded housing for operating under severe environmental conditions.

### **5.2.3. Wireless Sensing**

Signals from sensors are usually transferred to the data acquisition (DAQ) systems via cables, which also transmit the excitation required for sensor measurements. Cable installation is, therefore, a substantial part of installing an instrumentation system, in terms of both cost and labor. Increasing physical size of the application also increases the required cabling, which could be huge for large-scale structures, while their layout is time consuming.

Wireless data transmission technology has rapidly developed for SHM applications with the promise of reducing system cost and installation time, and providing flexibility. Wireless sensors based on MEMS have been introduced, which offer low-cost, low-power, compact and easy-to-install alternatives to traditional sensors. However, the wireless technology for civil infrastructure applications is still under development and more research is being done for its durability, energy consumption, signal quality and interference issues. Synchronization is also a major consideration in wireless sensing, which creates additional challenge for instrumentation control over traditional wired channels.

Compared to traditional wire-based systems, wireless structural monitoring systems have a unique set of technical challenges. First, wireless sensing units will most likely employ batteries that have a limited supply of energy. Batteries are probable in the short-term because current power harvesting techniques cannot yet provide a reliable, convenient, and low-cost solution for powering typical wireless structural sensors. In terms of power consumption, wireless transceivers often consume greater amounts of energy than any of the other components in the wireless sensor design. Local data processing targeted to balance data transmission and energy consumption is desirable.

Secondly, the transmission of data in a wireless network is inherently less reliable than in cable-based networks; reliability decreases as the communication range becomes further. Thirdly, the limited amount of wireless bandwidth usually impedes high-speed real-time data collection from multiple sensors. Lastly, time delays encountered during data transmission between different wireless sensing units due to sensor blockage or clock imprecision needs to be thoroughly considered (Lynch and Loh 2005).

### **5.3. DATA ACQUISITION SYSTEMS AND COMMUNICATION**

The data acquisition system (DAS) is a very critical component of structural health monitoring that is related with the acquisition of the data, including data collection, signal processing, synchronization, digitization and storage. The data from the sensors are transmitted with a cable or wireless connection to the data acquisition unit, and the data from a number of channels have to be received without time delay or loss of information. Signal conditioning is usually necessary to improve the quality of the signals, and most data acquisition systems are equipped with signal conditioning components. One of the most challenging aspects of data acquisition is handling different types of sensors and signals.

A data acquisition system with different components and alternative data transmission protocols is proposed in the following. Depending on the monitoring objectives and applications, this proposed system can be modified and expanded. For example, maintenance related considerations such as performance of mechanical and electrical components and structural issues such as stresses at critical locations can be incorporated. Figure 5.7 shows a possible data acquisition scheme to accommodate various types of sensors to be implemented on the bridge. Information on some of the sensors shown in this diagram can be found in Appendix A.

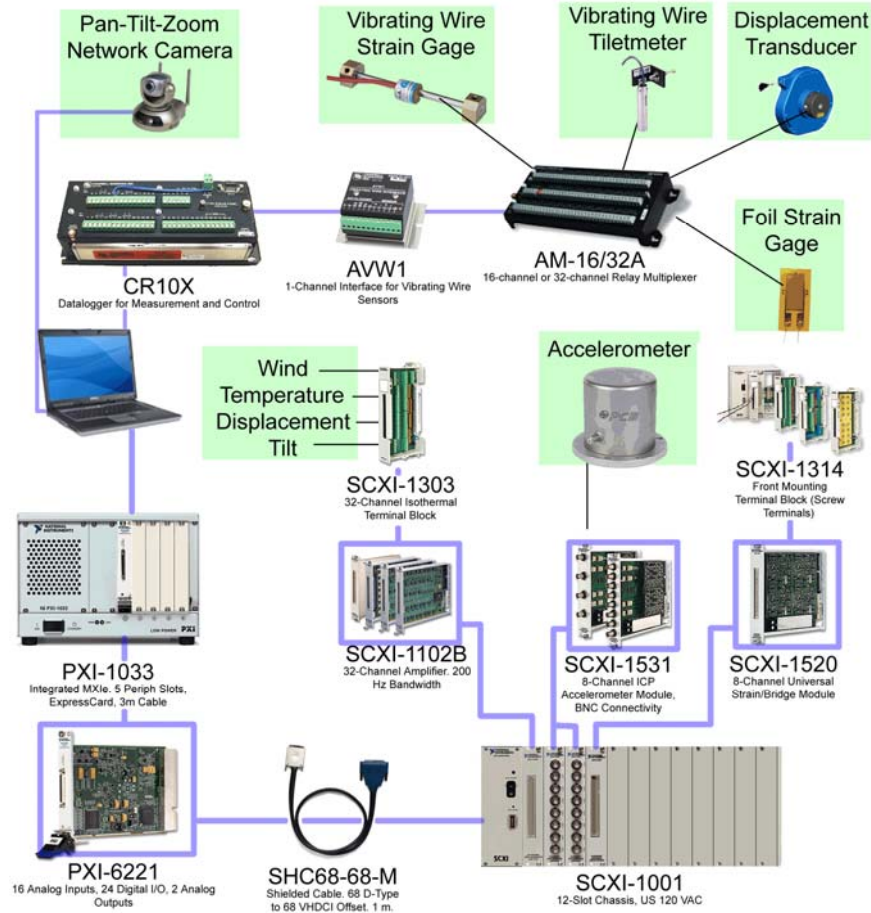


Figure 5.7 – Sensor array + DAQ scheme

In real-life bridge monitoring applications, the data acquisition equipment need to be installed in permanent protective enclosures located either in the control room or on the bridge piers that are hidden from view by casual passersby. The sensors can be connected by short cables routed through watertight conduit or wireless sensors can be employed for eliminating the need for cables. Since two leaves of the movable bridge are physically separated from each other, it is necessary to provide data transmission between leaves of the bridge. Three options are proposed for connection of the two sides:

OPTION A

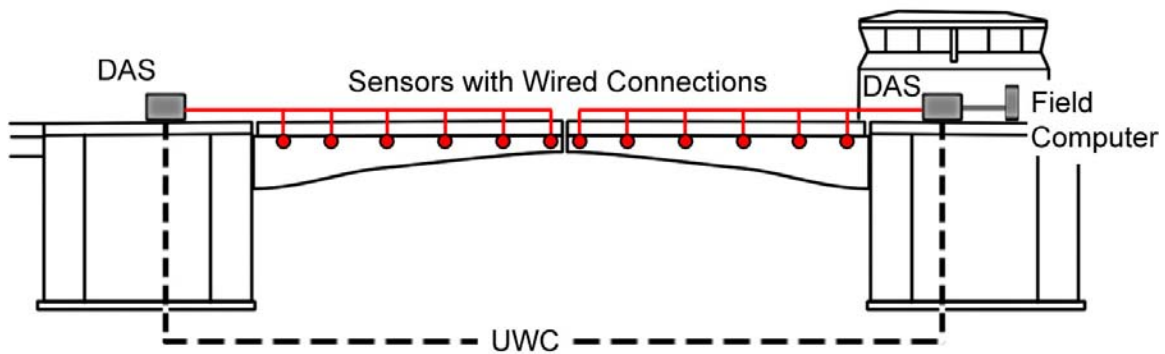


Figure 5.8 – Data transmission with two data acquisition systems via under-water cable

OPTION B

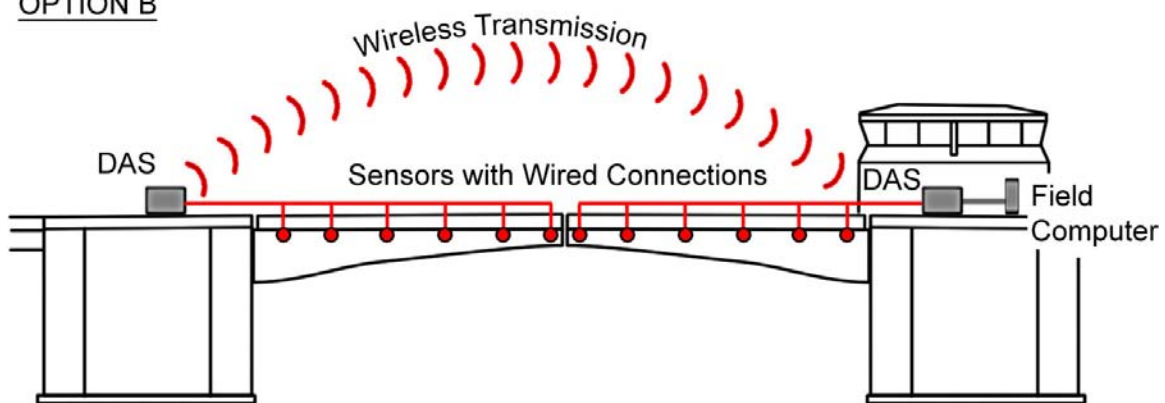


Figure 5.9 - Data transmission with two data acquisition systems via wireless connection

For the first two options (A and B), identical instrumentation and data acquisition systems (DAS) are utilized for the two sides and the DAS on the far side is connected to the other DAS via spread spectrum radio link, or underwater cables across the channel. The DAS in the operator office is connected to the host computer directly by data cable.

## OPTION C

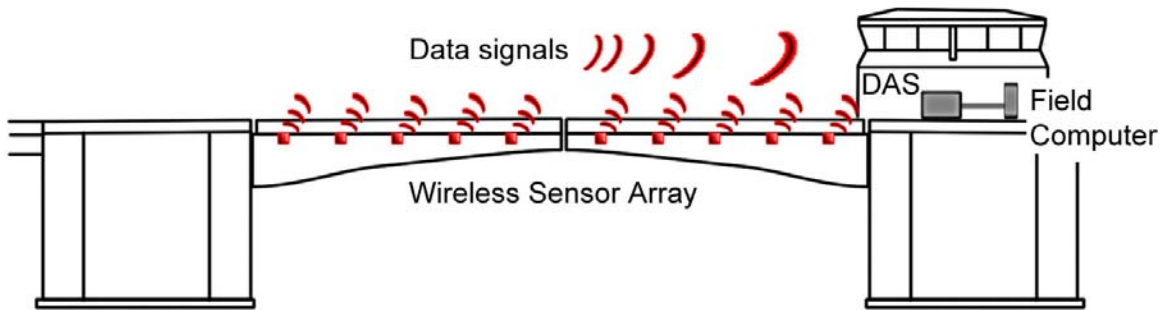


Figure 5.10 – Data transmission with wireless sensor array

For option C, wireless sensors and a single data acquisition system are used. Wireless sensors on the far span transmit signals to the DAS located in the control room. The DAS is again connected the host computer. Since no cables are involved for data transmission from sensors, physical separation is not a problem. Power supply for the wireless sensors is provided by batteries; therefore, periodic battery replacement or recharging will be necessary.

### **5.4. CRITICAL COMPONENTS OF MOVABLE BRIDGES FOR MONITORING**

In this section, we focus on specific electrical, mechanical and structural components and elements that are candidates for monitoring. These components and elements were identified based on the site visits and meetings with FDOT personnel, evaluation of inspection reports and finite element simulations conducted for various scenarios. Possible measurements and sensing methods are also briefly reviewed along with measurement needs for maintenance, safety and operation.

#### **5.4.1. Electrical Motors**

The electrical motors generate the torque required for the opening and closing of the bridge.



Figure 5.11 – Electrical motor

High amperage, high temperature, vibration and high revolution speed are indicators of improper functioning. The amperage can be measured with electrical current measurement. Temperature probes may be used to detect overheating. Excessive or abnormal vibration can be detected by accelerometers attached on the motor case. A generic RPM sensor will be useful to measure the speed of revolution, therefore, to indicate a problem in the motor or the mechanical system that generates additional resistance to the opening/closing torque.

#### **5.4.2. Gear Boxes**

The gear boxes contain the assembly that transmits the torque generated by the motor to the shafts, similar to a differential. When the gear boxes suffer deterioration, or lack proper lubrication, some change in the sound during operation is noted. Oil viscosity is also an important parameter for the proper functioning of the gear box. Similar to the electrical motors, abnormal vibration is an indicator of wear in the gears.



Figure 5.12 – A gear box

The acoustic print can be checked via acoustic measurements during each operation and automatically decided if there is a significant change. Small MEMS sensors can be used to measure the viscosity, density, temperature and mass flow of motor oil. Oil samples can also be taken intermittently and tested in materials labs. Again, accelerometers should be used to monitor the vibrations, and the rotation speed can be measured with RPM sensors.

### **5.4.3. Open Gears / Racks**

The motor torque is transferred to the pinion, the final gear on the mechanical assembly, through the drive shafts. The open gears are the main gears, which are part of the leaf main girder and receive the torque from the pinion. Open gears are present for movable bridges with and without Hopkins Frames. The usual rack-pinion type bascule bridges have the rack assemblies directly below the main girder, whereas in bridges with Hopkins Frames, the main gears are closer to the centerline of the leaf. Excessive strain, out-of-plane rotation and misalignment are common problems for open girders. The loading sequence problems mean that the drive shafts begin rotation in delayed sequence.

This has an adverse effect on the condition of the open girders, usually by causing impact loading. Routine maintenance is required on the gear teeth. Unless they are kept lubricated at all times, wear and corrosion due to grinding of the rack and the pinion will occur.



Figure 5.13 – Open gear / rack

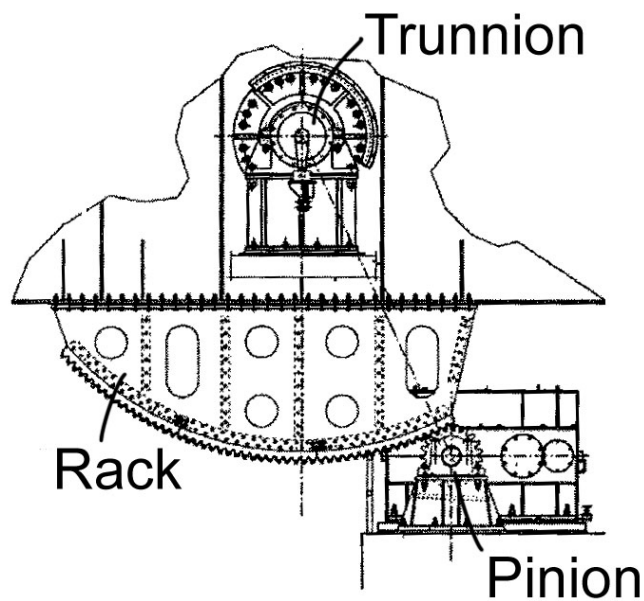


Figure 5.14 – Rack details (Patton 2006)

We propose placing strain gages on the open gear frame and on the main girder plate around the gear to measure excessive load effects and determine abnormal load sequence of the shafts. Tilt-meters give information on alignment and out-of-plane rotations. Impact loadings can be detected by an accelerometer placed anywhere on the gear. Lack of lubrication and areas of corrosion can also be determined through use of computer vision algorithms. A video camera or any imaging device can be positioned within sight off the teeth of the rack, and the detection algorithms can run in real time to process the image and detect regions lacking lubrication or showing corrosion.

Image segmentation (IS) is the process of partitioning a digital image into multiple regions. The goal of segmentation is to change the image into datasets that are meaningful and easier to analyze. The result of IS is a set of regions that collectively cover the entire image, or a set of contours extracted from the image. Each pixel in a region is similar with respect to a certain characteristic, which can be surface corrosion and/or indentation.

The procedure to obtain a digitized image or convert to digital format can be automatically supplied throughout the process. Usually, a searching area is defined to shorten the processing time, by confining the calculations to that area only, as shown on the right in Figure 5.15. In this search area, pixel histograms for all three color channels were generated and then grouped into blocks according to certain thresholds that represent areas of interest, in this case corrosion or indentation. Figure 5.16 summarizes this procedure, with the figure on the left showing the histogram of pixel intensities, and on the right, regions determined from the histogram, which are mapped to the original coordinates. Figure 5.17 shows the identified features on the main gear.



Figure 5.15 – Area for searching is defined

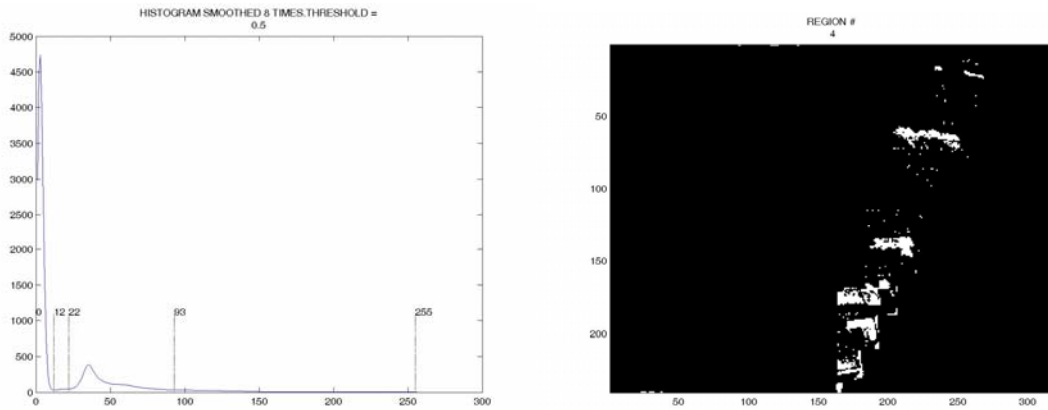


Figure 5.16 – Histogram of the pixel intensities and determination of interest regions

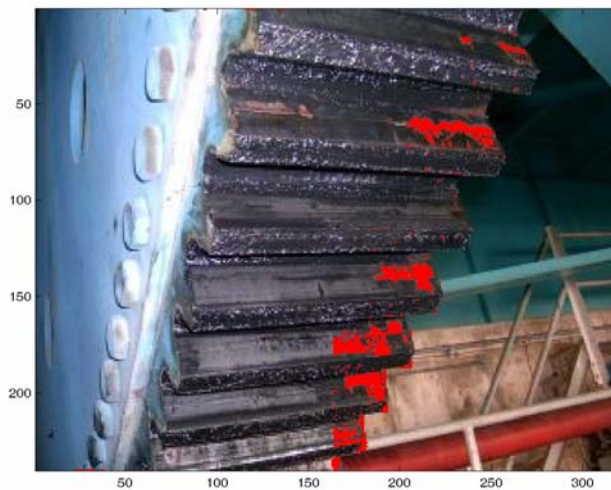


Figure 5.17 – Detection of corrosion/indentation

The total surface of the rack can be scanned with a stationary camera during opening and closing of the girders. With this algorithm, corrosion/indentation can be expressed as percentage of the total area, and raise a red flag for thresholds to be defined. Tracking the condition of the teeth would be an invaluable tool for maintenance of the gear.

#### 5.4.4. Hopkins Frame

Hopkins Frames are compact systems that include all the machinery in an enclosed case. Hopkins frames do not have drive shafts, since the open girders are close to the center of the leaves. Excessive strain and impact loading are critical parameters to be monitored on the gears. Due to its compact design, it is more challenging to instrument and monitor different mechanical components of the Hopkins frame.



Figure 5.18 – Hopkins frame girder

#### 5.4.5. Trunnions

Trunnions are the pivot points of the leaves; therefore, for their operation they need proper lubrication at all times. During opening and closing, Even a perfectly tuned and maintained leaf is expected to show some friction. Any disruption to alignment of

leaves or any part of the mechanical system would increase the friction. Also, improper lubrication on the trunnions should directly add up to the friction torque that needs to be overcome. Friction is calculated from the difference of opening and closing torques. A good review for the procedures to obtain friction values can be found in "Handbook of Bascule Bridge Balance Procedures" (Malvern, Li and Jenkins, 1982).

FDOT maintenance engineers indicated that by experience, trunnion lubrication is a major factor for friction. A modified balance test as described previously, which will help monitor the condition of the trunnion and indicate the best schedule to maintain.



Figure 5.19 – Trunnion

The alignment of the trunnion is critical to prevent premature wear of the trunnion bearings and to reduce out-of-plane web distortions that introduce fatigue damage. Misalignment in the trunnion axis can cause additional load on the trunnion-hub assembly and distress on the main girder plate, causing distortions, and eventually web buckling. Trunnion misalignment is also a major cause of wobble that can result in mismatch of the leaf tips, disturbing regular operation (Malvern et al. 1982; Besterfield et al. 2001; Koglin 2003; Patton 2006).

Therefore, the alignment and distress on the trunnion assembly should be controlled. The misalignment of the trunnions can be identified from a modified balance test involving both trunnions simultaneously (Figure 5.20). The torque on the drive shafts

can be measured by use of a strain gage assembly mounted on the shaft, following the directions given by Malvern et al. (1982). Strain rosettes or chevrons can be attached on the shaft to obtain the torsional strain. The application does not require any intrusion or alteration. Similar measurements have been performed successfully in the past. It is desirable to improve the accuracy by using an array of rosettes and averaging the data, as torque sensors do. These strain gages will measure the torsional strain, and the torque will be calculated accordingly. Since the shaft is the connecting element between the motor and the trunnion, and is responsible for transmitting the required power for opening and closing operations, its condition is directly related to the structural integrity and functioning of the movable bridge. Any distress on the shaft will indicate either degradation on the shaft, motor, gears, rack, or overloading of the bridge during operation.

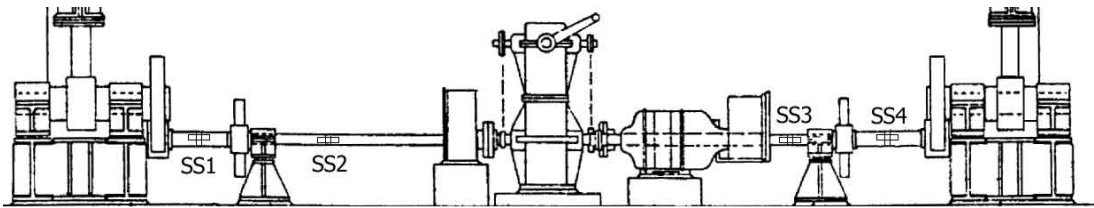


Figure 5.20 – Instrumentation for the mechanical components  
(Adapted from Christa McAuliffe Bridge Construction Plans)

The bridge balance test is being performed for all movable bridges in Florida, and the details of this test were explained in the previous sections. Torque vs. rotation angle of the girder will be monitored and the friction factors will be calculated remotely for all opening and closing actions of the bridge (Figure 5.21).

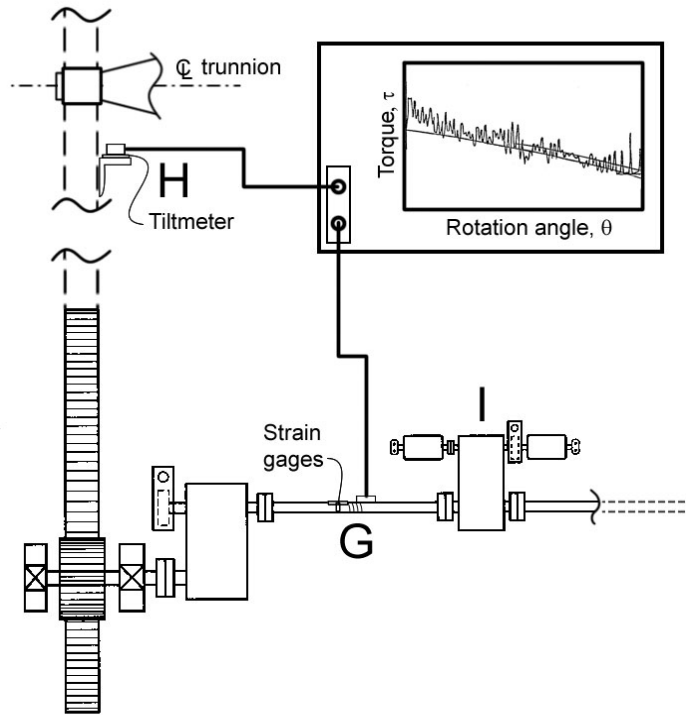


Figure 5.21 – Instrumentation of mechanical components

The motor RPM indicates how much power is needed during the operation of the bridge. External forces such as strong wind or internal effects such as friction or misalignment will cause the drive motor to produce more power, increasing the RPM. Therefore, monitoring the motor RPM as part of the instrumentation system will provide information about the condition and performance of the bridge together with other measurements.

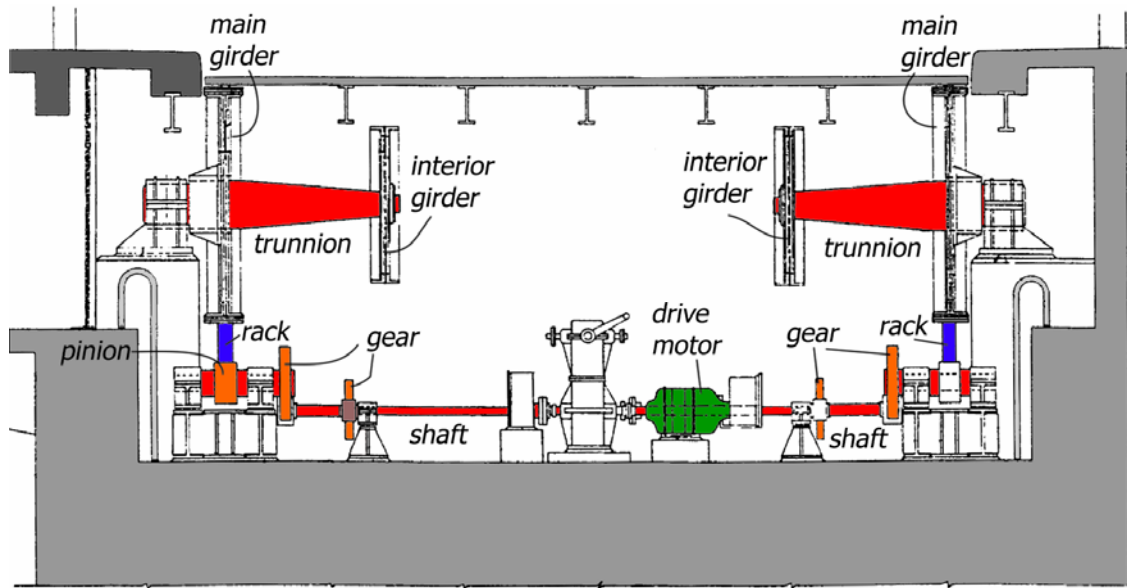


Figure 5.22 – Mechanical system of the representative movable bridge  
(Adapted from Christa McAuliffe Bridge Construction Plans)

#### 5.4.6. Live Load Shoes

Live load shoes are support blocks that the girders rest on while in the closed position. The live load shoes can be located forward of the trunnions, holding the main girder up, or behind the trunnions resisting the upward movement of the counterweight. The former type is the most common type, and is the type used for the Christa McAuliffe Bridge. Cracking and wear are rarely seen on the live load shoe, but mainly the operational problems such as full contact are of concern. If misaligned or improperly balanced, the bridge may not fully sit on the live load shoe. In that case, the dead load and traffic load are transferred to the gears and shafts, which cause damage on mechanical assemblies. Small gaps also lead to the girders pounding on the live load shoes, which results in further misalignment, additional stresses, fatigue damage and excessive wear.

Existence of a gap can be determined with linear displacement gages at closed position to ensure the bridge is fully seated. Impact loading due to pounding can also be detected with accelerometers. A load cell can be used to obtain the reaction force at the live load shoe. This would inform if there is full contact or not, as well as leaf

misalignment and balance. Changes in the balance condition should be reflected on the LLS reaction. However, using load cells may also be intrusive, since it has to be placed on the live load support. The leaf alignment is very important and it should be maintained. Therefore, certain modifications would be necessary to use load cells.



Figure 5.23 – Live load shoe (LLS) (sketch adapted from Christa McAuliffe Bridge construction plans)

#### 5.4.7. Span Locks

Span locks on double-leaf bascule spans tie the tip ends of two cantilevered bascule leaves together and force the leaves to deflect equally and prevent a discontinuity in the deck as traffic crosses the span. Most span locks consist of a rectangular lock bar supported by a pair of guides on one leaf that engages a single receiver on the opposite leaf. During operation, the lock bar slides across bronze shoes mounted in the rectangular guide and receiver housings. The housings are usually mounted to the side of the bascule girders or in the webs of transverse member (e.g. floorbeam or cantilevered bracket) that frames into the bascule girders. Lock bars are typically driven or retracted directly using a linear actuator (e.g. electric or hydraulic) or mechanical system with electric motor, speed reducer, and a series of crank arms, links and shafts (Patton 2006).

Span locks are one of the members that fail the most. They are sometimes destroyed due to deterioration, or incorrect operation, and sometimes the mechanism

failure prevents the function. The alignment and the stresses on the locking bar should be monitored to ensure the locks are in order.



Figure 5.24 – Span lock

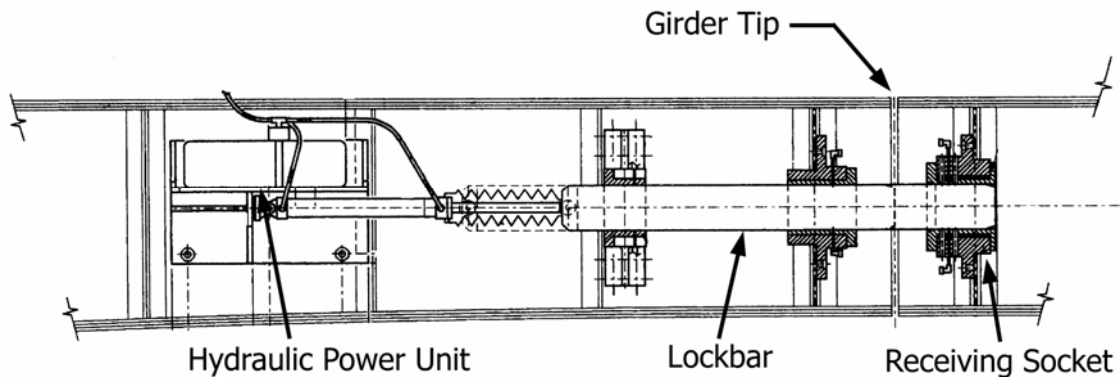


Figure 5.25 – Instrumentation for the span lock  
(Adapted from Christa McAuliffe Bridge construction plans)

Strain gages at the tip of the girders can indicate continuity between two leaves as a result of span lock connectivity. It may be possible to monitor lock bar also. Stresses on the locking bar will indicate whether the lock is on or off and also inform span lock

failure. This component is planned to reduce span lock failures due to overloading or the bridge operator overriding the opening action while the lock is in place, assuming a limit switch failure. Further on-site investigation need to be carried out for gage installation, running cables and access requirements.

#### **5.4.8. Bridge Operation (Opening/Closing)**

Bridge opening and closing operations induce additional stresses on the structural and mechanical components of movable bridges due to mechanical and dynamic forces, as well as increased wind forces. The misalignment of the girders due to deformation or thermal effects also causes damage that even leads to malfunction.



Figure 5.26 – Opening/closing of the leaf

Opening and closing operations should be tracked with tiltmeters, reflecting the angle of opening in real-time. Environmental conditions should also be monitored and correlated with the operation by using a wind station permanently located at the site.

#### **5.4.9. Longitudinal Displacement**

Longitudinal displacement, mainly due to thermal elongation, becomes a major concern especially for longer span bridges. Elongation causes bending on the piers, which may reflect on the cracking, and may even disrupt the opening/closing operation.

Displacement and temperature sensors should be placed to detect the amount of longitudinal displacement. These measurements should also be correlated to operational measurements during opening and closing.

#### **5.4.10. Main Girders and Floor Beams**

Main girders and floor beams form the main frame of the spans. They are made from both rolled and built-up sections with welded plates. The frame is generally manufactured at the shop and then installed at the site. There is usually a tiny margin of error, since all the dimensions should match with the hubs and the opposite span (if there is any) for proper operation, including the effects of camber and additional dead load from the deck and other parts.

Corrosion is a main concern on the bridge girders, especially on exposed surfaces. Corrosion leads to section loss and reduced capacity. Various corrosion sensors, which were summarized in sensor and sensor network sections previously, can be employed as part of the SHM instrumentation. Additionally, any misalignment, bending, or deformation can also cause an increased strain on the structure. The sensor layout given in Figure 5.28 can provide the distribution of stresses on the girders and indicate damage and deterioration, which will trigger preventive maintenance to avoid catastrophic failures.



Figure 5.27 – Main girders in open position

Transverse beams can be instrumented to track flexural behavior. This is done by using two linear gages horizontally along the top and bottom edges of the web, leaving sufficient clearance for the fillet end stress concentrations at the boundary.

Tiltmeters provide monitoring of the angle of rotation at the tip of the span. The tiltmeter readings will serve two functions: checking the leveling between girders on both sides for alignment during opening/closing and ensuring that the tips are in correct position for the locking maneuver. Accelerometers can be used to register the vibrations caused by environmental effects and vehicular traffic. Vibration frequencies also indicate if there is change in structural system such as due to imbalance or due to span lock failure.

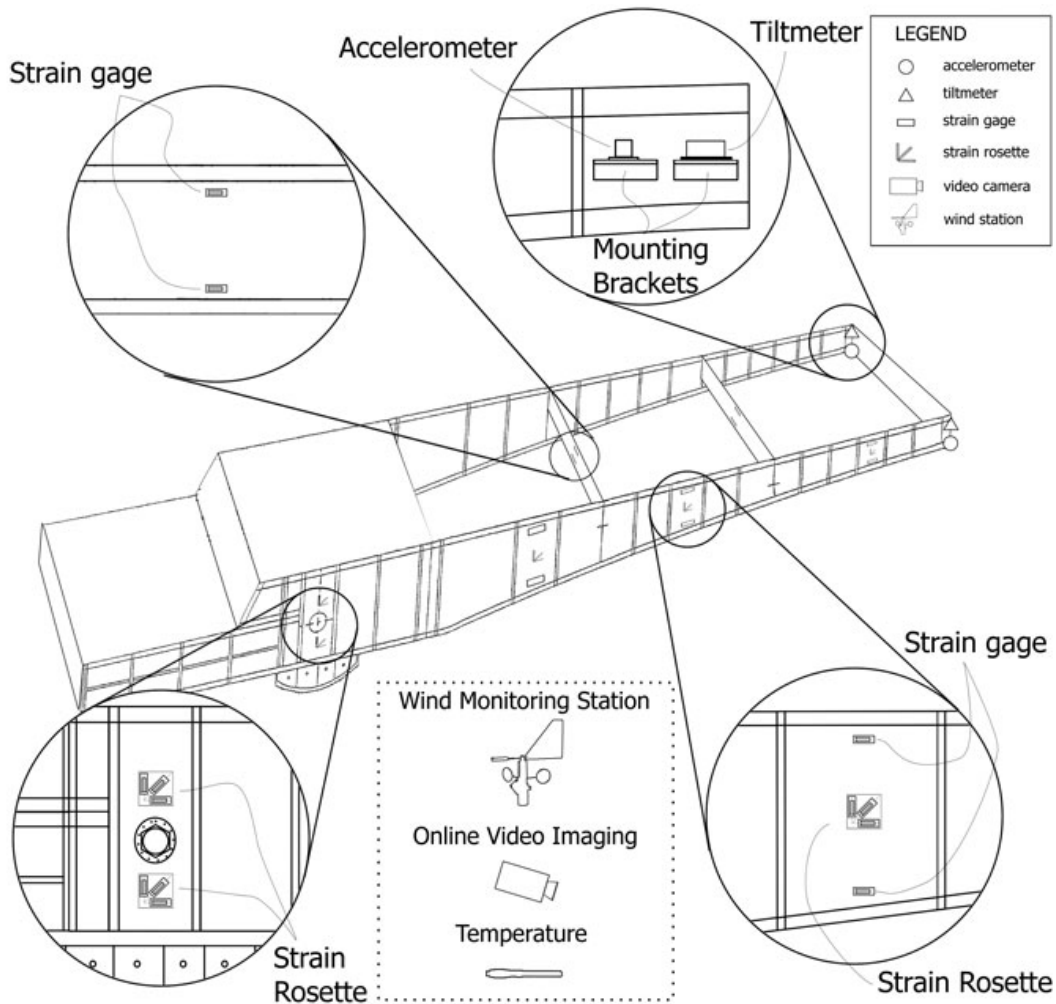


Figure 5.28 – Possible instrumentation for movable bridge structural components

As shown previously in the finite element model, connection between the trunnion and girder is a critical area where stress concentrations occur and has to be monitored because its damage can result in complete malfunction and require extensive repair. Instrumentation with strain rosettes is suggested because panel shear is the most likely cause of excessive stresses.

Main girder failure modes will be tracked considering bending and web shear. Stresses caused by bending will be measured by linear strain gages attached horizontally on the web close to the top and bottom flanges. The gages must have sufficient clearance to avoid fillets and stress concentrations. The shear stress on the center of the web panel will be measured by a strain rosette, located as shown in Figure 5.28. The rosette can

measure normal and shear strains in the plane of the gage, to be compared with the shear capacity of the section.

Wind monitoring will be used for determining the input load on the structure caused by air currents. Bascule bridges are slender and lightweight, and are significantly affected by strong wind forces, especially when they are open. Measured wind speed and direction will also be useful during hurricane-strength winds, indicating excessive force on the girders. In addition to wind, ambient temperature and structural member temperatures need to be monitored. Past studies have shown that temperature differentials can cause considerably higher stresses than stresses induced by vehicular traffic (Catbas and Aktan 2002). Finally, a video camera can be a complementary element as providing vehicular traffic data to be correlated with other sensor readings, informing bridge owners about accidents and suspicious activities. In addition, computer vision can be employed for purposes such as tracking corrosion of the gears.

## **5.5. DATA PROCESSING AND SOME NEW ANALYSIS METHODS**

For all options (Option A, B and C) explained in the previous section, data will be collected by a data acquisition system installed at the bridge site. The data will be analyzed at different levels to obtain information about the condition of the bridge. There are different metrics (features) at each level of analysis and these metrics can be sent via Internet connection to a main server to be stored. With the level of the analysis, the complexity of analysis methods and algorithms increases accordingly. For example, Level 1 refers to the raw data indicators and it represents the information obtained from the raw data without detailed analysis. Then Level 2, which can be referred as ‘identification stage’, will be carried out by using different analysis methods and different metrics to detect any damage, deterioration or ‘considerable change’ in measurements over the monitoring period. Afterwards, more rigorous analysis will be conducted for Level 3 to localize and quantify these ‘changes’, damage or deterioration. Finally, the Level 4 will be used to predict the future behavior, as summarized in Table 5.1.

Table 5.1 Monitoring of the structure in different levels (some of the proposed metrics and methodologies)

Level 1	Level 2	Level 3	Level 4
Displacement, Acceleration, Strain, Rotation, Corrosion, and Other Level 1 Measurements	Natural Frequency, MAC, Statistical Patterns such as from Mah. Dis. of the AR coefficients, and Other Level 2 Methodologies	Flexibility, Curvature, Reliability Index, and Other Level 3 Methodologies	Bayesian Updating, and Other Level 4 Methodologies

Based on the instrumentation design and the data collection regime, it is possible to collect, store and analyze various types of data sets. The writers' experience is that this process is rather iterative, especially at the early stages primarily influenced by the preliminary evaluation of data. The writers propose the following for the movable bridges: Maximum readings for each high speed gages such as strain gage and accelerometer can be saved on hourly basis. To ensure that the entire time history is captured, short duration windows of strain and acceleration are scanned for the peak absolute values in each gage. If the peak absolute value for each gage exceeds the previously recorded values for the current hour, the old peak time histories are overwritten by the new ones. All sensor readings as well as temperature and wind speed, and also a jpeg image from the video are recorded when a peak is detected. For long-term monitoring, it is important to continuously monitor strain and temperature relationship with a slower scan rate. Some of the critical components such as structural components subjected to high stresses or stress reversals due to traffic or wind induced inputs, can be monitored at different intervals or based on triggering.

At the end of each hour, the recorded data corresponding to peak values as well as others can be loaded onto the main server through an Internet connection from the on-site computer. The data from all gages are also recorded and transferred to the main server when the measurements are above a threshold level. For the part of the instrumentation application involving mechanical components, data can be recorded at the critical times such as during opening and closing of the bridge leaves. For each opening/closing event,

shaft torsion, leaf angle, drive motor RPM and the video can be collected by the DAS, transferred to the computer and archived in the main server.

Tip Displacement Level	0.863 in	
Acceleration	0.255 g	
Strain Near Trunnion	36.425 $\mu\epsilon$	
Rotation at Tip	1.75 deg	
Corrosion (Girder)	0.013 in	

 Green
  Yellow
  Red

Figure 5.29. Some of the proposed metrics for Level 1 monitoring (raw data indicators)

Figure 5.29 shows Level 1 monitoring with the raw data indicators. The on-site computer will store only the designated long-term monitoring raw data such as slow speed continuous strain-temperature or short duration high-speed vibration data. The rest can be overwritten afterwards unless an operator decides to save the data. All processed data and analysis results along with the designated raw data will be permanently stored. As explained before, after Level 1 monitoring, different types of analyses can be conducted. Several novel approaches and methodologies are being adapted, developed and implemented by the UCF researchers to obtain the necessary useful information from collected data. Some of these methodologies can be listed as statistical pattern recognition approaches, parameter estimation by using model updating and optimization, reliability based monitoring and the use of computer vision for structural health monitoring. While the writers employ many different methods and approaches, brief

overviews of the some novel methodologies researched by the writers are summarized in the following sections.

### 5.5.1. Statistical Pattern Recognition

Statistical pattern recognition has great promise for handling large amounts of data while detecting changes and deviations over the monitoring duration. The process of pattern recognition starts with a sensor that collects the data to be classified. Then, a feature extraction mechanism computes numeric or symbolic information from the data, which are referred as the features. Finally, the classifier is fed with the extracted features and the decision is made by classifying these features. This process is summarized in Figure 5.30.

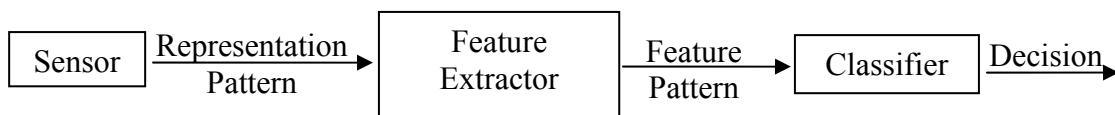


Figure 5.30. Pattern classifier (adapted from Webb 1999)

Pattern recognition is the classification (or recognition) of different data vectors (also referred as patterns) (Shalkoff 1992; Webb 1999). In statistical pattern recognition, statistical methods are used to define decision boundaries between patterns (Jain et al. 2000). It has found a lot of application areas in the fields of electrical engineering, computer science, medical sciences and many others. Recently, pattern recognition concepts have been also applied to civil engineering applications in the context of SHM.

Statistical pattern recognition has many components. They include linear discriminant functions, non-linear discriminant functions (neural networks), feature extraction and selection, supervised learning, unsupervised learning (clustering), decision trees, and outlier detection. In this text, a very brief overview about some of the components, which are directly related to this study, will be given.

*Feature selection and extraction:* Feature selection and extraction seeks to compress the data set into a lower dimensional data vector so that classification can be

achieved. Obviously, the features should be selected very carefully so that maximum separation can be achieved with the minimum number of features because the high dimensional features often cause problems, which is also referred as ‘curse of dimensionality’. Some of the features used for SHM are mentioned throughout this text.

Supervised Learning vs. Unsupervised Learning: The terms supervised and unsupervised learning refer to the learning process when there is training data available or not available respectively. Regression analysis (continuous data) and group classification (discrete data) are types of supervised learning whereas clustering and outlier analysis are often referred as unsupervised learning types. In SHM, the term unsupervised learning implies that there is no available data from the damaged systems.

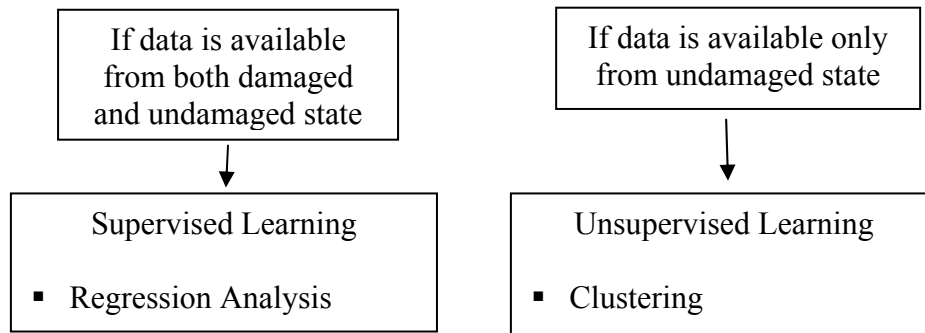


Figure 5.31 – Supervised and unsupervised learning for SHM

### SHM as a Statistical Pattern Recognition Paradigm

Recently, a new definition of SHM was given by Sohn et al. (2001). The authors stated that SHM is a statistical pattern recognition process and it is composed of the following four portions.

- Operational evaluation (how is damage defined, what are the conditions in the operational environment, what are the limitations on acquiring data?)
- Data acquisition (selecting the types, number and places of the sensors and defining the other hardware, data normalization), data fusion (the integration of different sets of data from different types of sensors) and cleansing (choosing the data to accept or reject)

- Feature extraction (identification of the metrics, which help to differentiate the damaged and undamaged structure) and data compression
- Statistical model development (models that will give the information about the damage state of the structure by analyzing the identified features)

Statistical pattern recognition can be used for Level 2 monitoring through use of many metrics as shown in Figure 5.32. There may be a number of metrics observed for monitoring of the structure at this level and some examples are shown in Figure 5.32 as natural frequency, Modal Assurance Criterion (MAC) and Mahalanobis distance (see Appendix B) of the AR model coefficients. There are a number of examples showing different methodologies for this type of monitoring, which can be addressed here. However, for the sake of brevity, those which are directly related to this study will be summarized in the following section. After this brief literature review, the studies conducted by the authors will be discussed.

Natural Frequency	1.243 Hz	
MAC	0.968	
Mah. Dis. of the AR Coeff	3.214E4	

 Green
  Yellow
  Red

Figure 5.32. Some of the proposed metrics for Level 2 monitoring (identification of damage)

Sohn and Farrar (2001) used an Auto-Regressive (AR) model for estimating the time history measurements from an undamaged structure. The AR coefficients of the models fit to subsequent new data are monitored relative the control limits. In another study, Sohn et al. (2001) applied two pattern recognition techniques to fiber optic strain gauge data obtained from a surface-effect fast patrol boat. Recently, Dr. Catbas and his students applied similar methodologies to identify different structural configurations of a

laboratory structure and details about this study is given in the Appendix B (Gul et al. 2007).

Worden (1997) used an Auto-Associative Network (AAN) for first level damage detection. The feature for the network is selected as the transmissibility function between two masses. More discussion about the applications of Neural Networks (NN) for damage detection can be found in (Chen et al. 1995; Masri et al. 1996; Kao and Hung 2003). Worden et al. (2000) used outlier detection methods for damage identification and applied it to four different cases. They also used Mahalanobis squared distance measure for outlier detection.

Elimination of environmental effects from the data is another very important issue and Principal Component Analysis (PCA) can be used for this purpose. PCA is a multi-variate statistical method, also known as proper orthogonal decomposition. A very attractive feature of the methodology is that environmental conditions do not need to be measured for the analysis. Giraldo and Dyke (2004) applied the method to the ASCE benchmark problem to identify damage under different environmental condition by using computer simulations. Yan et al. (2005) verified the methodology by using experimental data and applied it to real life data coming from Z24 Bridge in Switzerland. These methodologies can be implemented at Level 2 monitoring to have more reliable information about the changes in the data.

The authors implemented different algorithms and approaches to construct a novel SHM methodology by using statistical pattern recognition. The theoretical background of statistical pattern recognition based SHM and experimental studies conducted at UCF Structures and System Research Laboratory are summarized in Appendix B. Figure 5.33 shows an example figure showing representative results of the statistical pattern recognition applications on a steel grid structure where damaged structure state is determined. Again, detailed information about the studies is given in Appendix B.

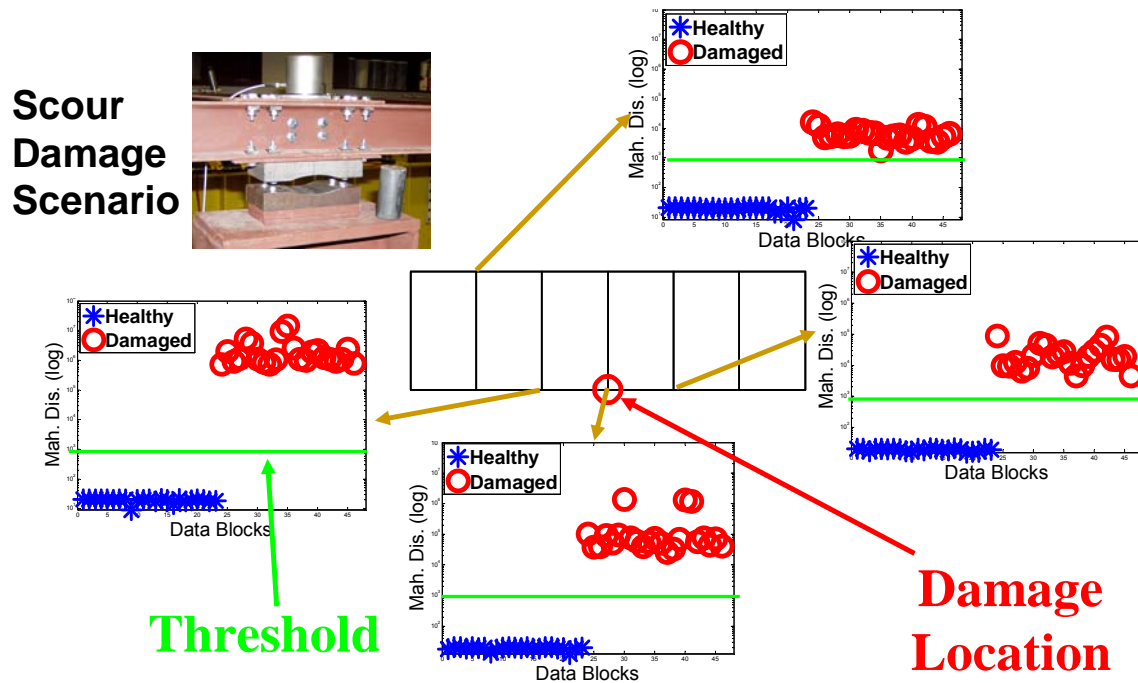


Figure 5.33 – Mahalanobis distance plots to detect damage case

### 5.5.2. Parameter Estimation with Sensor Fusion and Model Updating

After Level 2 monitoring, a more detailed and comprehensive analysis level can be defined by using different approaches to SHM such as model updating using sensor fusion, detailed modal analysis, Bayesian updating, computer vision and reliability analysis. Some of the methodologies developed by the authors for condition assessment of civil infrastructure can be found in literature (Catbas and Aktan 2002; Catbas et al. 2006). In this section, example studies regarding parameter estimation by using optimization conducted at UCF Structures and Systems Research Laboratory will be explained. Figure 5.34 shows some of the proposed metrics for Level 3 monitoring.

Flexibility	0.432 in/kip	
Curvature	0.255 1/in	
BC (Spring Stiffness)	45.698 kip/in	
Reliability Index	2.685	

 Green  
  Yellow  
  Red

Figure 5.34. Some of the proposed metrics for Level 3 monitoring (quantification and localization)

Parameter estimation is the procedure through which the unknown variables of an analytical structure, whether stiffness, cross section area, elastic modulus or moment of inertia or boundary condition stiffness, are updated using measured experimental measurements. In real-world scenarios, structural member properties may differ from their expected or “published” values due to variances from fabrication, construction or destructive events such as damage or fatigue problems that occur over the service life of the structure. Using optimization methods and experimental data sets, one can minimize the error between the analytical and measured responses, updating the unknown parameters. The updated model can then serve as a starting point, or baseline model for future analysis and critical decision making (Francoforte et al. 2007). In the following section the basic formulations are given without going into the details and example studies conducted in UCF Structures and Systems Research Laboratory will be presented.

The classical matrix formulation for FEM force-displacement relationship is

$$\{F\} = [K]\{U\} \quad (5.1)$$

where  $\{F\}$  is force vector,  $\{U\}$  is vector of displacements and/or rotations and  $[K]$  designates the structure stiffness matrix.

Since data over the entire set of degrees of freedom are generally not measured, the formulation in above equation can be partitioned according to measured and unmeasured DOF. Partitioning the force displacement relationship gives

$$\begin{Bmatrix} F_a \\ F_b \end{Bmatrix} = \begin{bmatrix} K_{aa} & K_{ab} \\ K_{ba} & K_{bb} \end{bmatrix} \begin{Bmatrix} U_a \\ U_b \end{Bmatrix} \quad (5.2)$$

where the subscripts  $a$  and  $b$  denote “measured DOF” and “unmeasured DOF”, respectively.

By using static condensation, the analytically determined forces,  $\{F_a\}$  can be solved in terms of the experimentally measured displacements and rotations,  $\{U_a\}^m$  where

$$\{F_a\} = \left( [K_{aa}] - [K_{ab}] [K_{bb}]^{-1} [K_{ba}] \right) \{U_a\} + [K_{ab}] [K_{bb}]^{-1} \{F_b\} \quad (5.3)$$

Since all of the unmeasured DOF are partitioned to  $\{F_b\}$ , part of the above equation will be equal to a zero vector and cancel the multiplied sub matrices  $[K_{ab}]$ ,  $[K_{bb}]^{-1}$  if there is no force on the unmeasured DOF. Then, an error function can be defined as the difference between the analytically determined forces,  $\{F_a\}$  and the experimental (applied) forces  $\{F_a\}^m$ , where  $\{e(k)\}$  denotes the error as a function of the unknown stiffness parameters and is given as

$$\{e(k)\} = \left( [K_{aa}] - [K_{ab}] [K_{bb}]^{-1} [K_{ba}] \right) \{U_a\}^m + [K_{ab}] [K_{bb}]^{-1} \{F_b\}^m - \{F_a\}^m \quad (5.4)$$

By using similar approach the error function based on the difference between analytically determined and experimentally measured displacements or rotations is

$$\{e(k)\} = \left( [K_{aa}] - [K_{ab}] [K_{bb}]^{-1} [K_{ba}] \right)^{-1} \left( \{F_a\}^m - [K_{ab}] [K_{bb}]^{-1} \{F_b\}^m \right) - \{U_a\}^m \quad (5.5)$$

Once test data are collected and the error functions are defined, an optimization algorithm is required in order to minimize the error between the analytically determined data and the experimental data. Optimization algorithms in general use iterative approaches to determine the best or optimal solutions for a given set of equations. A Spreadsheet Parameter Estimation (SPE) algorithm developed by Dr. Catbas and his students is utilized for optimization of the error functions and for updating the unknown stiffness parameters. The summary of the methodology is seen in Figure 5.35.

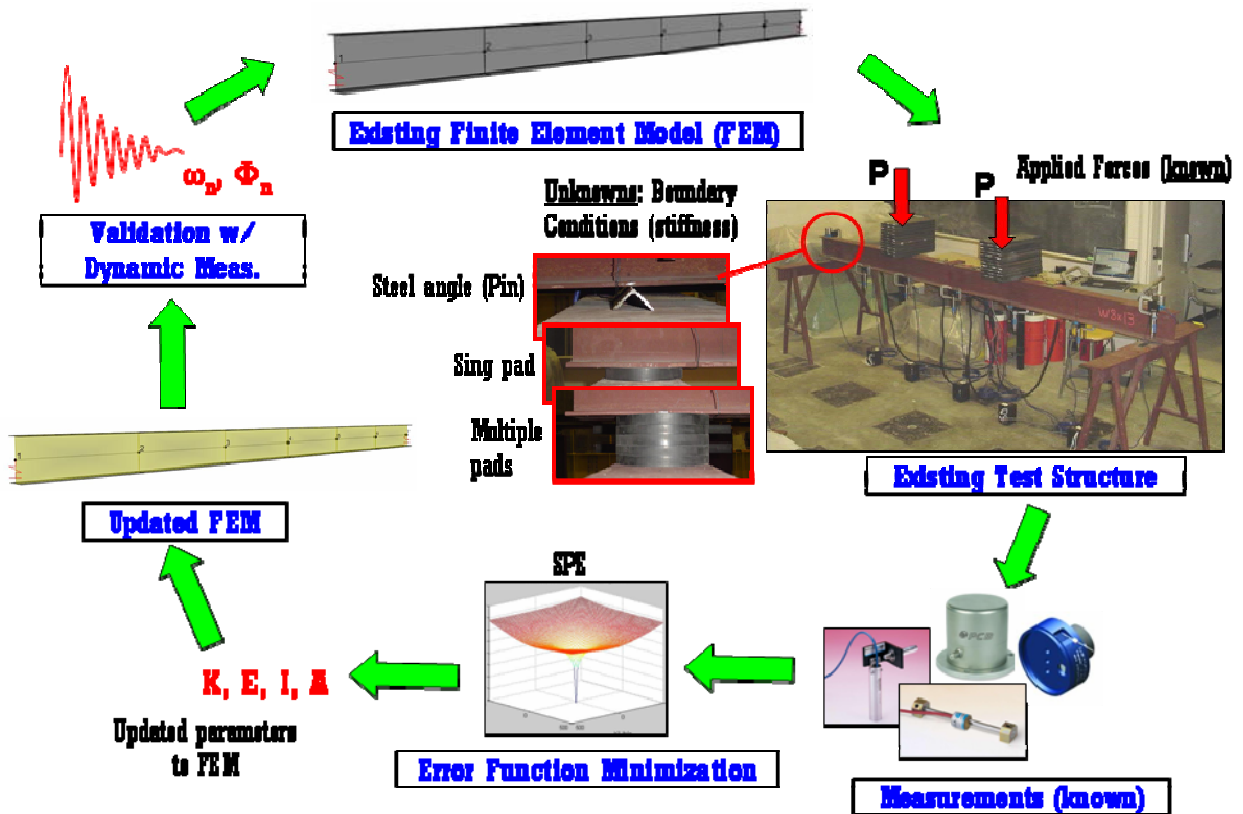


Figure 5.35 –General methodology for parameter estimation and model updating

A number of static and dynamic tests are conducted by using a simply supported beam. More information about the beam and the sensor distribution on the beam can be found in Appendix B. During the tests, different types of pads are used at the boundaries. Then the SPE was used to identify the unknown stiffness parameters at the boundaries and update the FEM. The following figure shows example results where five Duro50 pads were used at the boundaries. Then the stiffness parameters at the boundaries were

estimated by using the methodology. We see that the stiffness values are identified as 6.5 kip/in for right support and 6.62 kip/in for left support.

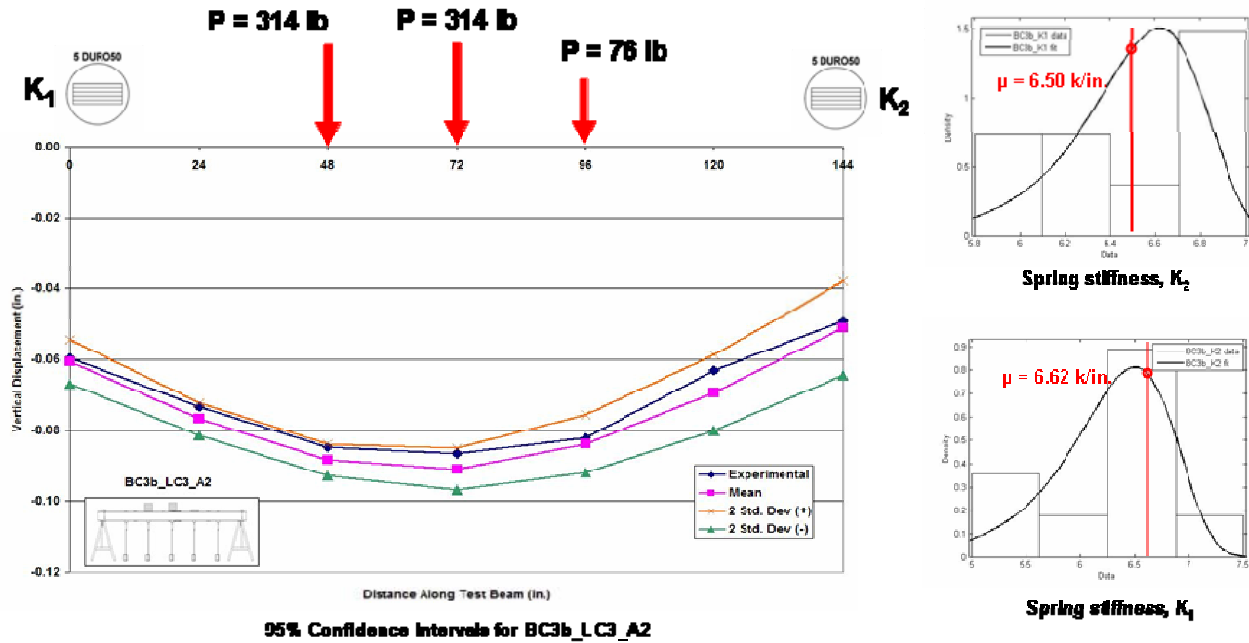


Figure 5.36 –Estimation of the stiffness parameters at the supports with statistical bounds

### 5.5.3. Estimation of Reliability using SHM Data

Sensor data can be used to track and model the deterioration or loss of capacity in monitored components. These models are supported by analytical derivations and previous study, and will be updated with new data. Finite Element or calibrated Finite Element models will be producing the component reliability indices using the data continuously fed by the sensors.

### Limit State Function

Limit states define the failure criteria according to a selected failure mode. All realizations of a structure can be put into one of the two categories

- Safe (load effect  $\leq$  resistance)
- Failure (load effect  $>$  resistance)

The state of the structure can be described using parameters,  $X_1, \dots, X_n$  where  $X_i$ 's are load and resistance parameters

A limit state function is a function  $g(X_1, \dots, X_n)$  of these parameters, such that

- $g(X_1, \dots, X_n) \geq 0$  for a safe realization
- $g(X_1, \dots, X_n) < 0$  for failure
- Each limit state function is associated with a certain limit state

Limit state functions are expressions defining the failure limit and generally in the form of  $g(R, Q) = R - Q$ , i.e., they indicate the spare capacity of the structure or the structural component. If the limit state function is positive, resistance is greater than the load effects, so the structure is safe. If the limit state function is less than zero, this case defines a failure since the load effect has exceeded the capacity. The curve or surface defined by  $g = 0$  is the failure surface dividing failure and survival spaces. Engineers' aim is always making  $g$  greater than zero, but how close to zero it may approach is related with the balance between risk and cost (Ditlevsen and Madsen 1996; Melchers 1999; Nowak and Collins 2000).

### **Reliability Index**

Reliability index is a unit of failure probability, which is the area under the limit state surface. In case a linear limit state function is considered;

$$g(X_1, X_2, \dots, X_n) = a_0 + a_1 X_1 + a_2 X_2 + \dots + a_n X_n \quad (5.6)$$

$X_i$  : uncorrelated random variables, with unknown types of distribution, but with known mean values and standard deviations

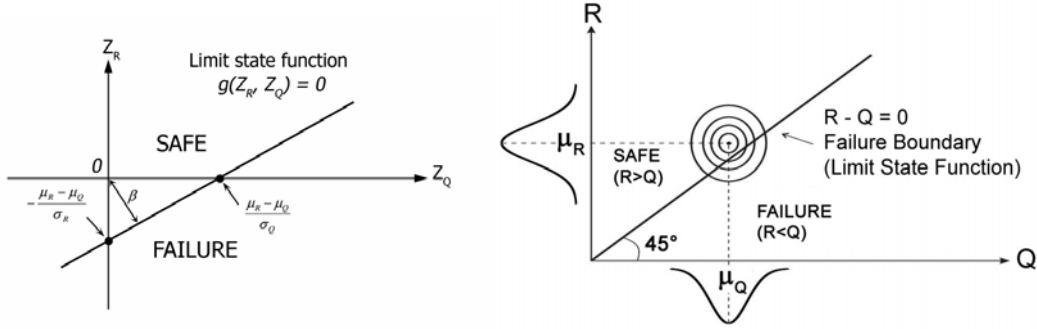


Figure 5.37 – Limit state functions (Nowak and Collins 2000)

Then, the reliability index,  $\beta$ , can be calculated as follows,

$$\beta = \frac{a_0 + \sum_{i=1}^n a_i \mu_{X_i}}{\sqrt{\sum_{i=1}^n (a_i \sigma_{X_i})^2}} \quad (5.7)$$

Therefore, as shown in Figure 5.37, the reliability index for a linear limit state is the shortest distance from the origin to the failure surface. If a non-linear limit state function  $g(X_1, \dots, X_n)$  is considered, then the limit state function can be linearized by applying a Taylor series expansion and taking the first-order terms;

$$g(X_1, X_2, \dots, X_n) \approx g(x_1^*, \dots, x_n^*) + \sum_{i=1}^n (X_i - x_i^*) \frac{\partial g}{\partial X_i} \quad (5.8)$$

where the derivatives are calculated at  $(X_1^*, \dots, X_n^*)$

Component reliabilities can be generated with the sensor-based degradation models for time functions of reliability. System reliability and component reliabilities can be monitored real-time, and different alert levels can be triggered when a value below a critical reliability index is calculated.

## Prediction and Bayesian Updating

Bayesian updating technique is a very powerful tool to make use of new data to refine the statistical parameters of an assumed or calculated distribution. The general formula for Bayesian updating method is shown below;

$$g(\theta | x) = \frac{f(x | \theta)g(\theta)}{\int f(x | \theta)g(\theta)d\theta} \quad (5.9)$$

where

$f(\theta | x)$  : conditional PDF of  $X$  given  $\Theta$  (sampling distribution)

$g(\theta)$  : PDF of  $\Theta$  (prior distribution)

$g(\theta | x)$  : posterior PDF of  $\Theta$  given  $x$  (posterior distribution)

$\theta$  : continuous parameter vector

$x$  : sample data

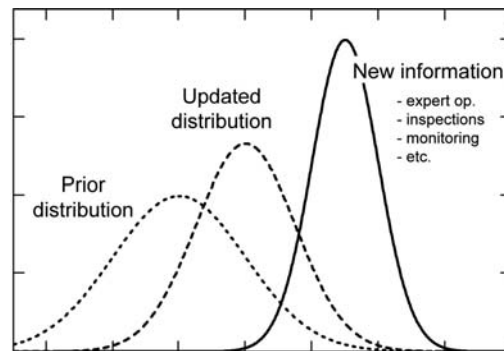


Figure 5.38 – Concept of Bayesian Updating

This technique is previously used successfully to update condition state of bridges when new visual inspection data is available. With time, the uncertainty of the estimated parameters increases rapidly due to epistemic randomness, but using Bayesian updating, new information is incorporated into the models to reduce that kind of uncertainty.

In the case of new monitoring data to be included in the existing knowledge, the following simplified formula can be used for Bayesian updating:

$$f''(\theta) = c \cdot L(\theta | x) f'(\theta)$$

where

$f'(\theta)$  : prior distribution

$L(\theta | x)$  : likelihood function for  $\theta$

$c = \left[ \int L(\theta | x) f'(\theta) d\theta \right]^{-1}$  : normalizing factor to adjust the probability area

For the case where both  $f'(\theta)$  and  $f(x)$  are normally distributed, the posterior function  $f''(\theta)$  is also normally distributed and has the mean value and standard deviation, respectively, as

$$\mu'' = \frac{\mu(\sigma')^2 + \mu'(\sigma)^2}{(\sigma')^2 + (\sigma)^2} \quad \sigma'' = \sqrt{\frac{(\sigma')^2(\sigma)^2}{(\sigma')^2 + (\sigma)^2}} \quad (5.10)$$

where

$\mu, \sigma$  : mean value and standard deviation of the a-priori distribution

$\mu', \sigma'$  : mean value and standard deviation of the new data

$\mu'', \sigma''$  : mean value and standard deviation of the updated distribution

If the distributions are non-normal, there may exist a closed form solution, but otherwise, Monte Carlo simulation can be used to calculate the posterior distribution.

As an example study, the simply supported beam shown in Figure 5.15 is tested for changing boundary conditions. Midspan displacement data was collected with a displacement sensor for the different boundary conditions, which are pin-support, single elastomeric pad and multiple elastomeric pads at the support locations, identical at both sides. The aim is to simulate deteriorating support conditions and how these changes can be tracked, translated into reliability analysis from monitoring data and future reliability can be predicted.

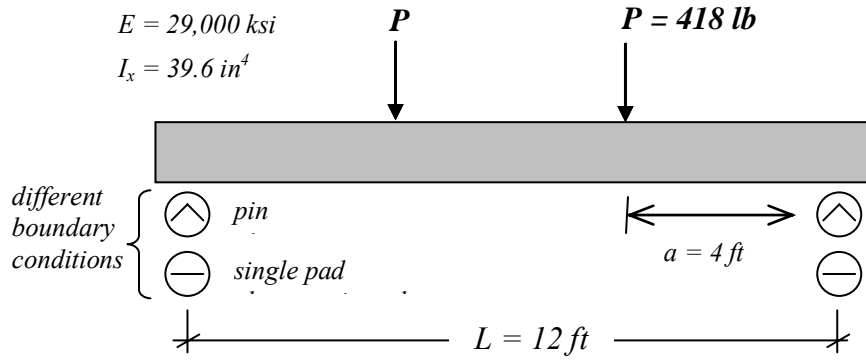


Figure 5.39 – Simple beam test for Bayesian updating demonstration

The theoretical midspan displacement value for the given loading is taken as the initial estimate of the displacement values. It is calculated according to the dimensional, material properties and loading as;  $\delta = 0.045 \text{ in}$  (midspan deflection).

The theoretical displacement value will define the mean value of the existing distribution, while uncertainty analysis needs to be conducted for defining the variability of the distribution. However, for a demonstration, the initial displacement was assumed to be normally distributed with a standard deviation of 0.001, to account for the uncertainties due to unknown actual parameters.

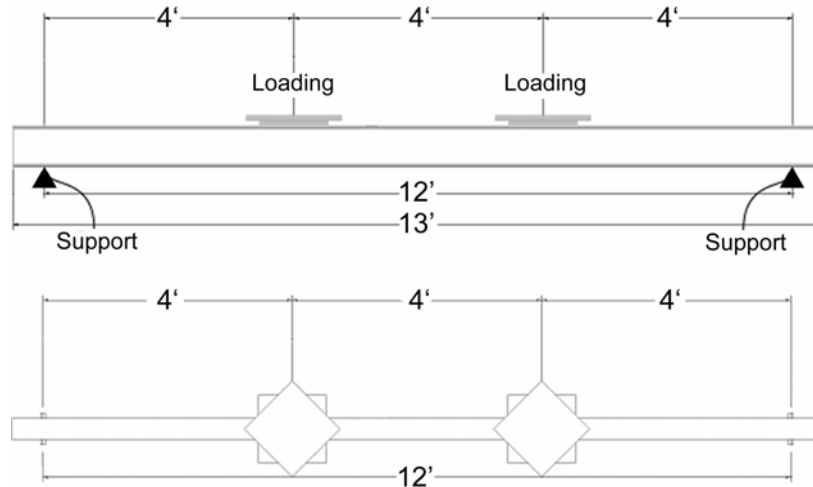


Figure 5.40 – Test beam

Having the initial information, i.e., the *a-priori* condition, it is desired to integrate the new data provided by sensor measurements. When new data is available, the previous knowledge should not be discarded, but updated through Bayesian updating. Figure 5.17 shows the distributions of the previous data (theoretical displacement value) and the most recent data (displacement gage at the midpoint for pinned end conditions).

In order to construct the reliability index, a limit state function needs to be defined. Since the displacement is the main parameter in this particular example, the limit state can be defined as the midspan deflection exceeding a pre-set value, which is set as  $\delta_{max} = L/800$ .

$$g_{disp}(\delta_{max}, \Delta) = \delta_{max} - \Delta \quad (5.11)$$

which forms the reliability index as;

$$\beta = \frac{\mu_{\delta} - \mu_{\Delta}}{\sqrt{(\sigma_{\delta})^2 + (\sigma_{\Delta})^2}} \quad (5.12)$$

where  $\Delta$  denotes the measured displacement

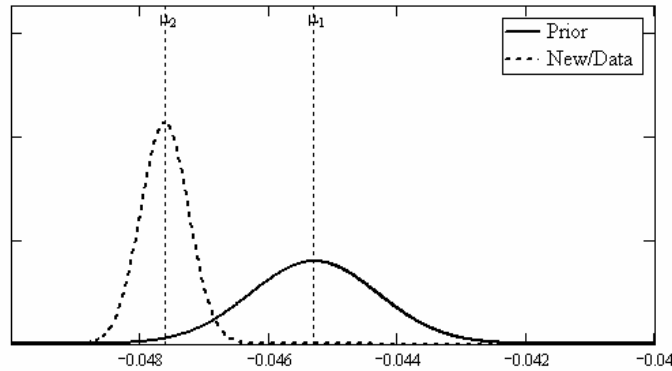


Figure 5.41 – Prior and new data for the test beam

The updating procedure generates the updated distribution, which involves less uncertainty than both distributions, and its mean value is closer to the distribution with higher confidence. Figure 5.24 shows the steps of updating the distributions with the

prior and recent information. On the right, the mean values are shown for the initial and the following reliability points, before and after updating. With each new data set, Bayesian updating is repeated, increasing the confidence of the data. Reliability indices are calculated based on the defined limit state.

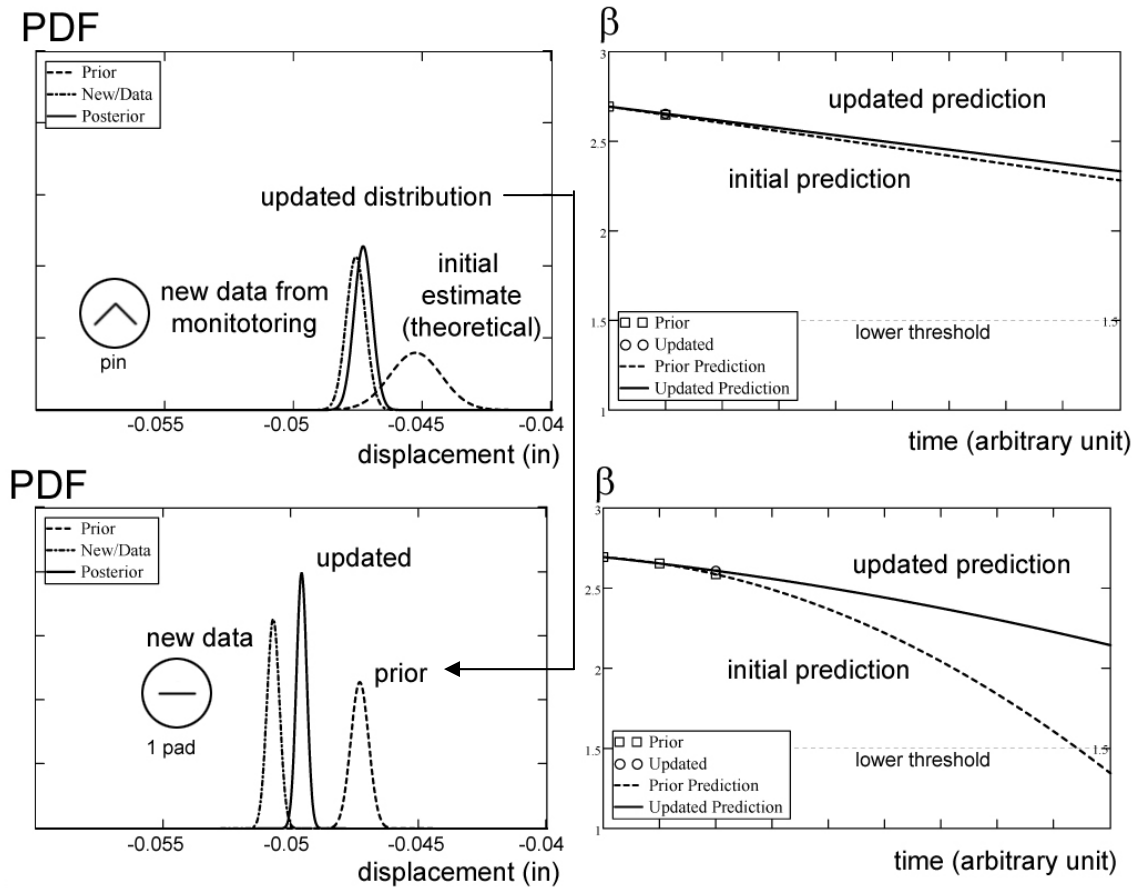


Figure 5.42 – Updating the available data and prediction with the first data set using Bayesian

The new data are incorporated into the previous data, creating a new distribution. The figure on the right hand side shows the difference in the prediction curves for the reliability index, based on curve fitting. The updated data also changes the curve fit, hence the prediction of future performance.

Making predictions are the ultimate tools for decision making in bridge management (Figure 5.43). The procedure will be applied to sensor data, which provides more accurate information to fine-tune the prior distributions. This way, predictions will

be much more accurate, since the information source is more reliable and accurate. Bayesian updating method is perfectly suitable for updating the condition with sensor measurements. An automated system can be coded, which would continuously update and adjust the parameters with the continuous input of sensors. The procedure is applicable to monitoring structural parameters, corrosion, motors and other components over time. Updated component reliability indices also form the updated system reliability automatically from parallel/series modeling.

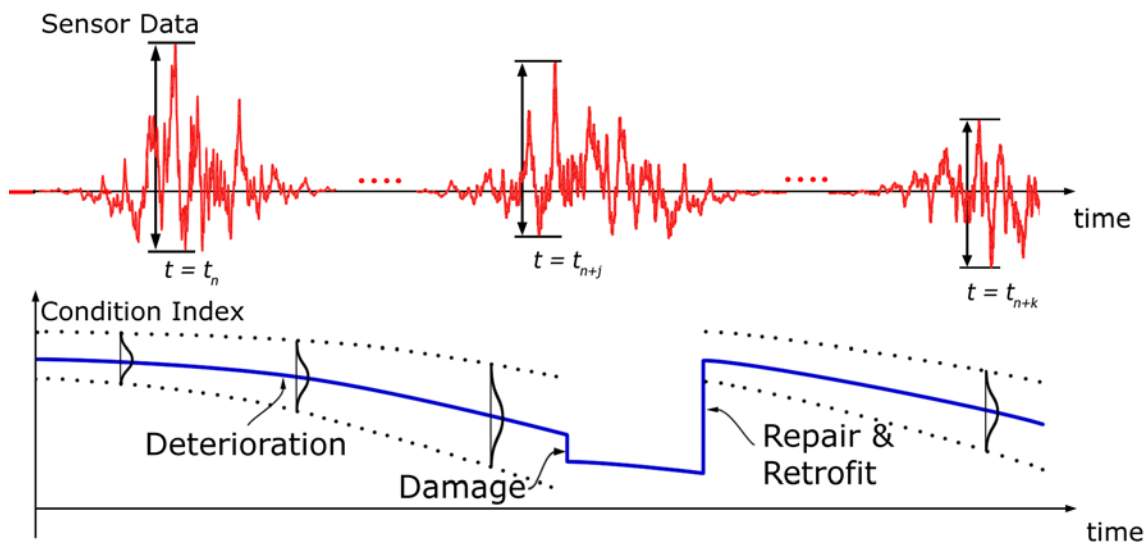


Figure 5.43 – Reliability based on SHM data

It is possible to expand the framework to employ life-cycle cost estimation, and add maintenance scheduling and optimization functions using the sensor-based, continuously updated system reliability monitoring data. The realization of such a framework would provide an invaluable tool for infrastructure management such as bridges, buildings and other constructed facilities (Susoy et al. 2006a; Susoy et al. 2007).

#### 5.5.4. Possible Use of Computer Vision Data for SHM

The writers believe that computer vision will be a key technology that will significantly improve SHM applications in the future. Computer-vision is processing of acquired images in order to detect and track certain features. Recently, computer vision applications have gained attention for SHM applications. This approach is being

implemented and improved at the UCF Structures and Systems Research Laboratory where a novel framework for real-life structures is being constructed. Basic methodology of the framework and preliminary results are described as follows;

Video streams are used in conjunction with computer vision techniques to determine the class, speed, and location of vehicles moving over the bridge. A database is constructed using information from the vehicles (loads) training sets, the experimental results from the sensors network and a finite element model. Then, this proposed system, by interpreting the images and correlating those with the information contained in the database, will evaluate the operational condition of the bridge.

All of this will be done in real time, without the necessity of processing large amounts of data after its acquisition. Additionally, video can be used to detect suspicious activities, i.e. the presence of persons, vehicles and/or objects in critical or prohibited, predetermined locations. Every day, at every moment, the bridge will be monitored and its condition will be assessed, preventing further damage and catastrophes and keeping the most critical legacy data, for further studies.

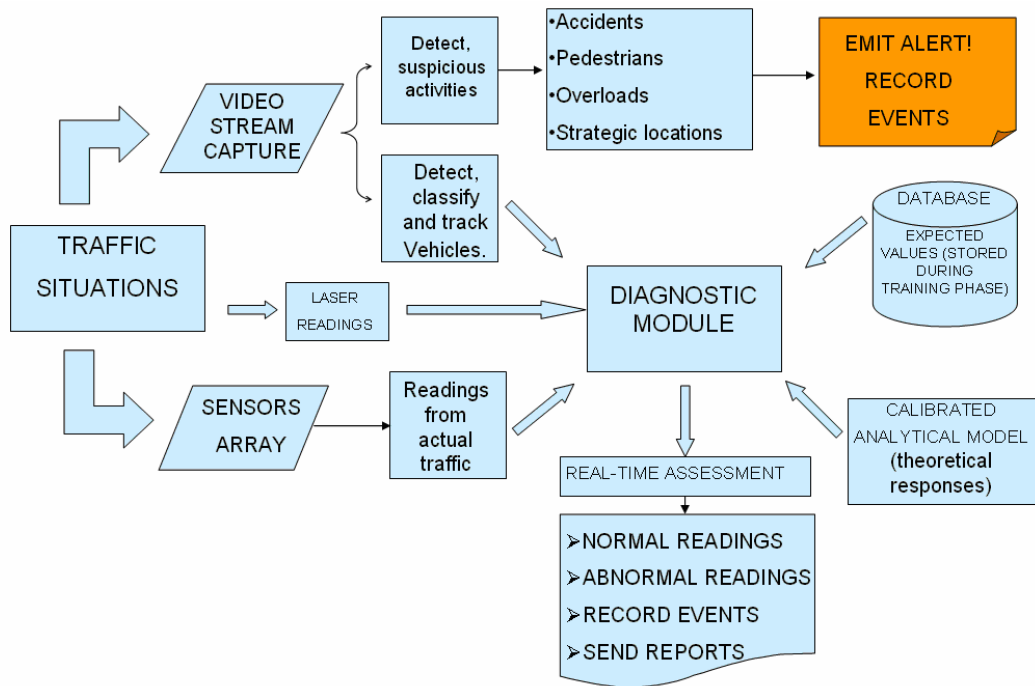


Figure 5.44 – Computer vision integration into SHM

The system will provide real-time continuous assessment: video cameras will be detecting, tracking, and classifying vehicles permanently, and sensors will be synchronized with the video input to detect the structural behavior. This feature will help prevention of catastrophic failures, notification of any abnormal behavior, generation of image and numerical records, remote visual monitoring, tracking of structural behavior and help in scheduling condition-based maintenance. The integration of computer vision into a SHM system is illustrated in Figure 5.44.

Identifying moving objects from a video sequence is a critical task for all vision systems. Some kind of mechanism is required to detect what is happening in the field of view of the camera. Any moving or out-of-place object is noted and has to be somehow detected. Once objects are detected, further processing is needed to indicate in which direction they are moving (tracking) and/or what kind of object is (classification). A common approach for identifying the moving objects is background subtraction, where each video frame is compared against a reference or background model. Pixels in the current frame that deviate significantly from the background are considered to be moving objects and belonging to the foreground. This pixel-based information is then clustered to identify regions in order to label, and classify objects.

Detection previously obtained will include false positives due to a variety of reasons. For example, background moving objects (leaves and branches, debris, shadows, occlusions, etc.) be considered foreground objects, leading to false results. To eliminate this identity mistakes data must be validated. The most common approach is to combine morphological filtering and connected components grouping to eliminate these regions. Connected component grouping is used to identify all regions that are connected and eliminates those that are too small to correspond to real interest moving points. In this way, the remaining noise is eliminated.

A bounding box is drawn around the object and its size (number of pixels) and centroid (location within the image) are calculated. Once each vehicle/object is detected and located in the image, its image coordinates have to be converted and mapped into the real world coordinates system. This is achieved by finding the intrinsic and extrinsic

camera parameters that establish the relationship between image (I) and world (W) coordinates. These parameters were found by knowing a set of points in the image and real world, establishing a system of equations and using singular value decomposition to get the final solution. This procedure is explained schematically in Figure 5.45.

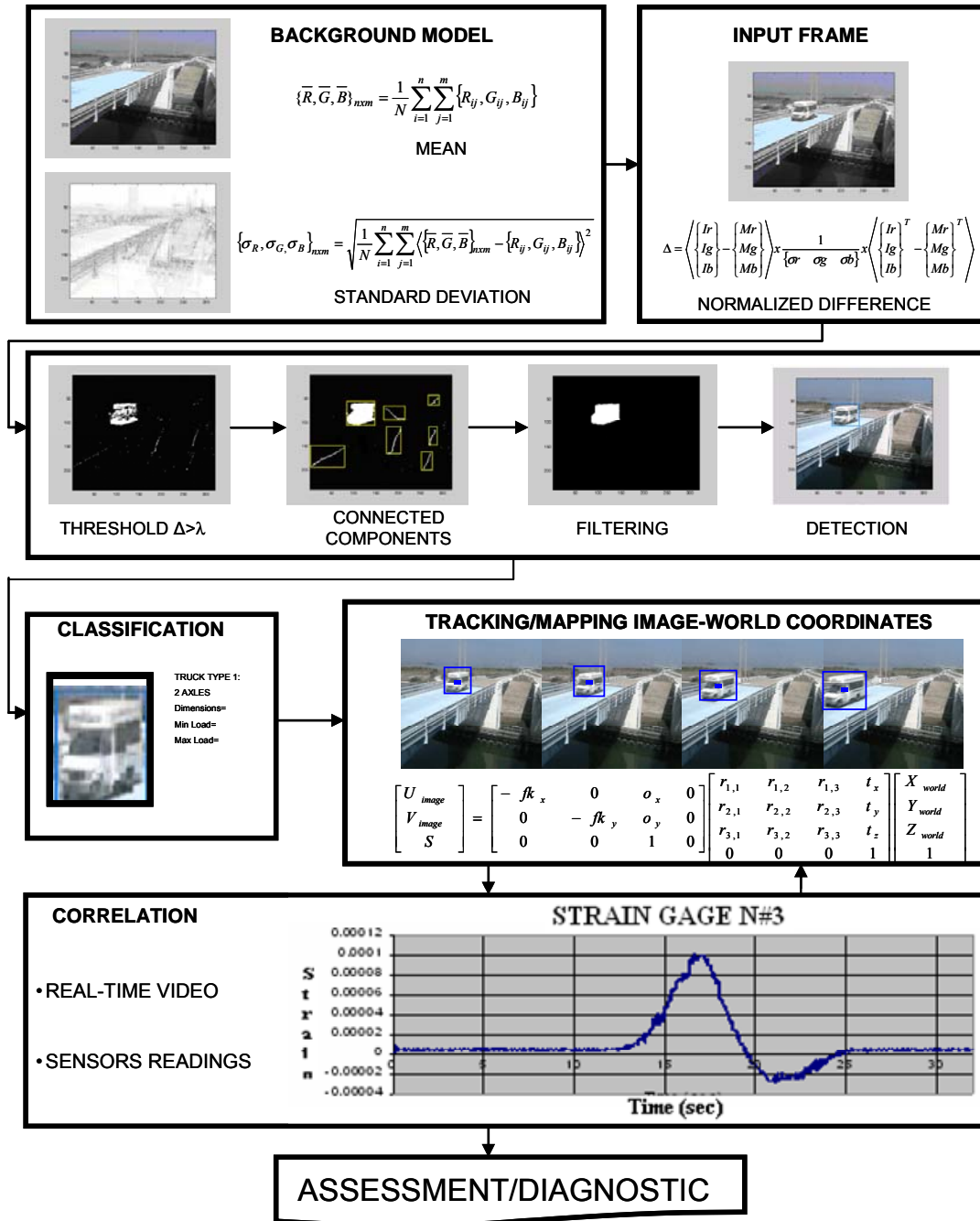


Figure 5.45 – SHM and computer vision integrated operation

Moving objects in two consecutive frames are matched allowing the calculation of its speed while moving along the bridge.  $v = d/t$  where  $v$  represents the speed,  $d$  is the distance between centroids of the same object for the two images, and  $t$  is the elapsed time between images (1/30 s. for two consecutive frames is the standard frame capture ratio for the type of camera used). To actually track a vehicle thru the video constrains like maximum speed, common motion, and minimum velocity are used. Additional information provided by color and size allows the building of an index-weighted matrix, which provides the most probably matching objects between the two frames. Estimation of the next position of the vehicle (centroid) is found. This value is fundamental when correlating sensor readings vs. load positions.

Finally, once an input is received from the vision module, the system will infer the structure health by comparing the expected results for those loads (from the database) with the actual readings (from the sensors array). Surveillance capabilities could also be added to discern between normal and suspicious activities and emit alerts if needed.

The proposed framework will also be capable of maintaining a permanent surveillance for safety monitoring. Video surveillance and monitoring is a rapidly growing area of video computing, particularly for suspicious activities, accidents and threats. The objectives of video surveillance and monitoring systems are to (1) detect moving objects in the video, (2) track objects throughout the sequence, (3) classify them into people, vehicles, animals, etc., and (4) recognize their activities. The system will be able to inform the bridge owner and/or other agencies in possible cases of accidents, pedestrians, overloads, suspicious activities including non-moving vehicles, persons around certain locations, presence of objects left on critical locations, etc (Zaurin and Catbas 2007).

## **5.6. DATA MONITORING FRONT PANEL**

An integrated monitoring system has been set up in the UCF Structures and Systems Research Laboratory, which allows monitoring various sensor data and video images. The front panel of the data acquisition system is shown in Figure 5.46. The

monitoring system is currently based on the two-span bridge model in the laboratory. The vision component of the system is acquiring real-time video images from the test setup, while at the same time monitoring the changes in other sensor measurements from other indicators and graphs. One component of the monitoring system is displacement, showing the displacements over the laboratory bridge structure at certain locations. Another section is strain, which shows the difference in strain values along the bridge. Tiltmeters, temperature sensors and accelerometers are also integrated into this system, controlled from corresponding dials and screens. For demonstration, a wind station has been set up in the laboratory, indicating the direction and speed of wind, which can be measured simultaneously with all other measurements. Currently, the system is programmed to emit visual and auditory alerts when certain threshold values are exceeded. It is possible to incorporate the advanced algorithms, which are under development by UCF researchers into this real-time system. These methodologies are to be mentioned in the following sections. The sensor, data acquisition and front panel setup is very flexible and easily modified to expand the capabilities according to the needs of any kind of monitoring application.

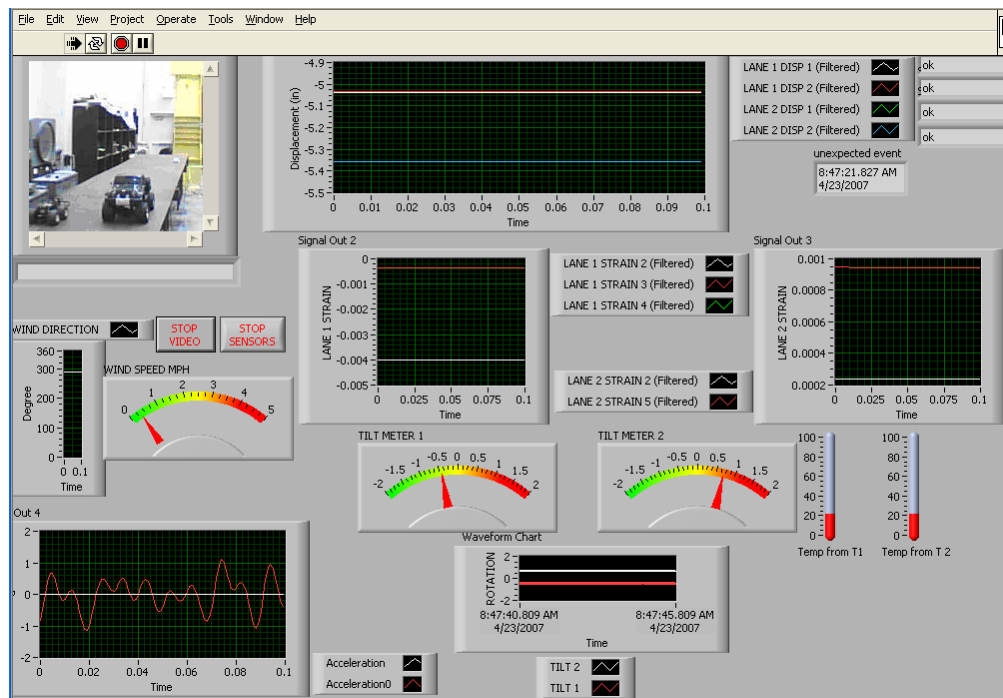


Figure 5.46 – Data monitoring for the laboratory health monitoring setup

A modified version of the existing monitoring system is proposed for day-to-day applications of actual bridges for the use of engineers and, if required, the public with various levels and limitations as illustrated in Figure 5.47. The sensor arrays and data acquisition systems of the framework should be tailored for the specific needs of the monitored bridge. The system, after collecting the data, should process the data at the server nodes supporting a database structure.

The main server can provide physical storage for the post-processed and filtered data, as well as other archived inspection and maintenance reports. The information on the main server can be accessible through the web. Security of the system is very critical since the bridges as well as the management system are important assets. Access to the database should be limited by defining users with passwords and their position, task and privileges. So, only certain sections of the database should be allowed to each user.

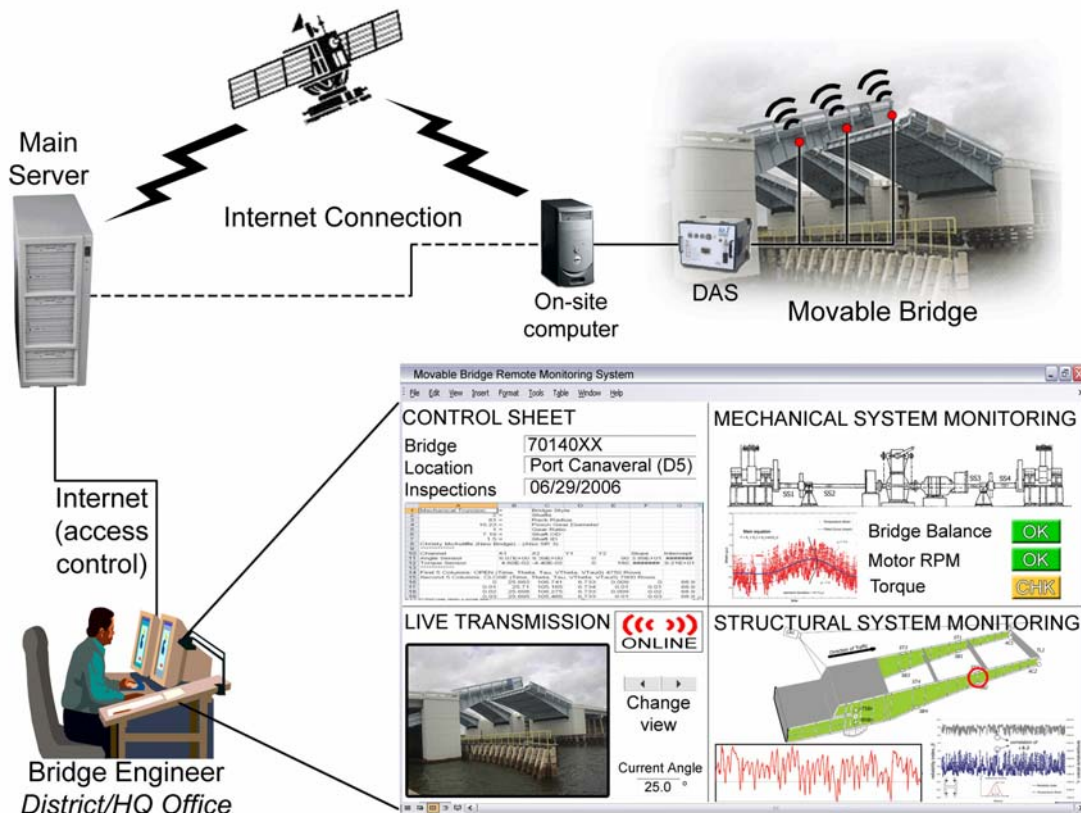


Figure 5.47 – Movable bridge remote monitoring system

Additionally, real-time data monitoring will be provided. The real-time mode displays data from any sensors at a particular location and live video streaming will be available. Streaming data can be observed by an authorized user from any remote site equipped with Internet access.

### 5.7. DATA MANAGEMENT AND INFORMATION TECHNOLOGIES

In the following schema, integration of Bridge Health Monitoring (BHM) and Bridge Management System (BMS) is illustrated. Sensors on the structure transmit signals to the data acquisition stations through wired or wireless connections, according to the SHM design. Raw data delivered by data acquisition stations are processed and converted into meaningful data, which is then logged into the database. Inspection reports from visual inspection of the structure are also added to the database in electronic format. Then, the integrated database containing bridge information, legacy data and condition state serves as a hub for all offices and districts for reaching, updating and sharing this information.

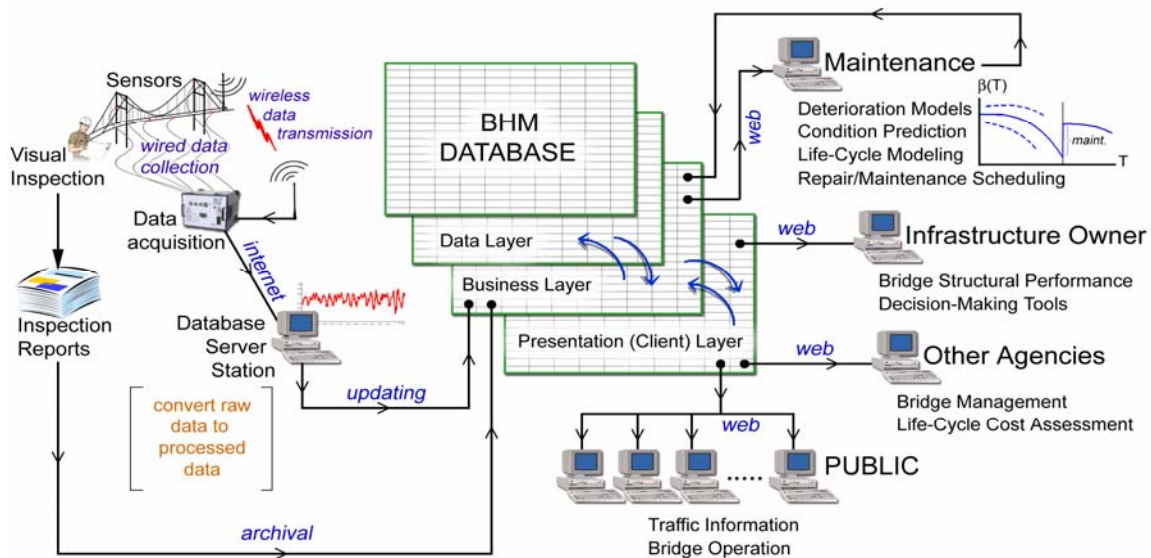


Figure 5.48 - Database implementation

Advantages of utilizing the Internet for bridge management and database applications are numerous. A system working on Internet will be much more convenient

for the users, who will have access with any kind of Internet connection. There will be no compatibility issues or installation and maintenance of software for each user, since regular internet browsers will be enough for all tasks. Intra-agency information sharing and collaboration is also maximized.

A typical database for SHM can be composed of three conceptual layers, each of which is associated with certain functions of its mechanism. These are;

1. Data Layer
2. Business Layer
3. Presentation (Client) Layer

An example of a database working schema is given in Figure 5.49.

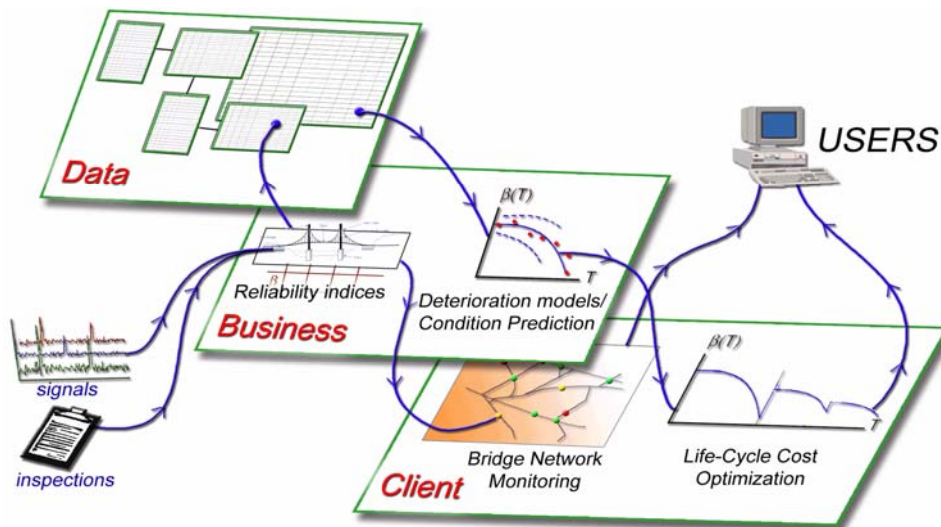


Figure 5.49 - Database functional layers

The data layer is static, representing stored physical data. The data layer is the foundation of the database, containing all data and tables. This layer is at the background and accesses only through the business layer. The business layer contains the rules, policies and algorithms for manipulating the data layer. Algorithms that determine the reliability indices from SHM data and store into appropriate fields/tables in the database

are parts of the business layer. The client layer is the interface that the user uses to interact and to send and receive information. When the user requests bridge network monitoring or life-cycle cost optimization display from the client layer, the business layer retrieves the necessary information from the data layer, converts into required format, and sends to the client layer for display.

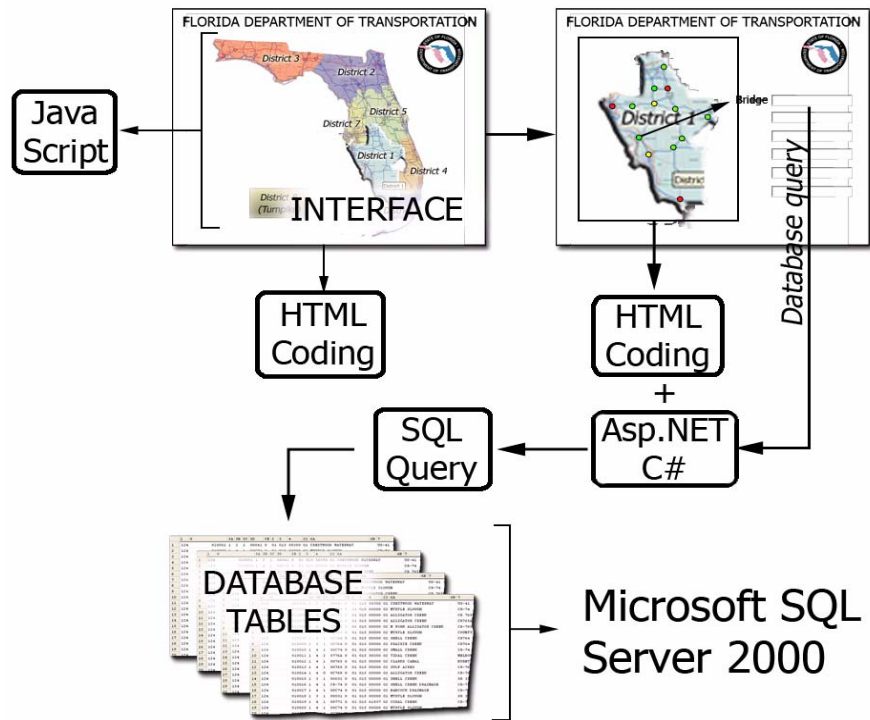


Figure 5.50 – Example framework for internet-based database

This database structure also allows life-cycle maintenance cost analyses using bridge deterioration models and effects and unit costs associated with each action. Optimum maintenance plans will be drawn for a given bridge lifetime, minimizing the total cost and assuring certain safety levels. This will be an ultimate tool for high-level management of bridges, allowing trade-off analysis and budget decisions with maximum efficiency.

## **6. CONCLUSIONS AND RECOMMENDATIONS**

This study aims to provide a general Structural Health Monitoring (SHM) framework to be applied for improved decision making for managing bridges. In the study, the components of an SHM system that are discussed include instrumentation, data collection, advanced techniques that enable high-level analysis and presentation of collected data, and data archival and management using information technology. Movable bridges in Florida are selected as the focus of this project, due to their different maintenance needs, and significantly higher maintenance costs than fixed highway bridges, making them a more critical bridge population and good candidates for monitoring.

### **6.1. CONCLUSIONS AND FINDINGS**

From analysis of movable bridge records, inspection reports, and site visits, the movable bridge population is identified to have a high deterioration rate for structural components. Structural components are subject to corrosion and adverse effects due to misalignments and operational wear. In addition, the mechanical and electrical systems are subject to frequent problems or breakdowns even if they are continuously inspected and maintained.

Among the FDOT movable bridge inventory, Christa McAuliffe Movable Bridge in Merritt Island, on SR-3 is selected as an average bridge according to the general characteristics, such as age, size, type and operation frequency. This bridge is assumed to be representative of most of the movable bridges in Florida, which have similar characteristics. In-depth analysis of the inspection reports over a 25 year period is conducted. It is seen that the orthotropic deck, movable components such as shafts, emergency drives, and locks and live load shoes exhibit low condition ratings. As a result, this bridge was rehabilitated twice in the 1990s. It is also observed that while rehabilitation improved the condition ratings, some components such as span lock ratings dropped shortly after the rehabilitation. In addition to the inspection results, finite element analyses are prepared and presented to help understand the critical response

locations and levels. The models are used to determine operating levels of stresses and deflection under various load conditions. The tip deflection under single AASHTO HL-93 truck and two HL-93 trucks+lane load are determined to be 1.65 in and 4.49 in, respectively. The serviceability limit for this bridge and deck type is determined to be 5.6 in. The maximum stresses under dead load and two HL-93 trucks+lane load around trunnion, at span lock and live load shoe are determined to be ~6-12 ksi, ~10 ksi, ~15 ksi, respectively. The frequencies and mode shapes are also sensitive to damage, imbalance and structural changes. For example, it is seen that additional modes appear when span lock failure is simulated. For the undamaged condition, the first three modes are at 3.69 Hz, 4.74 Hz and 9.04 Hz. The load rating is determined to be lowest right above the live load shoes. The inventory and operating rating values under two HL-93 trucks+lane load at this location are 0.98 and 1.27, respectively. However, it is seen that under one HL-93 truck traveling at 50 mph, the lowest system reliability index is determined to be 5.79 which is far above the 3.5 (AASHTO LRFD for new design) and 2.5 (AASHTO LRFR for existing bridges). These results are valuable to determine the monitoring locations, sensing requirements and expected ranges. Analyses based on finite element modeling of this bridge, inspection data and data collection from balance tests revealed that the complex structural, mechanical and electrical systems are very sensitive to maintenance neglects, therefore, need to be monitored closely.

## **6.2. INSTRUMENTATION PLAN**

A proposed instrumentation plan on structural components, which would enable tracking of the current condition and deterioration, is presented. The proposed SHM instrumentation is based on site visits and meetings with several maintenance and repair engineers at different districts, analysis of inspection records, and analytical models and simulations. The following are found to be candidates for instrumented monitoring, in addition to various common structural components:

- Electrical Motors
- Gear Boxes
- Open Gears / Racks
- Hopkins Frame
- Trunnions
- Live Load Shoes
- Span Locks

Issues associated with these components and possible monitoring solutions are documented in the report. The main purpose of the instrumentation plan is to provide a better tracking system of maintenance issues, which would increase the maintenance efficiency and indicate critical service needs to reduce breakdowns.

A major benefit of a monitoring system is that any sudden change in the capacity or partial/total collapse of a bridge can be detected and “seen” instantly. Especially after a catastrophic natural or man-made event, such as hurricane, or vessel/vehicle impact, rapid condition evaluation of bridges is imperative. During or in the aftermath of a widespread disaster, such a system would be the key for strategic emergency response operations, by determining whether the bridges are operational, critically damaged, or failed. This will allow the establishment of safe routes as well as the prioritizing of emergency repair operations.

Coupled with appropriate sensors and sensing networks, advanced analysis techniques such as statistical pattern recognition methodologies, reliability based monitoring, and computer vision oriented SHM enable processing of data for generating useful information through a series of algorithms. The aim is to provide useful information quickly, and these methodologies are currently in development to indicate the condition scientifically, detect anomalies and damage, and provide predictions and future trends based on the results extracted from collected data. Problems caused by physical scatter and discrepancy of current data collection and storage systems can be overcome by establishing an innovative mechanism of information management system where all the data is collected in standard formats and transferred to a central database, where raw and processed data are logged and stored. This database is to serve all clients of different layers within the organization up to the level of their involvement with the information and authorization by the system. In addition to serving as a data terminal, the system can provide means of efficient communication among all branches in lateral and vertical dimensions.

### **6.3. RECOMMENDATIONS AND FUTURE STUDY**

For a complete Structural Health Monitoring system, the integration of the monitoring components is necessary. Remote monitoring and integrated data archival methods are presented to make the maximum and most efficient use of the collected data. Based on the framework defined in this report, it is possible to build a monitoring system for a movable bridge that covers whole aspects from sensor installation to user controls.

The proposed instrumentation plan was aimed at addressing maintenance, operation and safety issues, and leading to more efficient management practices for movable bridges. A continuous monitoring system, with relatively little investment, can help track the bridges' degradation. Therefore, projections for the structural performance can be made over the long-term and preventative maintenance work can be better scheduled. In addition, this approach should eliminate or significantly reduce unexpected breakdowns by providing instant warnings to maintenance personnel. Proactive maintenance is a much more efficient practice than repairing the bridge after extensive damage is discovered, or in case of a breakdown, which prompts costly and time-consuming emergency repairs. Costs associated with traffic delays will also be reduced. We note that the integrated monitoring framework proposed in this report is developed in parallel to efforts of the Federal Highway Administration Long Term Bridge Performance Program (LTBPP). The LTBPP focuses on continuous bridge monitoring applications for developing improved knowledge on performance and degradation, better design methods and performance predictive models, and advanced management decision-making tools. In light of the findings from the current studies, it is recommended that complete SHM systems are adapted and implemented to complement current bridge management systems. An application such as described in this report is expected to mitigate the problems and reduce maintenance costs. Further studies and pilot applications are necessary to test and evaluate new technologies and algorithms as well as to quantify the cost-benefit ratio of integrated SHM applications. This way, the approach can be further improved and customized according to user needs and other challenges that can only be discovered through real-life applications.

## 7. REFERENCES

- "Manual for Maintenance Inspection of Bridges", AASHTO, 1983.
- "Guide Manual for Condition Evaluation and Load and Resistance Factor Rating (LRFR) of Highway Bridges, 1st Edition", AASHTO, 2003a.
- "Manual for Condition Evaluation and Load and Resistance Factor Rating (LRFR) of Highway Bridges" American Association of State Highway and Transportation Officials, AASHTO, 2003b.
- "Development of a Model Health Monitoring Guide for Major Bridges" Drexel Intelligent Infrastructure and Transportation Safety Institute, Aktan, A. E., Catbas, F. N., Grimmelsman, K. A. and Pervizpour, M., 2003.
- Aktan, A. E., Chase, S., Inman, D. and Pines, D. (2001a). "Monitoring and Managing the Health of Infrastructure Systems". Proceedings of the 2001 SPIE Conference on Health Monitoring of Highway Transportation Infrastructure, Irvine, CA, March 6-8.
- Aktan, A. E., Pervizpour, M., Catbas, F. N., Grimmelsman, K. A., Barrish, R. A., Curtis, J. and Qin, X. (2001b). "Information Technology Research for Health Monitoring of Bridge Systems". Proceedings of the Structural Faults & Repair 2001 Conference, London, UK, July 4-6, 2001.
- "AASHTO LRFD Bridge Design Specifications" Washington, DC., American Association of State Highway and Transportation Officials (AASHTO), 2002.
- Anderson, O. D. (1976). "Time Series Analysis and Forecasting the Box-Jenkins Approach." Butterworth & Co, UK.
- Asmussen, J. C. (1997). "Modal Analysis Based on the Random Decrement Technique - Application to Civil Engineering Structures." Doctoral Dissertation, University of Aalborg, Aalborg.

- "Parametric Finite Element Modeling and Full-Scale Testing of Trunnion-Hub-Girder Assemblies for Bascule Bridges" A Report on a Research Project Sponsored by the Florida Department of Transportation, Besterfield, G., Kaw, A. and Crane, R., 2001.
- Box, G. E., Jenkins, G. M. and Reinsel, G. C. (1994). "Time Series Analysis: Forecasting and Control". Prentice-Hall, New Jersey.
- Burkett, J. L. (2005). "Benchmark Studies for Structural Health Monitoring using Analytical and Experimental Models." MS Thesis, Department of Civil and Environmental Engineering, University of Central Florida, Orlando, FL.
- Buxton-Tetteh, B. (2004). "Development of User Cost Model for Movable Bridge Openings in Florida." MS Thesis, Civil Engineering, Florida State University, Tallahassee, FL.
- Catbas, F. N. and Aktan, A. E. (2002). "Condition and Damage Assessment: Issues and Some Promising Indices." *Journal of Structural Engineering, ASCE*, **128**(8): 1026-1036.
- Catbas, F. N., Brown, D. L. and Aktan, A. E. (2006). "Use of Modal Flexibility for Damage Detection and Condition Assessment: Case Studies and Demonstrations on Large Structures." *Journal of Structural Engineering, ASCE*, **132**(11): 1699-1712.
- Catbas, F. N., Ciloglu, S. K. and Aktan, A. E. (2005). "Strategies for Condition Assessment of Infrastructure Populations: A Case Study on T-beam Bridges." *Structure and Infrastructure Engineering Journal, SIE*, **1**(3): 221-238.
- Catbas, F. N., Shah, M., Burkett, J. and Basharat, A. (2004). "Challenges in Structural Health Monitoring". Proceedings of the 4th International Workshop on Structural Control, 195-202, Columbia University, New York, June 10-11.
- Chen, H. M., Qi, G. Z., Yang, J. C. S. and Amini, F. (1995). "Neural Network for Structural Dynamic Model Identification." *Journal of Engineering Mechanics, ASCE*, **121**(12): 1377-1381.

- Ditlevsen, O. and Madsen, H. O. (1996). "Structural reliability methods". Wiley, Chichester ; New York.
- Dunn, P. F. (2005). "Measurement and Data Analysis for Engineering and Science". McGraw-Hill, New York, NY.
- "Structures Design Guidelines" Florida Department of Transportation, FDOT, 2004.
- "Recording and Coding Guide for the Structural Inventory and Appraisal of the Nation's Bridges" FHWA, Federal Highway Administration (FHWA), 1995.
- "Transportation Asset Management Case Studies, FHWA-IF-05-040: Bridge Management Experiences of California, Florida, and South Dakota" Office of Asset Management, Federal Highway Administration (FHWA), 2005.
- "Transportation Asset Management Case Studies, Bridge Management: Experiences of California, Florida and South Dakota", FHWA, 2003.
- "Bridge Inspector's Reference Manual" Publication No. FHWA NHI 03-001, FHWA Report, 2002.
- Francoforte, K., Gul, M. and Catbas, F. N. (2007). "Parameter Estimation Using Sensor Fusion and Model Updating". Proceedings of the 25<sup>th</sup> International Modal Analysis Conference (IMAC), Orlando, FL, February 19 - 22.
- Giraldo, D. and Dyke, S. J. (2004). "Damage Localization in Benchmark Structure Considering Temperature Effects". 7<sup>th</sup> International Conference on Motion and Vibration Control.
- Gul, M. and Catbas, F. N. (2006). "An Integrated System Identification Framework for Structural Condition Assessment Using Ambient Vibration Data." *Journal of Engineering Mechanics, ASCE*, **under review**.

- Gul, M., Catbas, F. N. and Georgiopoulos, M. (2007). "Application of Pattern Recognition Techniques to Identify Structural Change in a Laboratory Speciment". Proceedings of the SPIE Smart Structures and Materials & Nondestructive Evaluation and Health Monitoring Conference San Diego, CA, March 18 - 22.
- Jain, A. K., Duin, R. P. W. and Mao, J. (2000). "Statistical Pattern Recognition: A Review." *IEEE Transactions on Pattern Analysis and Machine Intelligence*, **22**(1): 4-37.
- Jain, A. K., Murty, M. N. and Flynn, P. J. (1999). "Data Clustering: A Review." *ACM Computing Surveys*, **31**(3): 264-323.
- Kao, C. Y. and Hung, S.-L. (2003). "Detection of Structural Damage via Free Vibration Responses Generated by Approximating Artificial Neural Networks." *Computers and Structures*, **81**: 2631-2644.
- Koglin, T. L. (2003). "Movable Bridge Engineering". John Wiley and Sons.
- Lynch, J. P. and Loh, K. (2005). "A Summary Review of Wireless Sensors and Sensor Networks for Structural Health Monitoring." *Shock and Vibration Digest, Sage Publications*, **38**(2): 91-128.
- "Handbook of Bascule Bridge Balance Procedures" Report submitted to Florida Department of Transportation, Malvern, L. E., Lu, S. Y. and Jenkins, D. A., 1982.
- Masri, S. F., Nakamura, M., Chassiakos, A. G. and Caughey, T. K. (1996). "Neural Network Approach to Detection of Changes in Structural Parameters." *Journal of Engineering Mechanics, ASCE*, **122**(4): 350-360.
- Melchers, R. E. (1999). "Structural Reliability Analysis and Prediction". John Wiley & Sons.
- Nair, K. K. and Kiremidjian, A. S. (2005). "A Comparison of Local Damage Detection Algorithms Based on Statistical Processing of Vibration Measurements". Proceedings

of the 2<sup>nd</sup> International Conference on Structural Health Monitoring and Intelligent Infrastructure (SHMII), Shenzhen, China.

Nowak, A. S. (1995). "Calibration of LRFD Bridge Code." *ASCE Journal of Structural Engineering*, **121**(8): 1245-1251.

Nowak, A. S. and Collins, K. R. (2000). "Reliability of Structures". McGraw-Hill.

Omega Engineering Inc. (1995). WMS-22A and WMS-22 Current Loop Wind Stations: Operator's Manual.

Patton, G. C. (2006). "Bascule Leaf Fabrication and Erection Tolerances: Where Structure Meets Machine". Heavy Movable Structures, Inc. Eleventh Biennial Symposium, Orlando, FL.

"Bridge Analysis and Rating Program - BAR7, V7.10" PennDOT Bureau of Information Systems Application Development Division, PennDOT, 2001.

"Remote Global Monitoring of the Michigan Street Bridge, Sturgeon Bay, Wisconsin" ITI technical report no. 19, Prine, D. W. and Fish, P. E., 1996.

Rackwitz, R. and Fiessler, B. (1978). "Structural Reliability under Combined Random Load Sequences." *Computers and Structures*, **9**: 489-494.

Shalkoff, R. J. (1992). "Pattern Recognition: Statistical and Neural Approaches". John Wiley & Sons, US.

Sohn, H. and Farrar, C. R. (2001). "Damage Diagnosis Using Time Series Analysis of Vibration Signals." *Smart Materials and Structures*, **10**: 1-6.

Sohn, H., Farrar, C. R., Hunter, N. F. and Worden, K. (2001). "Structural Health Monitoring Using Statistical Pattern Recognition Techniques." *Journal of Dynamic Systems, Measurement, and Control*, **123**: 706-711.

- Susoy, M., Catbas, F. N. and Frangopol, D. M. (2006a). "Implementation of Structural Reliability Concepts for Structural Health Monitoring". Proceedings of the 4<sup>th</sup> World Conference on Structural Control and Monitoring, San Diego, CA, July 11-13.
- Susoy, M., Catbas, F. N. and Frangopol, D. M. (2006b). "Reliability-Based SHM of a Long-Span Bridge." *Journal of Engineering Structures, Elsevier (submitted)*.
- Susoy, M., Catbas, F. N. and Frangopol, D. M. (2007). "Structural Health Monitoring Development using System Reliability". Proceedings of the 10<sup>th</sup> International Conference on Applications of Statistics and Probability in Civil Engineering (ICASP10), University of Tokyo, Japan, July 31 - August 3.
- Thompson, P. D., Sobanjo, J. O. and Kerr, R. (2003). "Florida DOT Project-Level Bridge Management Models." *Journal of Bridge Engineering, ASCE*, **8**(6).
- "Bridge Study Analyzes Accuracy of Visual Inspections"  
[http://www.tfhr.gov/focus/jan01/bridge\\_study.htm](http://www.tfhr.gov/focus/jan01/bridge_study.htm), Turner-Fairbank Highway Research Center, 2005.
- "Bridge Study Analyzes Accuracy of Visual Inspections"  
[http://www.tfhr.gov/focus/jan01/bridge\\_study.htm](http://www.tfhr.gov/focus/jan01/bridge_study.htm), Turner-Fairbanks Highway Research Center, 2005.
- Webb, A. (1999). "Statistical Pattern Recognition". Oxford University Press, New York, NY.
- Wong, K.-Y. (2005). "Design of Structural Health Monitoring System for Long-Span Bridges." *Structure and Infrastructure Engineering*, **3**(2): 169-185.
- Worden, K. (1997). "Structural Fault Detection Using a Novelty Measure." *Journal of Sound and Vibration*, **201**(1): 85-101.
- Worden, K., Sohn, H. and Farrar, C. R. (2000). "Damage Detection Using Outlier Analysis." *Journal of Sound and Vibration*, **229**(3): 647-667.

- Worden, K., Sohn, H. and Farrar, C. R. (2002). "Novelty Detection in a Changing Environment: Regression and Interpolation Approaches." *Journal of Sound and Vibration*, **229**(3): 647-667.
- Xu, R. and Wunsch, D. (2005). "Survey of Clustering Algorithms." *IEEE Transactions on Neural Networks*, **16**(3): 645-678.
- Yan, A.-M., Kerschen, G., De Boe, P. and Golinval, J.-C. (2005). "Structural Damage Diagnosis under Varying Conditions - Part I: A Linear Analysis." *Mechanical Systems and Signal Processing*, **19**: 847-864.
- Zaurin, R. and Catbas, F. N. (2007). "Computer Vision Oriented Framework for Structural Health Monitoring of Bridges". Proceedings of the 25<sup>th</sup> International Modal Analysis Conference (IMAC), Orlando, FL, February 19 - 22.

## **APPENDIX A. SENSORS AND DATA ACQUISITION SYSTEMS**

### **A.1.SENSOR TECHNOLOGY**

Sensing technology is advancing very rapidly, allowing networks of large numbers of sensors to be deployed practically and with relatively low cost. Many new types of sensors are now available for various types of applications. Sensors are now used in almost all fields and industries, from medical to aerospace. Introduction of wireless transmission for sensor signals made a huge impact on the feasibility of instrumentation applications by reducing the cost and trouble of installing the cables and wires for large-scale projects.

### **A.2.GENERAL TYPES OF SENSORS**

#### **Strain Gage**

The strain gage is one of the most widely used strain measurement sensors. It is a resistive elastic unit whose change in resistance is a function of applied strain. Strain gages measure the expansion and contraction of material due to mechanical stress or thermal effect. Like all transducers, these sensors rely on indirect measurements for determining strains. Two common sensor types are the electrical resistance strain gage and the fiber optic strain gage.

The metallic foil-type strain gage consists of a grid of wire filament (a resistor) of approximately 0.001 in. (0.025 mm) thickness, bonded directly to the strained surface by a thin layer of epoxy resin. Their rugged construction and flexibility make them suitable for static and dynamic measurement with a high degree of accuracy. The measuring grid is formed by etching Constantan foil, which is then completely sealed in a carrier medium composed of polyimide film.

When a load is applied to the surface, the resulting change in surface length is communicated to the resistor and the corresponding strain is measured in terms of the electrical resistance of the foil wire, which varies linearly with strain. The foil diaphragm

and the adhesive bonding agent must work together in transmitting the strain, while the adhesive must also serve as an electrical insulator between the foil grid and the surface.

When selecting a strain gage, one must consider not only the strain characteristics of the sensor, but also its stability and temperature sensitivity. Unfortunately, the most desirable strain gage materials are also sensitive to temperature variations and tend to change resistance as they age. For tests of short duration, this may not be a serious concern, but for continuous, long-term monitoring applications, one should include temperature and drift compensation.

Bonded resistance strain gages have been proven to be reliable. They are relatively inexpensive, can achieve overall accuracy of better than  $\pm 0.10\%$ , are available in a short gage length, are only moderately affected by temperature changes, have small physical size and low mass, and are highly sensitive. Bonded resistance strain gages can be used to measure both static and dynamic strains. This is the type of strain gage used in the demonstration study of movable bridge instrumentation.

### Strain Rosette

A wire strain gage can effectively measure strain in only one direction. To determine the three independent components of plane strain, three linearly independent strain measures are needed, i.e., three strain gages positioned in a rosette-like layout.

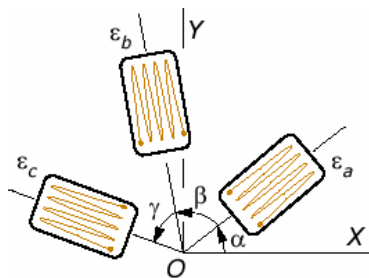


Figure A.1 – A strain rosette

The following coordinate transformation equation is used to convert the longitudinal strain from each strain gage into strain expressed in the x-y coordinates,

$$\epsilon_{x'} = \frac{\epsilon_x + \epsilon_y}{2} + \frac{\epsilon_x - \epsilon_y}{2} \cos 2\theta + \epsilon_{xy} \sin 2\theta \quad (\text{A.1})$$

Applying this equation to each of the three strain gages results in the following system of equations,

$$\begin{cases} \epsilon_a = \frac{\epsilon_x + \epsilon_y}{2} + \frac{\epsilon_x - \epsilon_y}{2} \cos 2\alpha + \epsilon_{xy} \sin 2\alpha \\ \epsilon_b = \frac{\epsilon_x + \epsilon_y}{2} + \frac{\epsilon_x - \epsilon_y}{2} \cos 2(\alpha + \beta) + \epsilon_{xy} \sin 2(\alpha + \beta) \\ \epsilon_c = \frac{\epsilon_x + \epsilon_y}{2} + \frac{\epsilon_x - \epsilon_y}{2} \cos 2(\alpha + \beta + \gamma) - \epsilon_{xy} \sin 2(\alpha + \beta + \gamma) \end{cases} \quad (\text{A.2})$$

These equations are then used to solve for the three unknowns,  $\epsilon_x$ ,  $\epsilon_y$ , and  $\epsilon_{xy}$ . For the example case study presented in the following sections, 45° strain rosette aligned with the x-y axes, i.e.,  $\alpha = 0^\circ$ ,  $\beta = \gamma = 45^\circ$ , for which the following set of equations are used for calculating the plane strains;

$$\begin{cases} \epsilon_x = \epsilon_a \\ \epsilon_y = \epsilon_c \\ \epsilon_{xy} = \epsilon_b - \frac{\epsilon_a + \epsilon_c}{2} \end{cases} \quad (\text{A.3})$$

### Vibrating Wire Strain Gages

Vibrating wire gages operate by generating a 'current pulse' to excite or 'pluck' the wire in the vibrating wire gauge. Immediately following excitation, the resonant frequency of the vibrating wire is measured. The pulse has a current source characteristic that provides automatic cable length compensation. Sensors on long cables will be pulsed with the similar energy as those on shorter cables. Produced frequency signal is measured by a precision frequency counter.

Any deformation of the vibrating wire changes its natural frequency, which may be expressed as:

$$f = \frac{1}{2L_w} \sqrt{\frac{F}{m}} \quad (\text{A.4})$$

where  $L_w$  is the length of wire;  $F$  is the tension on the wire; and  $m$  is the mass per unit length for the wire. Expressing mass,  $m$  in terms of material density,  $\rho$ , cross-sectional area,  $a$ , and gravitational acceleration,  $g$ , the equation will yield:

$$m = \frac{W}{L_w \cdot g} = \rho a L_w \Rightarrow f = \frac{1}{2L_w} \sqrt{\frac{Fg}{\rho a}} \quad (\text{A.5})$$

Expressing the tension force,  $F$ , in terms of strain:

$$F = \epsilon_w E a \Rightarrow f = \frac{1}{2L_w} \sqrt{\frac{\epsilon_w E g}{\rho}} \quad (\text{A.6})$$

where  $E$  is the Young's modulus, and  $\epsilon_w$  is the strain in the wire.

Inserting the specified parameter values of the vibrating wire material ( $E = 30 \times 10^6$  psi,  $\rho = 0.283$  lb/in<sup>3</sup>,  $g = 386$  in/s<sup>2</sup>):

$$f = \frac{101142}{L_w} \sqrt{\epsilon_w} \quad (\text{A.7})$$

$$\text{and } \epsilon_w = \frac{97.75 L_w^2}{T^2} \quad (\text{A.8})$$

Therefore, with this equation, the strain is related to the natural period of the wire. Since the signal is in terms of frequency, there is no loss of signal while traveling along long cables.

Arc-weldable and spot-weldable versions are available for easy mounting on steel surfaces. These gages can also be used on concrete, by using studded end-blocks, which

are embedded into the concrete. Vibrating wire strain gages are very stable and durable. The advantage of vibrating wire gages over resistance-based gages is their self temperature compensation making them more suitable for long-term measurements. However, their sampling rate is rather slow, therefore, dynamic events such as traffic and vibration cannot be measured.

## **Accelerometer**

With strain gages, accelerometers are the most commonly used sensor in structural monitoring. A brief summary of the most common accelerometer types is presented and their inherent benefits/drawbacks summarized.

Force balance accelerometers are spring mass devices which feature high sensitivity over a relatively low frequency range. The ability to make low frequency measurements with high accuracy makes this class of accelerometers particularly well suited for seismic and general structural monitoring applications. Because of their exceptional resolution, this class of accelerometer became the standard for permanent structural monitoring systems. However, due to their high costs and evolving sensor technologies, other types of accelerometers are becoming more popular.

Piezoelectric accelerometers incorporate a crystal sensing element which has the property of emitting a charge when subjected to a force. As these are active electrical systems, the crystals produce an electrical output only when they experience a change in load, they cannot perform true static measurements. Typical piezoelectric accelerometers offer higher measurement and frequency ranges than force balance accelerometers at the expense of resolution and inability to measure down to 0 Hz. Lower costs are another advantage of piezoelectric accelerometers over FBA's.

Capacitive accelerometers measure acceleration by monitoring a change in electrical capacitance. Within these sensors, the sensing element consists of two parallel plate capacitors acting in a differential mode. These capacitors operate in a bridge circuit, along with two fixed capacitors, and alter the peak voltage generated by an oscillator when the structure undergoes acceleration. Like the force balance accelerometer,

capacitive accelerometers typically operate in a low frequency range. Unlike piezoelectric accelerometers, these sensors can measure down to 0 Hz. The principal advantage of capacitive accelerometers is their low cost, making them attractive for dense sensor arrays; however, the resolution of these sensors is typically less than either force balance or piezoelectric accelerometers.

## **Wind**

Wind plays a major role on the movable bridges, due to their relatively slender structure. The leaves sustain significant wind loading especially when open and the mechanical drive system opening and closing them is also affected. An inexpensive option for these measurements is the WMS-22B series sensor capable of monitoring wind speed and direction at discrete locations on a bridge. The WMS-22 Current Loop Wind Station measures wind speed and direction and converts each parameter into 4 to 20mA output signals for use by process control or monitoring systems. No external power is required since the encoding electronics for wind speed and for wind direction are isolated and powered from their respective 2-wire current loops (Omega Engineering Inc. 1995). These stations are capable of measuring wind speed from 1 to 136 miles-per-hour (mph) with 1 mph resolution. For wind direction, the station offers 0° to 360° capability with 2° resolution.

## **Displacement**

The most basic type of these devices measure displacement via a flexible cable that extracts from and retracts to a spring-loaded drum. They convert mechanical motion into electrical signals that can be measured. An internal spring helps maintain tension on the cable and the threaded drum rotates a precision rotary sensor that produces an electrical output proportional to the cable travel. These displacement transducers are very easy to configure, setup and make measurements. The advantages of using these sensors are that they are easy to install, cost effective, reliable and have minimal signal conditioning requirements.

## **Tiltmeters**

Tiltmeters measure the change of inclination of a surface or a component. They usually encompass a pendulum mass; therefore, rotation of the device induces spring forces due to earth's gravitation. Tiltmeters might be based on electrical resistance or vibrating wire principles, similar to strain gages.

Vibrating wire tiltmeters are also comprised of a pendulous mass, which is under the force of gravity. As tilt increase or decreases, the mass attempts to rotate beneath the elastic hinge point and the tension in the vibrating wire changes, altering the natural frequency. Like the vibrating wire strain gages, an electromagnetic coil plucks the vibrating wire in order to read the natural frequency. Some advantages of using vibrating wire tiltmeters is that they combine high range with high sensitivity, and have excellent long-term stability. Since the sensor outputs readings in units of frequency, there is little attenuation over long cable lengths.

### **A.3. DATA ACQUISITION SYSTEMS CURRENTLY IN USE AT THE UCF STRUCTURES AND SYSTEMS RESEARCH LABORATORY**

Various data acquisition devices and systems are currently in use and/or being tested in the UCF Structures and Systems Research Laboratory.

#### **A.3.1. VXI SYSTEM**

An acquisition system from VXI and Agilent technologies is currently being used. From the accelerometers, the continuous electrical signal is conditioned before being discretized into finite values by the digitizer. After the signal is digitized, the PC link enables the data to be stored to the computer.

There are two cards that plug into the VXI mainframe. As mentioned previously one is the digitizer and the other links to the PC via IEEE 1394 fire wire. Currently, the digitizer card is limited to 16 channels but provides similar constraints to real-life monitoring whereby instrumentation must be limited due to time and economic reasons.

One of the most powerful aspects of this digitizer and acquisition system is that all the time data is collected simultaneously as opposed to a finite difference in each channels recording history. In addition to collecting data, the PC link card is also used as the controller for the electro-seis shaker. The shaker cable connects to the PC link and then the settings are configured with the testing software.



Figure A.2 – Signal conditioning

### A.3.2. NATIONAL INSTRUMENTS SYSTEM

There are many advantages to using a DAQ system from National Instruments (NI). As stated before, health-monitoring systems may require integration of multiple DAQ systems in order to run different sensors that may not work on a particular DAQ. The following components are available in the laboratory, which are sufficient for building a data acquisition network:

- SCXI 1001 chassis
- SCXI-1520 universal strain gage module
- SCXI-1314 terminal input block
- PXI 1033 chassis
- PXI 6221 controller card
- Labview software

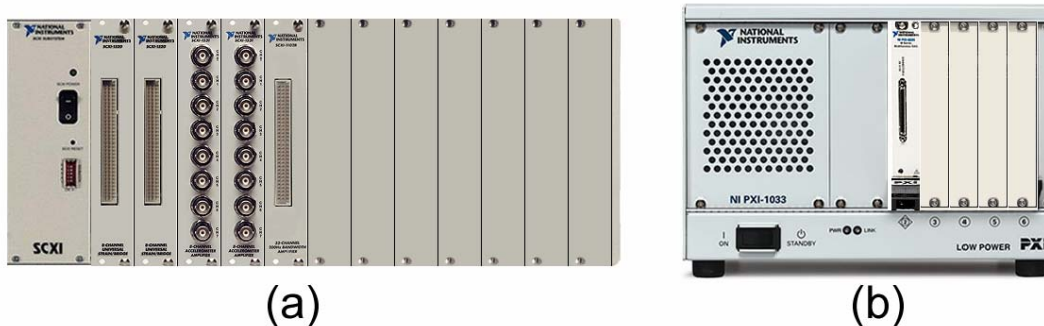


Figure A.3 – National Instruments system in the laboratory; (a) SCXI 1001 chassis, (b) PXI 1033 chassis

One SCXI-1520 universal strain gage module is to be inserted into one of the free slots on the SCXI 1000 chassis. The 1520 module is pre-wired to accommodate a wide variety of strain gages.

### A.3.3. CAMPBELL SCIENTIFIC

The Campbell Scientific datalogging equipment used in the laboratory includes the following:

- CR10X datalogger
- AM16/32 Multiplexer
- AVW1 Vibrating Wire Gage Interface
- PS100 12V Power Supply

The CR10X is a rather inexpensive and robust data collection unit, found extensively in environmental and civil monitoring applications. The CR10X datalogger is a rugged unit capable of running in some of the most demanding environments, and in temperatures ranging from  $-25^{\circ}\text{C}$  to  $+50^{\circ}\text{C}$ . The unit has 2 Mbytes of internal storage capacity, allowing for up to 524,288 data values per MByte, where high-resolution data (5 decimal characters) equals 4 bytes and low-resolution data (4 decimal characters) equals 2 bytes. The CR10X is capable of sampling rates from real-time to 64Hz and up to 750Hz using burst measurements over short intervals. Analog inputs allow for 6

differential or 12 single ended measurements, as well as accommodations for resistance measurements (resistive bridge-based), as well as excitation outputs of -2.5V to +2.5V.

Because it is relatively inexpensive, up to 4 multiplexers can be used with one CR10X datalogger, allowing hundreds of sensors to be run at a time. Two separate modes, “2x32” and “4x16” allow for scanning of 32 sensor input channels, each having 2 lines and for scanning of 16 sensor input channels, each having 4 lines respectively. The maximum number of sensors that can be multiplexed is limited to: 32 single-ended or differential analog sensors not requiring excitation (thermocouple) or 16 single-ended or differential sensors requiring excitation (full bridge strain gages). In a differential measurement, the voltage on the H input is measured with respect to the voltage on the L input. A single-ended measurement is used to measure voltage at a single-ended input with respect to ground. Although often used in conjunction with the CR10X, the multiplexer is only good for indoor, non-condensing environments. Separate enclosure units can be purchased to protect the system if it is used outdoors. Like the CR10X, the AM16/32 can be used in temperatures ranging from -25°C to +50°C.

#### **A.3.4. OTHER DATA ACQUISITION SYSTEMS**

One of the emerging technologies in the field of health monitoring today is the use of wireless communication systems to measure and record field data. Wireless devices such as sensors allow measurements to be made from remote locations without the need for long cables. By reducing the need for cables running from the sensor to the DAQ, overall costs of the health monitoring system can be greatly reduced. Wireless sensors may also be used in locations that would otherwise be inaccessible, if using conventional gages. The system we have is comprised of 3-USB base stations, 4 V-Link wireless DAQ transceivers and 2 G-Link wireless accelerometer systems from Microstrain, Inc.

The V-Link wireless transceivers feature bridge completion, on board sensor excitation, programmable offsets and gains, and differential and single ended inputs. Samples can be triggered and stored on the onboard 2 Mbytes flash memory or streamed

real-time from up to 200 feet away. Its rechargeable battery system allows for ~230 hours on continuous operation. These units feature a sweep rates from 32 Hz (low-speed) up to 2 KHz (high-speed). An integrated analog to digital converter allows for 12 bits resolution of data. Each V-Link transceiver is programmed to communicate with a base station running at 925 MHz frequency.



Figure A.4 – Microstrain data acquisition and transmitter

## APPENDIX B. RELATED LABORATORY STUDIES

The Structures Laboratory of the University of Central Florida is capable of accommodating various types of experimental studies. The laboratory has also been a test bed for investigating, installing and developing sensing systems and analysis methods of structures based on monitoring data.

Shown below is an instrumentation study on a steel beam, on which strain, displacement, accelerometer, and tilt measurements via different sensor types were employed.

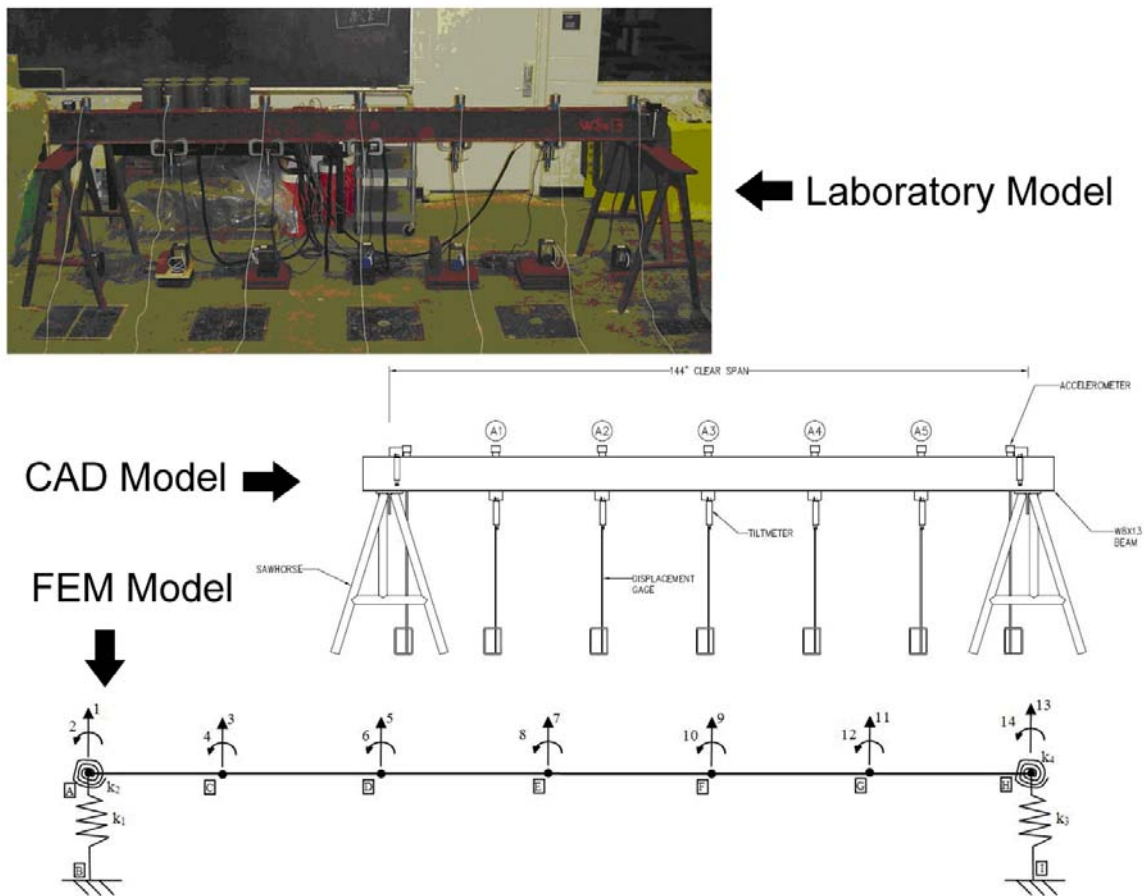


Figure B.1 – Test beam



Figure B.2 – Some tests performed on the test structure

The aim of the tests was to check the sensors and data acquired before deploying them in the field for monitoring actual structural components, and also, to develop and enhance current analysis techniques by comparing test results to mathematical and finite element models. From comparative analysis results, it was seen that experimental parameters are in a good correlation with the updated FEM.

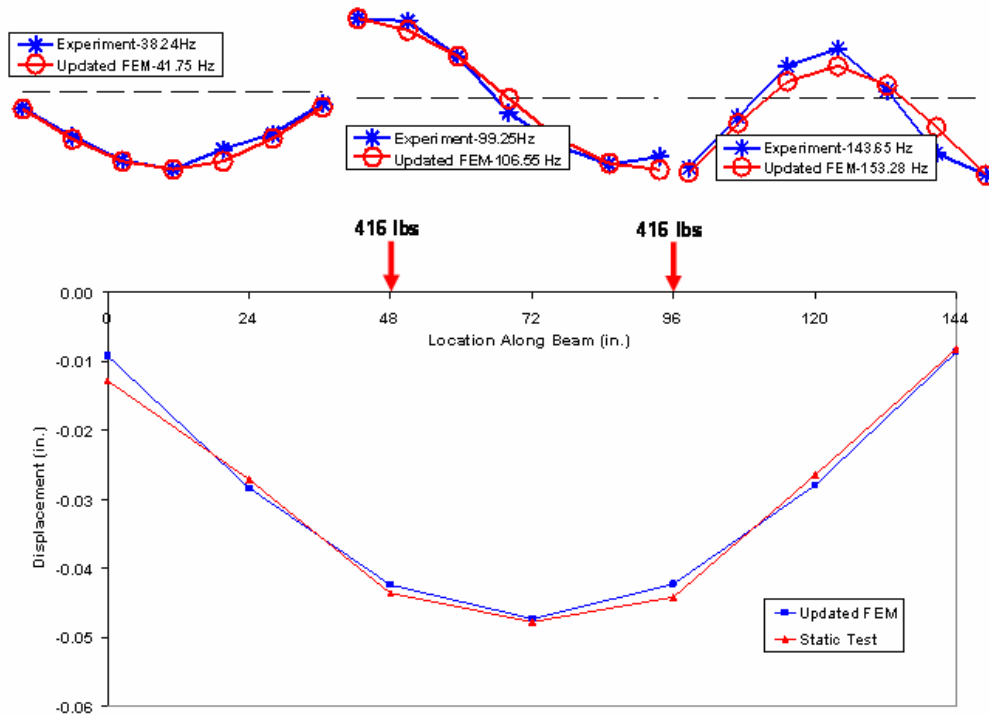


Figure B.3 – Analysis results from the instrumented beam

Another significant test setup in the laboratory is the grid structure. This structure is being used to conduct monitoring tests, in which this structure is modified to represent single-span or double-span bridges, or run damage scenarios.

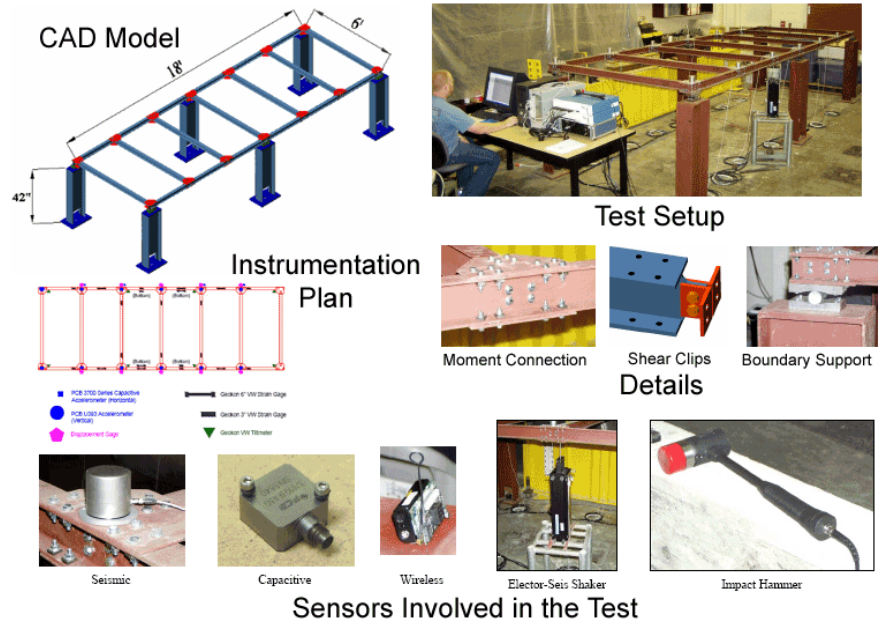


Figure B.4 – Grid structure in the laboratory

Among many results obtained from the numerous test on this structure, a couple of them show that damage can be detected by using sensor networks and developed analysis techniques.

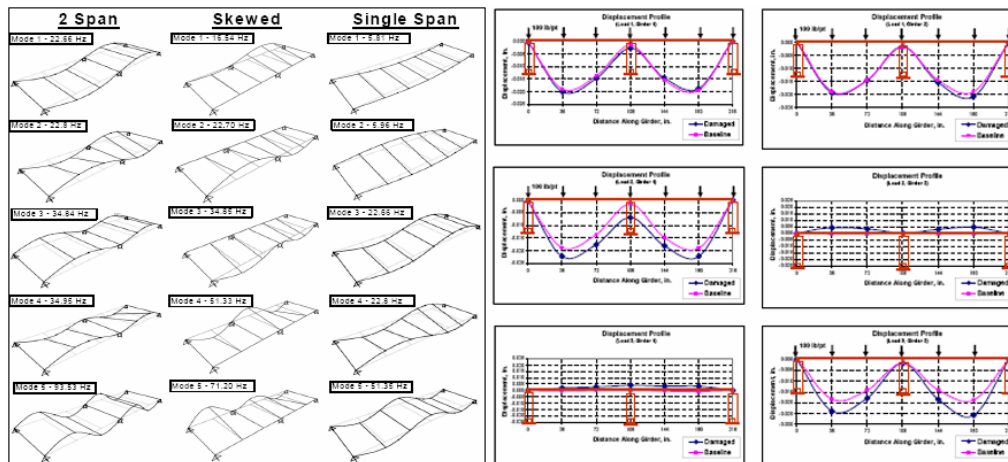


Figure B.5 – Results of dynamic analysis and damage scenarios

## **Statistical Pattern Recognition Applications to SHM**

In the literature, statistical pattern recognition has generally been used in conjunction with time series modeling of structural response data. Auto-Regressive models are highly utilized for this purpose. After constructing the AR models of the time history data, the model coefficients are used as damage indicating features. Then any statistical pattern recognition algorithms can be applied by using these features.

The researchers have implemented pattern recognition algorithms to identify damage in different test specimens. One example is given here to show the methodology implemented by the authors. After giving the overview of the methodology, discussions about the algorithms applied are given in the following sections without going into the details.

The analysis procedure applied in this study is similar to the approach used by Sohn et al. (2001) in the sense that AR model coefficients are used as features for outlier detection. However, in this analysis Random Decrement (RD) is applied to each channel to normalize the data before constructing the Auto Regressive (AR) models. After normalizing (averaging) the data using RD, AR models are fitted to the averaged data. Then the coefficients of these models are used as the damage indicating features and they are fed to the outlier detection and clustering algorithms (Figure B.6).

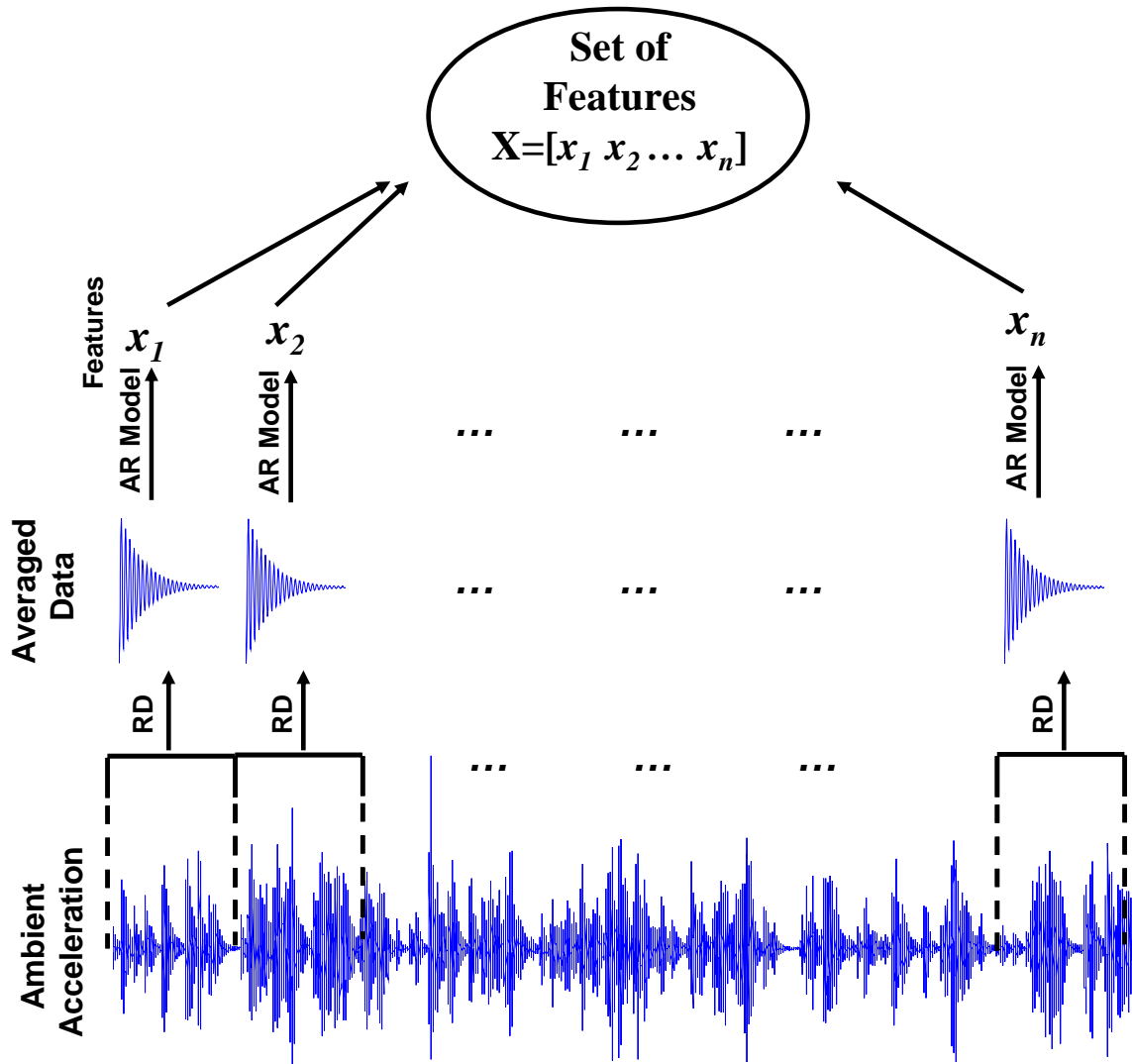


Figure B.6 – General Methodology

Random Decrement: The basic idea behind the method will be briefly summarized in the following paragraph, however more comprehensive information can be found in Asmussen (1997). Moreover, detailed discussions about its application for ambient data analysis is given in Gul and Catbas (2006) where the authors combined Complex Mode Indicator function (CMIF) with RD method to extract several features, such as modal frequencies, mode shapes, scaled and pseudo flexibilities, from ambient test data.

The random response of a system at a particular time consists of three components, which are the step response due to the initial displacements, the impulse response from initial velocity, and a random part due to the load applied to the structure. By taking the average of data segments, every time the response has an initial displacement bigger than the trigger level, the random part due to random load will eventually vanish and become negligible. Additionally, since the sign of the initial velocity can be assumed varying randomly in time, the resulting initial velocity will also be zero, leaving a pseudo-free response of the system (Asmussen 1997).

Time Series Analysis - Auto Regressive (AR) Model: Time series analysis is a common method for novelty detection applications to detect damage (Sohn and Farrar 2001; Sohn et al. 2001; Worden et al. 2002; Nair and Kiremidjian 2005). AR, ARX and ARMA (Auto-Regressive Moving Average) models were some of the time series analysis methods employed in that studies. Here, brief descriptions about the theory behind AR modeling will be presented. Preliminary results related to the AR modeling are presented in the following sections.

An AR model estimates a function's value at time  $t$  based on a linear combination of prior values. The model order (generally shown with  $p$ ) determines the number of past values, which will be used to estimate the value at  $t$  (Anderson 1976). The basic formulation of a  $p$  order AR model is defined as follows.

$$x(t) = \sum_{i=1}^p \phi_i x(t - i\Delta t) + e(t) \quad (\text{B.1})$$

The identification of the model requires determining the unknown coefficients of the AR model by using the data points. The AR coefficients can be computed in different ways. The coefficients can be computed from autocorrelation estimates, from partial autocorrelation coefficients, and from least-squares matrix procedures. In this text, the least square formulation will be given as an example. The formulation is summarized in the following paragraph.

Let us assume there are  $m$  data points. Then, the following set of linear equations can be written by using  $m - 1$  blocks of data, which consists of  $p + 1$  data points.

$$\begin{bmatrix} x_1 & x_2 & \cdots & x_p \\ x_2 & x_3 & \cdots & x_{p+1} \\ \vdots & \vdots & \ddots & \vdots \\ x_{m-p} & x_{m-p+1} & \cdots & x_{m-1} \end{bmatrix} \begin{Bmatrix} \phi_p \\ \phi_{p-1} \\ \vdots \\ \phi_1 \end{Bmatrix} = \begin{Bmatrix} x_{p+1} \\ x_{p+2} \\ \vdots \\ x_m \end{Bmatrix} \Rightarrow [x]\{\phi\} = \{x\} \quad (\text{B.2})$$

To solve the unknown coefficients,

$$\{\phi\} = ([x]^T [x])^{-1} [x]\{x\} \quad (\text{B.3})$$

Here,  $([x]^T [x])^{-1} [x]$  is so called pseudo inverse (note that  $[x]$  is not necessarily square) of  $[x]$  and the unknown coefficients can in fact be considered as least square solution.

A very crucial point here is the determination of the model order. Among many model order determination criteria, partial auto-correlation can be applied to determine the model order. For this study, the partial auto-correlation function is defined as the last AR coefficient (Box et al. 1994). To determine the model, the partial auto-correlation function is calculated for increasing  $p$  values and the correct model order is set to the  $p$  value whose auto-correlation function value is under a pre-set threshold value.

Clustering and Outlier Detection: Clustering can be described as defining groups in the data set where the data points in the same groups (clusters) are similar to each other and dissimilar to the data points in the other clusters. More details about the topic and different clustering approaches can be found in the studies by Jain et al. (1999) and Xu et al. (2005).

$K$ -means clustering is a very simple, yet powerful, unsupervised learning algorithm to cluster a given data set. The basic idea behind the method is to define  $k$  clusters in the data set by minimizing the following objective function

$$V = \sum_{j=1}^k \sum_{i=1}^n \|x_i^{(j)} - c_j\| \quad (\text{B.4})$$

where  $x_i^{(j)}$  is  $i^{\text{th}}$  data point in cluster  $j$  and  $c_j$  is the center of the cluster  $j$ . First, an initial partition with  $k$  clusters is selected. Then new partitions are generated by assigning each data point to its closest cluster. Afterwards, new clusters are recorded and the centers of the new clusters are calculated. This procedure is repeated until the cluster membership is stabilized (Jain et al. 2000).

Outlier detection, however, is detection of clusters, which deviate from other clusters so that they are assumed to be generated by another system or mechanism. Outlier detection is one of the most common pattern recognition concepts, which is applied to SHM problem as mentioned in detail in the previous sections of this text. Therefore, a special emphasize will be put on outlier detection.

The outlier detection problem for univariate (1D) data is relatively straightforward meaning that the outliers must be removed from one end or the other of the data set distribution. There are several discordance tests but one of the most common is based on deviation statistics and it is given by the following

$$z_{\xi} = \frac{x_{\xi} - \bar{x}}{\sigma} \quad (\text{B.5})$$

where  $x_{\xi}$  is the potential outlier and  $\bar{x}$  and  $\sigma$  are the sample mean and standard deviation, respectively. The multivariate equivalent of this discordance test is known as the Mahalanobis squared distance and given as

$$Z_{\xi} = (x_{\xi} - \bar{x})^T \Sigma^{-1} (x_{\xi} - \bar{x}) \quad (\text{B.6})$$

where  $x_{\xi}$  is the potential outlier vector and  $\bar{x}$  is the mean vector and  $\Sigma$  is the sample covariance matrix. By using the above equations, the outliers can be detected if the Mahalanobis distance of a data vector is bigger than a pre-set threshold level. The

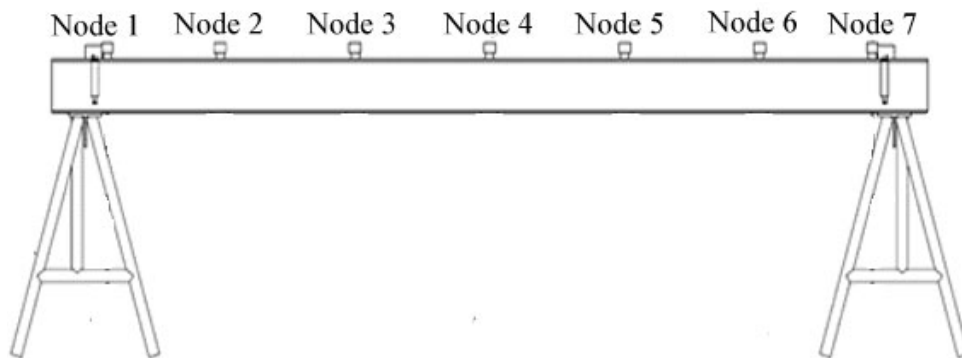
determination of this threshold level is critical and can be determined by using previous observations or simulations (Sohn et al. 2001).

### Experimental Study

The model used for the experimental tests is a simply supported steel W8x13 I-beam. The overall length of the beam is 156 in, while the clear span is 144 in. The beam rests on two steel sawhorses each measuring 3 feet in height. The setup can be seen in Figure B.7 and more information about the tests can be found in the study by Francoforte et al. (2007).



(a) Instrumented steel beam



(b) Node numbers

Figure B.7 – Test setup

Although it is a simple laboratory specimen, a very interesting, if not unique, aspect of this study is that the beam is densely instrumented with a number of sensors and is tested for many different structural configurations (different boundary conditions). The total number of dynamic and static sensors is 29 (seven accelerometers, seven displacement gages, seven tiltmeters and eight strain gages); however only the results obtained with data coming from accelerometers will be presented in this text.

The Boundary Conditions (BC) of the structure are modified by changing the material that sits on the support (between the sawhorses and the beam). The material can be a neoprene pads (different configurations of two types of pads) or a steel angle. Although a number of BC is applied during the tests, only four of them are used in this study and they are summarized in Table B.7.1. It should be noted that the first BC is also referred as the baseline case throughout the text.

Table B.7.1 – The BC applied to the test beam

Name	Boundary Condition
BC1	Pin supports at each support
BC2	4 Duro50 pads at node 1; Pin/shims at node 7
BC3	5 Duro50 pads at each support
BC4	5 Duro70 pads at each support

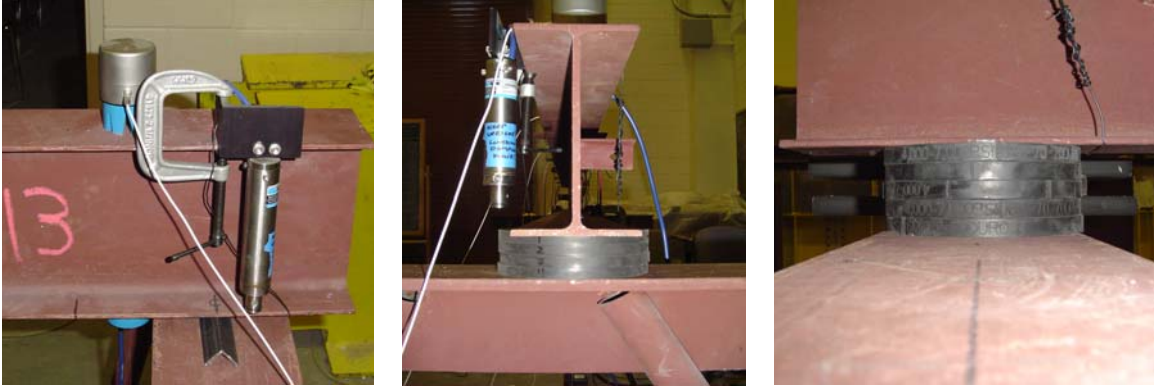


Figure B.8 – Example pictures showing different BC (a) The pin support for BC1  
(b) Four Duro50 pads for BC2 (c) Five Duro70 pads for BC4

Please note from Figure B.8(a) that the accelerometers are not placed exactly on the supports. The reason for this is that the accelerometers were positioned right above the displacement gages and the displacement gages could not be placed under the supports. So, when the term ‘support points’ is used in the following sections, the reader should understand ‘the points at the vicinity of the supports’. Figure B.8(b) and Figure B.8(c) show some of the other BC.

*Framework of the Analysis and Results:* As explained before, the ambient data is first processed (averaged) by using the random decrement method. A pseudo-free response of the system is obtained when RD is applied to data. Then, the AR models are fitted to the averaged data to obtain the damage indicating features (please refer to Figure B.6).

There are a number of different crucial parameters for the analysis such as the size of the data blocks, the reference channel for RD and the model order of AR models. A sensitivity analysis concerning these parameters can reveal important information, however, it is beyond the scope of this study. The ambient data is collected from each channel for approximately 10 minutes with a sampling frequency of 800 Hz. 18 blocks with 50000 points with no overlap are used for each BC. Reference channel for RD is node 2 and each data block has 1024 points after averaging with RD. The model order  $p$  for AR models is 10 and obtained by using partial auto-correlation function (Box et al.

1994). Figure B.9(a) shows an example of the ambient data collected from the beam. In Figure B.9(b), two graphs are overlaid one of which is the pseudo-impulse response function estimated with RD. The same figure also shows the data estimated by using the AR model. As it can be seen from Figure B.9(b) and (c), the averaged and estimated data matches almost perfectly, which indicates that the AR model fitted to the data is working reasonably well.

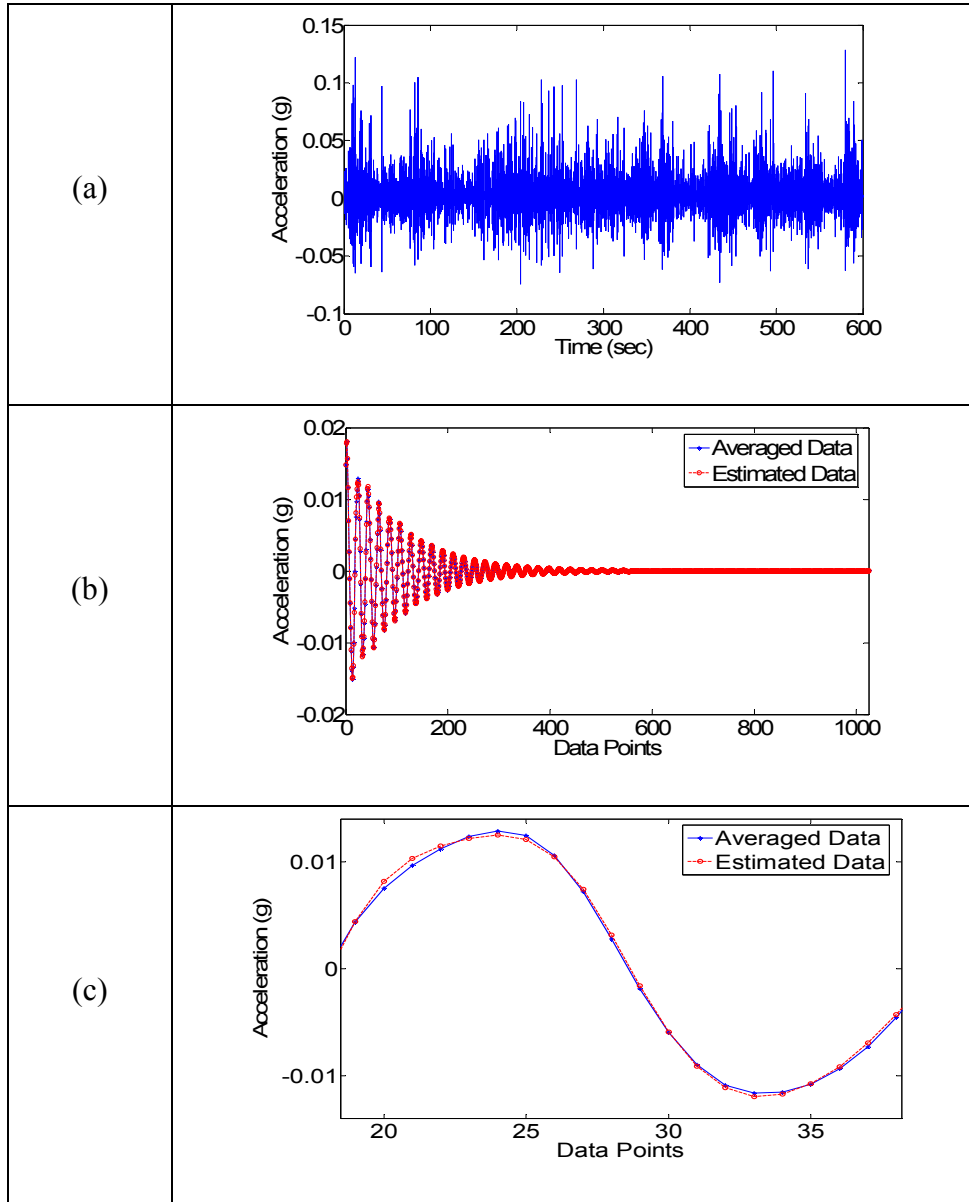


Figure B.9 – Time history data (a) Ambient data (b) Data after averaging with RD plotted with the data estimated with AR (c) A closer look at the figure in (b)

After constructing the AR models, the coefficients of these models are used as the damage indicating features. Please note that, for each BC, there are 18 data blocks, which means there are 18 sets of feature vectors each containing 10 AR coefficients. Then, all of these features are used to calculate the Mahalanobis distance between the features coming from different BC. The same features are also fed to K-Means to see if the data coming from different BC can be clustered properly.

Figure B.10 compares the features coming from BC1 and BC2 for the seven nodes. The first half of the features (blue stars) is coming from BC1 whereas second half of them (red circles) represents the BC2. It is clearly seen from Figure B.10(a) that the two BC can be well separated by using Mahalanobis distance. However, Figure B.10(b) shows that the same BC cannot be differentiated with the same features by using K-Means clustering. Mahalanobis distance works also quite well for classifying BC1 and BC3 as it is shown in Figure B.10(c). Unlike the previous case, K-Means works reasonably good for these cases (Figure B.10(d)) yet it does not perform as well as Mahalanobis distance. For example, patterns could not be classified correctly for nodes 3 and 7.

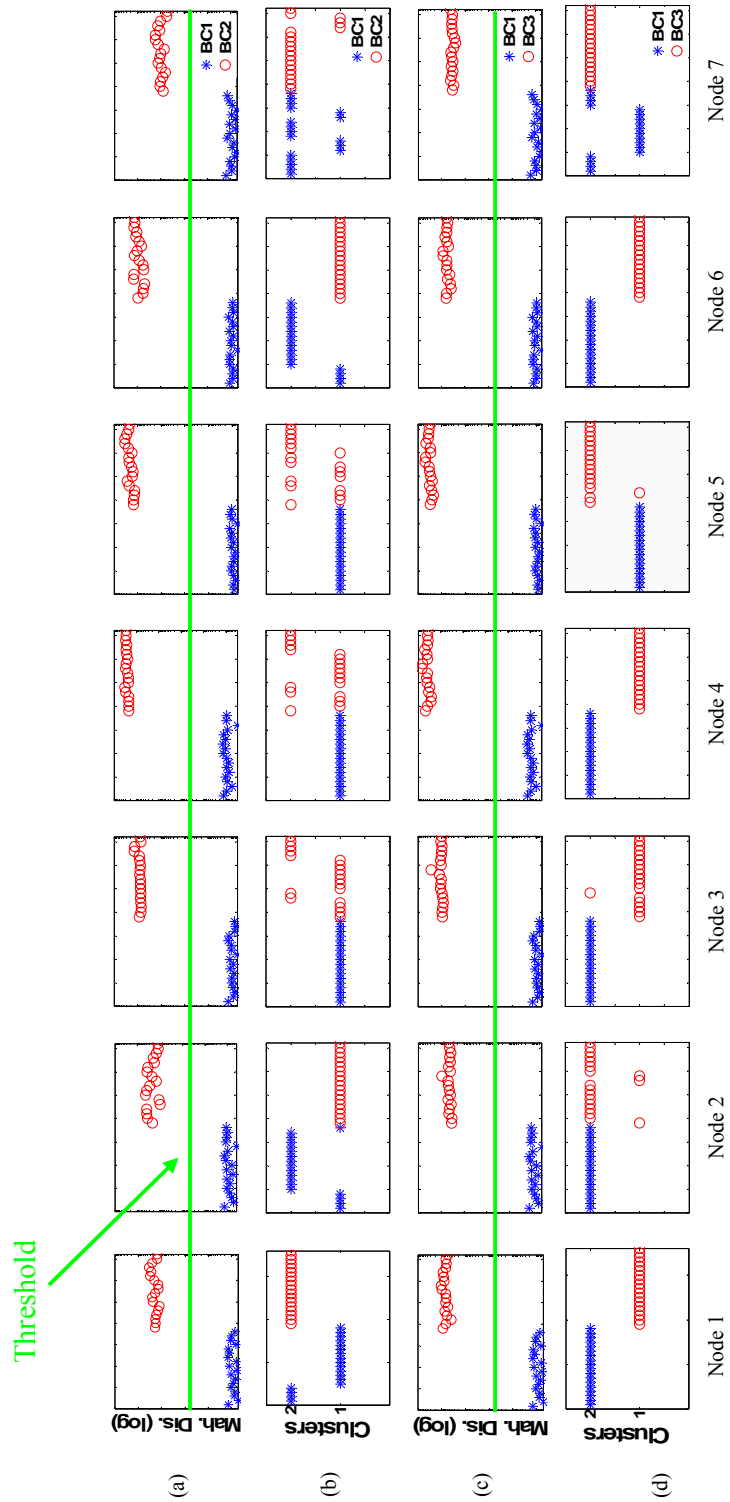


Figure B.10 – Analysis results for BC1, BC2 and BC3 (a) Mahalanobis distance of the AR coefficients for BC1 and BC2 (b) Clustering of the AR coefficients for BC1 and BC2 (c) Mahalanobis distance of the AR coefficients for BC1 and BC3 (d) Clustering of the AR coefficients for BC1 and BC3 (each point in the figures is coming from one data block)

Another important thing we should notice from Figure B.10(a) and (c) is that although the difference between data sets are clearly seen with Mahalanobis Distance, no information about the location of the change is obtained. This is a very important point and it should be explored with further investigation in future studies.

Now, the same algorithms are used to see if three different BC can be separated from each other. The previous analysis results showed that there was a change in the structure. However, here it is not only shown that there have been changes in the data but also these changes are different from each other. Figure B.11 shows the Mahalanobis distances for BC1, BC3 and BC4 for node 1, 4 and 7. It is clearly seen from Figure B.11 that three different cases can be differentiated from each other, which mean we can not only understand that there is a problem but also see if this problem is different than the problems before.

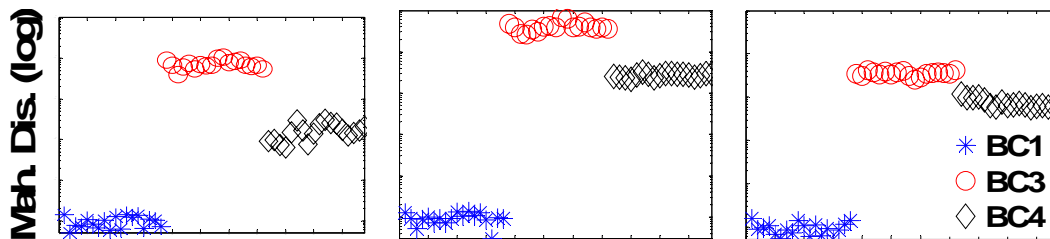


Figure B.11 – Mahalanobis distance of the AR coefficients  $f$  for BC1, BC3 and BC4 (each point in the figures is coming from one data block)

## Steel Grid Tests

To ensure the effectiveness of the methodology, it is also applied to a steel grid, which is constructed at University of Central Florida (UCF) Structures and Systems Research Laboratory (Figure B.12). This steel structure is an excellent specimen to verify the methodology since it is possible to increase the level of indeterminacy and the uncertainty of the model. The model is specially designed to have the dynamic properties of short to medium span bridges. Its basic properties can be found in the study by Burkett (2005).

Different damage scenarios are applied to the grid as can be seen in Figure B.13. The first scenario is a relatively obvious case to identify where a pile loss is simulated by removing the roller support between the grid and the column (Figure B.13 (a)). The second damage case is simulated by fixing the end supports to simulate some unintended rigidity at the supports caused by different reasons, i.e. corrosion (Figure B.13(b)). The last, and probably most challenging case is the reduced stiffness case where only for bolts at the supports are removed (Figure B.13(c)).



Figure B.12 – The physical grid model and test setup



(a) Scour



(b) Restraint Support



(c) Reduced Stiffness

Figure B.13 – Damage scenarios applied to the steel grid

Since K-Means clustering did not perform satisfactorily, only Mahalanobis distance will be used for outlier detection for the steel grid. Before going to the damage cases, two different data sets coming from the healthy condition of the grid were

analyzed. These data sets were acquired more two years apart by using the same structure. This is done to determine the threshold indicating if there is a structural change or not. Figure B.14 shows Mahalanobis distance plots for different nodes and it is seen that the threshold value can be set as  $10^3$ .

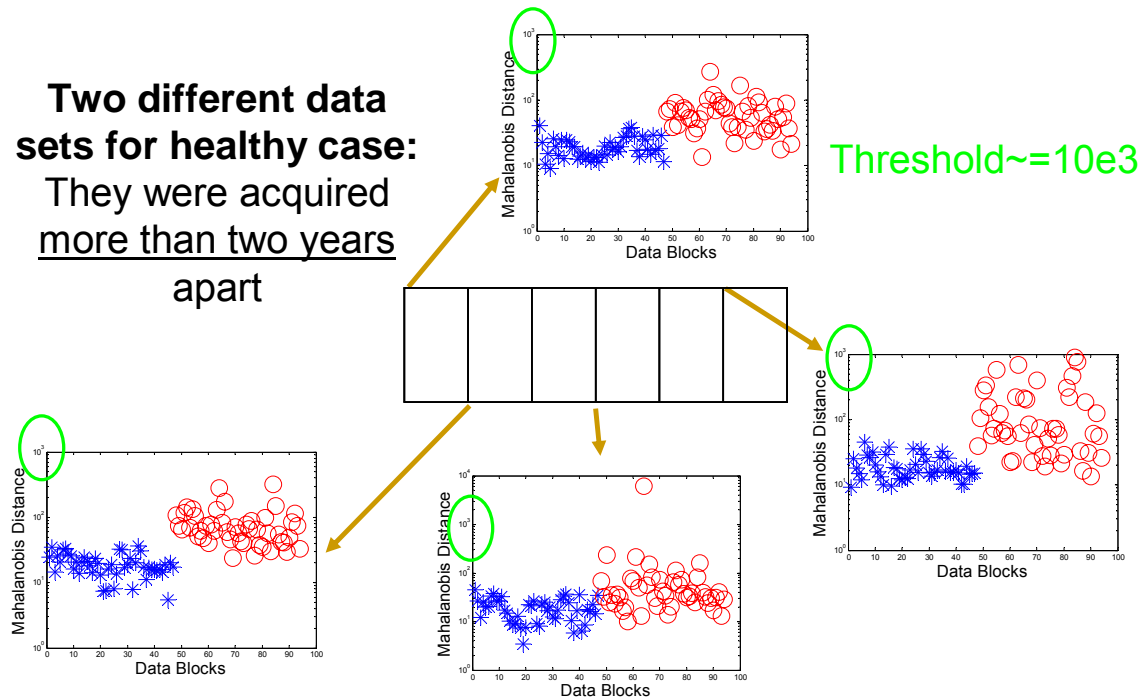


Figure B.14 – Determining the threshold value for the grid

The following three figures (Figure B.15, Figure B.16 and Figure B.17) show the Mahalanobis distance plots for the damage cases. As Figure B.15 shows, the damaged case is clearly identified since all the values coming from the damaged structure is well above the threshold value. This is expected since the induced damage was obvious. As we look at Figure B.16, we see that most of the values are still above the threshold value; however some false negatives are also observed. For the last damage case, Figure B.17 shows that number of false negatives is even more; whereas a distinction between healthy and damaged case is still observable. This is a reasonable result since removing just four bolts in the structure can be considered as a slight damage case.

## Scour Damage Scenario

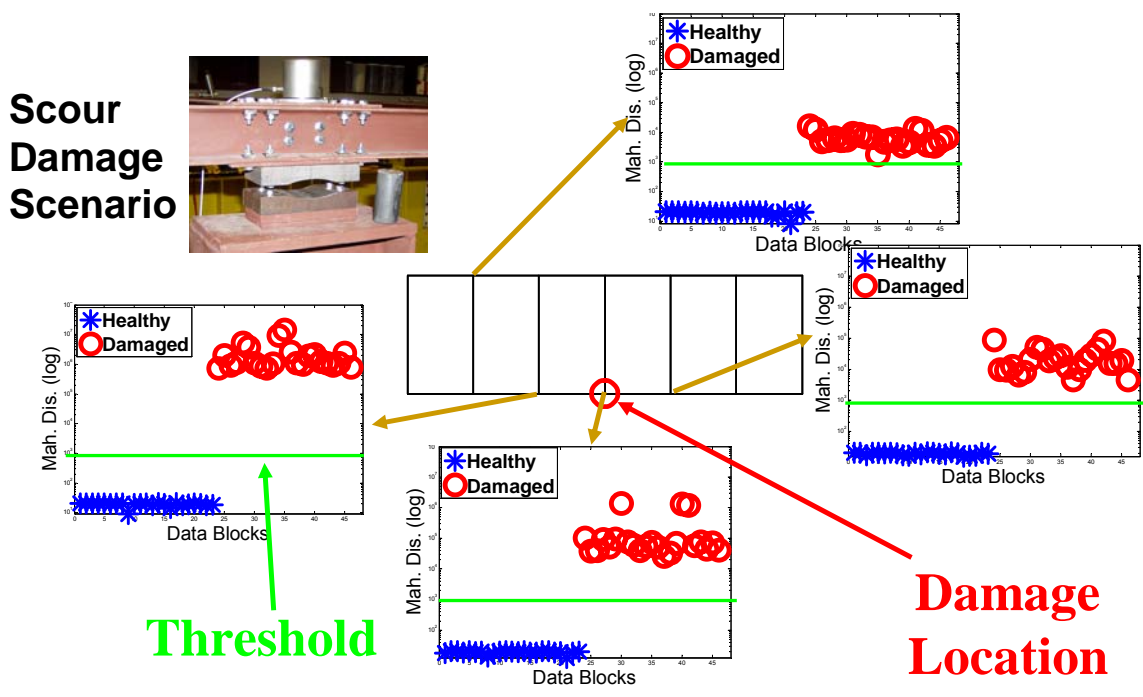


Figure B.15 – Mahalanobis distance plots for scour case

## Two Joints Restraint Damage Scenario

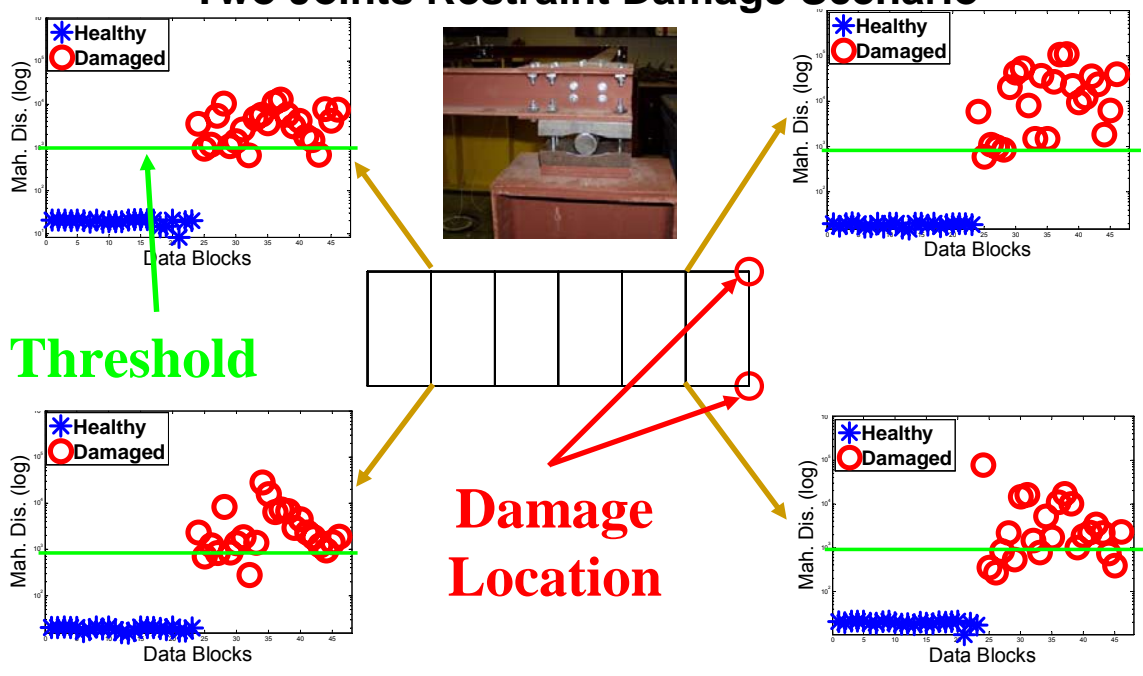


Figure B.16 – Mahalanobis distance plots for restraint supports

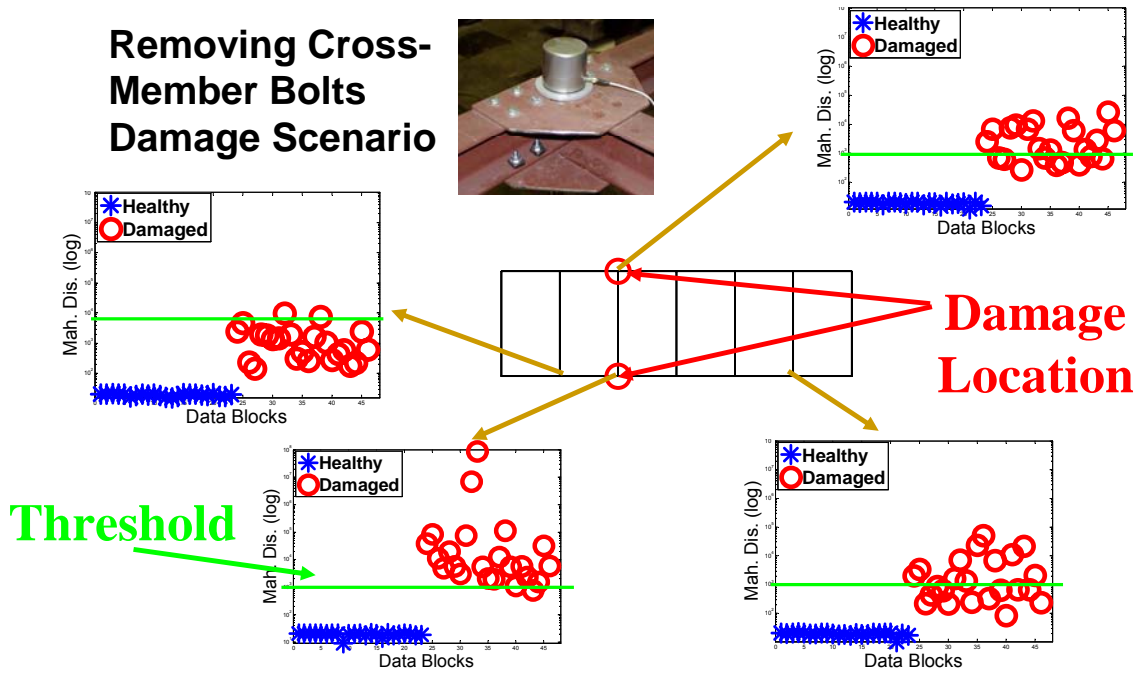


Figure B.17 – Mahalanobis distance plots for reduced stiffness

## **APPENDIX C. INSTRUMENTATION COMPANIES AND MARKET SEARCH**

### **A.1. COMPANIES RELATED WITH SHM SENSOR DEVELOPMENT**

The sensor market search has been conducted over the sensors currently in use in the UCF Structures and Systems Research Group, and some comparable gages. The aim of preparing this list is to provide some examples of current commercially available sensing instruments and general characteristics. The list does not cover the whole spectrum of gage types, and only a number of leading brands are included. Not all information and specifications are available, and the information is time sensitive, therefore, the reader is advised that the information is valid only at the time of the inquiry. This information should not be used without checking for updates, which are very frequent in the sensor industry.

#### **Acellent Technologies, Inc. ([www.acellent.com](http://www.acellent.com))**

Acellent's SMART technology is designed to be easily integrated into new or existing structures to automate inspection and maintenance procedures. The SMART Layer sensor network, SMART Suitcase signal generation and collection unit, and ACCESS Software Suite comprise a complete system that provides complete solutions for structural health monitoring. The SMART Layer sensor network is a thin dielectric film with an embedded network of distributed piezoelectric actuators/sensor and can be manufactured in a variety of sizes, shapes, and complexity. They can be used as PZT transducers, fiber optic sensors, strain gages, temperature sensors, and much more. The portable SMART Suitcase data acquisition instrument is direct wire connected to the sensors, but can be remotely controlled through Ethernet or Internet and is compatible with third-party sensors. These systems are custom-designed and range anywhere from \$8,000 to \$30,000 depending on design, size, and application.

### **Advanced Corrosion Monitoring (ACM) Instruments ([www.potentiostat.com](http://www.potentiostat.com))**

ACM has been developing and supplying various corrosion monitoring instrumentations since 1985. Custom elements, especially logging techniques, can be created to the structure owner's specification. ACM often builds a PC into their instruments. By adding internet connection either via a LAN, phone line, or mobile phone, data can be retrieved from any PC connected to the internet. ACM has several engineers with plenty of experience in corrosion monitoring. They claim to be able to build any system to meet the customer's needs.

### **Analog Devices, Inc. ([www.analog.com](http://www.analog.com))**

Analog Devices specializes in high-performance analog, mixed-signal, and digital signal processing integrated circuits. They develop and supply some high-performance signal conditioning devices and MEMS and provide custom-designed solutions. Their sensors include:

- 1-, 2-, and 3-axis accelerometers
- Gyroscopes
- Analog and digital temperature sensors.

There are several systems available for data acquisition and processing: data converters, display electronics, integrated systems, etc. Their data acquisition systems are, in most cases, custom designed and, therefore, application-specific. They have several communications solutions, including RF, cellular handset ICs, optical networking, and other wireless options.

### **Geokon, Inc. ([geokon.com](http://geokon.com))**

Geokon is one of the leading designers and manufacturers of a broad range of high quality geotechnical instrumentation. They are world leaders in vibrating sensor technology. They offer sensors that measure:

- Strain
- Load
- Concrete stress
- Displacement
- Temperature
- Tilt

Since vibrating wires use frequency output rather than voltage, sensor signals can be transmitted over long cables (>2000 m) without significant degradation of signal caused by cable resistances which can arise from water penetration, temperature fluctuations, contact resistance, or leakage to ground. This results in excellent long-term stability suited for long-term measurements in adverse environments.

Geokon also makes rugged dataloggers, multiplexers, and software to operate all types of vibrating wireless sensors. Some of their datalogging equipment and software models are compatible with the Campbell Scientific CR10X and with Microsoft Excel.

**Measurement Computing Corp. ([www.measurementcomputing.com](http://www.measurementcomputing.com))**

Measurement Computing is a pioneer and leader in low-cost data acquisition boards for ISA, PCI and USB personal computer interfaces. They provide an extensive line of signal conditioning products and low-cost, rugged data loggers. Acquired by National Instruments in April 2005, the company markets its products worldwide through direct sales, a distribution network, and the Worldwide Web.

**MicroStrain, Inc. ([www.microstrain.com](http://www.microstrain.com))**

MicroStrain makes data acquisition equipment and tiny sensors that are used in a wide range of applications, including civil structures, unmanned military vehicles, and automobile engines. They offer sensors to monitor:

- Strain
- Temperature
- Displacement
- Acceleration
- Angle and angular rate
- Differential voltage.

Their award-winning Wireless Web Sensor Network allows the transmission of data from 1,000 unique sensors to one web-based receiver, enabling massive amounts of

data to be shared globally in real time. All of MicroStrain's wireless sensors and dataloggers comply with IEEE 802.15.4 (and Zigbee) standards.

The Agile-Link software allows users to fully configure and communicate with the entire line of Dashlink products, including, but not limited to, V-Link, G-Link, and SG-Link wireless sensors. The graphical user interface makes interacting with wireless sensor nodes effortless with virtual plug-and-play operability.

**Omega Engineering, Inc. ([www.omega.com](http://www.omega.com))**

Omega offers more than 100,000 state-of-the-art products for measurement and control of:

- Temperature
- Humidity
- Pressure
- Strain
- Force
- Flow
- Level
- pH
- Conductivity
- Voltage

They also offer several solutions for wireless connectivity between their sensors and data acquisition devices as well over the Ethernet and Internet. Most of their sensors and dataloggers set up with virtual plug-and-play ease.

Omega's OM-CP-Series Windows software includes an Excel button on the toolbar to allow simple one-click data export to Microsoft Excel. One click of the Excel icon will automatically open Excel and format the data into a spreadsheet. The software can collect and display real-time data from any OM-CP-Series logger directly connected to the user's PC, a LAN, or even remotely through the use of an OM-CP-RF-Series RF transceiver.

**PCB Piezotronics, Inc. ([www.pcb.com](http://www.pcb.com))**

PCB Piezotronics, Inc. is a leading manufacturer and worldwide supplier of laboratory and industrial grade sensors servicing a vast array of applications and markets. Utilizing piezoelectric, piezoresistive, capacitive, and strain gage technologies, PCB

produces a wide variety of sensors for the measurement of both static and dynamic events used for test, measurement, monitoring, and feedback control in industrial, military, educational, commercial, and research applications. PCB is particularly known for having popularized integrated electronic piezoelectric sensors (IEPE), known also by PCB's trademarked name ICP<sup>®</sup> sensors (Integrated Circuit Piezoelectric).

They manufacture over 3,000 products to meet the diversified needs of the worldwide sensor market. Their sensors are compatible with virtually any datalogger or acquisition system that accepts analog voltage input and include:

- Acceleration and vibration
- Acoustic
- Strain
- Force
- Impact
- Load
- Pressure
- RPM
- Shock
- Speed and velocity
- Tilt
- Torque

**Picarro ([www.picarro.com](http://www.picarro.com))**

Picarro serves customers in the life science, environmental monitoring, and high tech manufacturing markets. They produce lasers for bio-instruments and ultra-trace gas sensors for environmental monitoring and high tech manufacturing. Picarro's ESP-1000 family of instruments is based on a revolutionary technology known as Cavity Ringdown Spectroscopy (CRDS). This innovative technique is used to detect and quantify trace amounts of chemicals for an expanding range of applications including semiconductor manufacturing, the development of clean diesel engines, petrochemical processing and monitoring of green house gases. The ESP-1000 uses precision lasers to measure miniscule amounts of specific chemicals in complex gas backgrounds

**Silicon Designs, Inc. ([www.silicondesigns.com](http://www.silicondesigns.com))**

Silicon Designs builds a wide range of accelerometers for OEM and instrumentation applications. Their capacitive design provides both DC and dynamic

response to acceleration. Integrated accelerometer electronics provide a high level, low impedance output to minimize environmental noise pickup, and no separate charge amplifiers are needed. These accelerometers are available with either a traditional analog output, for use with conventional data acquisition systems using A/D converters, or with a digital output, suitable for direct integration with microprocessors. Their products offer a wide variety of standard g-ranges, form factors, and output styles to suit any application. Custom accelerometer packaging, outputs, and screenings are available on a per case basis. The company is also capable of electronic, circuit, system, and product design; micro-machining and thin-film development; and hybrid, micro-sensor, and PC board design. Silicon Designs' Accelerometers are being used by the US Military, NASA, and in the automotive, transportation, and agricultural industries

**Summation Research, Inc. ([www.summationresearch.com](http://www.summationresearch.com))**

Summation Research, Inc. (SRI) is an engineering and manufacturing company providing high performance data acquisition, satellite telemetry, and communication products and systems to defense, government and commercial markets worldwide. They specialize in unique off-the-shelf and custom solutions requiring expertise and innovation in RF, analog, and digital signal processing. Through its PMD sister company, SRI supplies industry-leading wireless sensor telemetry products for test and operational measurement, sensing, and data logging. Through the use of advanced digital signal processing technologies, PMD wireless sensor telemetry transmitters are easily programmed to work with a wide variety of sensors measuring temperature, torque, strain, pressure, and other critical parameters in locations that are difficult or impossible to reach with wires or slip rings.

**Intecorr International ([www.intecorr.com](http://www.intecorr.com))**

Intecorr's SmartCET makes it possible to monitor localized pitting corrosion along with general corrosion. It is "smart" because it processes the data onboard and provides operators information on a real-time basis. Key features are reduced cost of installation, accuracy, ease of use, intrinsically safe, online, and real-time monitoring of

corrosion rate and pitting. The units facilitate electrochemical measurement of corrosion and scaling for industrial applications and are available in either Intrinsically Safe or non-Intrinsically Safe models. SmartCET is installed directly adjacent to a corrosion probe and connected to it using three-pair cabling. The system can support up to 16 SmartCET units up to a maximum hardwired distance of 3,900 feet. FieldCET software is used for data acquisition and trending.

## A.2. SENSORS MARKET SEARCH

### A.2.1. ACCELEROMETER

Company	Analog Devices, Inc.		Microstrain
Unit Name/Number	ADXL Low-g Series	ADXL High-g Series	G-Link
Function	MEMS	MEMS	Triaxial Piezoelectric
Price	\$3.75 - \$12.00	\$7.00 - \$10.50	\$495
Wireless?	No	No	Yes
RF Carrier			916 MHz
RF Range			100 ft
Channels	1-, 2-, and 3-axis	1- and 2-axis	3 axes
Memory/Data Storage			2 MB
Data Rate	0.55 - 6 kHz	0.4 kHz	19.2 kbs
Data Range	+/- 1.2 to 18 g	+/- 35 to 250 g	+/- 2g or +/- 10g
Shock Limit			500g
Frequency Range			
Sensitivity	57mV/g to 1.5 V/g	8 to 55 mV/g	
Resolution			12 bits (ADC)
Accuracy	5 to 20%	5%	
Nonlinearity			
Output Noise			
Temperature Response			
Strain Sensitivity			
Excitation Provided	2 - 6 V	4.75 to 5.25 V	
Excitation Required			
Record Interval			32 to 2048 samples per sec
Continuous Sample Rate			1000 samples per sec
Battery Life			273 hrs
Computer Interface			Agile-Link
Notes	Analog and digital models available	Analog only	802.15.4 compatible

Company	Silicon Designs	PCB Piezotronics	
Unit Name/Number	2265 Series	PCB 393C	2420 Series
Function	1-axis analog	Quartz Seismic	3-axis digital
Price	\$461 - \$526		\$1179 - \$1279
Wireless?	No	No	No
RF Carrier			
RF Range			
Channels	1 axis	1 axis	3 axes
Memory/Data Storage			
Data Rate			
Data Range	2 to 200 g	2.5 g peak	2 to 200 g
Shock Limit	2000 g	100 g	2000 g
Frequency Range	0-400 thru 0-3000 Hz	0.025 to 800 Hz	0-400 thru 0-2000 Hz
Sensitivity	20 to 2000 mV/g	1,000 mV/g	0.625 to 62.5 mg/pulse
Resolution		0.0001 g	
Accuracy		5 to 10%	
Nonlinearity	0.3 to 1.0% FS		0.5 to 1.0% FS
Output Noise	8 to 200 micro-g per root Hz		
Temperature Response	50 - 200 ppm/deg.C	<0.03% / deg.F	150 - 300 ppm/deg.C
Strain Sensitivity		0.001 g / microstrain	
Excitation Provided			
Excitation Required	5.0 VDC	18 to 30 V	5.0 VDC
Record Interval			
Continuous Sample Rate			
Battery Life			
Computer Interface			
Notes		398 models of accelerometer are available	

### A.2.2. STRAIN

Company	Microstrain	Geokon	
Unit Name/Number	SG-Link	VK-4100	4000
Function	High Speed Strain Gage/Datalogger	Vibrating wire	Vibrating wire
Price	\$495		
Wireless?	Yes	No	No
RF Carrier	2.4 GHz		
RF Range	70 m (300 m with high-gain ant.)		
Channels	2--1 Full Bridge, 1 Single-Ended		
Memory/Data Storage	2 MB		
Data Rate			
Data Range		2500 $\mu\epsilon$	3000 $\mu\epsilon$
Shock Limit			
Nominal Resistance			
Gage Range			
Frequency Range		1400 - 3500 Hz	450 - 1200 Hz
Coil Resistance		180 Ohm	150 Ohm
Fatigue			
Sensitivity			
Accuracy		2%	0.10%
Resolution	+/- 1 microstrain - 12 bits (ADC)		
Nonlinearity		2%	0.50%
Temperature Characteristics		12.2 $\mu\epsilon$ /deg.C	12.2 $\mu\epsilon$ /deg.C
Excitation Provided	3 VDC		
Excitation Required			
Record Interval	32 – 2048 samples per sec		
Continuous Sample Rate	617 - 736 Hz		
Battery Life	3.4 hrs		
Computer Interface	Agile-Link		
Notes	802.15.4 compatible		

Company	Omega		PCB Piezotronics
Unit Name/Number	SG Series	KFG Series	240A03
Function	Foil strain gage	Foil strain gage	Quartz strain sensor
Price	\$49 - \$145 (basic)	\$80 - \$140 (basic)	
Wireless?	No	No	No
RF Carrier			
RF Range			
Channels			
Memory/Data Storage			
Data Rate			
Data Range			
Shock Limit			
Nominal Resistance	120, 350, 100 Ohms	120 +/- 0.4 Ohms	
Gage Range	3% or 30,000 $\mu\epsilon$	5% or 50,000 $\mu\epsilon$	300 $\mu\epsilon$
Frequency Range			
Coil Resistance			
Fatigue	10,000 cycles	10,000 cycles	
Sensitivity			10 mV / microstrain
Accuracy			
Resolution	Continuous	Continuous	0.001 microstrain
Nonlinearity			$\leq 2\%$
Temperature Characteristics	11 ppm/deg.C (Steel) 23 ppm/deg.C (Aluminum)	10.8 ppm/deg.C (steel)	
Excitation Provided			
Excitation Required			20 to 30 VDC
Record Interval			
Continuous Sample Rate			
Battery Life			
Computer Interface			
Notes	There are dozens of shapes and sizes from which to choose		

### A.2.3. TEMPERATURE

Company	Analog Devices, Inc.	
Model Name/Number	AD- and TMP- Series	AD- and TMP- Series
Function	Analog IC transducer	Digital IC transducer
Price	\$0.40 to \$6.51	\$0.59 to \$2.95
Wireless?	No	No
Temp Range	-55 to 150 deg. C (varies)	-55 to 150 deg. C (varies)
Error	+/- 0.5 to 2.5 deg. C	+/- 0.5 to 3 deg. C
Resolution	1 micro-A per deg. K 5 to 28 mV per deg. C	10- to 16-bit 0.025 to 0.3 deg. C per LSB
Excitation Provided	2.7 to 30 V	2.65 to 7 V

### A.2.4. TILT

Company	Geokon
Unit Name/Number	6350
Function	Vibrating wire
Wireless?	No
Price	
Data Range	+/- 15 deg.
Sensitivity	
Resolution	8 arc sec
Accuracty	0.10%
Linearity	1.50%
Thermal Zero Shift	0.01% per deg. C
Operating Frequency	1400 - 3500 Hz
Coil Resistance	180 Ohm
Notes	

### A.2.5. WIRELESS NETWORKING

Company	Omega	Summation Research	
Unit Name/Number	OM-CP-RFEXT-KIT	ST-540	SR-540
Function	RF Range Extender	Data transmitter	Data receiver
Price	\$599 per extender \$999 per pair	\$1,645 (1-channel) \$2,395 (4-channel) \$3,145 (8-channel)	\$2,745
Frequency	900 MHz	915, 868, or 433 MHz	915, 868, or 433 MHz
Transmit Power	100 MW		
Transmit Range	600 to 1500 ft (indoor) 0.5 to 1 mi (outdoor)	500 ft	
Number of Channels		1, 4, or 8	16
Sample Rate		9.5 or 17 ksps	
Sample Resolution		12- or 18-bit	
Accuracy		0.5% typical 0.1% possible	
Analog Output			0-5, 0-10, +/-5, +/- 10 VDC
Digital Output			12-bit
Computer Interface	RS-232C or serial		RS-232
Data Rate	2.4 thru 57.6 kbs		115 kbs
Notes	Remotely mount any OM-CP Series datalogger		

### A.2.6. CORROSION

Company	ACM	
	Gill AC	Field Machine
Unit Name/Number	Galvanostat	Portable Galvanostat
Function	No	No
Wireless?		\$20,000
Price	4	12
Channels	600 V or 1000 A	12 V
Max Power	110/230 VAC 50-60 Hz	110/230 VAC 50-60 Hz or 12 VDC
Power Supply	<3 microvolts	<4 microvolts
Noise		
Potentiostat		
Compliance Voltage	+/- 15 V	+/- 12 V
Sweep Range	+/- 3 V	+/- 3 V
Sweep Resolution	25 microvolts	25 microvolts
Frequency Response	30 kHz	30 kHz
Measurement Accuracy	21 Bit A/D	21 Bit
Measurement Resolution	1 microvolt	1 microvolt
Sweep Rate	200 mV/second	200 mV/second
Frequency Response Analyzer		
Frequency Range	10 microHz to 30 kHz	10 microHz to 30 kHz
Sample Rate	1 MHz	1 MHz
ADC	12 Bit	12 Bit
Galvanostat Resolution	1 microvolt	1 microvolt
Notes	For laboratory use	For field use